



HAL
open science

Cyclic aromatic nanoribbons

Luc Soliman

► **To cite this version:**

Luc Soliman. Cyclic aromatic nanoribbons. Organic chemistry. Université de Bordeaux, 2024. English. NNT: 2024BORD0177 . tel-04784586

HAL Id: tel-04784586

<https://theses.hal.science/tel-04784586v1>

Submitted on 15 Nov 2024

HAL is a multi-disciplinary open access archive for the deposit and dissemination of scientific research documents, whether they are published or not. The documents may come from teaching and research institutions in France or abroad, or from public or private research centers.

L'archive ouverte pluridisciplinaire **HAL**, est destinée au dépôt et à la diffusion de documents scientifiques de niveau recherche, publiés ou non, émanant des établissements d'enseignement et de recherche français ou étrangers, des laboratoires publics ou privés.

THÈSE PRÉSENTÉE
POUR OBTENIR LE GRADE DE
DOCTEUR DE
L'UNIVERSITÉ DE BORDEAUX

ÉCOLE DOCTORALE DES SCIENCES CHIMIQUES

Chimie Organique

Par Luc SOLIMAN

Nanorubans cycliques aromatiques
Cyclic aromatic nanoribbons

Sous la direction de :
Fabien DUROLA

Soutenue le 27/09/2024

Membres du jury :

Dr DUROLA Fabien, Chargé de Recherche, Université de Bordeaux/CNRS, Directeur de thèse
Pr. NOWAK-KROL Agnieszka, Professor, Universität Würzburg, Rapporteur
Dr. WEISS Jean, Directeur de recherche, Université de Strasbourg/CNRS, Rapporteur
Pr. SAUVAGE Jean-Pierre, Professeur émérite, Université de Strasbourg, Examineur
Pr. ZAKRI Cécile, Professeure, Université de Bordeaux, Examinatrice

Summary

Résumé.....	13
Introduction.....	13
Résumé.....	14
Conclusion générale	23
Chapter 1: From allotropic forms of carbon to the synthesis of new forms of nanocarbons.27	
I. Carbon and allotropy	27
a. Natural allotropes of carbon.....	27
b. Synthetic allotropes of carbon.....	27
II. Polycyclic aromatic compounds.....	29
a. Planar nanocarbons	29
b. 3D nanocarbons	35
c. Macrocyclic nanocarbons	40
III. The Perkin Strategy.....	44
a. Evolution of the Perkin reaction	44
b. Synthesis of the building blocks.....	46
c. PACs obtained with the Perkin Strategy	46
d. Macrocycles	50
IV. Thesis project: The synthesis of topologically non-trivial nanoribbons	54
References.....	57
Chapter 2: Synthesis of topologically non-trivial macrocycles	61
I. Introduction	61
II. Synthetic strategy involving two bifunctional building blocks	63
a. Synthesis of building blocks	63
b. Macrocyclization in stoichiometric conditions	66
III. Synthesis of the macrocycles through controlled assembly	68
a. Synthesis of the monoprotected building blocks	68
b. Synthesis of the trimer with acetic acid functions	72
c. Synthesis of the flexible intermediate functionalized with glyoxylic acids	73
d. Toward the synthesis of the macrocycles.....	74
Conclusion	81

References.....	82
Chapter 3: Phenanthrocyclophanes	83
I. Introduction	83
II. Microcycles: naphthalenophenanthrocyclophanes	84
III. Phenanthroparacyclophanes and substituted coronenes.....	94
a. Synthesis of macrocycles with a D_{2h} symmetry.....	94
b. Synthesis of an asymmetric coronene.....	98
c. Synthesis of macrocycles with a D_{3h} symmetry.....	100
Conclusion	102
References.....	103
Chapter 4: Macrocyclic hexamer of phenanthrenes	105
I. Introduction	105
II. Capping a brominated trimer with Suzuki-Miyaura coupling.....	108
a. Presentation of the strategy	108
b. Synthesis of the building blocks.....	109
III. Controlled assembly of monoprotected building blocks.....	112
a. Synthesis of the building blocks.....	112
b. Synthesis of the complementary trimers	114
c. Synthesis of the macrocycles.....	117
Conclusion	119
References.....	120
General conclusion	123
Experimental Part	125
General.....	125
Synthetic procedures	126
Chapter 2:	126
Chapter 3:	138
Chapter 4:	144
Crystallographic Data	152
Single crystal X-ray diffraction.....	152
References.....	154

Je me souviens d'un appel téléphonique passé en 2021 pour postuler à une thèse sur la synthèse de nanorubans topologiquement non triviaux. Alors que mon interlocuteur me présentait la longue synthèse nécessaire pour obtenir les produits, je me souviens avoir dit : « 3 ans c'est long il y aura le temps ». Sache Fabien tu avais raison, c'est super court en fait.

Tout d'abord je souhaite remercier une dernière fois les membres du jury pour avoir pris le temps de lire mon manuscrit et d'assister à ma soutenance de thèse.

Merci au personnel administratif du CRPP : Emilie, Béatrice, Eva, Corinne et Caroline. Vous m'avez accueilli dans le laboratoire, vous m'avez aidé avec les (nombreuses) tâches administratives, les ordres de missions, les avenants de contrats... Merci à toi Cécile pour tout ce que tu réalises en tant que directrice du laboratoire, tu es à l'écoute des doctorants et tu te bats pour que les conditions dans lesquelles nous réalisons notre thèse soient idéales. Lorsque j'ai postulé à la bourse JSPS, tu as pris le temps de m'écrire une recommandation pour mon dossier, lorsque j'ai formé mon jury de thèse, tu as accepté d'en faire partie et de lire mon manuscrit.

A tous les membres de l'équipe M3, passés et présents, merci. Ludmilla tu as pris le temps de me montrer les ficelles du laboratoire quand je suis arrivé. Fred j'ai passé des moments excellents dans le labo avec toi. On venait du même endroit et on avait les mêmes délires. Je pense aussi à Katia, Mengting, Vincent, Jouke, Dandan, Abhijit, Hugo, Fabricia, Gabi, Wilson, Monike et Jiri pour les moments partagés au cours des trois dernières années. Merci Xavier pour les discussions entre deux manips, ton aide sur la RMN qui tombe en panne tous les trois mois et les commandes de produits, Mathieu pour ton aide quand j'avais des problèmes avec certaines machines. Pierre, grâce à toi j'ai pu obtenir de magnifiques structures RX pour mes produits et je t'en remercie. Merci à toi Corine pour ton aide et le côté administratif de la thèse, Rodolphe pour nos discussions scientifiques, ce que tu fais pour l'équipe et pour m'avoir encouragé à sortir de ma zone de confort pendant ma thèse et pour la suite de ma carrière. Enfin Harald et Andrej, pour toute votre aide et vos précieux conseils pendant ces trois dernières années. Harald, je ne saurai jamais assez te remercier pour avoir pris le temps de relire tous mes chapitres, la rédaction du ChemComm, les repas chez toi et les petites discussions dans ton labo quand la GPC tournait.

Au cours de ma thèse j'ai aussi pu encadrer d'incroyables stagiaires dont Loonis, Elsa et Youssef. Je voudrais vous remercier pour l'aide que vous m'avez apportée pendant ces stages. Cela a été un plaisir de travailler avec vous et de vous encadrer. Je vous souhaite la meilleure des réussites pour la suite de vos études !

J'aimerais remercier toute l'équipe OMC à l'Institut des Sciences Chimiques de Rennes pour leur accueil chaleureux et plus particulièrement Ludovic Favereau pour avoir accepté de tout m'apprendre sur les mesures chiroptiques et photophysiques de composés luminescents.

Un remerciement particulier à ma famille pour leur soutien indéfectible. A mes parents, merci d'avoir cru en moi et de m'avoir donné les fondations nécessaires pour réussir. Merci à mes

amis alsaciens, Alex, Etienne, Xavier, Caitlyn, Maëva, Pierrick, avec qui j'ai gardé contact pour m'avoir soutenu à distance et le temps de quelques visites à Strasbourg.

Quand j'ai commencé ma thèse au CRPP, je faisais partie d'un groupe d'une dizaine de nouveaux doctorants, venant de partout en France. On s'est pour la plupart retrouvé dans un nouvel environnement avec des projets exigeants. Au fil des ans de nouvelles personnes nous rejoignaient. On s'est rapproché et on a partagé des moments incroyables pendant ces trois ans. Elodie, Auriane, Ludovic, Antoine V., Clément, Luna (et Ilan !), Ilies, Romain, Camille, Mathieu, Antoine B., Marion, Gaby, Antonin et tous ceux que j'ai oubliés : merci pour ces trois ans. Merci pour votre soutien, pour tous ces moments passés ensemble. Que ça soit autour d'un verre, d'un café, d'un jeu de cartes, à la salle d'escalade, j'ai apprécié chaque moment passé avec vous et je chérirai ces souvenirs très longtemps. J'ai été très heureux de tous vous rencontrer et partager cette expérience avec vous.

Pour finir, si j'ai pu faire cette thèse dans d'aussi bonnes conditions, c'est aussi en grande partie grâce à toi Fabien. Quand on s'est appelé pour la première fois pour discuter de la thèse, j'ai tout de suite senti qu'on était sur la même page : les défis de synthèses, obtenir des structures uniques : faire de la belle chimie. On a souvent rigolé du fait que dans la recherche il faut souvent une grande part de chance : je pense que la plus grande chance que j'ai eu c'est de pouvoir faire cette thèse sous ta supervision. Pour moi, ça a tout de suite cliqué : ta gentillesse, ton humour, ta passion pour la chimie ; je pouvais discuter de tout avec toi. Surtout, tu m'as laissé beaucoup de liberté pendant cette thèse, tout en me supportant au maximum. Que ça soit pour les stratégies de synthèse, pour proposer de petits side-projects, les conférences, le jury de thèse et surtout pour la suite de ma carrière au Japon, tu m'as toujours supporté dans tous mes projets. Plus que tout, j'ai adoré l'autonomie dont je disposais, tant au laboratoire que dans l'organisation de ma thèse. Cette thèse, elle a eu des bas, mais elle a eu des très haut aussi. Cette thèse, c'était un défi de synthèse, c'était un défi humain mais si je devais la refaire depuis le début avec les mêmes choix, je le referais sans hésiter. Merci pour cette thèse, merci pour cette formidable expérience, merci pour ton accompagnement incroyable, ta bienveillance, ton support. C'est peut-être la fin de mon séjour à Bordeaux mais j'espère pouvoir te recroiser à de multiples occasions.

A vous tous, pour ces trois incroyables années,

Merci

Abbreviations

ACID: Anisotropy of the Induced Current Density

AcOEt: ethyl acetate

COSY: Correlation Spectroscopy

CNB: Carbon Nanobelt

CNT: Carbon Nanotube

CPL: Circularly Polarized Luminescence

CPP: Cycloparaphenylene

DBU: 1,8-diazabicyclo[5.4.0]undec-7-ene

DCM: dichloromethane

DMF: dimethylformamide

DMSO: dimethyl sulfoxide

ECD: Electronic Circular Dichroism

eq.: equivalent

GPC: Gel Permeation Chromatography

GNB: Graphene Nanobelt

GNR: Graphene Nanoribbon

PAHs: polycyclic aromatic hydrocarbons

PACs: polycyclic aromatic compounds

h.d.: high dilution

M: molar, mol/L

MIMA: Mechanically interlocked molecular architecture

MS: Mass Spectrometry

MWCNT: Multi-Walled Carbon Nanotube

NMR: Nuclear Magnetic Resonance

rt: room temperature

SWCNT: Single-Walled Carbon Nanotube

TADF: Thermally Activated Delayed Fluorescence

THF: tetrahydrofurane

UV-vis: ultraviolet-visible

XRD: X-Ray Diffraction

Résumé

Introduction

La synthèse de macrocycles conjugués à partir de fragments aromatiques polycycliques a fait l'objet de recherches approfondies au cours des dernières décennies en raison de leurs structures et propriétés physiques inhabituelles. Notre équipe a développé une voie de synthèse pour la formation de nouveaux composés aromatiques polycycliques carboxy-substitués basée sur une version modifiée de la réaction historique de Perkin. Cette stratégie permet la formation d'une grande variété de molécules conjuguées, linéaires ou ramifiées, planes ou torsadées, et s'est même révélée très efficace pour la formation de composés macrocycliques. Les techniques de protection et de déprotection mises au point permettent d'assembler de manière contrôlée un grand nombre d'éléments et de concevoir des molécules aux formes de plus en plus atypiques. Au cours des dernières années, notre groupe a développé la synthèse de cyclo-poly-[5]hélécènes avec des formes persistantes de figure-de-huit ou de rubans de Möbius. Toutefois, malgré leurs géométries similaires à celles de rubans cycliques torsadés, ces composés ne peuvent pas être strictement considérés comme tels en raison des liaisons simples restantes reliant les fragments [5]hélécènes entre eux. Les stratégies de synthèse existantes ont été adaptées pour aboutir à la conception d'équivalents entièrement condensés de ces poly-[5]hélécènes macrocycliques, qui présenteraient alors des topologies non triviales de nanorubans torsadés. Nous rapportons dans ce manuscrit les différentes approches tentées pour la synthèse de ces nouvelles structures moléculaires.

En utilisant des briques élémentaires bifonctionnelles à base de phénanthrène et de naphthalène, les réactions de macrocyclisation n'ont pas conduit aux composés attendus, mais plutôt à des macrocycles à deux éléments seulement. Ces macrocycles plus courts et tendus ont été obtenus sous forme de mélanges racémiques de produits très énantiostables, en raison de la proximité étroite entre les deux parties aromatiques orthogonales. Les énantiomères ont été séparés par HPLC chirale et leurs propriétés photophysiques et chiroptiques ont été étudiées. Des recherches complémentaires ont conduit à la formation de phénanthrocyclophanes, des macrocycles impliquant un phénanthrène et un benzène, utilisés ensuite pour la formation photochimique de coronènes fonctionnalisés. D'autres approches synthétiques basées sur l'assemblage contrôlé des briques élémentaires ont été explorées. En utilisant des éléments bifonctionnels monoprotégés, deux précurseurs flexibles complémentaires furent envisagés. Le premier est composé d'un phénanthrène central substitué par deux unités naphthalènes monoprotégées. Une fois déprotégé, ce précurseur flexible peut réagir par réaction de Perkin dans des conditions de haute dilution avec un autre équivalent de phénanthrène bifonctionnel pour donner un précurseur flexible de nanoruban cyclique « Figure-de-8 ». Si en revanche ce précurseur était engagé avec son homologue complémentaire, composé d'un naphthalène central et de deux phénanthrènes monoprotégés, cela pourrait conduire à la synthèse d'un nanoruban plus large avec trois torsions à 180° : un ruban de Möbius.

Résumé

Si la stratégie de Perkin nécessite seulement des composés acides aryles acétiques et acides aryles glyoxyliques, ces derniers ne sont pas toujours accessibles par voie commerciale. Notre groupe a donc mis en place une stratégie rapide et efficace permettant la synthèse des deux briques complémentaires à partir d'un seul composé aromatique dibromé. Une première réaction d'échange halogène-lithien permet de d'obtenir un composé dilithié qui peut réagir *in situ* avec un dialkoxyoxalate pour donner un diester aryle glyoxylique. Ce diester peut être saponifié en conditions douces pour donner la brique élémentaire diacide glyoxylique. Enfin ce diacide peut être réduit pour former la brique diacide acétique. Cette approche, appliquée à partir d'un 1,5- dibromonaphtalène, a permis d'obtenir la brique élémentaire naphthalène diacide acétique **II-3** (Figure 1).

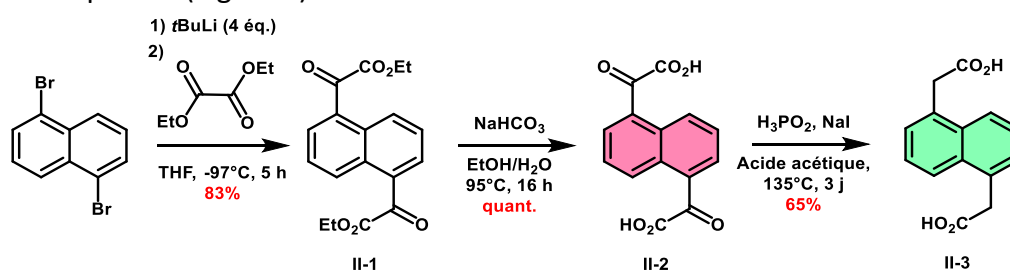


Figure 1. Synthèse du naphthalène diacide acétique.

Le 3,6-dibromophénanthrène, lui, n'est pas facilement disponible. La condensation du *p*-bromobenzaldéhyde en présence de zinc et de TiCl₄ permet d'obtenir un dibromostilbène. Ce dernier peut être transformé en 3,6-dibromophénanthrène grâce à une réaction de photocyclisation. Notre approche peut alors être utilisée et mène en deux étapes à la brique élémentaire phénanthrène diacide glyoxylique. Cette voie de synthèse est cependant limitée par l'étape de photocyclisation menant au dibromophénanthrène et la faible solubilité du diacide final. Une approche différente a donc été envisagée et un dérivé de diacide phénanthrène diglyoxylique a pu être synthétisé à partir de la 9,10-phénanthrènequinone. Ce réactif commercial est tout d'abord dibromé puis réduit en dibromobisalkoxyphénanthrène. Notre stratégie de synthèse mène ensuite à la formation de 9,10-dialkoxyphénanthrènes diacides glyoxyliques (Figure 2).

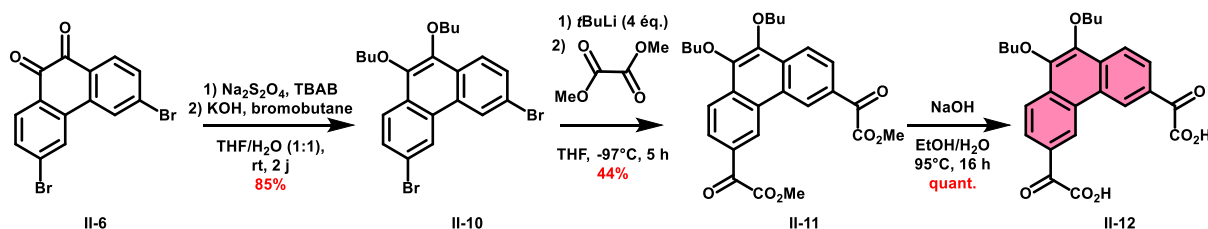


Figure 2. Synthèse du diacide bisbutyloxyphénanthrène diglyoxylique.

Une fois les deux précurseurs acides obtenus, ils ont été engagés dans une réaction de macrocyclisation dans des conditions stœchiométriques en haute dilution (Figure 3). Les conditions utilisées lors de cette réaction devaient mener aux précurseurs macrocycliques flexibles de la figure-de-huit (cyclisation 2+2) et du ruban de Möbius (cyclisation 3+3) lors de

la même réaction. Cependant un seul produit de macrocyclisation a été isolé à la fin de celle-ci. Les analyses RMN ^1H et HRMS réalisées sur le composé isolé ont permis de déterminer que celui-ci correspondait en fait à un macrocycle **II-13** à deux unités seulement (cyclisation 1+1).

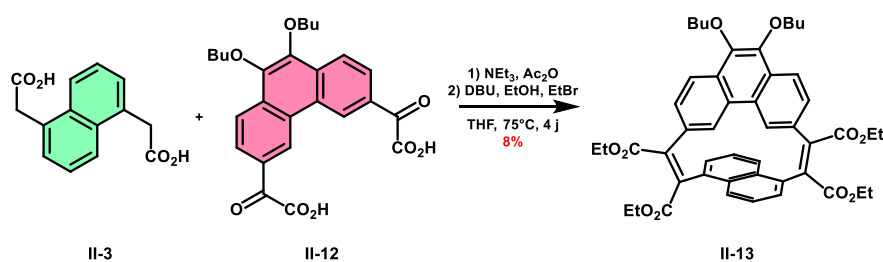


Figure 3. Synthèse du phénanthrocyclophanediène.

Malgré différentes modifications du protocole expérimental, cette réaction n'a jamais mené à la formation de macrocycles flexibles à quatre ou six unités. La macrocyclisation dans des conditions stœchiométriques de briques élémentaires diacides ne donnant pas les précurseurs flexibles désirés, une nouvelle stratégie de synthèse était nécessaire. Grâce à des techniques de protection, il est possible d'obtenir des briques élémentaires bifonctionnelles monoprotégées. Ces briques peuvent réagir avec des briques complémentaires pour former des intermédiaires flexibles et bifonctionnels par réaction de Perkin. Deux intermédiaires complémentaires peuvent ensuite être utilisés dans une réaction de macrocyclisation pour donner le macrocycle flexible précurseur du ruban de Möbius. Enfin, la réaction d'un de ces intermédiaires avec la brique élémentaire complémentaire manquante peut mener à la formation du macrocycle flexible précurseur de la figure-de-huit (Figure 4).

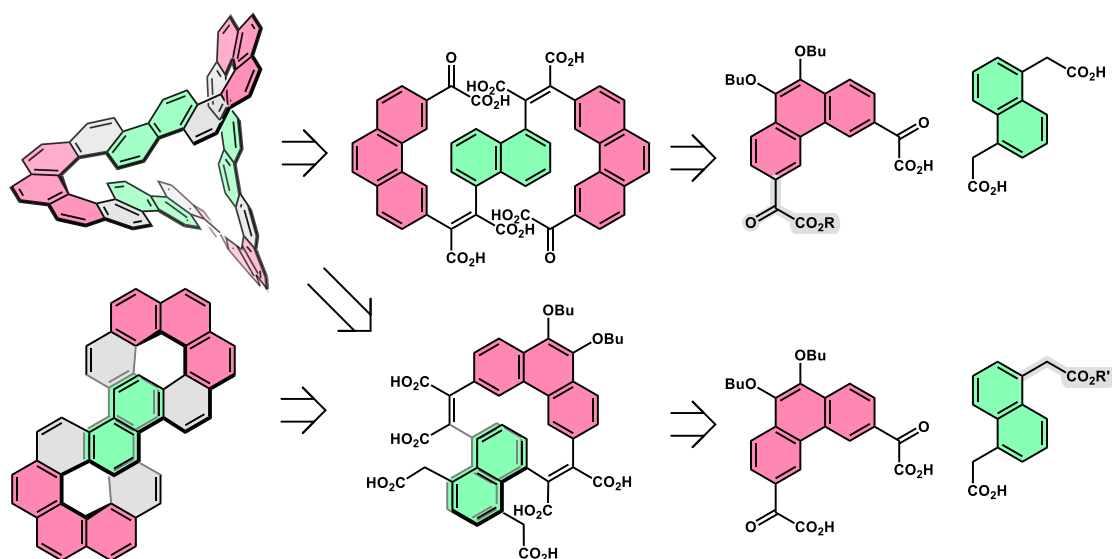


Figure 4. Approche synthétique reposant sur l'utilisation de briques élémentaires monoprotégées.

De manière similaire à la synthèse des briques élémentaires bifonctionnelles, une stratégie de synthèse et de purification de briques monoprotégées utilisables dans des réactions de Perkin a été mise au point dans notre équipe. Une brique diester glyoxylique ou acétique, préalablement synthétisée, est engagée dans une réaction de saponification en présence d'un équivalent de base. Une succession de filtrations à pH contrôlé permet de séparer les trois produits du mélange statistique ainsi obtenu (Figure 5). Si cette approche permet la synthèse

de nombreuses briques élémentaires monoprotégées, dont le 1,5-naphtalène diacide acétique monoprotégé **II-15**, elle ne permet toutefois pas la synthèse d'un phénanthrène diacide glyoxylique monoprotégé. Lors de la réaction de monosaponification du phénanthrène diester, un mélange comprenant seulement le diester et le diacide est étonnamment obtenu. Une approche alternative, basée sur la monoesterification d'un phénanthrène diacide glyoxylique à l'aide du diazométhane a donc été envisagée, sans succès.

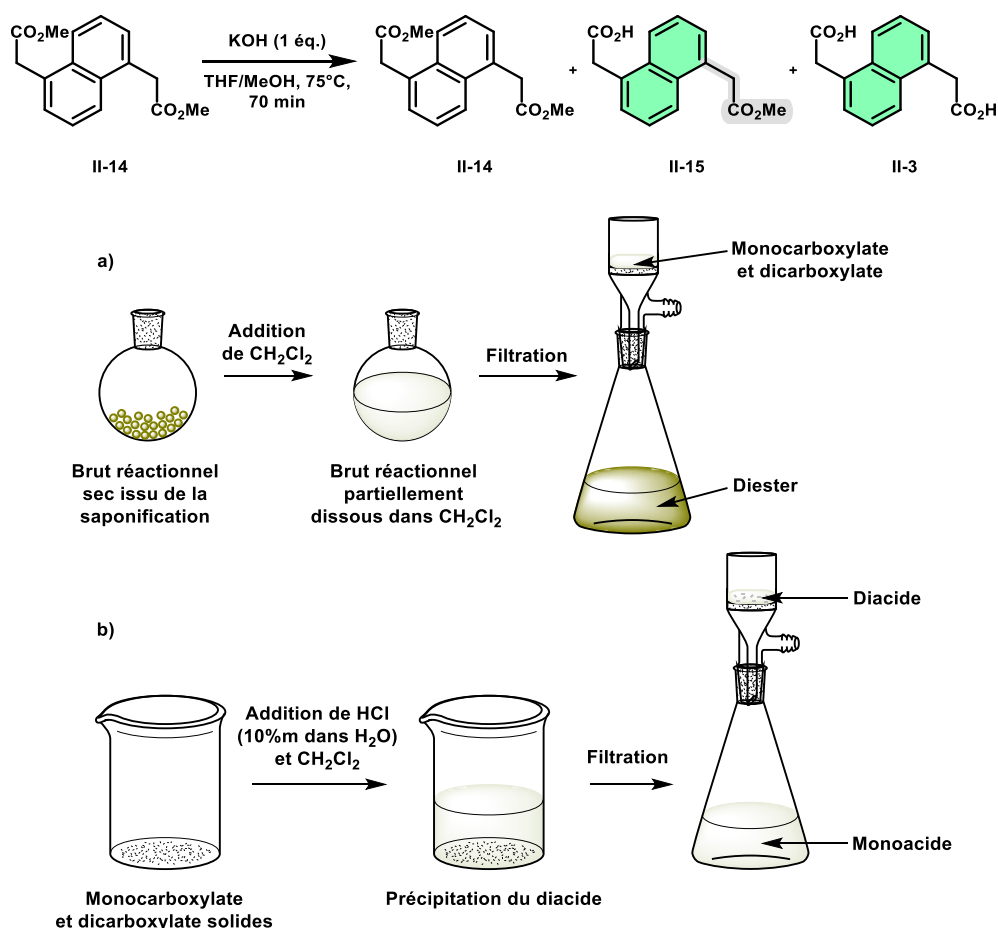


Figure 5. Synthèse et purification d'un naphtalène diacide acétique monoprotégé.

Avec seulement le 1,5-naphtalène diacide acétique monoprotégé, un seul des deux intermédiaires flexibles nécessaires pour cette seconde stratégie est accessible, limitant la synthèse des macrocycles au précurseur flexible de la figure-de-huit. Deux équivalents de naphtalène monoprotégé ont donc été engagés dans une réaction de Perkin avec un équivalent de phénanthrène diacide glyoxylique. Une fois la réaction terminée et traitée, la purification du produit par chromatographie sur colonne de gel de silice a permis d'isoler non seulement le produit désiré **II-17**, mais aussi le produit de condensation d'un phénanthrène avec un seul naphtalène monoprotégé **II-18** (Figure 6).

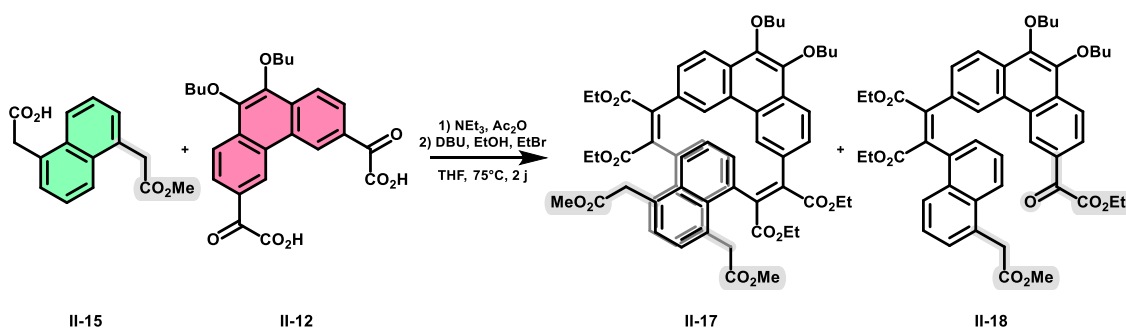


Figure 6. Synthèse des intermédiaires flexibles di- et mononaphthalènes.

Bien qu'inattendu, l'obtention de ce produit à deux unités présente un grand intérêt en termes de stratégie de synthèse en apportant une nouvelle approche pour la synthèse des macrocycles entièrement condensés. Celle-ci se base sur la photocyclisation du composé **II-18**, afin de bloquer la potentielle condensation intramoléculaire lors de la réaction de Perkin. La saponification du benzo-[5]hélécène obtenu permettrait d'obtenir un produit rigide, fonctionnalisé par une fonction acide acétique et une fonction acide glyoxylique. Cette brique pourrait enfin être utilisée dans une réaction de macrocyclisation pour d'obtenir un mélange de macrocycles 2+2 et 3+3 en partie rigidifiés. La synthèse du composé flexible a été optimisée et celui-ci a pu être rigidifié en benzo-[5]hélécène bifonctionnel. La saponification de ce dernier s'est malheureusement révélée très problématique et cette approche synthétique n'a pas pu être menée jusqu'au bout (Figure 7).

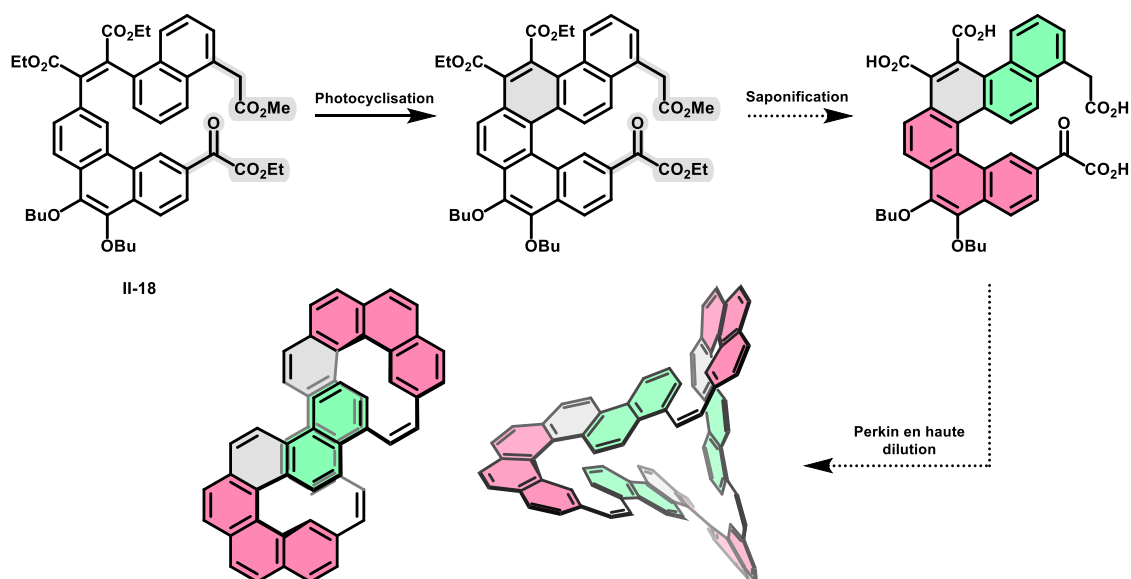


Figure 7. Approche alternative pour la synthèse de macrocycle entièrement condensés.

L'intermédiaire flexible **II-17** a été saponifié avec succès et engagé dans une réaction de macrocyclisation avec un équivalent de phénanthrène diacide glyoxylique. Malgré plusieurs tentatives, le macrocycle flexible attendu lors de cette réaction n'a pas été obtenu. Afin de favoriser la formation du macrocycle, en préorganisant les fonctions acétiques dans l'espace, le produit flexible **II-17** a été engagé dans une réaction de photocyclisation pour former un dibenzo-[7]hélécène fonctionnalisé par deux fonctions ester acétique **II-24**. De manière

surprenante, la saponification de ce produit n'a pas pu être réalisée (Figure 8a). En inversant les étapes, le dibenzo-[7]hélécène fonctionnalisé par des acides acétiques **II-25** peut cependant être obtenu à partir de l'intermédiaire flexible saponifié d'abord puis photocyclisé (Figure 8b). Le produit a effectivement été obtenu mais en faible quantité et avec de nombreux produits secondaires, identifiés comme étant des produits partiellement rigidifiés ou issus de transestérifications indésirables. Des conditions optimisées permettant la synthèse de ce précurseur rigide doivent encore être explorées. Une fois obtenu en quantité suffisante, ce dibenzo-[7]hélécène pourra être engagé dans une réaction de macrocyclisation menant à un précurseur partiellement rigide de macrocycle figure-de-huit.

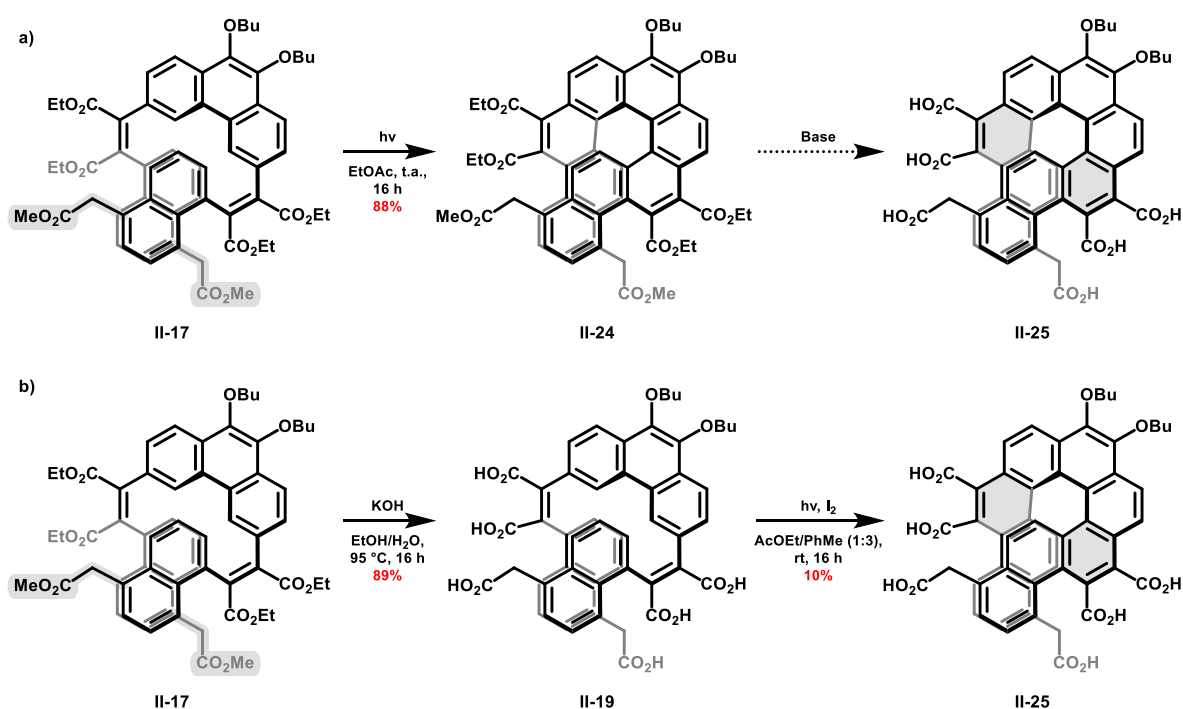


Figure 8. Synthèse du précurseur dibenzo-[7]hélécène **II-25**

Bien qu'inattendu, le macrocycle à deux unités **II-13** présente une structure assez intéressante : un phénanthrène et un naphthalène orthogonaux, liés entre eux par des ponts maléïques conjugués. Des monocristaux du produit ont permis d'obtenir une structure après analyse par diffraction des rayons X. La résolution de ces cristaux a confirmé la structure du macrocycle, obtenu comme mélange racémique de deux énantiomères. En raison de la faible distance entre le phénanthrène et le naphthalène, la rotation de ce dernier est impossible et ce produit est donc parfaitement énantiostable (Figure 9).

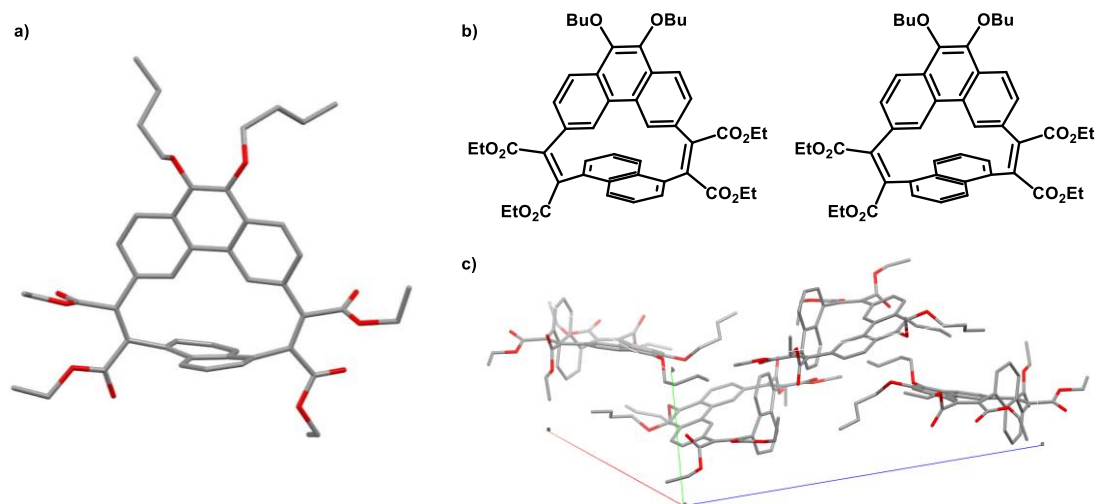


Figure 9. Structure obtenue par diffraction des rayons X de macrocycle à deux unités II-13 et représentation de ses deux énantiomères.

Grâce à la versatilité de notre approche, une famille de quatre macrocycle a été synthétisée. Les énantiomères ont été ensuite séparés par HPLC chirale avec l'aide de notre collaborateur Dr. Michal Šámal (IOCB, Prague). Une seconde collaboration avec le Dr. Ludovic Favereau (ISCR, Rennes) a permis de mesurer les propriétés photophysiques et chiroptiques de ces composés. Ceux-ci se sont révélés être fluorescents à température ambiante, avec une exception pour le composé fonctionnalisé par des imides cycliques qui présente une luminescence retardée à température ambiante. Des mesures et calculs complémentaires sont cependant nécessaires pour déterminer la nature de cette émission retardée. Les mesures de dichroïsme électronique circulaire et de luminescence polarisée circulairement ont pu être effectuées. Les spectres obtenus, opposés pour chaque paire d'énantiomères, ont ensuite permis de déterminer les facteurs de dissymétrie g_{lum} et g_{abs} (Figure 10).

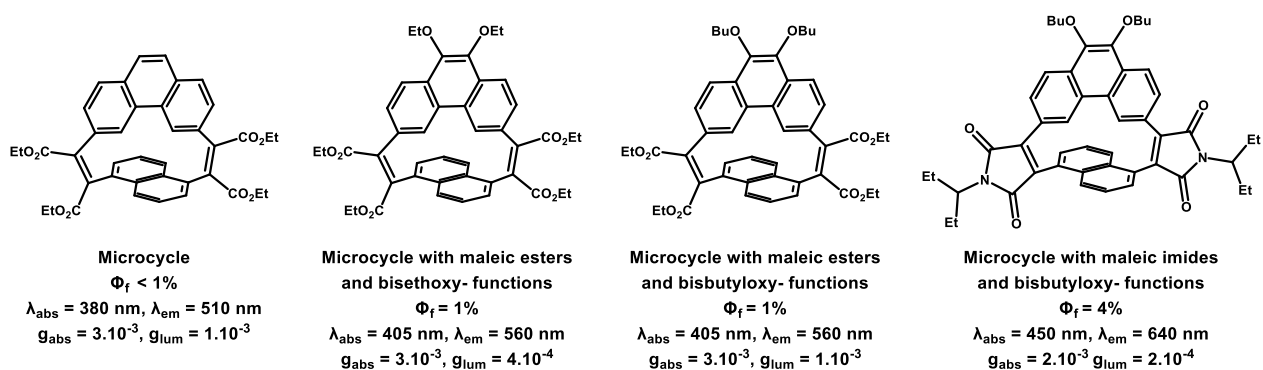


Figure 10. Macrocycles chiraux synthétisés et leurs propriétés photophysiques et chiroptiques.

L'utilisation d'une brique élémentaire 3,6-phénanthrène a permis d'obtenir de manière reproductible des macrocycles à deux unités en raison de l'angle entre les substituants sur le noyau aromatique. En appliquant la même approche synthétique mais en utilisant une brique *p*-phénylène à la place d'une brique 1,5-naphtalène, des macrocycles à deux unités mais moins tendus ont été obtenus. Ces macrocycles, cette fois-ci achiraux, ont pu être utilisés comme précurseurs flexibles menant à des coronènes tétra- ou hexa-fonctionnalisés. Trois

coronènes ont ainsi pu être synthétisés et des monocristaux de ceux substitués par des esters ont pu être obtenus, analysés par DRX, et leurs propriétés photophysiques ont été étudiées (Figure 11).

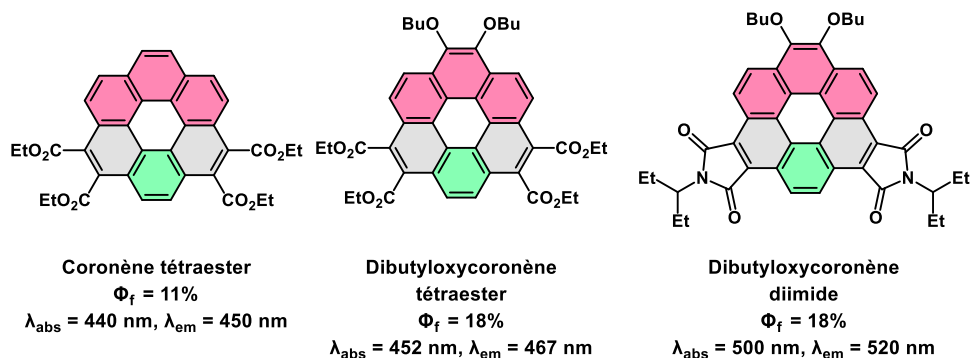


Figure 11. Coronènes fonctionnalisés et leurs propriétés photophysiques.

La synthèse du composé **II-18** a montré qu'il est possible d'obtenir des intermédiaires fonctionnalisés par un ester glyoxylique et un ester acétique. En utilisant cette méthode il serait alors possible de réaliser des synthèses de composés asymétriques, tel qu'un coronène hexafonctionné de manière symétrique mais par trois groupes différents. La synthèse de ce composé peut être imaginée à partir du bisbutyloxyphénanthrène diacide glyoxylique et d'un phénylène diacide acétique monoprotégé. La première étape serait une réaction de Perkin statistique entre ces deux précurseurs. Lors de cette étape, il est nécessaire de former un imide cyclique sur le pont maléique. En effet, une saponification de déprotection est nécessaire avant de passer à la suite de la synthèse. De récents résultats obtenus dans l'équipe ont montré qu'il était possible de saponifier sélectivement les fonctions esters sur un produit d'une réaction de Perkin sans affecter des imides cycliques. Ces conditions permettent de garder la fonction imide puis de former un second pont maléique fonctionnalisé avec des fonctions esters. Une photocyclisation de Mallory permettrait d'obtenir le coronène dissymétrique final (Figure 12).

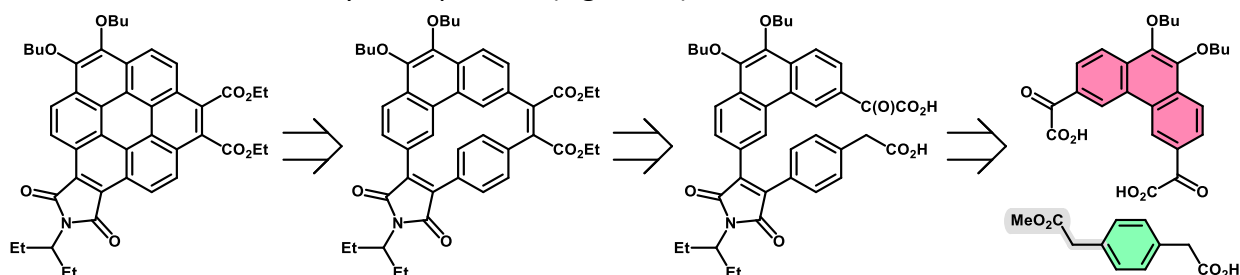


Figure 11. Rétrosynthèse d'un coronène asymétrique.

Plusieurs tentatives de réaction de Perkin statistique ont été tentées mais ont pour le moment donné les mêmes résultats : contrairement à la réaction conduisant à la formation d'un pont maléique fonctionnalisé par des esters, l'introduction du 3-aminopentane mène systématiquement à une décarboxylation de la fonction acide glyoxylique restée libre dans le produit de mono-condensation. Si l'on change les conditions afin d'avoir le même intermédiaire fonctionnalisé par des esters, celui-ci est bien formé sans que l'on observe de décarboxylation. L'utilisation du phénanthrène diglyoxylique monoprotégé permettrait de

réaliser cette synthèse beaucoup plus facilement et d'autres approches de synthèse sont actuellement étudiées dans ce but.

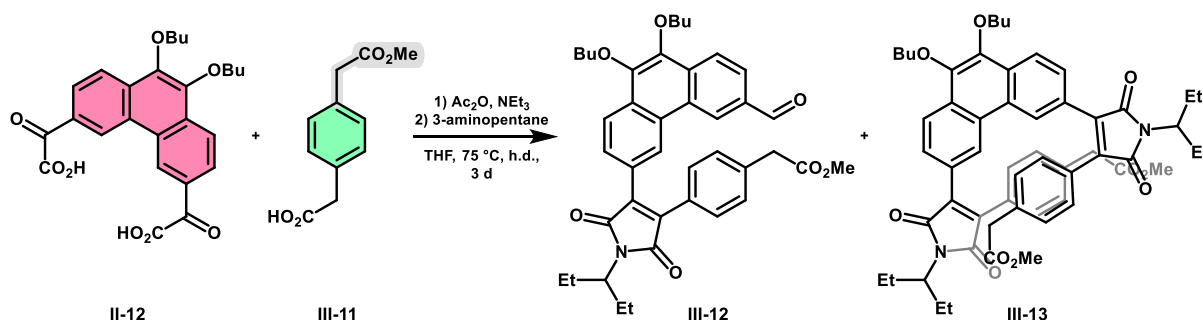


Figure 12. Tentative de synthèse d'un phénanthrène monosubstitué pour la synthèse d'un coronène asymétrique.

En parallèle de ces projets, un projet secondaire reposant sur la synthèse d'un macrocycle composé de six phénanthrènes liés entre eux par des liaisons simples a été mené. Ce projet s'inscrit dans la continuation des résultats obtenus en thèse par Antoine Robert, un précédent doctorant, avec la synthèse du tétramère macrocyclique de phénanthrènes. Antoine avait alors observé, lors de la purification d'un intermédiaire par chromatographie par exclusion stérique, la formation d'un produit secondaire qu'il a identifié comme étant la version hexamérique plutôt que tétramérique du macrocycle flexible. Des simulations ont montré que l'une des conformations stables de ce produit final rigidifié aurait la forme d'une figure-huit. Une première tentative de synthèse a été réalisée en utilisant un mélange stœchiométrique de biphényles diacides dans des conditions plus concentrées que celles utilisées par Antoine, pour favoriser la formation d'oligomères plus longs avant la cyclisation finale. Seuls des polymères linéaires ont été obtenus suite à cette tentative. Une seconde approche plus contrôlée a donc été tentée qui repose sur la réaction entre deux intermédiaires flexibles complémentaires issus de briques de type biphenyle monoprotégées (Figure 13).

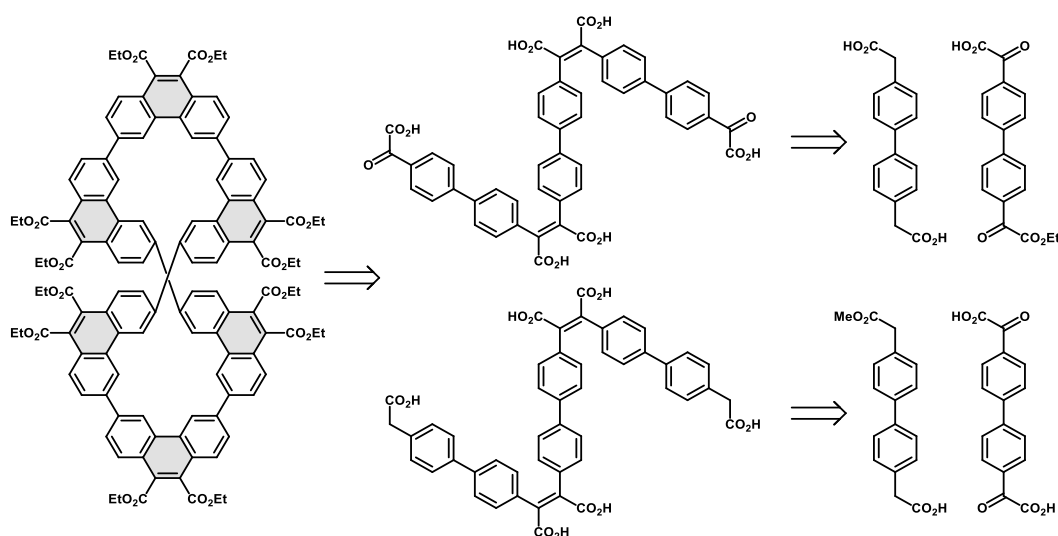


Figure 13. Rétrosynthèse de l'hexamère macrocyclique de phénanthrènes.

Deux stratégies de synthèse ont été pensées pour réaliser la synthèse des deux intermédiaires. La première consiste à synthétiser un précurseur commun grâce à une réaction de Perkin entre un 4,4'-biphényle diacide glyoxylique et un *p*-bromobenzène acide acétique. Le produit obtenu serait alors couplé à un benzène fonctionnalisé par un ester boronique et une fonction acide acétique ou glyoxylique pour former, au choix, les intermédiaires flexibles désirés. La synthèse du premier intermédiaire dibromé a été réalisée avec succès mais des saponifications indésirables lors de la seconde réaction de couplage, dues aux conditions basiques de la réaction de Suzuki-Miyaura, ont remis en question l'efficacité de la stratégie. L'approche habituelle de notre groupe, basée sur l'assemblage contrôlé de briques élémentaires, a donc été considérée. Les différentes briques nécessaires pour cette stratégie ont pu être synthétisées et utilisées dans des réactions de Perkin menant, après saponification, à l'obtention des deux intermédiaires flexibles et complémentaires.

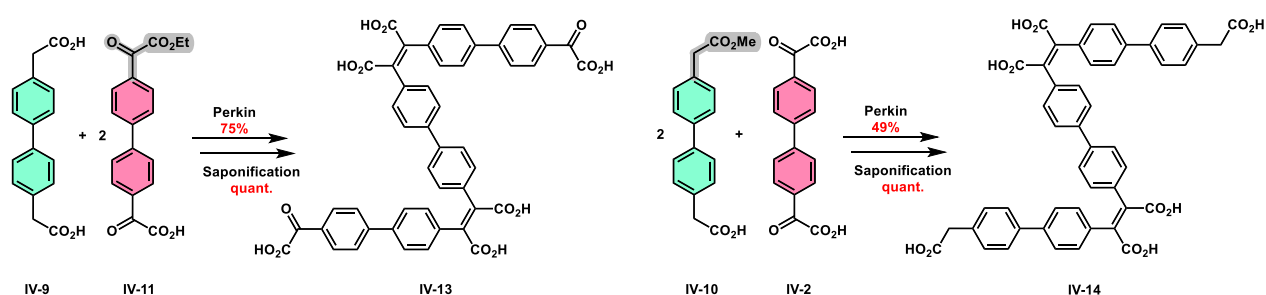


Figure 14. Synthèse des deux intermédiaires flexibles pour la synthèse d'un macrocyclique flexible de phénanthrènes.

Ces deux composés ont finalement été engagés dans une réaction de macrocyclisation pour donner un hexamère macrocyclique de biphényles. Après caractérisation, ce macrocycle a été engagé dans une réaction de photocyclisation pendant une nuit. Malheureusement, c'est un mélange de composés partiellement rigidifiés qui a été obtenu. Afin de favoriser la formation des liaisons C-C lors de cette étape finale, les esters lors de la réaction de Perkin ont été remplacés par des imides cycliques. Un second macrocycle flexible a ainsi pu être isolé mais cette fois la réaction de photocyclisation s'est montrée totalement inefficace : peu importe les conditions utilisées, le macrocycle ne subit aucune transformation.

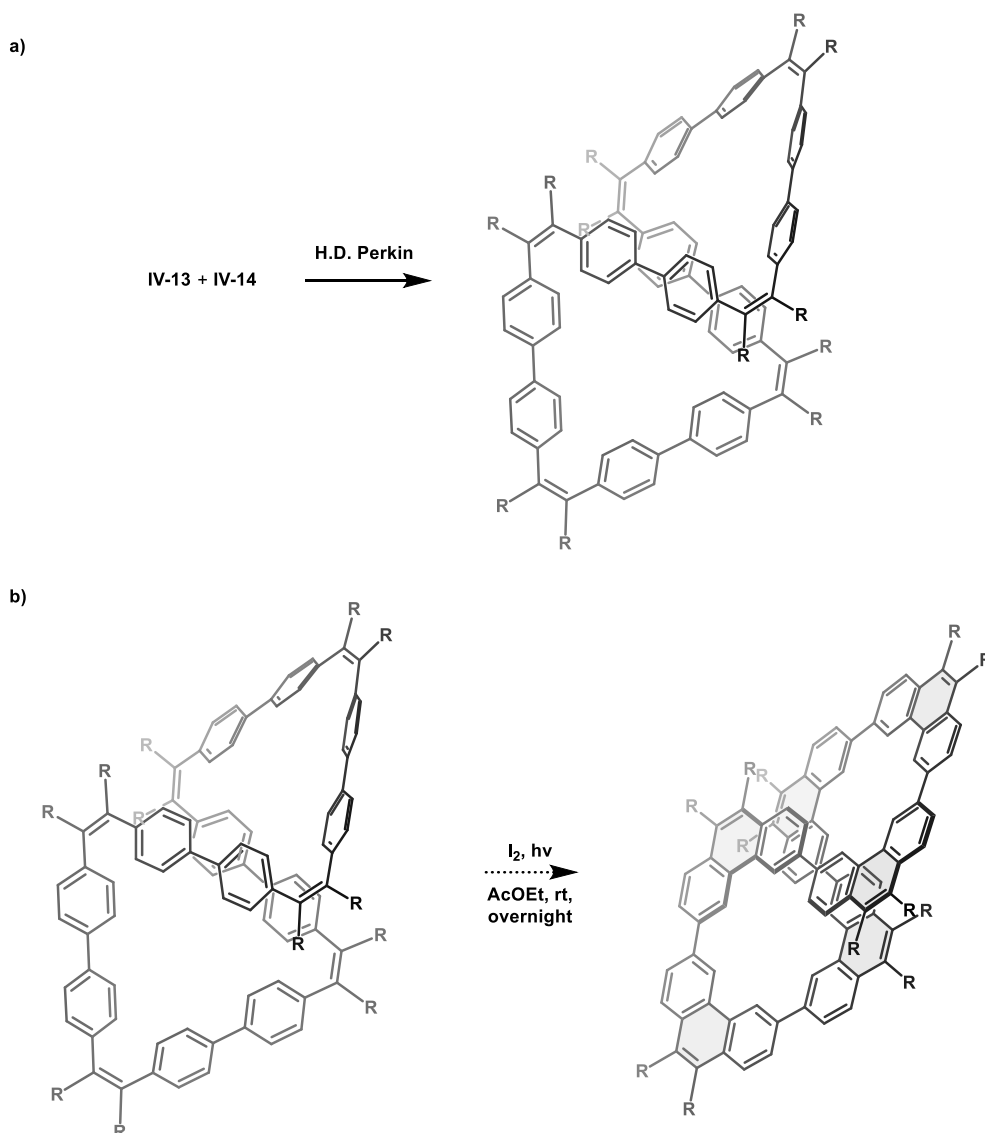


Figure 14. Synthèse d'hexamères macrocycliques de biphényles (a) et tentative de photocyclisation de ce dernier (b).

Conclusion générale

Au cours de la dernière décennie, la stratégie de synthèse développée dans notre groupe s'est avérée être un outil puissant et polyvalent pour la formation de composés aromatiques polycycliques de grande taille. Des intermédiaires conjugués flexibles sont d'abord formés par condensation de Perkin d'acides aryles glyoxyliques avec des acides aryles acétiques. Les intermédiaires flexibles obtenus peuvent ensuite être rigidifiés par différents moyens. Cette stratégie a conduit à la formation d'une grande variété de molécules conjuguées, linéaires ou ramifiées, plates ou torsadées, et s'est même avérée très efficace pour la formation de composés macrocycliques. De plus, des techniques de protection et de déprotection ont permis l'assemblage contrôlé des briques élémentaires. Cela a conduit à la synthèse de macrocycles aux structures atypiques telles que des polyhélicènes macrocycliques en forme de figure-de-huit ou de nanorubans de Möbius, et même un cyclophane ponté par trois [5]hélicènes. Parmi ces derniers exemples de macrocycles obtenus dans notre équipe, certains présentent des orbitales moléculaires dont la surface nodale est un ruban cyclique

de topologie non triviale. Ces particularités ne s'étendent cependant pas à la topologie des macrocycles eux-mêmes, car les liaisons simples reliant les parties [5]héliçènes permettent de dessiner ces macrocycles avec un graphe plan. Des macrocycles homologues entièrement condensés avec une topologie non triviale ont été conçus et de nouvelles stratégies de synthèse ont été adaptées.

Une première approche, s'appuyant sur deux briques élémentaires bifonctionnelles complémentaires à base de naphthalène et de phénanthrène, a été tentée. Cette méthode n'a pas conduit aux précurseurs flexibles à quatre unités souhaités de macrocycles topologiquement non triviaux mais, en raison de la géométrie du phénanthrène bifonctionnel, plutôt à un macrocycle de type cyclophane contenant seulement deux unités aromatiques orthogonales. Une deuxième approche, basée sur l'assemblage contrôlé du bon nombre de blocs de construction, a donc été envisagée. Deux précurseurs bifonctionnels flexibles complémentaires doivent être synthétisés et utilisés pour atteindre la formation de deux des macrocycles souhaités. Le phénanthrène monoprotégé n'ayant pu être obtenu, cette approche a été limitée à la synthèse du précurseur contenant un phénanthrène central et deux naphthalènes périphériques mais ce dernier n'a pas non plus abouti au précurseur du macrocycle en forme de huit après une réaction avec un autre équivalent du bloc de construction phénanthrène. Un équivalent hélicoïdal pré-rigidifié de ce précurseur a été conçu pour favoriser la formation du macrocycle cible, mais sa synthèse reste à optimiser.

Lors de la première approche pour la synthèse des macrocycles topologiquement non triviaux, plusieurs blocs de construction à base de phénanthrène bifonctionnalisés en 3,6 ont été synthétisés. En raison de la disposition en pince de leurs fonctions acide glyoxylique, la réaction de Perkin à haute dilution impliquant de tels composés et un autre équivalent de bloc de construction bifonctionnel a toujours conduit à des macrocycles contenant deux unités uniquement. Les macrocycles chiraux uniques obtenus en utilisant ces blocs de construction ont montré une énantio-stabilité infinie, en raison de leurs structures hautement contraintes. Leurs propriétés photophysiques et chiroptiques ont été étudiées et ont montré des facteurs de dissymétrie habituels en ECD et CPL, bien qu'avec de faibles rendements quantiques. Le remplacement du bloc de construction à base de naphthalène par un bloc de construction à base de phénylène plus court a conduit à des phénanthroparacyclophanes. Ces composés se sont avérés être de bons précurseurs pour la formation de coronènes tétra- et hexasubstitués fluorescents. Plusieurs approches pour la synthèse d'autres coronènes symétriques et asymétriques ont été testées mais sans succès.

Enfin, la synthèse ciblée d'un hexamère macrocyclique de phénanthrènes, observé par hasard dans notre groupe plusieurs années auparavant, a été tentée. Une première stratégie de synthèse, combinant les réactions de couplage de Perkin et de Suzuki-Miyaura, a été initialement étudiée mais la fragilité de l'ester, même dans des conditions faiblement basiques, a mis fin à cette voie. Une seconde approche, plus longue mais plus usuelle, a finalement été utilisée, avec des blocs de construction bifonctionnels et monoprotégés réagissant ensemble pour former des trimères flexibles complémentaires. Ces trimères ont été synthétisés et engagés ensemble dans une réaction de Perkin formant un macrocycle pour

donner un hexamère cyclique d'unités biphényles. La rigidification de ce macrocycle n'a cependant été que partielle. Un second macrocycle a donc été synthétisé, avec des imides cycliques sur les ponts maléiques. Ce second macrocycle s'est finalement avéré non réactif lors de la photocyclisation de Mallory. De nouvelles conditions de photocyclisation totale de l'ester fonctionnalisé devraient être trouvées et permettraient, espérons-le, d'obtenir un hexamère macrocyclique de phénanthrènes avec une conformation en forme de figure-de-huit.

A notre grand regret, les macrocycles de topologie non triviale n'ont pas pu être obtenus. Malgré de nombreuses difficultés inattendues, un intermédiaire dibenzo-[7]héliène fonctionnalisé par des acides acétiques a pu être synthétisé, bien qu'en quantité insuffisante pour poursuivre la synthèse. Le voie de synthèse menant à ce précurseur d'un macrocycle en forme de huit a cependant été tracée (à travers la sueur, les larmes et les solvants organiques). Des structures uniques, luminescentes, de type cyclophane ont été obtenues et caractérisées de manière inattendue. Finalement, deux précurseurs cycliques de macrocycles flexibles en forme de huit ont été obtenus.

Bien que les limites de la stratégie de synthèse développée par notre groupe aient commencé à apparaître, de nouveaux outils et opportunités de synthèse ont également émergé. Les phénanthrènes 3,6-disubstitués pourraient être utilisés comme éléments de base favorisant la formation de macrocycles à deux unités. Par la suite, le naphthalène peut être substitué par des naphthalènes fonctionnalisés ou des acènes plus longs, ou le phénanthrène peut également être remplacé par un autre noyau aromatique le même angle entre ses fonctions acides. Des résultats préliminaires ont également montré qu'il était possible d'effectuer la réduction glyoxylique en acétique sur des produits de la réaction de Perkin encore fonctionnalisés avec des acides glyoxyliques, afin de former leurs homologues acides acétiques. Ce résultat encourageant peut grandement faciliter certaines stratégies en permettant des synthèses plus convergentes. Enfin, des résultats antérieurs obtenus en laboratoire ont montré que la réaction de Perkin était compatible avec les noyaux aromatiques contenant des hétéroatomes, tels que les thiophènes et la pyrazine. L'inclusion de composés N-hétérocycliques tels que les bipyridines dans des produits Perkin flexibles pourrait conduire à des composés allostériques, ainsi qu'offrir une possibilité de rigidification réversible, contrôlée par métallation et démétallation.

Chapter 1: From allotropic forms of carbon to the synthesis of new forms of nanocarbons

I. Carbon and allotropy

a. Natural allotropes of carbon

Allotropy is defined as the ability of certain simple bodies to exist in several different crystalline or molecular forms. For example, oxygen exists in the form of dioxygen but also ozone O_3 . Carbon exists naturally in the form of amorphous carbon or in three crystallized forms. Diamond, a face-centered cubic crystalline form with half of the tetragonal sites occupied, is the best-known allotropic form of carbon (Figure 1a). Another known natural form of carbon is graphite, a superposition of graphene sheets composed of carbons coordinated to three others by sp^2 bonds (Figure 1b). Due to the superposition of the layers, it is an anisotropic material. Finally, lonsdaleite is another natural allotropic form of carbon, although much rarer. It is a hexagonal crystallographic structure composed of sp^3 carbon (Figure 1c), synthesized the year of its discovery under high pressure (13 GPa) at high temperature ($>1000\text{ }^\circ\text{C}$).¹

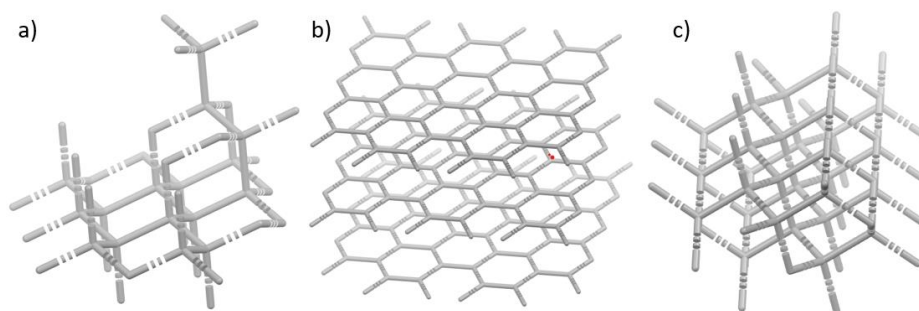


Figure 1. Unit cells representation of diamond (a), graphite (b) and lonsdaleite (c).

b. Synthetic allotropes of carbon

Synthetic allotropes of carbon also exist. Among them are fullerene, an allotropic form of carbon with a spherical and highly symmetrical shape and existing in several sizes. A particularly well-known member of this family is the first fullerene synthesized, C_{60} , dubbed *buckminsterfullerene* due to its resemblance to a football. It was synthesized in 1985 by the team of Kroto and Smalley by laser irradiation on graphite.² Fullerene C_{60} is a spherical molecule composed of sixty carbons linked together by sp^2 bonds and organized in six- or five-membered rings, responsible for the curvature of the molecule. The synthesis of C_{60} has been possible in large quantities (of the order of g/d) since 1990. The vaporization of graphite electrodes by an electric current under a helium atmosphere at low pressure gave fullerene C_{60} as the major product.³ Since these two innovations, several sizes of fullerene have been obtained, ranging from C_{20} , the smallest possible fullerene,^{4,5} to gigantic compounds such as C_{500} , observed by mass spectrometry (MS) and often obtained as poorly soluble isomeric mixtures (Figure 2).^{6,7} The synthesis and study of new fullerenes is an active area of research due to their electronic properties which makes them good candidates as an antimicrobial agent,⁸ in organic electronic compounds⁹ or in host/guest systems.^{10,11}

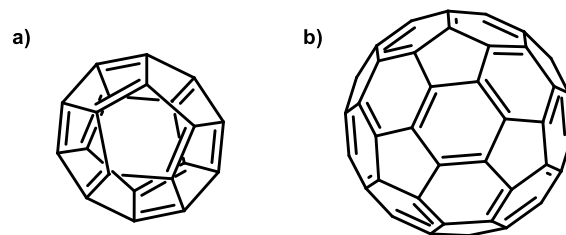


Figure 2. Fullerene C₂₀ (a) and buckminster fullerene C₆₀ (b).

The folding of a single sheet of graphene into a tube gives a new allotropic form of carbon called carbon nanotubes. The first major breakthrough in carbon nanotube research was made by Iijima and his team. During their research on fullerenes, the first example of a multi-walled carbon nanotube, abbreviated MWCNT, was obtained using a protocol similar to the one that gave fullerenes by electro-vaporization.¹² But carbon nanotubes are not limited to MWCNTs, various types of single-walled nanotubes also exist. These different types can be determined by representing the SWCNT by a sheet of graphene folded on itself. The way the sheet is folded gives a characteristic parameter, the chirality of the nanotube. The folding can be described by two directional vectors a_1 and a_2 (Figure 3). A third one, the chirality vector C_h , is then defined and can be decomposed in two components, depending on a_1 and a_2 , so $C_h = n.a_1 + m.a_2$. Three fundamental types of SWCNTs are obtained: zigzag nanotubes when $m = 0$, armchair nanotubes when $n = m$ and chiral nanotubes in all the other cases. The electronic properties are strongly linked to the chirality vector: all armchair nanotubes and those of the others where the difference between n and m is a multiple of three are metallic, the others are semiconducting.^{13,14} As materials, CNTs display extraordinary mechanical and physical properties: being extremely lightweight but with a high stiffness and tensile strength,¹⁵ they may be used as fiber sheets,¹⁶ transparent conductive films,¹⁷ or in biological sensors.¹⁸

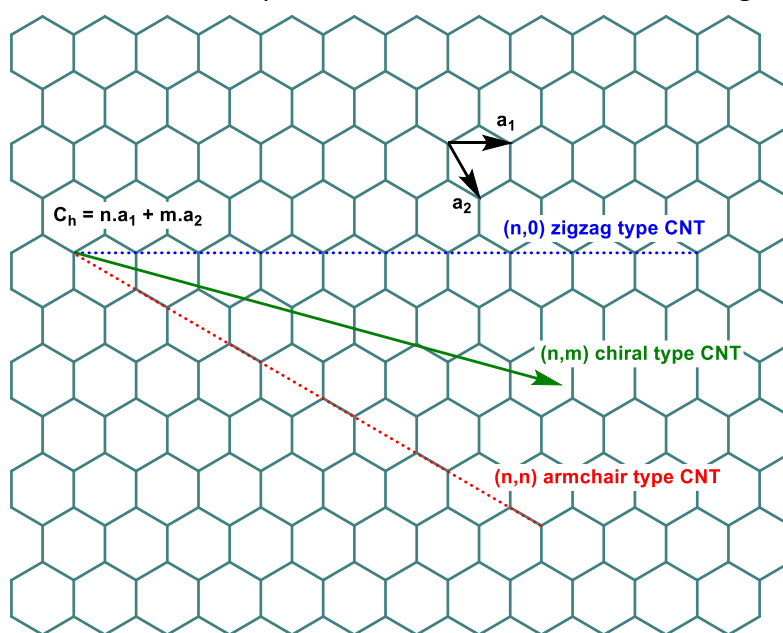


Figure 3. Representation of an unfolded carbon nanotube and the vectors characterizing the different types of CNTs.

Finally, graphene is another synthetic allotrope of carbon. It is a two-dimensional material composed of a single hexagonal layer of sp^2 carbons.¹⁹ Graphite is in reality a superposition of graphene sheets, and its mechanical exfoliation by Geim and Novolosev made possible the first isolation and characterization of graphene in 2004.²⁰ This discovery earned them a Nobel Prize in 2010 and launched a wave of research on this innovative subject. Interest in graphene grew such that in 2013, more than 16 000 articles on this field were published.²¹ The properties of graphene are indeed exceptional: thermal conduction (5000 W/cm/K),²² electrical conduction ($105 \text{ cm}^2/\text{V/s}$),²³ 200 times more resistant than steel;²⁴ graphene is a promising material, as well as its derivatives.²⁵ Graphene, however, has the disadvantage of having a band gap of 0 eV (i.e. being a metal),²⁶ which restricts its use in electronic materials despite its incredible conductivity. The use of destructive syntheses leads to nano-graphenes with non-zero band gaps, but such syntheses do not allow atomic level precision on the structure of the material.^{27,28} This is why one area of research focuses on the use of constructive synthesis methods to synthesize nanotube-like compounds with precise control over their structure and atomic composition.^{29,30}

II. Polycyclic aromatic compounds

a. Planar nanocarbons

The use of constructive synthesis techniques leads to graphene analogues with precise structures. Such an approach with structural control leads to carbon architectures with a modular bandgap. These “pieces” of graphene are called graphene nanoribbons or nanographenes.³¹ Lithography methods or opening of carbon nanotubes have been a method to obtain such compounds, but effective constructive synthesis techniques have long remained missing. It is only recently that numerous surface and solution synthesis strategies have enabled the targeted synthesis of nanographenes in an efficient manner. For example, Müllen and Fasel in 2010 report the synthesis of graphene nanoribbons from dibromoarene monomers on an Au(111) surface.³² This synthesis relies on thermal sublimation of the monomers on the metal surface, which will lead to dehalogenation and the formation of a diradical species that will polymerize. A final annealing at 400 °C or 440 °C leads to intramolecular cyclodehydrogenation and the formation of a linear graphene nanoribbon (Figure 4).

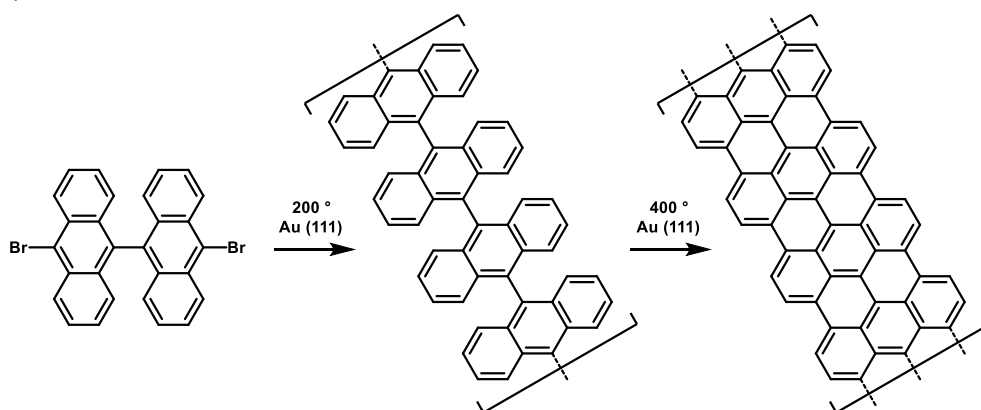


Figure 4. Surface assisted synthesis of $N = 7$ armchair type GNR on Au(111).

By using monomers of different shapes, it is possible to modify the structure of the nanoribbon and obtain chevron-type GNRs or obtain a junction of three GNRs (Figure 5). This revolutionary approach was later applied to obtain other forms of GNR.³³⁻³⁵

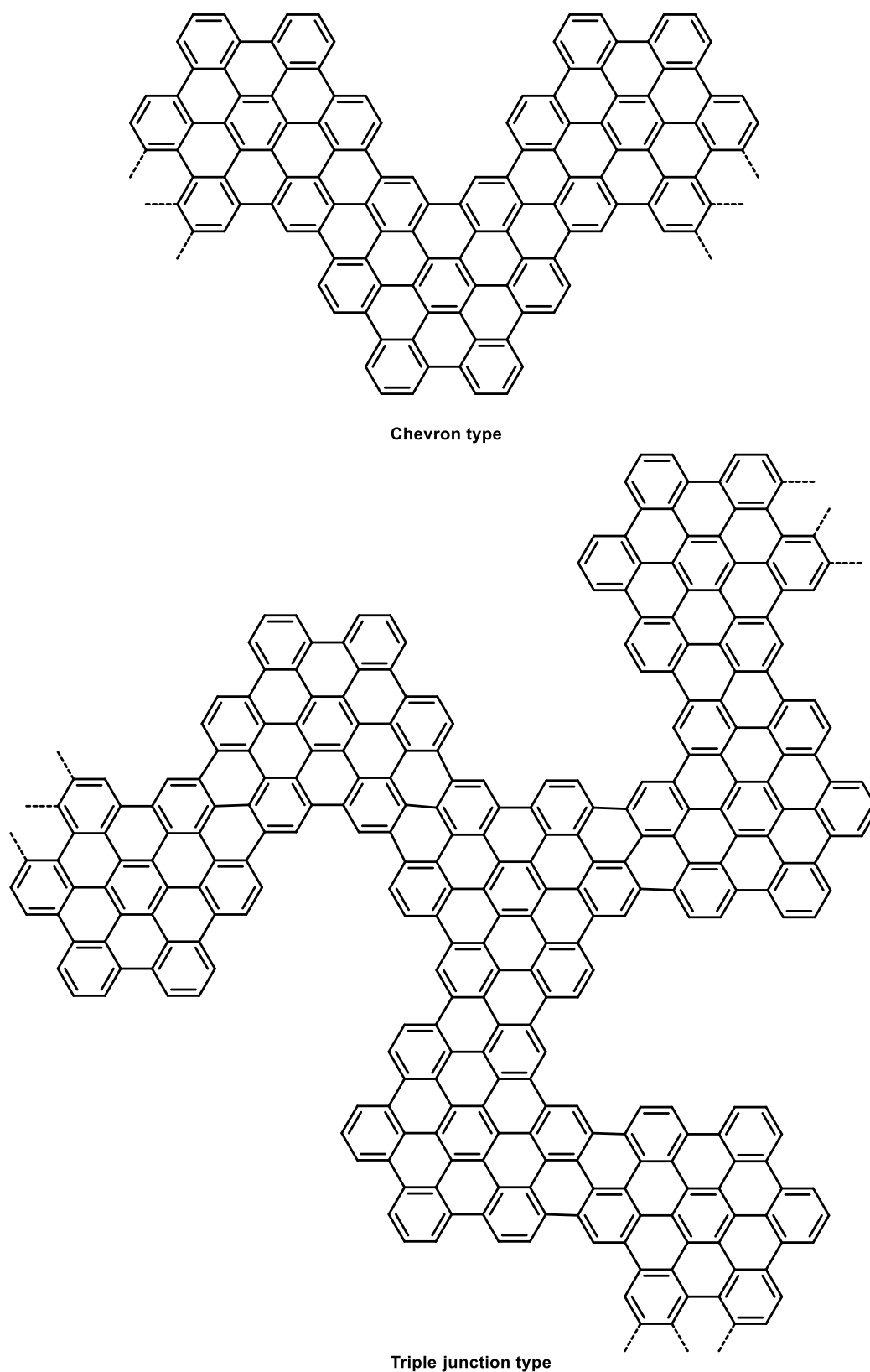


Figure 5. Chevron type GNR and junction of three GNRs accessible through the strategy of Müllen.

Following their work on aluminum surfaces, Amsharov's team developed another approach for precise on-surface synthesis of GNR. This synthesis, called HF zipping, is based on the fusion of cycles by activation of C-F bonds. This strategy allowed the synthesis of several GNRs on an aluminum surface,^{36,37} but also on a TiO₂ surface (Figure 6).³⁸

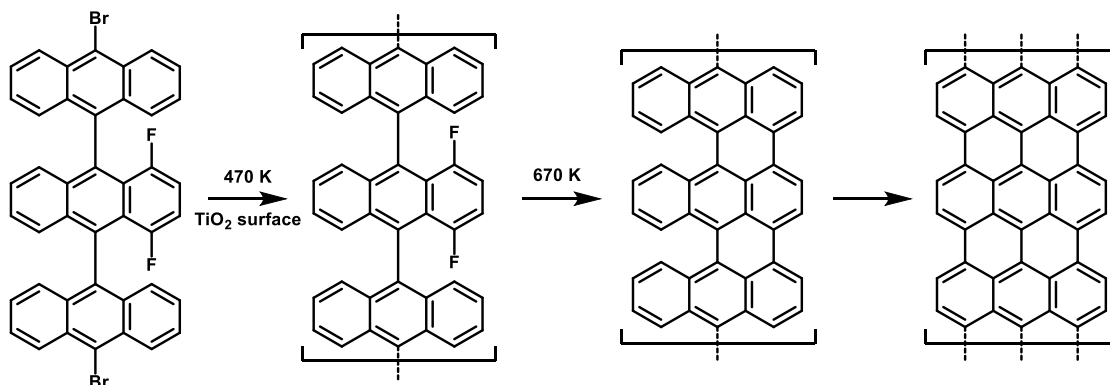


Figure 6. Surface assisted synthesis of $N = 7$ armchair type GNR by "HF-zipping" on TiO₂.

It is also possible to obtain GNRs with solid state chemistry techniques. Few examples are reported in the literature, but Rubin and his team described the synthesis of armchair type GNRs by light- or thermally induced topochemical polymerization in a diarylbutadiyne crystal. In this way, the synthesis of an armchair type GNR was obtained from topochemical polymerization of 1,4-bis(6-methoxy-methoxynaphthalen-2-yl)butadiyne (Figure 7).³⁹ Once the aryl-substituted polybutadiene obtained, treatment at 300 °C produced the GNR. This method allows the synthesis of GNRs without any solvent or oxidant. However, the distance and angles between molecules in the starting structure must be ideal to promote polymerization.

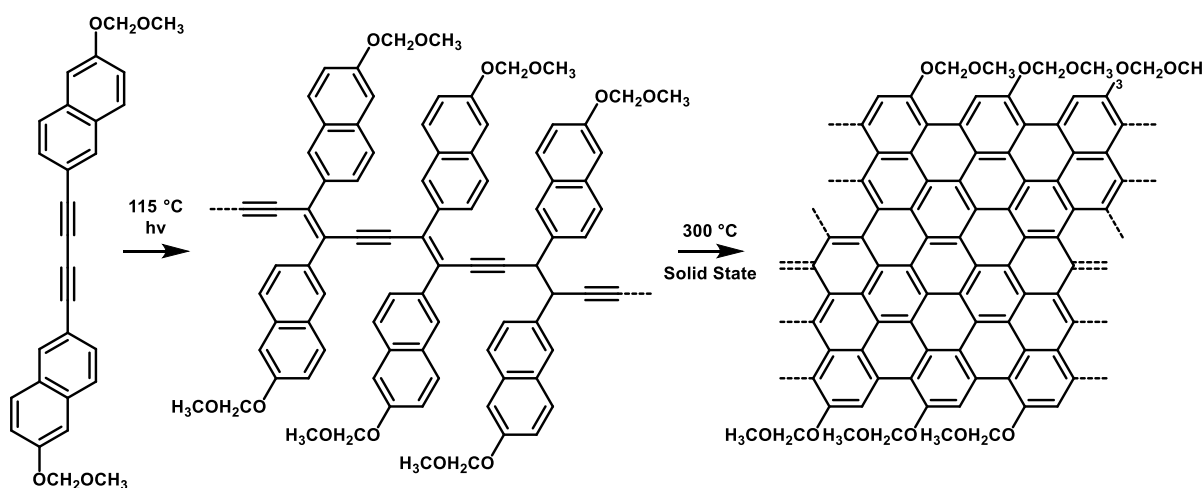


Figure 7. Solid state synthesis of $N = 12$ armchair type GNR by light- and thermal-induced polymerization in a crystal, followed by heating at 300 °C.

To overcome this problem, Rubin and his team decided to use butadiyne precursors functionalized with anilides (Figure 8).⁴⁰ The introduction of such functions allows the alignment of monomers in the crystal by hydrogen bonds. The amide functions are then

removed at high temperature (400-600°C). This strategy led to the synthesis of an armchair type GNR with $N = 8$, otherwise impossible to obtain with solution chemistry.

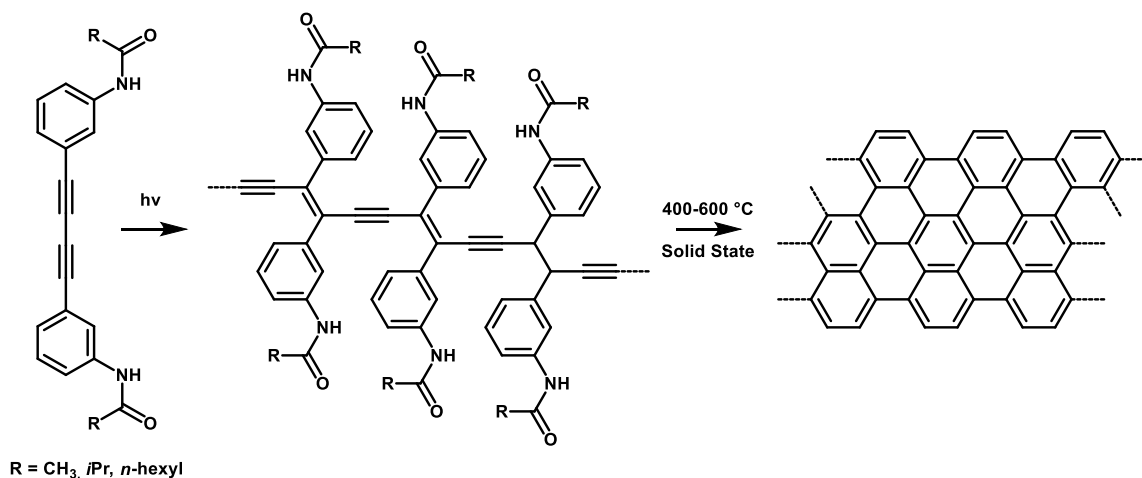


Figure 8. Solid state synthesis of $N = 12$ armchair type GNR by light -induced polymerization in a crystal, followed by heating at 400-600 °C.

In parallel to these approaches using surface chemistry, new solution chemistry synthesis techniques efficiently gave GNRs. The most common strategy used for the synthesis of GNRs in solution is to assemble several arene-functionalized monomers, then rigidify the resulting polyphenylene precursor in a cyclodehydrogenation reaction to give the corresponding GNR. Many examples of GNR formation in solution exist, but these syntheses often suffered from insufficient polymerization, poor solubility of the polymers and the presence of numerous defects. Nevertheless, in 2008 Müllen and his team reported the first solution synthesis of a soluble GNR.⁴¹ The copolymerization of 1,4-diiodo-2,3,4,5,6-tetraphenylbenzene and diboronic hexaphenylbenzene ester by Suzuki-Miyaura coupling followed by FeCl_3 -assisted cyclodehydrogenation forms the $N = 9$ armchair type GNR precisely (Figure 9). This is the first example of an armchair type GNR obtained by solution polymerization. The presence of long alkyl chains gives the ribbon excellent solubility in most organic solvents, allowing separation by size exclusion column and the measurement of relative molecular weights by mass spectrometry.

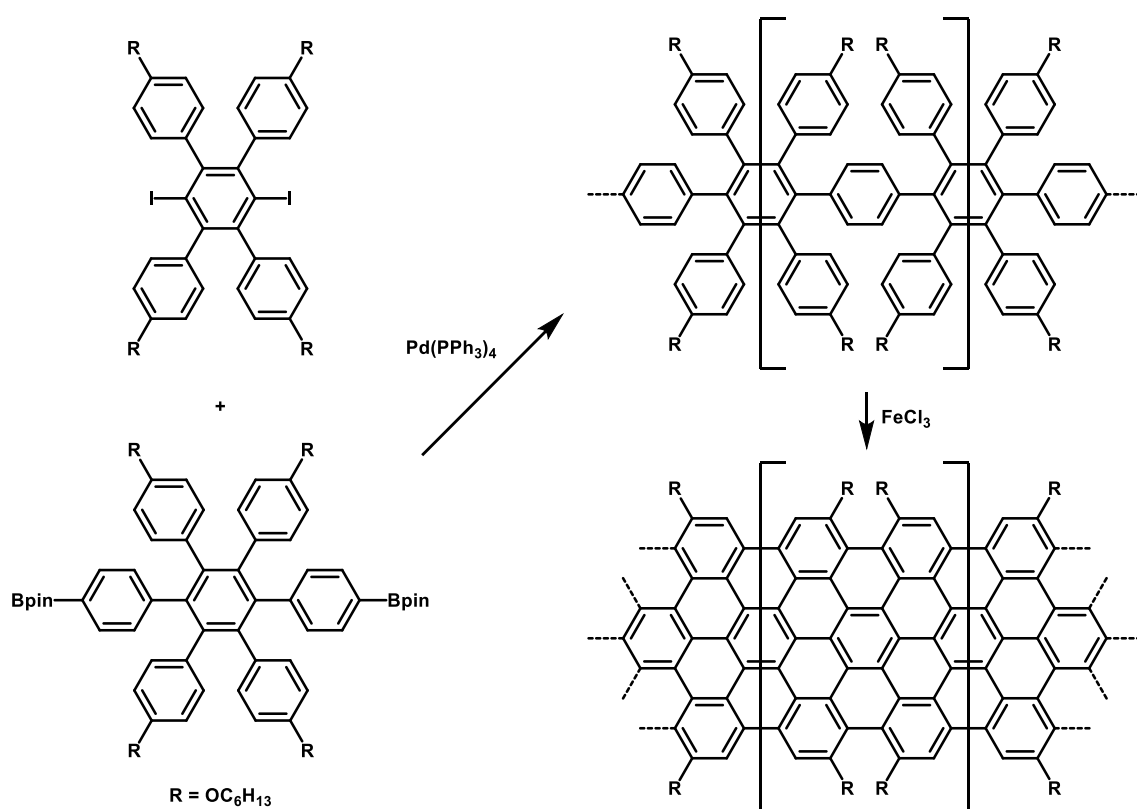


Figure 9. Solution synthesis of $N = 9$ armchair-type GNR through Suzuki-Miyaura coupling and FeCl_3 -mediated decyclohydrogenation.

The use of building blocks of different sizes by Jo and his team, such as phenyls and bifunctional naphthalenes, gave polybenzoiophenacenes (Figure 10) and polynaphtho-fused armchair type GNRs respectively.⁴²

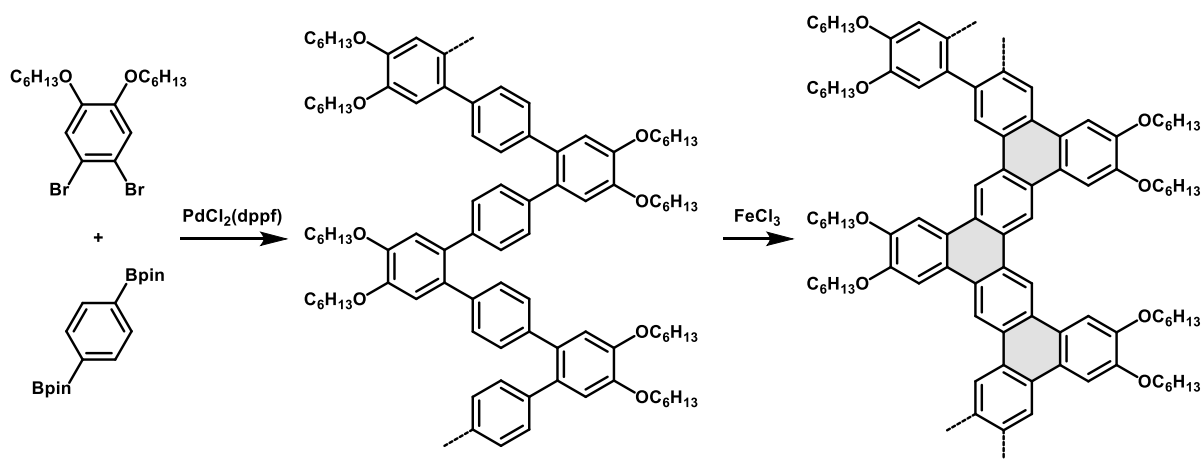


Figure 10. Solution synthesis of a polybenzoiophenacene via Suzuki-Miyaura coupling and FeCl_3 -mediated decyclohydrogenation.

Yamamoto coupling, forming single bonds between two sp^2 carbons using a $\text{Ni}(\text{cod})_2$ catalyst, is another coupling reaction commonly used for the synthesis of graphene nanoribbons in

solution. The first solution synthesis of a GNR obtained by Yamamoto coupling was described by Müllen in 2012.⁴³ This is based on the coupling of two dichloroarene monomers containing thirteen benzene rings, followed by cyclodehydrogenation to give a chiral GNR (Figure 11a). The length of the polymer obtained by this approach could not, however, be controlled. A chevron type GNR, similar to the one reported by Müllen (Figure 5), was obtained by Sinitskii by Yamamoto coupling,⁴⁴ but also by Fischer, by combining ring-opening alkyne metathesis polymerization (ROAMP) and the Diels-Alder reaction (Figure 11b).⁴⁵

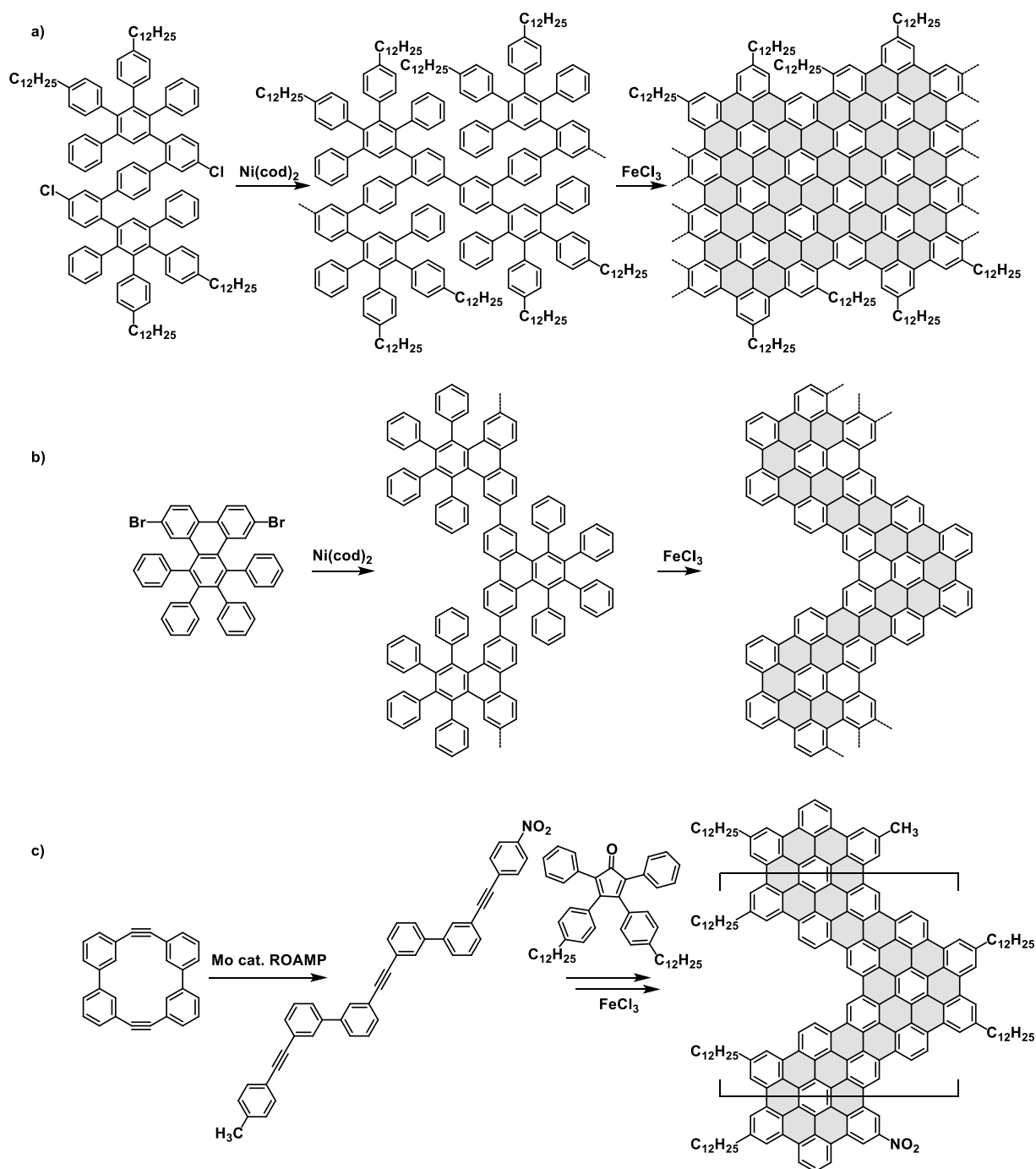


Figure 11. Synthesis of chiral-type (a), chevron-type GNR via Yamamoto coupling (b) and chevron-type GNR via ROAMP and Diels-Alder reactions (c).

b. 3D nanocarbons

Due to the sp^2 character of the carbons inside graphene, it is very often considered as a planar 2D material. Defects, such as five- or seven-membered rings, may however exist in the structure, creating deformations and influencing the electronic, optical and magnetic properties of the material.⁴⁶

Inspired by the structure of C_{60} fullerene, the replacement of benzene rings by five-membered rings creates deformations of nanographene and gives it a concave structure similar to a bowl. These “geodesic” nanocarbons have the particularity of copying the closed ends of carbon nanotubes. Corannulene, the smallest of the carbon nanobowls, was obtained by Barth and Lawton in 1966 by a multi-step synthesis from methyl 4,5-methylenephenanthrene-3-carboxylate (Figure 12).⁴⁷

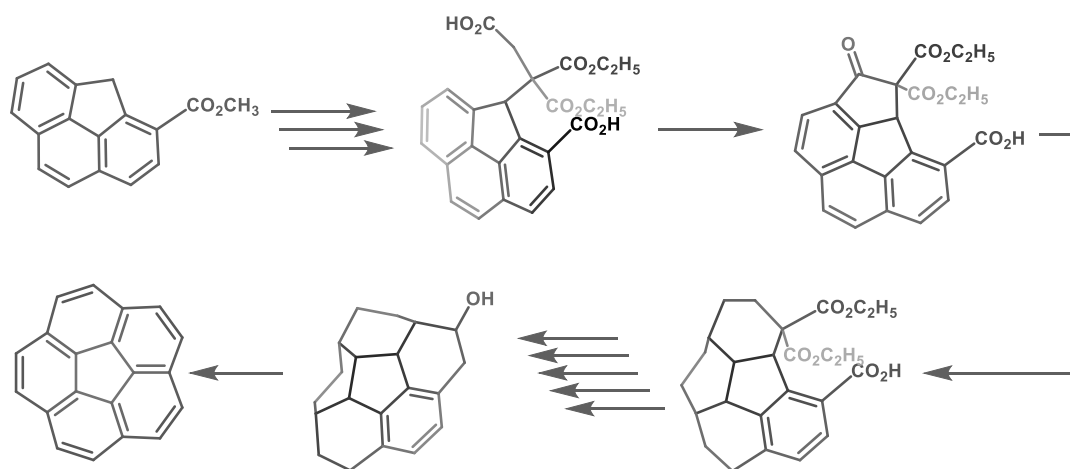


Figure 12. Synthesis of corannulene by Barth and Lawton.

In 2012, Scott and coworkers synthesized and characterized the end of a (5,5)NCT in 3 steps from corannulene using vacuum flash pyrolysis in a manner similar to the first synthesis of fullerene (Figure 13a).⁴⁸ This key synthesis was subsequently used as a starting point to form SWCNTs from this nanobowl,⁴⁹ and to obtain $C_{70}H_{20}$ carbon nanocones (Figure 13b).⁵⁰

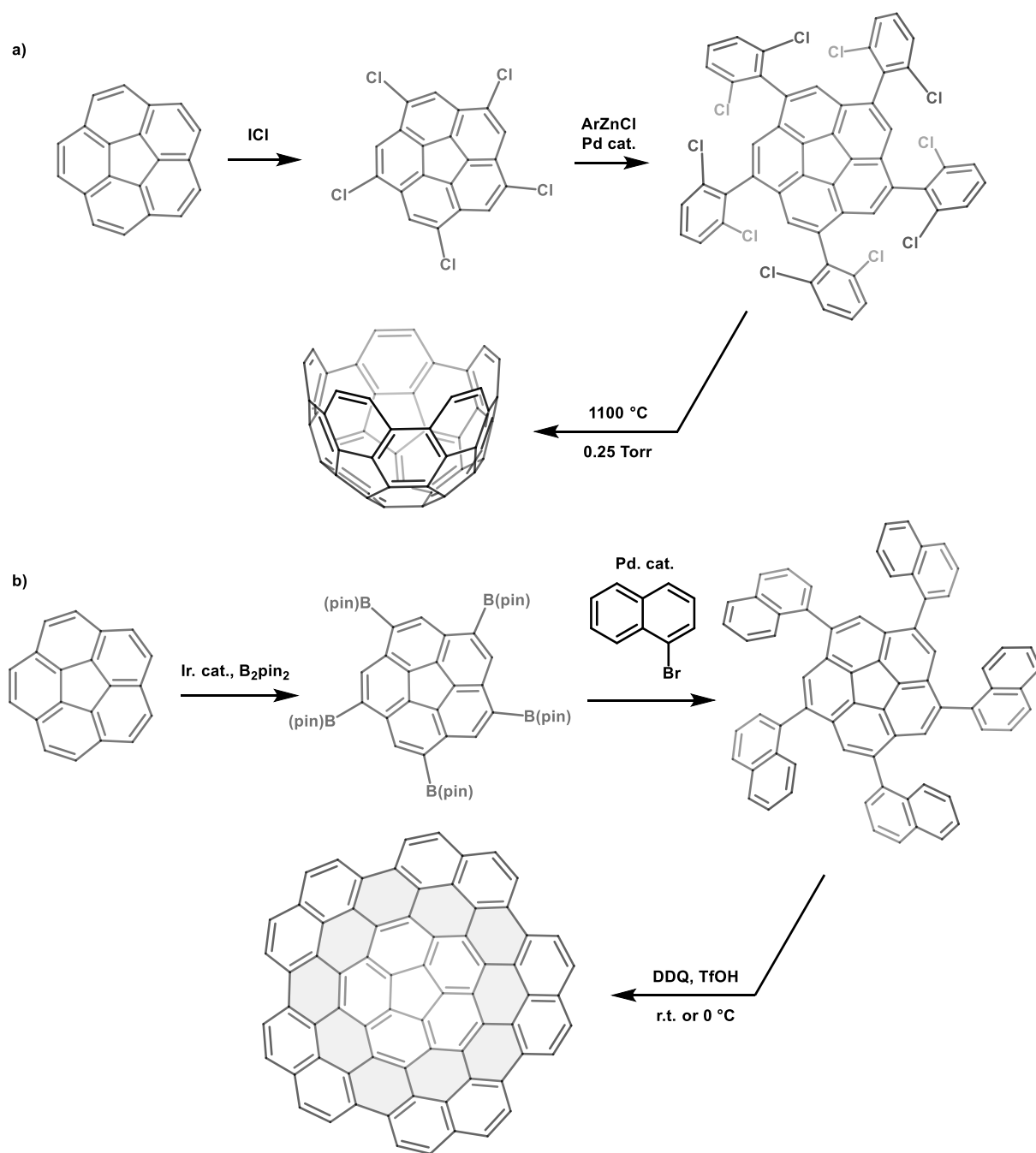


Figure 13. Synthesis of a nanobowl comparable to the end of (5,5)CNT (a) and a nanocone (b).

These examples involve five-membered rings to induce deformations in nanographene, but recent examples of nanographenes including seven- or eight-carbon rings have been reported. These compounds will often adopt a saddle shape with a negative curvature and increased solubility compared to compounds made entirely of hexagonal rings. Thanks to Wynberg's work on the dehydrogenation of heterohelicenes, the Scholl reaction could be used to form heptagonal rings during the graphitization step.⁵¹ These results were then completed by Itami and Scott with the synthesis a distorted nanographene including heptagonal and pentagonal defects (Figure 14).⁵² The coupling of biphenyl units on corannulene gave a flexible precursor which, after dehydrogenation with DDQ, adopts a conformation with a negative curvature once the five heptagonal cycles are formed.

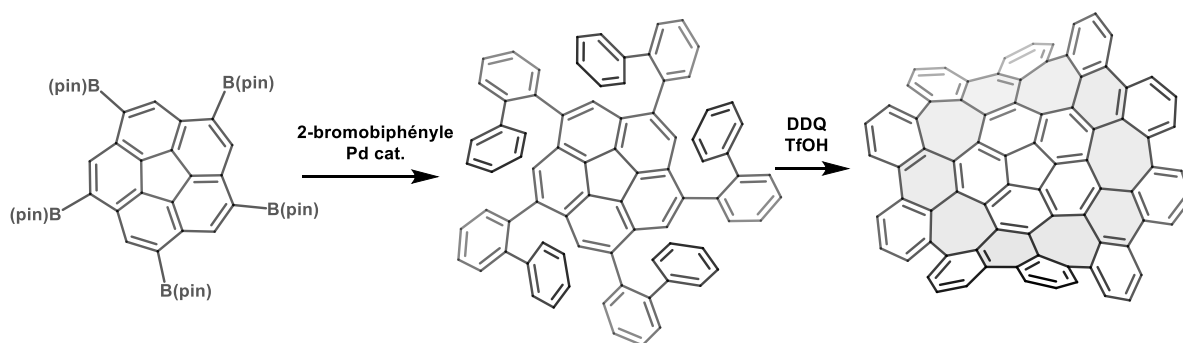


Figure 14. Synthesis of a distorted nanographene by Scholl reaction.

The use of the Scholl reaction to form seven-membered rings is now an established strategy used for the synthesis of nanographenes with negative or atypical curves. By combining the strategies used for the synthesis of hexabenzocoronene with a substituted corannulene, two nanographenes with different curvatures were obtained by Martin's group (Figure 15).⁵³ The first has a positive curvature induced by corannulene and the presence of hexagonal rings. The second, however, has a positively curved part, induced by corannulene, and a negatively curved part by the presence of a heptagonal ring.

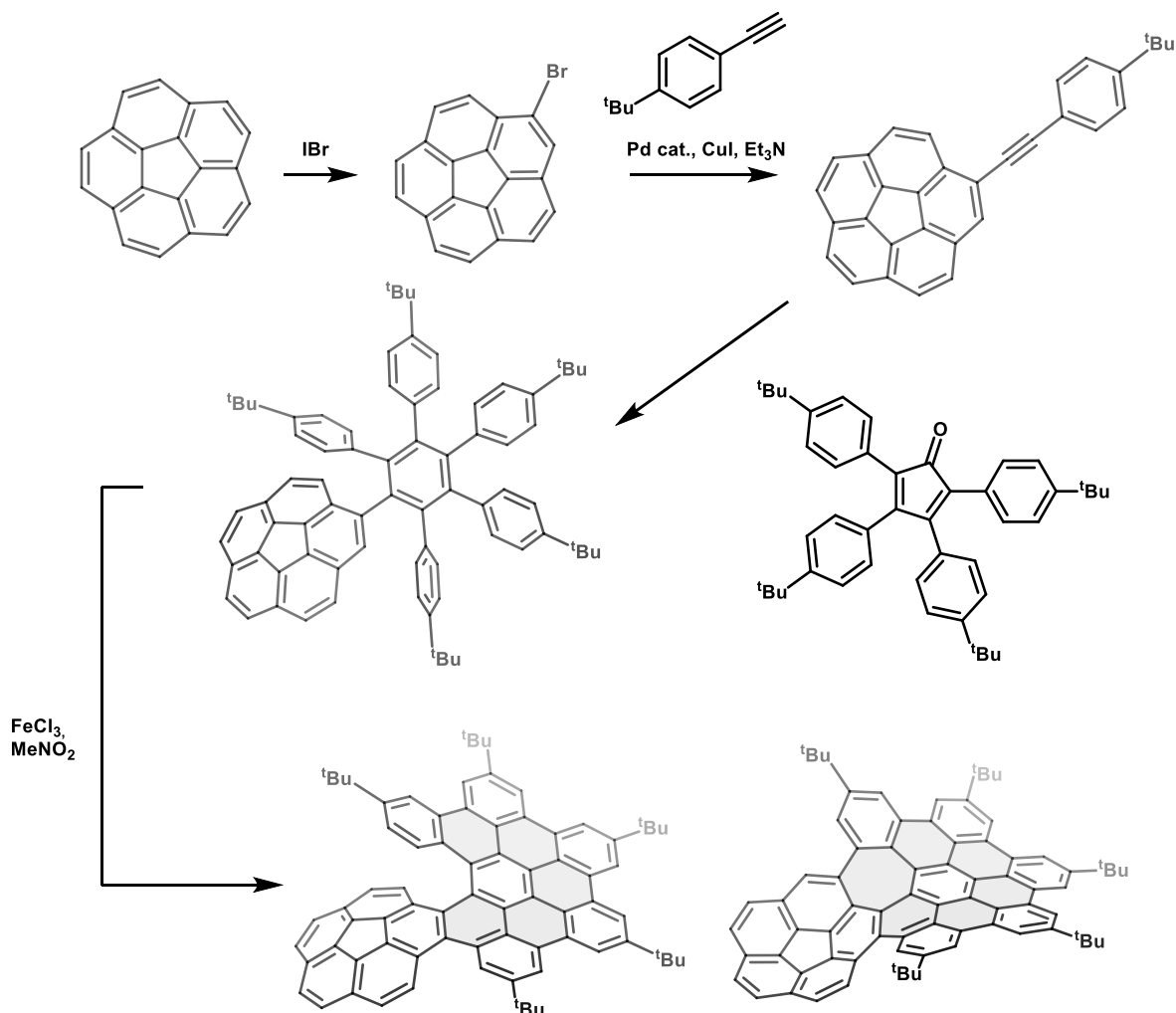


Figure 15. Synthesis of nanographenes with positive and positive-negative curvatures.

Another way to deplanarize graphene is sterical crowding. When an acene bears very bulky functions, the latter may twist it. Some of these compounds are called twistacenes because of the deformation along their aromatic acene backbone. Many examples of very crowded and strongly twisted acenes, often naphthalenes or anthracenes, have been described. Derivatives of naphthacene^{54,55} and longer acenes have also been reported.

A notable example of a twisted acene is 9,10,11,12,13,14,15,16-octaphenyldibenzo-[a,c]naphthacene, synthesized by Pascal *et al.* and published in 1997.⁵⁴ This twistacene was obtained by diazotization of an anthranilic acid in the presence of a hexaphenylisobenzofuran (Figure 16). The oxide such obtained is then deoxygenated in the presence of zinc to give the desired product. The structure obtained by single-crystal X-ray diffraction revealed that the end-to-end twist angle of the acene is 105°, making it the twistacene with the largest deformation along the axis for several years.

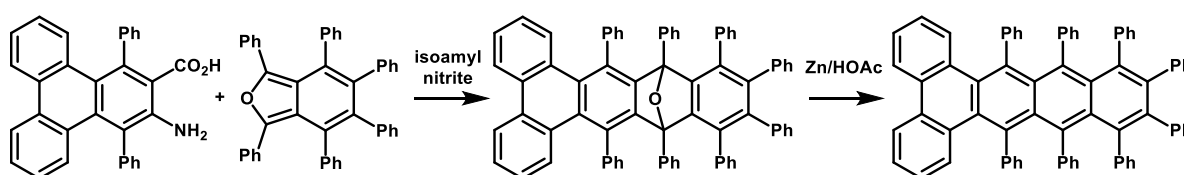


Figure 16. Synthesis of 9,10,11,12,13,14,15,16-octaphenyldibenzo-[a,c]naphthacene.

The synthesis and structure of 9,10,11,20,21,22-hexaphenyltetrabenzo[a,c,l,n]pentacene was then published by the same team.^{56,57} The treatment of 1,2,4,5-tetrahalobenzenes with *n*BuLi gave a 1,4-benzadiyne which can react *in situ* with diphenylphenanthrofurans during a Diels-Alder reaction to give the oxidized precursor of pentacene (Figure 17). This precursor is then deoxygenated in the presence of TiCl₃ and *n*BuLi to give the final twistacene. The structure obtained by single crystal XRD revealed an end-to-end twist angle of 144°, but the molecule contains also smaller acene fragments, including naphthalenes, an anthracene and naphthacenes, for which the twist can be determined. The twists measured for each of these substructures are 60° for the naphthalene, 88° for the anthracene and 116° for the naphthacene, each one representing a new record of distortion for the corresponding acene.

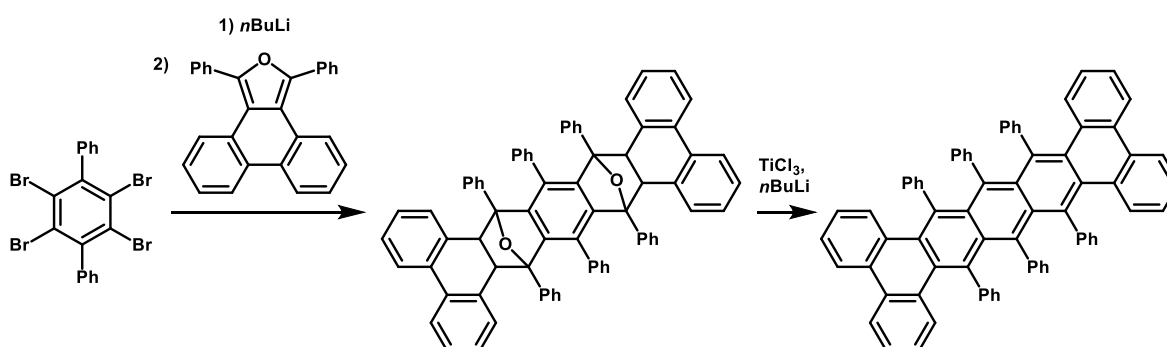


Figure 17. Synthesis of 9,10,11,20,21,22-hexaphenyltetrabenzo[a,c,l,n]pentacene by Pascal and co.

This record has been broken 12 years later, not by Pascal, but by Kilway and her team. The addition of phenyllithium to a quinone precursor gave a diol intermediate which was then reduced in the presence of SnCl₂ to give the desired acene (Figure 18). This strategy not only greatly optimized the synthesis of twistacenes previously developed by Pascal (Figure 17) but

also increased the family of twisted acenes.⁵⁸ The structure of hexacene synthesized by Kilway *et al.* reveals an end-to-end twist of 184° , a new record of longitudinal twist reported for an acene. The deformations measured in its smaller acene subsections (64.6° for naphthalene, 96.4° for anthracene, 128.1° for tetracene and 159.2° for pentacene) also constitute new torsion records.

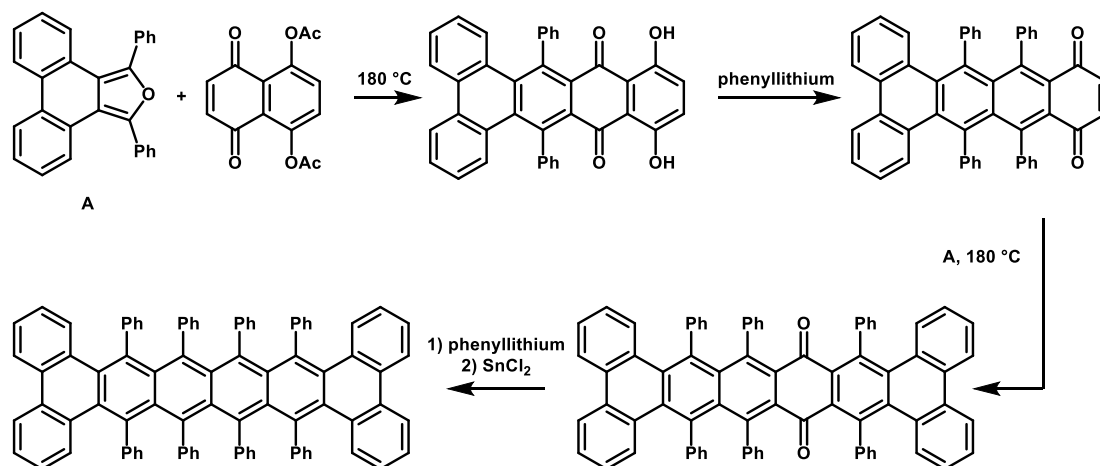


Figure 18. Synthesis of 9,10,11,12,21,22,23,24-octaphenyltetrabenzo[*a,c,n,p*]hexacene by Kilway and co.

Whereas acenes consist of linearly fused benzene rings, helicenes are a family of compounds composed of angularly fused benzene rings.⁵⁹ The intramolecular steric repulsion imposed by the π system will lead to a helical shape and therefore to a planar chirality. Carbohelicenes and heterohelicenes can be characterized by their size (the number of fused benzene rings), their pitch (the dihedral angle between the two terminal rings) and their chirality (Figure 19). Historically, helicene synthesis is based on the assembly of elementary building blocks to form a flexible system which can subsequently be rigidified. These synthetic routes are often non-stereoselective and result in a racemic mixture of [*n*]helicenes. Their racemization is extremely rapid in the case of [4]- and [5]helicenes, and much slower in the case of [6]helicene and larger systems.

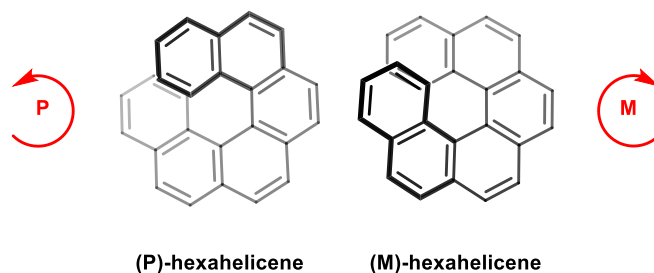


Figure 19. Axial chirality of helicene induced by their helical conformation.

The synthesis of the first helicene, the [4]helicene, was realized in 1913 by Lieb and Weitzenböck.⁶⁰ Despite the weak steric repulsion, the π system is already distorted. It was only several years later that the synthesis of a [5]helicene was reported by Weitzenböck (Figure 20).⁶¹

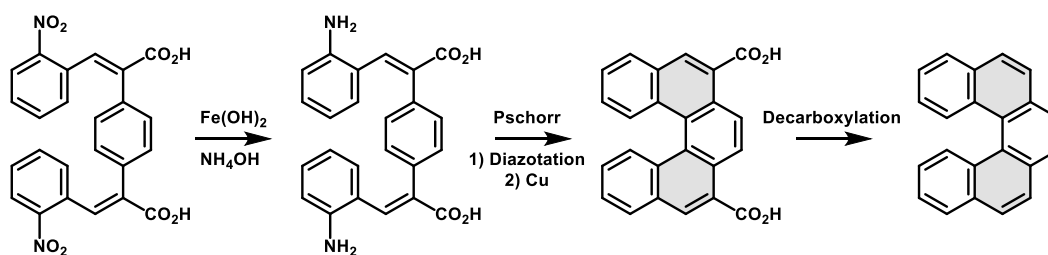


Figure 20. Synthesis of the first [5]helicene via Pschorr reaction.

This synthesis is based on the condensation of two *o*-nitrobenzaldehydes with *p*-phenylenediacetic acid, followed by a reduction of the nitro groups to amine functions, a Pschorr cyclization and a double decarboxylation. The formation of the helicene during the condensation step, however, competes with that of the linear compound, making this synthesis inefficient. It was not until 1933 that this synthesis was improved,⁶² and in 1952 that the first structure by X-ray diffraction was produced.^{63,64} It took several additional years for the synthesis of a [6]helicene to be reported.^{65,66} The resolution of this helicene by the formation of a charge transfer complex⁶⁷ contributed to launching a growing interest in the study of the chiroptical properties of carbohelicenes.⁶⁸ Despite this innovative aspect, few results relating to it were reported at this time and helicenes long remained scientific curiosities. Schölz's historic work on the photochemical synthesis of a [4]helicene,⁶⁹ followed a few weeks later by the photochemical synthesis of a [7]helicene by Martin's team (Figure 21),⁷⁰ has then initiated the exponential growth of this field.

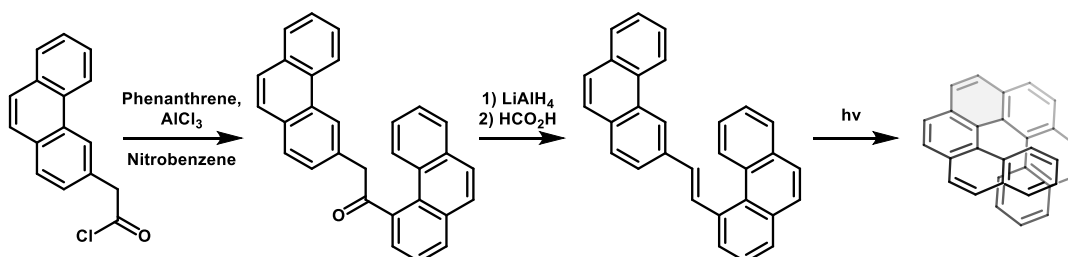


Figure 21. Photochemical synthesis of a [7]helicene by Martin and coworkers.

Works on oxidative photocyclodehydrogenation opened the way to the synthesis of larger helicenes,⁷¹ but the scale on which it is possible to carry out these syntheses remains a limiting factor. The procedure requires high dilution in a pure solvent to prevent $[2\pi+2\pi]$ dimerizations, limiting production to a maximum of a few hundred milligrams when carried out in a liter of solvent. However, interest in helicene chemistry was growing and numerous non-photochemical syntheses were also reported in the literature.

c. Macrocyclic nanocarbons

It is also possible to deform aromatic cores by connecting two ends with a fairly short link. By linking two opposite positions on a pyrene with alkyl chains, Bodwell *et al.* were able to obtain a family of pyrenophanes containing bent pyrenes (Figure 22).⁷²

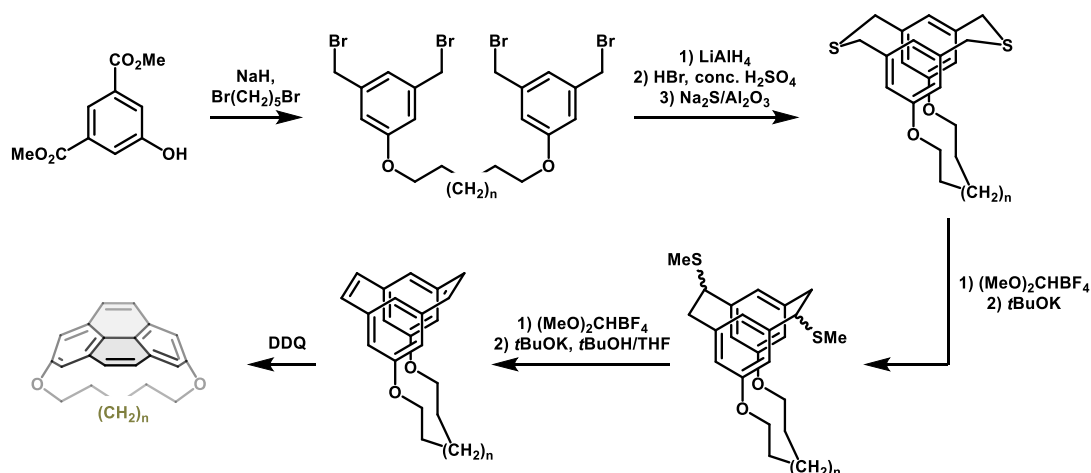


Figure 22. Synthesis of bent pyrenophanes by Bodwell.

By constraining, for example, an aromatic core with a cyclophane, the tension applied by the latter will induce a twist. In this way, Tanaka and co. were able to obtain a naphthalene triple decker with a twist of 32° .⁷³ Their synthesis is based on the coupling between mercaptomethylnaphthalenes and bromomethylnaphthalenes (Figure 23). The photoinduced desulfurization of the mixture of tetrathia[3,3][3,3]naphthalenophane finally makes it possible to obtain [2,2][2,2]naphthalenophane.

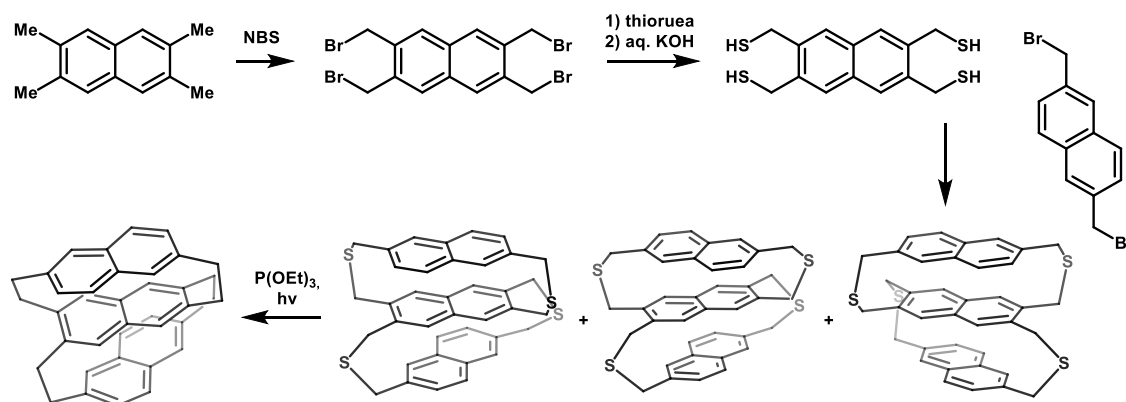


Figure 23. Synthesis of triple decker naphthalenophane.

In the same manner as rational synthesis of GNRs mimics and improves the properties of graphene, the synthesis of macrocyclic polycyclic aromatic compounds can aim at forming cylindrical compounds, that is to say CNT segments. The properties of CNTs are dependent on their structure and no known destructive synthetic strategy allows to produce structurally uniform CNTs.⁷⁴ Because of this and also due to the challenging synthesis imposed by the ring strain, molecules representing CNTs segment have long been of interest. Their synthesis has long remained elusive, but in 2008, Bertozzi and co. reported for the first time of [9]-, [12]- and [18]-cycloparaphenylenes (CPPs) using a novel aromatization reaction (Figure 1a).⁷⁵ The main challenge was to address the strain energy of the bent aromatics. To resolve this problem, Bertozzi and her team built the strain sequentially, thanks to the use of the 3,6-*syn*-dimethoxy-cyclohexa-1,4-diene moiety as a camouflaged aromatic ring. Once the

macrocycles were formed and isolated, they were treated with lithium naphthalenide at low temperatures to give the final CPPs. This method allowed fast access to three different macrocycles, although in modest yields. Soon after this report, the first size-selective synthesis of CPPs would be reported by Itami and Yamago.^{76,77} These reliable strategies opened the way for the synthesis of a wide range CPPs and functional derivatives. In 2013, Itami and his group pushed further the development of new CPPs by publishing a bicyclic CPP (Figure 24b).⁷⁸ This synthesis is one of the first examples of a carbon nanocage. The inability to use sp² carbon as a single unit led to approaches relying on the assembly of bigger building blocks. Isobe's group developed the idea of using *meta* trisubstituted phenyl as a planar trigonal building block to access new tridimensional nanocarbons.⁷⁹ Using known biaryl couplings, this method allowed the synthesis of π electrons rich compounds mimicking known nanocarbons and rapidly paved the access to hypothetical nanocarbons, such a polluxene.⁸⁰ A linear diboryl precursor was first synthesized dimerized via Ni-mediated Yamamoto coupling. After addition of two phenyl to the resulting decagonal macrocycle, a final coupling forms the final bridge and gives polluxene as a racemic mixture.

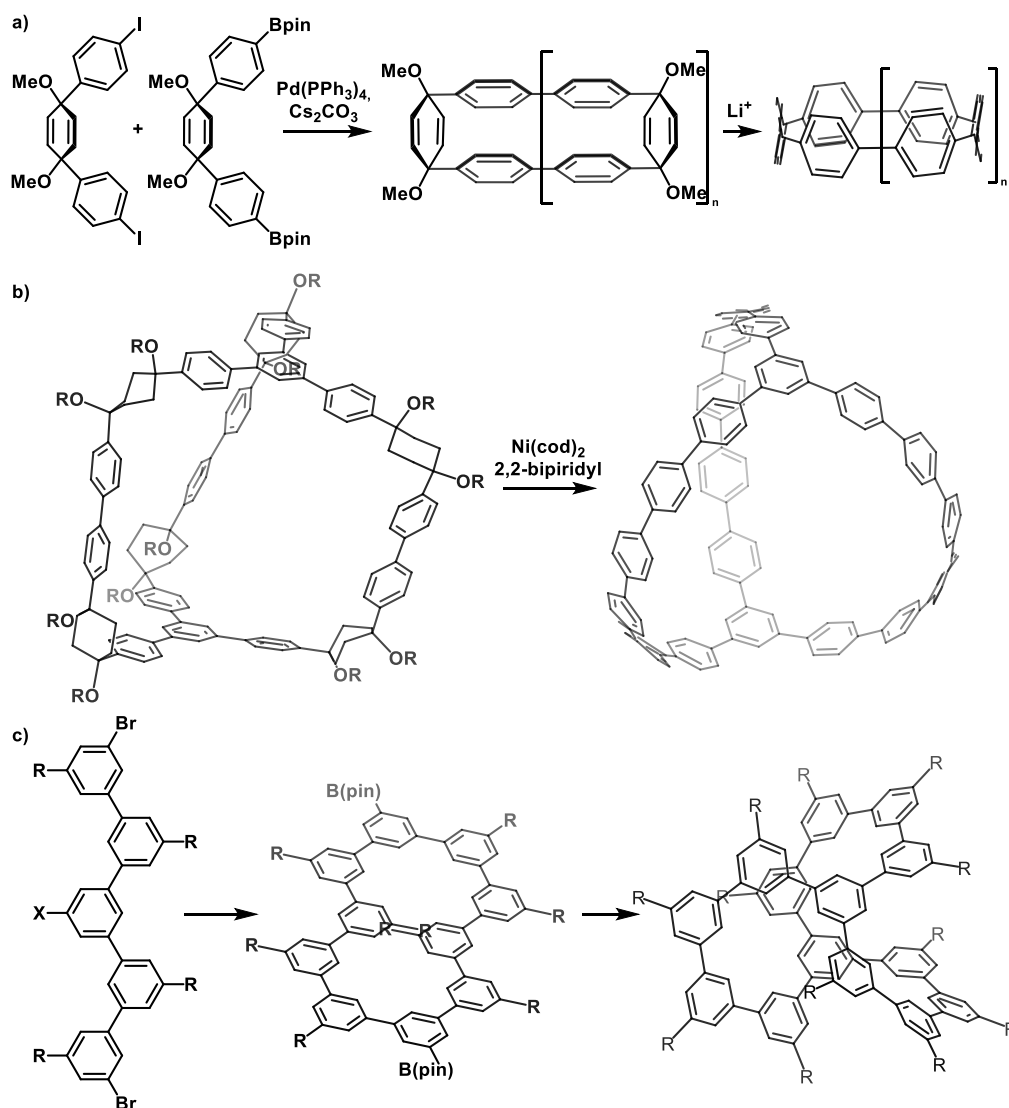


Figure 24. Synthesis of CPPs by Bertozzi(a), a CPP cage by Itami (b) and a phenine polluxene by Isobe (c).

More condensed carbon nanotube segments are the carbon nanobelts (CNBs). CNBs are defined as macrocyclic compounds composed of fully fused benzene ring and requiring the cleavage of at least two bonds to be opened.³⁰ CNBs can be classified just like CNTs, depending on their chiral index n, m . With the first attempts at the synthesis of CNBs starting as early as 1957,⁸¹ they remained elusive until the report of a series of armchair nanobelts by Itami and coworkers the last decade (Figure 25).^{82,83} Successive stereoselective Wittig reactions allow the synthesis of macrocycles with only little strain, and fully condensed carbon nanobelts were obtained by a final nickel-mediated Yamamoto cyclization.

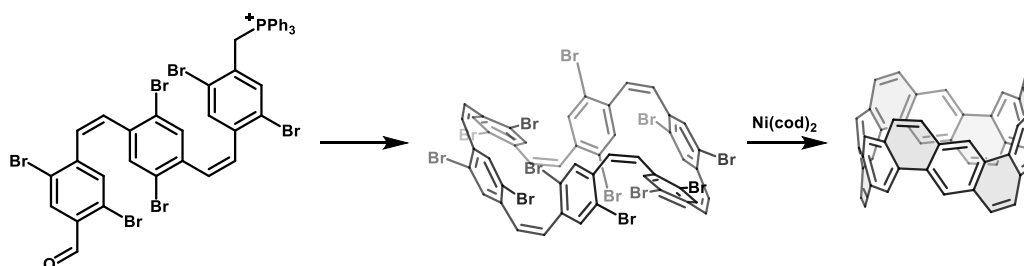


Figure 25. Synthesis of an armchair type carbon nanobelt by Itami.

Using the bent benzene analogue strategy used for the synthesis of CPPs, Miao reported in 2019 the synthesis of a chiral CNB, the final fusing of the benzene rings being this time realized by a Scholl reaction.⁸⁴ Finally, Itami and Chi reported the first examples of zigzag CNBs almost at the same time. The strategy used by Itami relied on successive Diels-Alder processes, followed by a final Diels-Alder dimerization (Figure 26a).⁸⁵ Chi's team also used successive Diels-Alder reactions to obtain non strained macrocycles functionalized with epoxydes (Figure 26b). A final reductive aromatization led to the zigzag CNB.⁸⁶

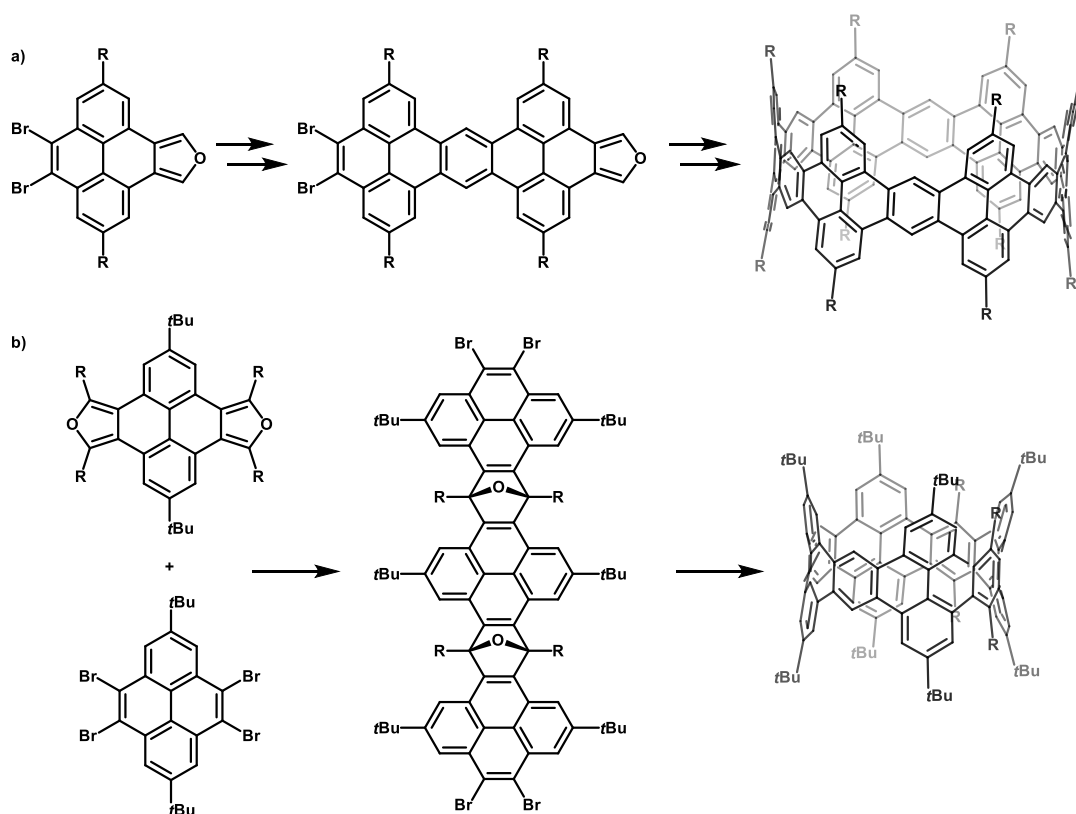


Figure 26. Synthesis of zigzag type CNB by Itami (a) and Chi (b).

Finally, macrocycles not representing segments of CNTs were also synthesized. For example, a saddle shape molecular belt capable of anion recognition in its cavity was reported by Stepien *et al.* in 2016.⁸⁷ This “octulene” was obtained by McMurry cyclooligomerization of a phenanthrene dialdehyde (Figure 27). Phenanthranes of two different sizes were each engaged in nickel-mediated Yamamoto couplings and gave the desired kekulene and octulene.

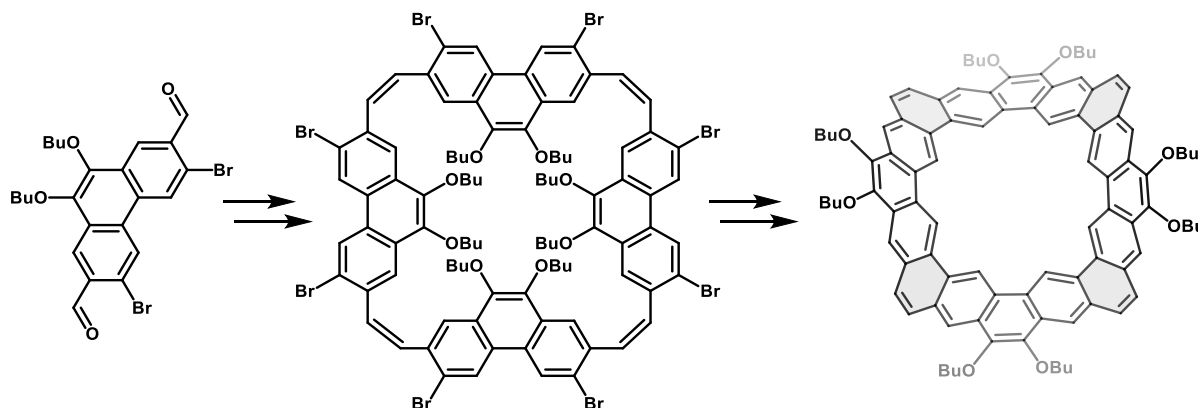


Figure 27. Synthesis of octulene by Stepien.

The development of new topologies of nanocarbons has been ever growing in the last years, and with the help of innovative synthetic strategies, unprecedented and atypical structures are being reported each year.

III. The Perkin Strategy

a. Evolution of the Perkin reaction

In 1967, Sir William Henry Perkin, an English chemist known for his discovery of mauveine, one of the first artificial dyes, created a new process now called the Perkin reaction.⁸⁸ This synthesis allows the formation of unsaturated carboxylic acids such as cinnamic acid by diastereoselective formation of a C=C bond by the condensation of an aromatic aldehyde with acetic anhydride. A modernized version of this reaction has been developed and used in our team for synthesizing new polycyclic aromatic compounds (PACs).⁸⁹ Our bottom-up synthetic strategy, dubbed the Perkin Strategy, is based on the assembly of small elementary bricks forming a flexible intermediate which can finally be rigidified to obtain new PACs functionalized with carboxylic functions (Figure 28).

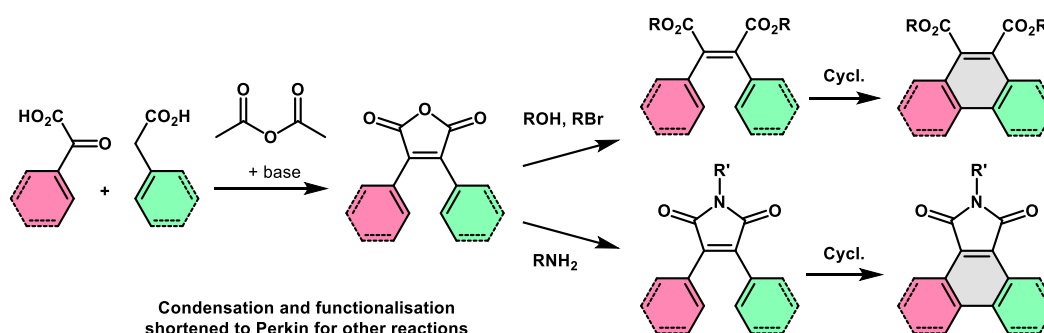


Figure 28. The Perkin Strategy.

The formation of the flexible intermediate with a disubstituted unsaturated bridge is possible through the condensation of aryl-glyoxylic acids and aryl-acetic acids. In the presence of acetic anhydride and in basic conditions, these two elementary building blocks will react to give a flexible intermediate composed of aromatic cores linked by maleic anhydride bridges (Figure 29).

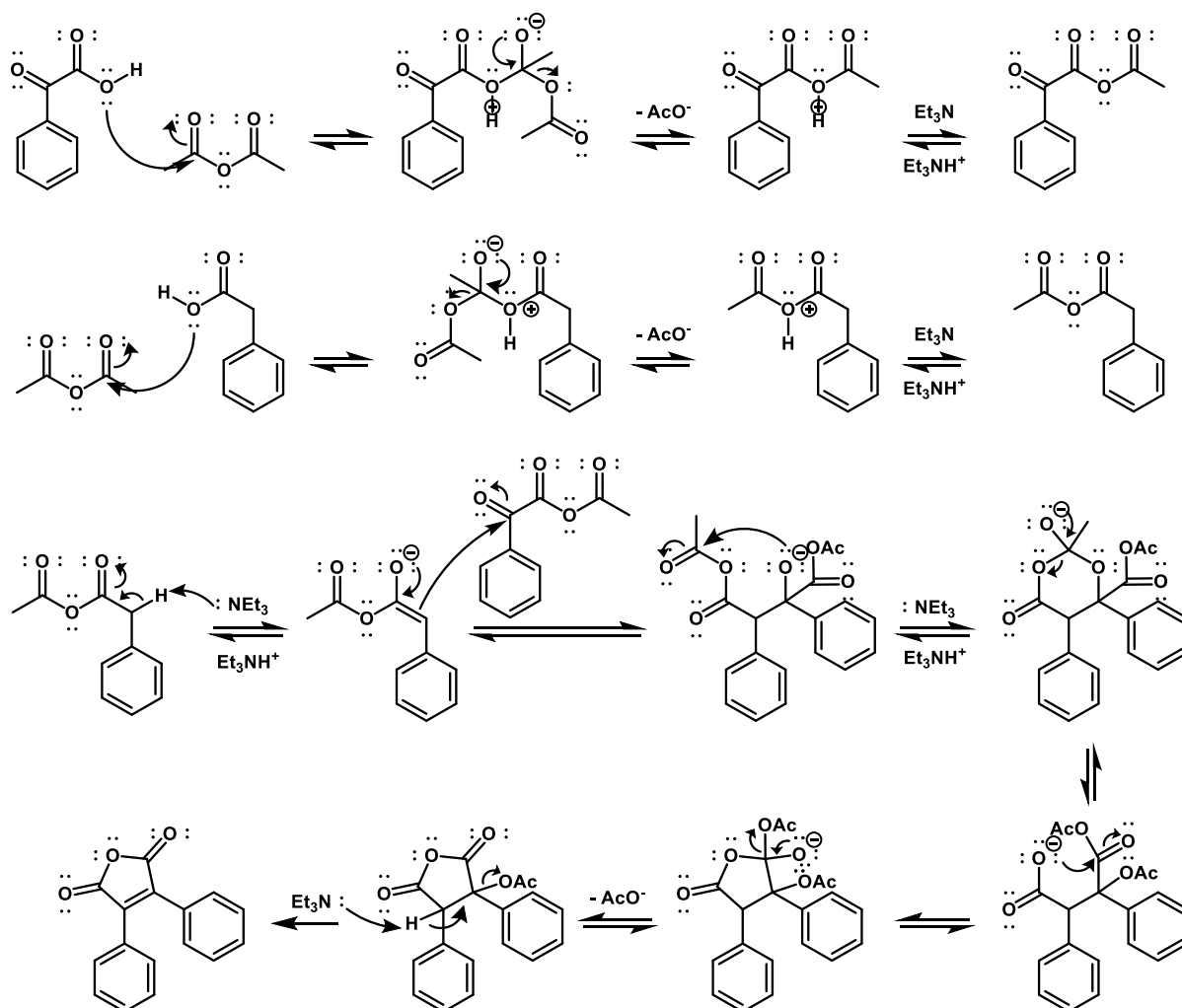


Figure 29. Supposed mechanism for the condensation step of the Perkin reaction.

This intermediate can then be functionalized *in situ* to give a flexible precursor having maleic diester bridges after reaction with a bromoalkane/alcohol mixture, or cyclic maleimides when using a primary amine. The two carboxylic functions on the maleic bridge provide solubility to the compound, while the *cis*-stilbene motif imposed during the condensation of the elementary building blocks makes it possible to envisage a rigidification of the intermediate by palladium-catalyzed dehydrobromination or by Mallory photocyclization. Initially, palladium-catalyzed dehydrobromination was preferentially used because it was considered more reliable.⁹⁰ The presence of bromines was, however, too great a constraint and this approach was abandoned in favor of Mallory photocyclization. This last step allows the formation of the missing C-C bonds and the obtaining of a new PACs.

b. Synthesis of the building blocks

To achieve the coupling between the two aromatic cores, at least two complementary acids are necessary. Some compounds are commercially available, but a large majority of them must be synthesized. The first approach to the building blocks relied on successive Friedel-Crafts acylations. For example, ethyl perylene-3-glyoxylate is obtained following a Friedel-Crafts acylation reaction on commercially available perylene.⁹⁰ A second acylation on this product gives access to diethyl perylene-3,9-diglyoxylate,⁹¹ which is not selectively accessible via bromination (Figure 30)

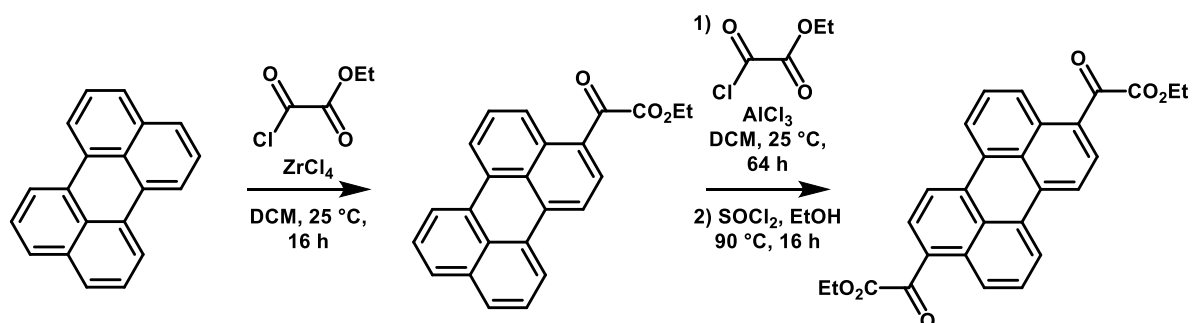


Figure 30. Synthesis of ethyl perylene-3-glyoxylate and diethyl perylene-3,9-diglyoxylate.

A second approach has later been developed to transform brominated arenes into the corresponding aryl-glyoxylic acid in a few steps. The latter can finally be reduced in mild conditions to give the aryl-acetic acid (Figure 31).

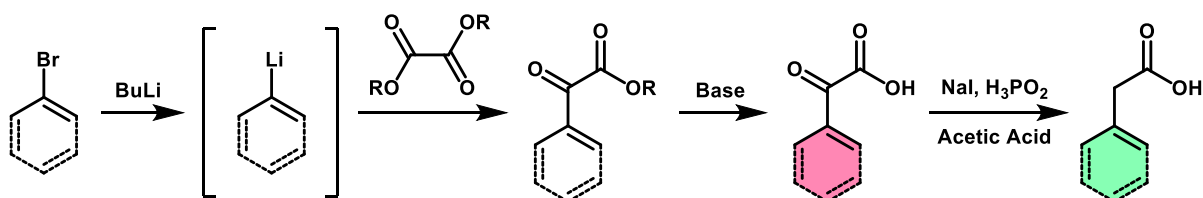


Figure 31. Synthetic strategy for aryl-glyoxylic and aryl-acetic acids from bromoarenes.

It is sometimes difficult to obtain the aromatic ring with the bromide functions at the desired positions, due to a decrease or deactivation of reactivity once another position is functionalized, and Friedel-Crafts acylation provides a nice alternative when it is the case. These complementary approaches provide access to mono- or polyfunctionalized compounds.

c. PACs obtained with the Perkin Strategy

Once the elementary bricks have been obtained and coupled, it is necessary to rigidify the flexible intermediate by creating the missing C-C bonds. The last graphitization steps were carried out using palladium-catalyzed dehydrobromination during the first tests of the Perkin strategy.⁹² This technique was often efficient but required the presence of bromine in the *ortho* position of one of the two reactive functions. Due to the restrictive synthetic constraint

imposed, this graphitization method was abandoned. Photochemical dehydrocyclization, or Mallory photocyclization,⁹³ is now favored for the final step of the synthesis. This method does not require bromine and therefore allows access to a greater diversity of starting blocks.

The wide range of available elementary building blocks, coupled with a direct and effective strategy eased the synthesis of new PACs of various sizes and shapes. The solubility provided by carboxylic functions has been taken advantage of during the synthesis of long linear PACs such as phenacenes, whose solubility decreases with increasing size due to their ease of forming aggregates. From different naphthalenes and chrysenes, soluble phenacenes of different sizes have been synthesized (Figure 32).⁹⁴

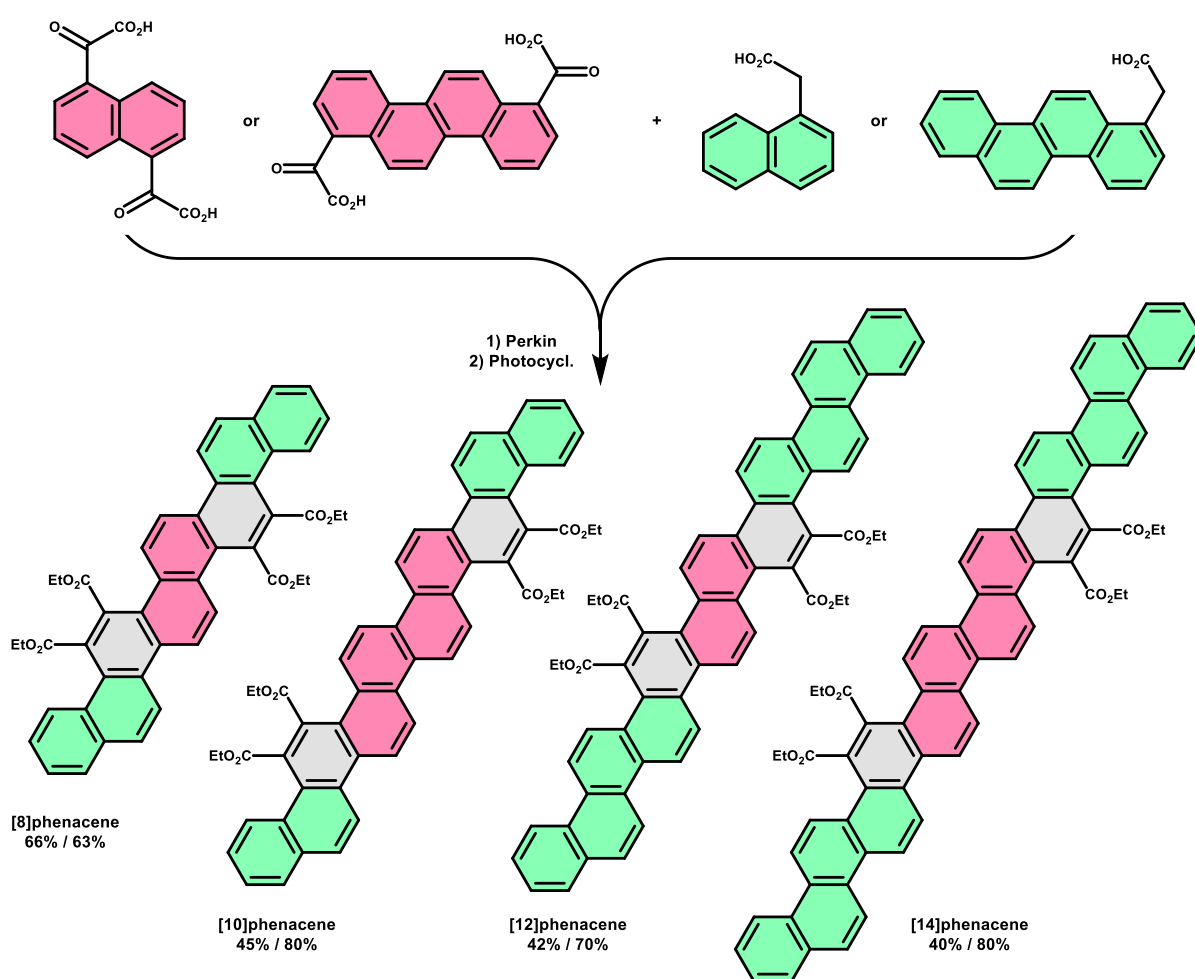


Figure 32. Synthesis of [8]-, [10]-, [12]- and [14]phenacene.

The solubility limits of these phenacenes are reached for [14]phenacene, despite the tetrafunctionalization and the presence of long alkyl chains on the ester functions. One solution to obtain longer soluble phenacenes is to use a synthetic approach allowing the introduction of more ester functions. By using protection techniques, it is possible to sequence the synthesis and obtain more complex products. The acetic ester function being not reactive during the Perkin reaction and easily accessible by statistical saponification, it can be used as a protective function. More surprisingly, the glyoxylic ester function as well

does not react during the condensation step. Perkin reactions using such building blocks yield flexible intermediates functionalized by glyoxylic or acetic esters. The latter can be saponified and then engaged in a second coupling before rigidification. This strategy was used for the synthesis of other phenacenes and proved successful, allowing the synthesis of a hexafunctionalized [14]phenacene,⁹⁵ then a soluble dodecafunctionalized [20]phenacene (Figure 33).⁹⁶

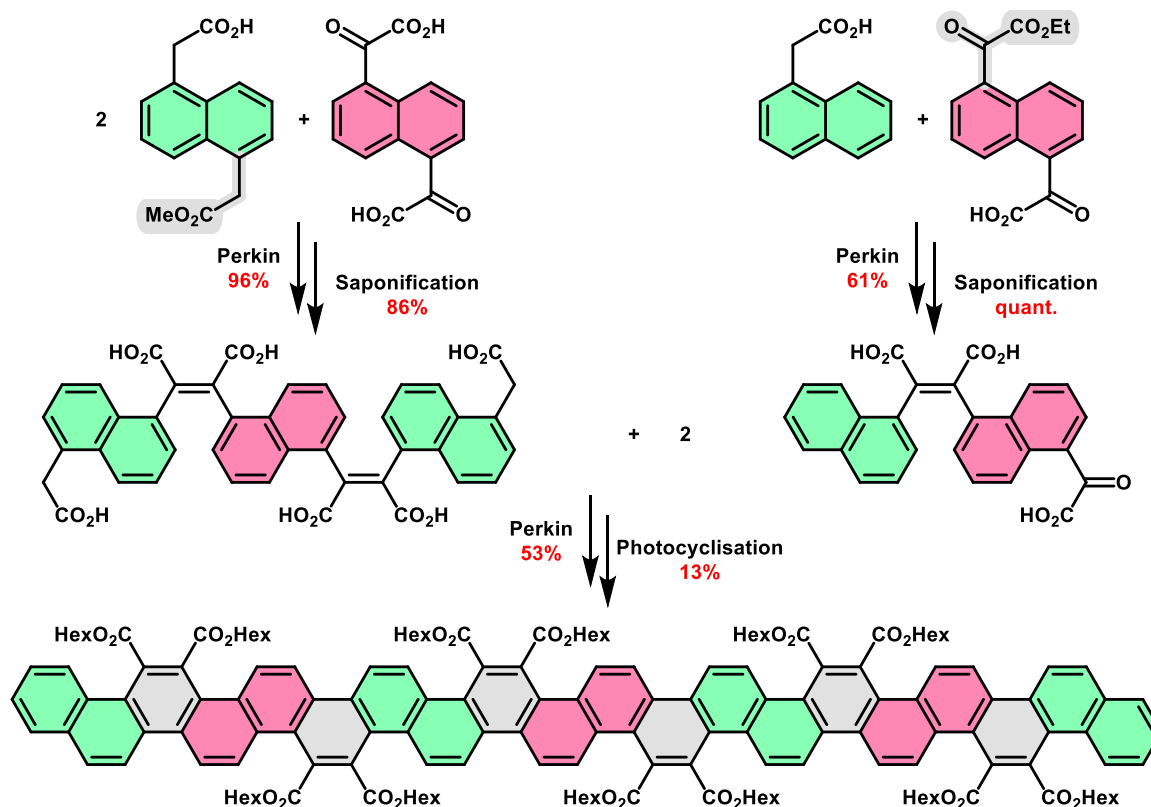


Figure 33. Synthesis of a [20]phenacene by successive Perkin reactions.

During the photocyclization of flexible phenacene precursors, the position of maleic bridges between alpha-positions of naphthalene units can only lead to the formation of linear compounds. The photocyclization reaction on compounds with a stilbene motif is, however, a known approach for helicene synthesis.⁹⁷ Obtaining regioisomers is therefore possible in the case where a photocyclization reaction is used on intermediates where several positions of the ring aromatic are reactive (Figure 34a).⁹⁸ When a mixture of isomers is obtained, different strategies are possible to obtain predominantly one or the other. In the case where the synthesis of linear compounds is to be favored, palladium-catalyzed dehydrobromination, although more restrictive, allows the majority of the latter to be synthesized (Figure 34b).⁹⁹ This may prove to be a judicious alternative to Mallory photocyclization when it is possible to easily obtain aromatic cores with bromide functions in the *ortho* position of the acid functions.

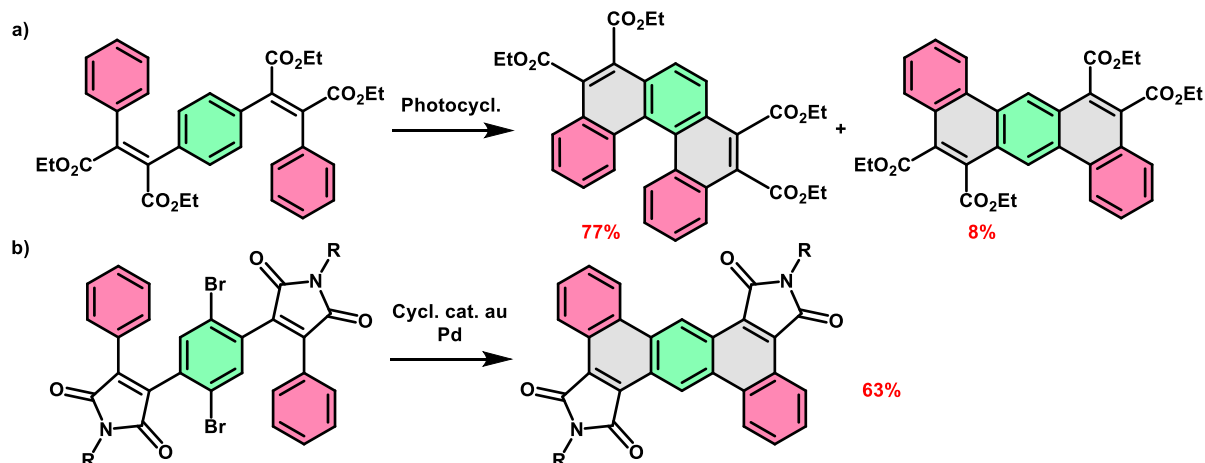


Figure 34. Regioselectivity of Mallory photocyclization (a) and palladium-catalysed deshydrobromination (b).

A second method consists of playing on the position of the acid functions on the aromatic cores. For example, by using chrysenes functionalized on the central phenyls rather than on the terminal ones, this approach logically leads to a double [7]helicene instead of a [10]phenacene (Figure 35).¹⁰⁰

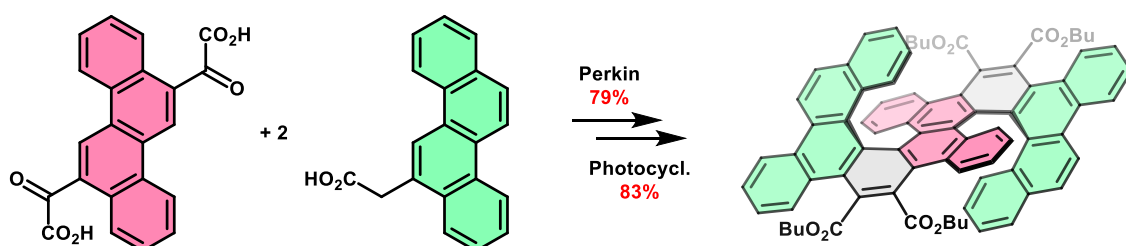


Figure 35. Synthesis of a double [7]helicene from chrysenes.

Finally, the mild photocyclization conditions avoid the overreaction of compounds of the [5]helicene type. On the other hand, it is possible to create further C-C bonds by oxidative dehydrocyclization in the presence of AlCl_3 .⁹⁸ This approach was used for the synthesis of a symmetrical dibenzocoronene from an extended [5]helicene obtained following a reaction Perkin.¹⁰¹ The helicene was planarized in the presence of AlCl_3 and thereupon presented a diene-type reactive site that could undergo a Diels-Alder reaction with maleic anhydride to form symmetrical dibenzo-coronene (Figure 36).

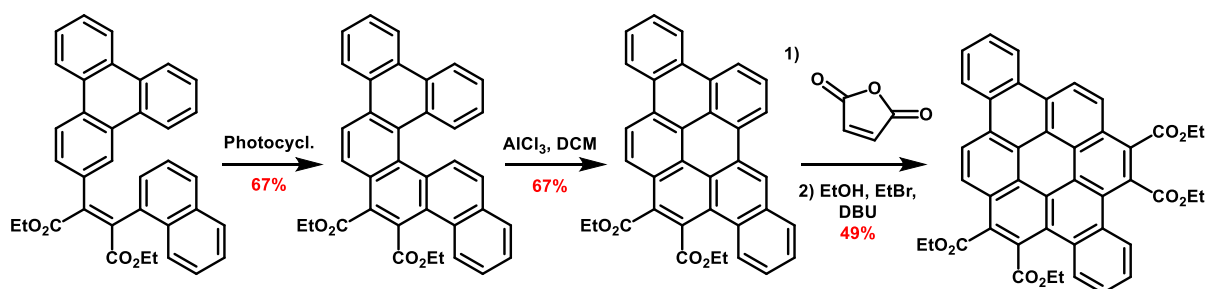


Figure 36. Synthesis of a dibenzocoronene.

d. Macrocycles

Prior to the development of protection techniques for the Perkin strategy, coupling tests of bifunctional elementary bricks were carried out. These tests showed that such reactions led not only to oligomers but also to conjugated macrocycles comprising four building blocks.^{95,102} The yields obtained for this type of macrocyclization reactions are very reasonable in such unoptimized conditions, for instance with a yield of 25% using “normal dilutions” for macrocycle containing four pyrene units (Figure 37a).¹⁰² When the solubility of the starting reagents allows it, it is possible to use a syringe pump to reach intermittent high dilution conditions during the reaction, without need for very large solvent quantities per amount of reactant. The formation of oligomers is then less probable and the yields are greatly improved (Figure 37b).⁹⁵ The aim of the synthesis of these macrocycles was to obtain graphene nanobelts. Unfortunately, the final rigidification steps of these compounds were unsuccessful.

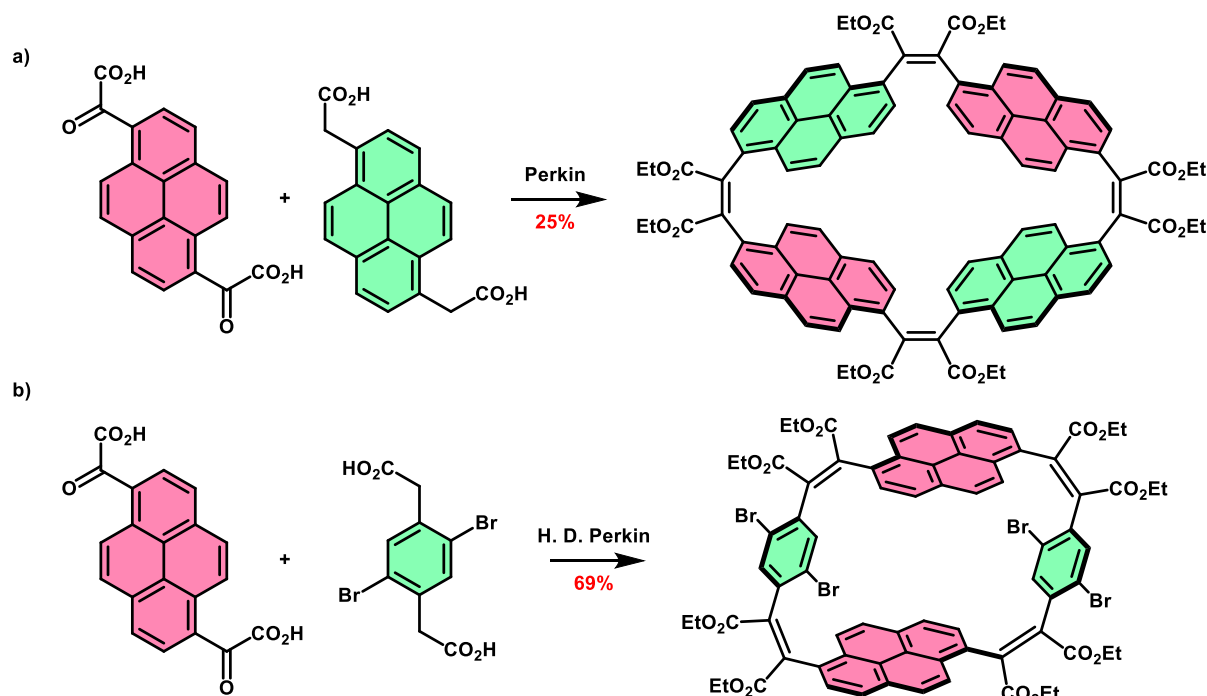


Figure 37. Graphene nanoring precursors synthesized by macrocyclisation reactions.

In order to simplify the final step, biphenyl type reagents have been developed. The single bond between the two phenyl groups allows their free rotation and facilitates access to a favorable configuration of the reactive sites during the Mallory photocyclisation. A biphenyl-maleate tetramer could thus be synthesized from a stoichiometric mixture of 4,4'-biphenyl-diglyoxylic diacid and 4,4'-biphenyl-diacetic diacid.¹⁰³ Once engaged in a photoinduced dehydrocyclization reaction, a macrocyclic phenanthrene tetramer was isolated (Figure 38). The small size of the macrocycle and the position of the single bonds on positions 3 and 6 of the phenanthrenes induce a strong tension and force the macrocycle to adopt a saddle-shaped conformation.

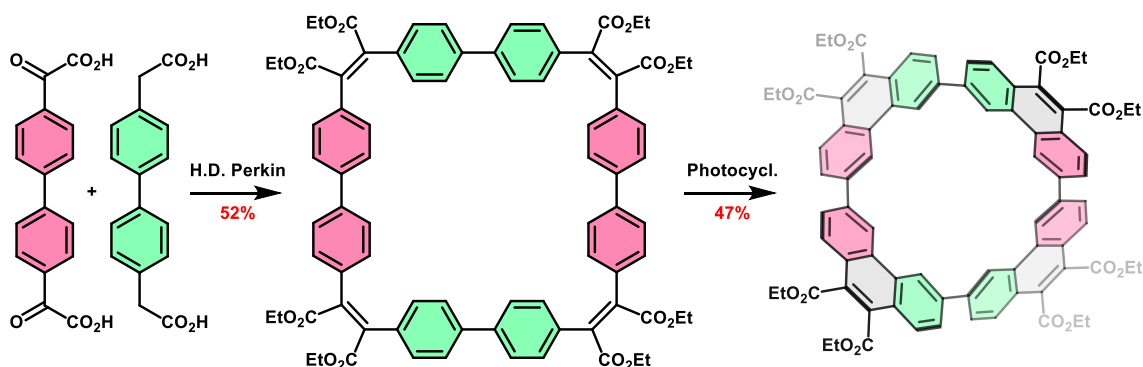


Figure 38. Synthesis of a macrocyclic tetramer of phenanthrene.

If the acetic brick is replaced by a 1,4-benzenediacetic diacid, a smaller macrocycle is obtained with a yield of 21% (Figure 39a).^{103,104} The photocyclization reaction is, however, more favorable and leads to the formation of a cyclo-bis-[5]helicene. It is a rigid, highly distorted macrocycle with a figure-of-eight shape and with two helicenes of the same helicity linked together by single bonds. By coupling high dilution conditions and protection techniques, it is possible to increase macrocyclization yields by reducing the number of potentially formed oligomers.¹⁰⁵ A diacetic trimer was synthesized from 4,4'-biphenyl-diglyoxylic acid and two equivalents of monoprotected phenylene 1,4-diacetic acid. After saponification, this intermediate reacts with biphenyl-4,4'-diglyoxylic acid to give the flexible macrocycle with a yield of 55% (Figure 39b). With this strategy, an additional step is necessary but the overall yield of the synthesis is improved (33% over 3 steps). A less direct but more controlled approach can therefore sometimes be more effective in obtaining this type of atypical macrocycles.

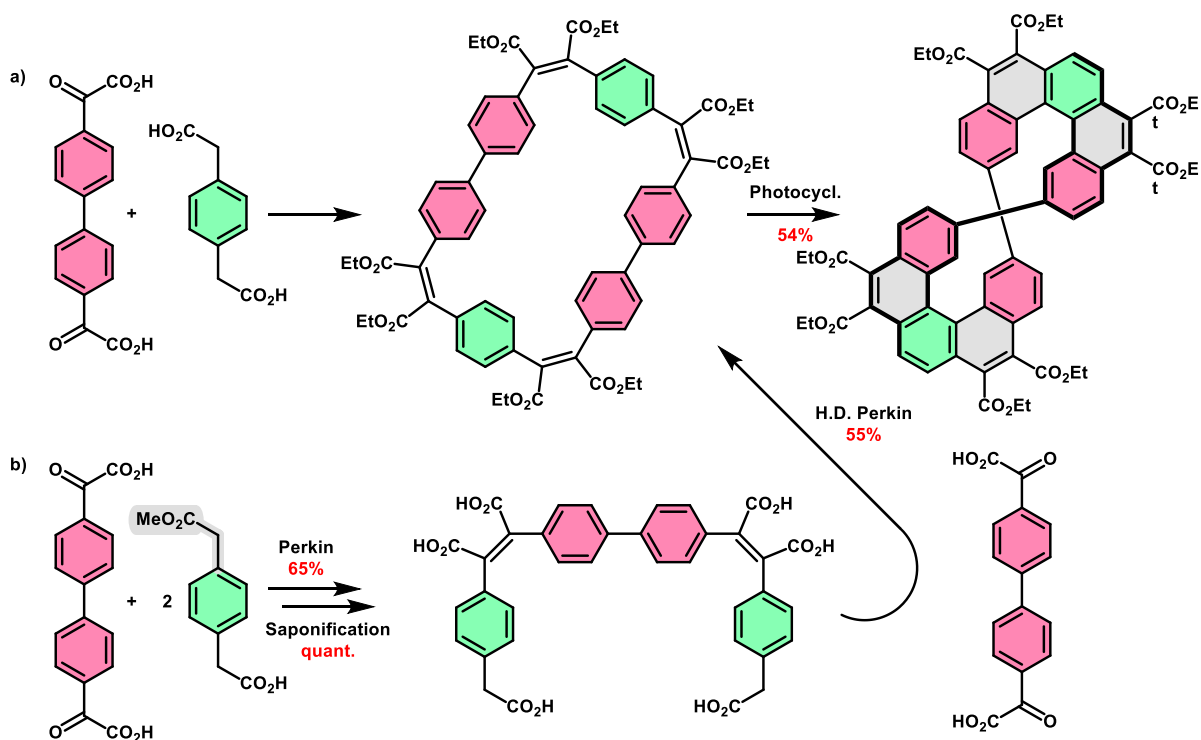


Figure 39. Synthesis of a cyclo-bis-[5]helicene from a stoichiometric mixture of building blocks (a) or from a controlled assembly (b).

The progressive and controlled assembly of basic building blocks allowed the formation of macrocycles with increasingly atypical and complex structures. Thus a triblock complementary to the one used in the previous synthesis (Figure 39b) was synthesized from benzene-1,4-diacetic acid and two equivalents of monoprotected biphenyl-4,4'-diglyoxylic acid.¹⁰⁵ With the two triblocks engaged in a Perkin reaction in high dilution, a flexible macrocycle composed of six units was obtained. After Mallory photocyclization, two cyclo-tris-[5]helicene diastereoisomers were isolated as racemic mixtures (Figure 40). The first is a cyclo-tris-[5]helicene of D_3 symmetry, with three [5]helicenes of the same helicity (MMM or PPP). The second has C_2 symmetry, with one [5]helicene of a helicity different from the other two (MPM or PMP). Single crystals analyzable by XRD were obtained for each of these macrocycles and their structure revealed that these structures possessed a persistent Möbius geometry. The macrocycle with C_2 symmetry has one twist while that with D_3 symmetry has three. The aromatic properties of these molecules were studied in collaboration with Rainer Herges. These studies have shown that within these macrocycles an external electronic current and an internal current, of respectively 48 and 24 π electrons, exist. These circuits of $4n \pi$ electrons and the odd number of twists in the macrocycles seem to indicate that the molecular orbitals of the latter have a Möbius topology and not a Hückel one. ACID calculations, however, showed that the situation was more complex. The expected Möbius aromaticity exists, located in the π system of the ribbon, but a signature of anti-aromaticity exists too, mainly located in the σ system. This unexpected double phenomenon illustrates the complexity of the notion of aromaticity when it is applied to large non-planar conjugated compounds.

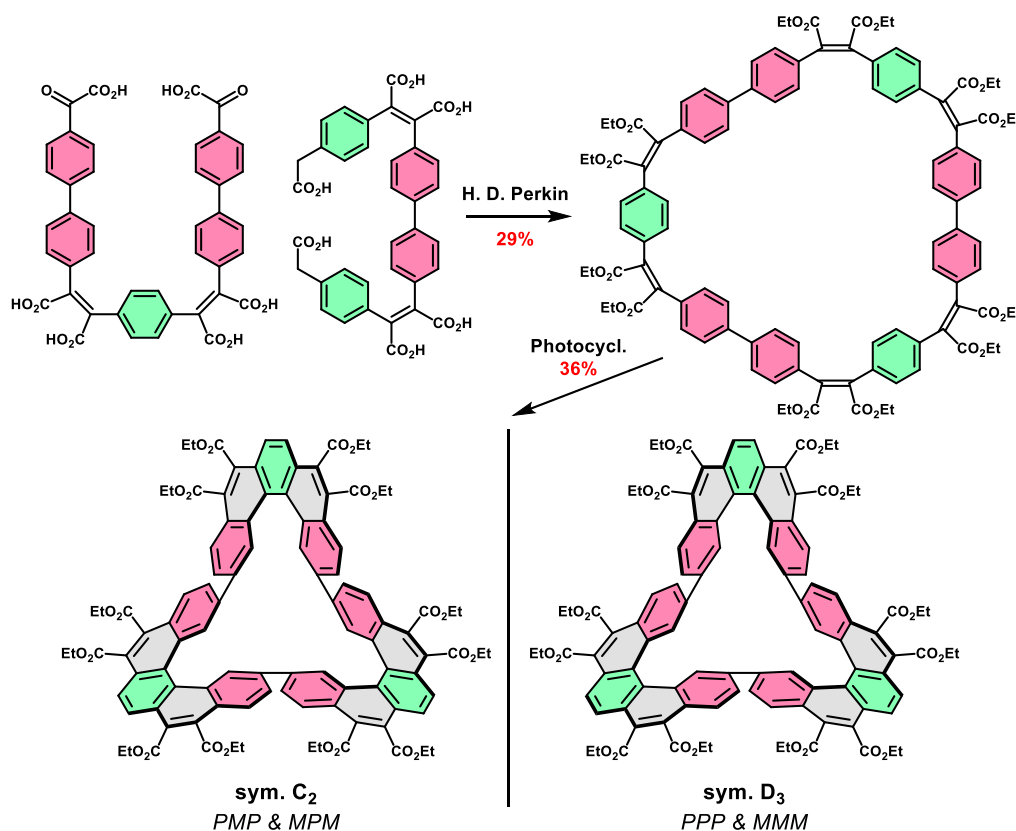


Figure 40. Synthesis of cyclo-tris-[5]helicene.

Cyclo-tris-[5]helicenes have molecular orbitals with a Möbius topology and manifest Möbius aromaticity on the π electron current, but they do not have a non-trivial topology, strictly speaking. This is due to the single bonds linking the [5]helicenes together. The presence of these connections means that it is not possible to consider the macrocycle as a ribbon (a single surface) and it is thus possible to draw it in two dimensions without any bonds crossing each other (Figure 41).

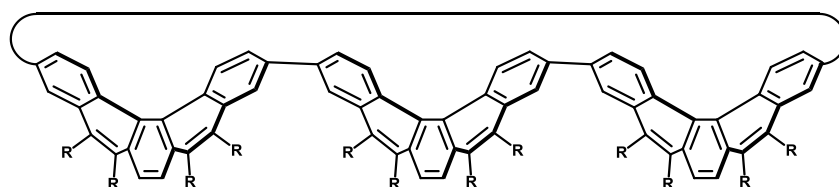


Figure 41. 2D representation of the cyclo-tris-[5]helicene with a D_3 symmetry.

Finally, obtaining trifunctionalized elementary building blocks compatible with the Perkin strategy allowed the synthesis of a cyclophane with three [5]helicene bridges.¹⁰⁶ For this, a 1,3,5-triphenylbenzene-4',4'',4'''-triglyoxylic acid was obtained in three steps from 4-bromoacetophenone. It was then engaged in a Perkin reaction with three equivalents of monoprotected biphenyl-4,4'-diglyoxylic acid to give a flexible triacetic intermediate. The latter was finally involved in a macrocyclization reaction in high dilution conditions, followed by a Mallory photocyclization reaction to give a rigid macrobicyclic cyclophane (Figure 42).

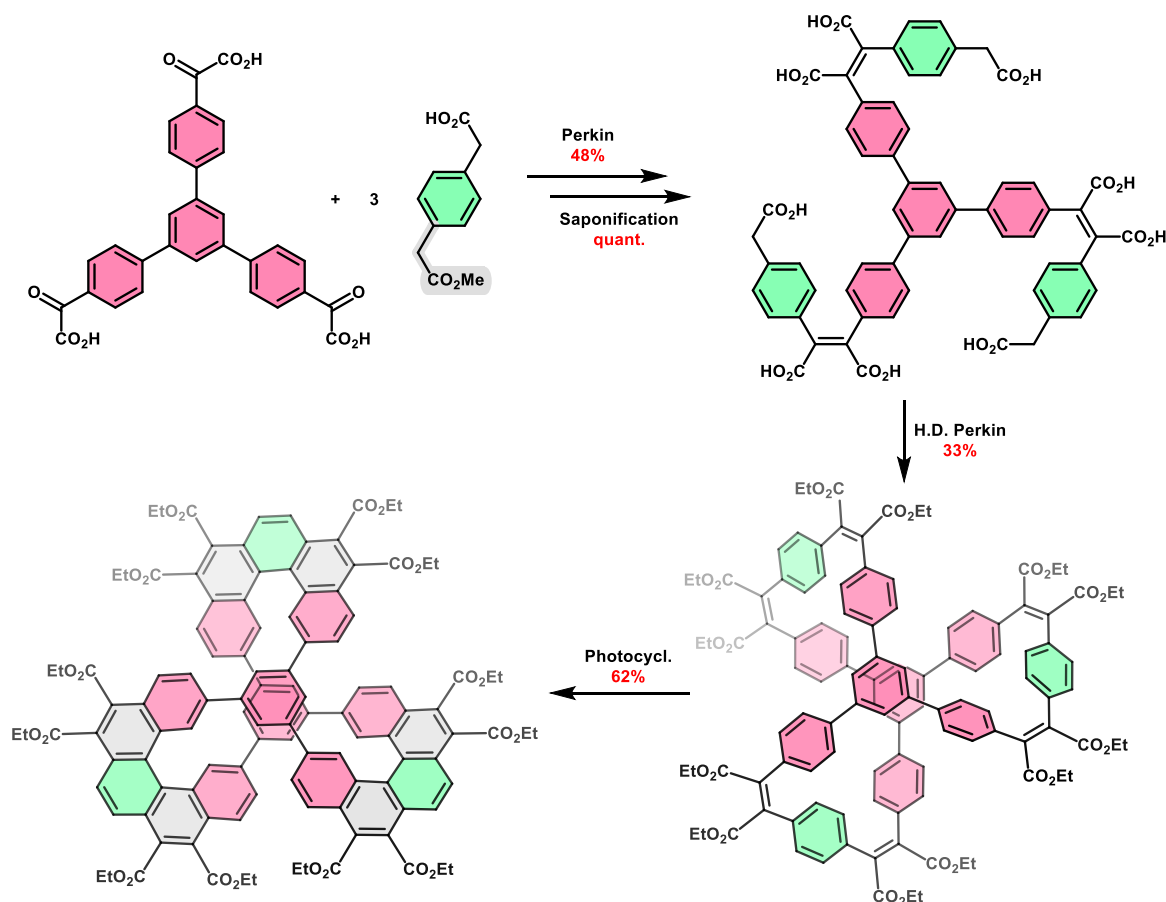


Figure 42. Synthesis of a macrobicyclic cyclophane bridged by three [5]helicenes.

Most systems with π - π interactions adopt a slipped-stack structure to minimize electrostatic repulsions between π electrons. In the case of this macrocycle, the structural rigidity imposed by the [5]helicenes force the central benzene rings to perfectly face each other. As these two central benzenes are planar and parallel, and the other benzene rings of the macrocycle deviate moderately from this plane, it was possible to perform analysis of the anisotropic current density. Using the AICD software, the induced current density of the macrocycle was calculated as a vector on the AICD isosurface. These calculations showed that there is an overall circuit of 78 π electrons, with the central rings acting as bridges between the helicenes.

IV. Thesis project: The synthesis of topologically non-trivial nanoribbons

In mathematics, topology is a branch of geometry which is interested in objects considered infinitely deformable and in their properties which are preserved by these deformations, without however involving ruptures. In three dimensions of space, an object is called topologically trivial if it can be represented in only two dimensions, with deformations, without any superposition of the parts of the drawing. This is the case of a loop, a wire simply closed on itself, which although it can be represented with a crossing (Figure 43b) can also be slightly deformed to be drawn as a circle (Figure 43a). On the other hand, if this thread is first knotted before being closed (Figure 43c), it can no longer be represented in two dimensions without crossing and the object thus obtained is topologically non-trivial.

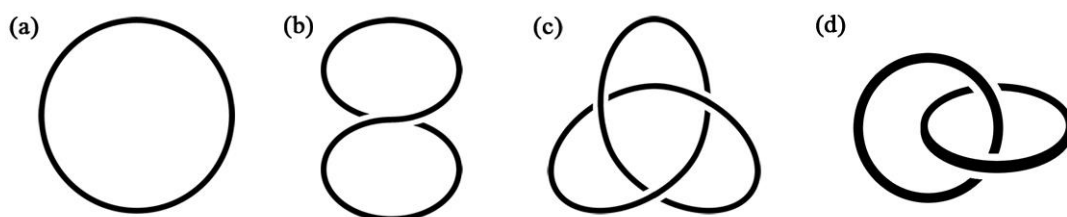


Figure 43. Representations of a loop without (a) or with a crossing (b), a single (c) and a multi-components (d) knots.

Single or multi-components knots (Figure 43d) constitute one of the largest families of topologically non-trivial objects that have been studied by mathematicians.¹⁰⁷ Some popular symbols are in fact objects with a non-trivial topology: the five interlocked Olympic Rings (Figure 44a), or the Borromean rings (Figure 44b). The trefoil knot (Figure 43c) belongs to the family of knots, where one thread, closed on itself, will form the necessary intertwining to give a non-planar graph.

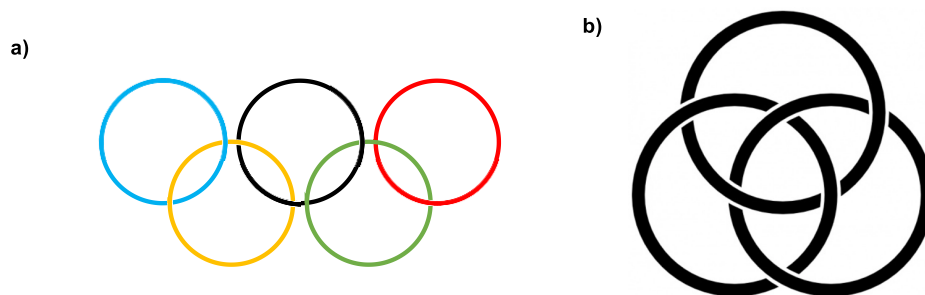


Figure 44. The Olympic Rings (a) and the Borromean rings (b).

In chemistry, topology entered laboratories when researchers tried to synthesize topologically non-trivial organic molecules, the main chain of which was considered as a string.^{108,109} This research was not very fruitful until the reasoned, reproducible and efficient obtaining of the first organic catenane, formed of two intertwined macrocycles, by Jean-Pierre Sauvage and his team in 1983,¹¹⁰ then by the formation of a trefoil knot in 1989.¹¹¹ Since then, chemical topology has inspired many other teams and particularly ambitious challenges have been taken up.¹¹² Thanks to high degrees of freedom between the components of such interlocked molecules, Sauvage's and Stoddart's pioneer work on topologically non-trivial compounds led them to develop the syntheses of molecular machines and they were both awarded a Nobel Prize in 2016, together with Feringa. In the last decades, the development of new synthetic strategies for the synthesis of PACs and PAHs allowed the synthesis of increasingly complex structures. Among them can be found catenated or trefoil knot CPPs (Figure 45), reported first by the team of Müllen,¹¹³ and later isolated by Itami and co.,¹¹⁴ but at the starting time of this thesis work, no examples of twisted CNBs were described yet in the literature.

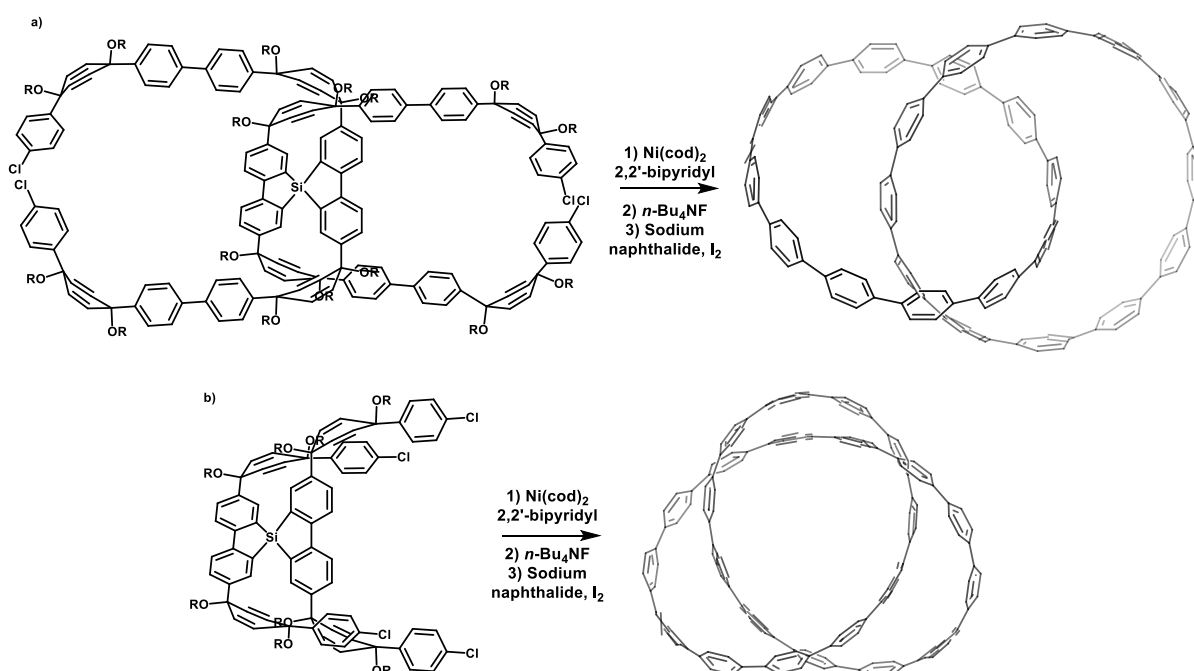


Figure 45. Synthesis of a catenated- (a) and trefoil knots-CPPs (b) synthesized by Itami.

The Perkin Strategy used in our team turns out to be a versatile and effective synthesis approach. The large library of multifunctional building blocks available and the use of protection techniques allows controlled assembly to obtain increasingly complex and atypical structures. The use of high dilution conditions disfavors the formation of oligomers to efficiently obtain macrocycles. Among the latest examples of macrocycles obtained by our research team, some of them have molecular orbitals whose nodal surface is a cyclic ribbon with a Möbius topology. Even though these three atypical molecules have persistent rigid geometries similar to twisted cyclic ribbons, considering of course that a benzene ring is a surface, they are not strictly topologically non-trivial due to the simple C-C bonds which still connect the helicenes between them (Figure 46)

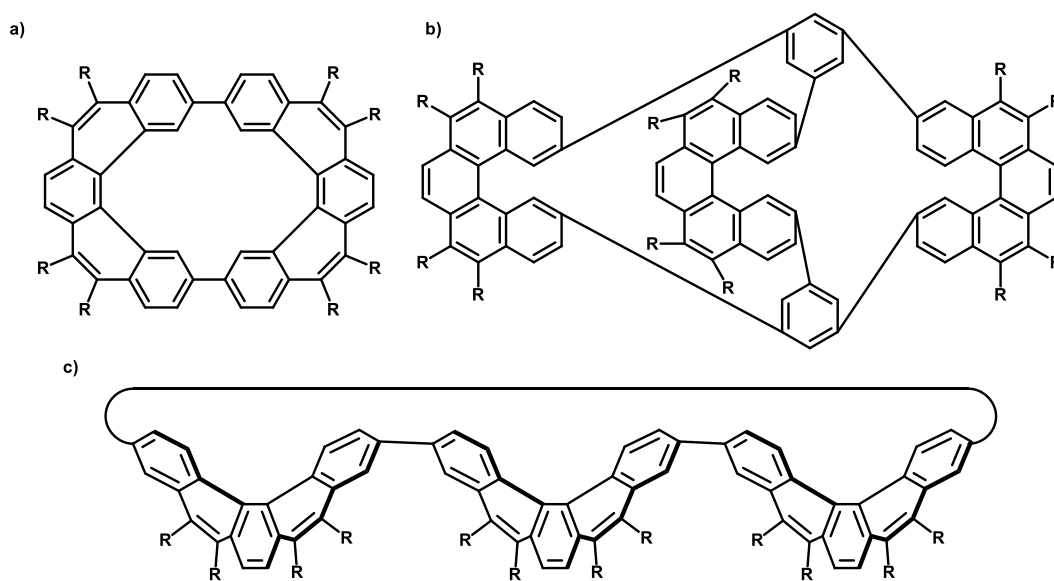


Figure 46. 2D representations of the cyclo-bis-[5]-helicene (a), macrobicyclic cyclophane (b) and the cyclo-tris-[5]helicene (c).

In order to eliminate this last defect, we adapted the existing synthesis strategies for each of these molecules in order to design their fully condensed counterparts and therefore the topologies would be non-trivial. This research work was entrusted to me and my goal was to synthesize these three fully condensed macrocycles over the course of the past three years. The first macrocycle, a figure-of-eight type nanoribbon (Figure 47a), would have the structure of ribbon with two 180° twists. The second one would be a nanoribbon with three 180° twists (Figure 47b), thus having only one side and one edge. Contrary to the other macrocycles, the last one would be a fully condensed bimacrocycle (Figure 47c). At the beginning of this thesis, there was no compound displaying a topologically non-trivial surface reported in the literature. These three structures would have been the first members of a new family of compounds with yet-to-be studied properties.

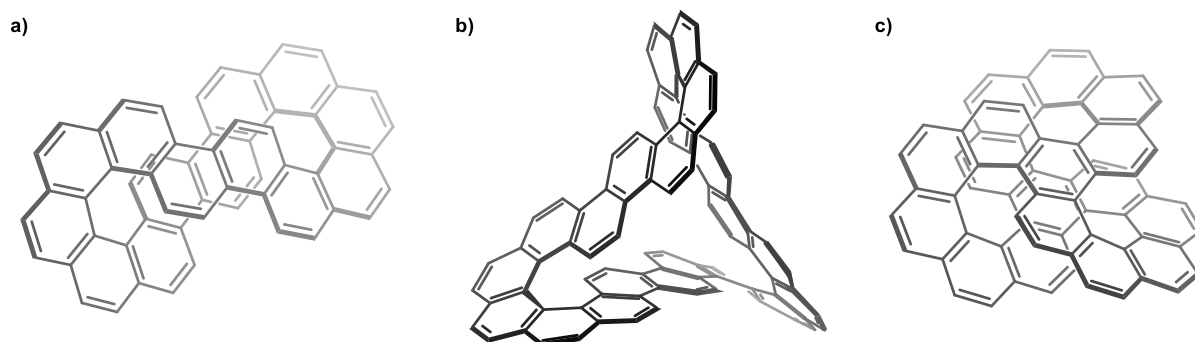


Figure 47. Polycyclic nanoribbons with a figure-of-eight shape (a), three 180° twists (b) and a bi-macrocyclic (c).

In this manuscript, we report the synthetic strategies that were used to attempt making these novel aromatic compounds. One building block used in the different strategy proved to be also valuable for the synthesis of two-block macrocycle. Two families of compounds were thus synthesized and their physical and chiroptical properties were studied. Finally, the targeted synthesis of a flexible macrocycle containing six phenanthrenes linked together by single bonds will be discussed in the last chapter.

References

- 1 F. P. Bundy and J. S. Kasper, *J. Chem. Phys.*, 1967, **46**, 3437–3446.
- 2 H. W. Kroto, J. R. Heath, S. C. O'Brien, R. F. Curl and R. E. Smalley, *Nature*, 1985, **318**, 162–163.
- 3 W. Krätschmer, L. D. Lamb, K. Fostiropoulos and D. R. Huffman, *Nature*, 1990, **347**, 354–358.
- 4 M. F. Jarrold, *Nature*, 2000, **407**, 26–27.
- 5 H. Prinzbach, A. Weiler, P. Landenberger, F. Wahl, J. Wörth, L. T. Scott, M. Gelmont, D. Olevano and B. v. Issendorff, *Nature*, 2000, **407**, 60–63.
- 6 H. Shinohara, H. Sato, Y. Saito, A. Izuoka, T. Sugawara, H. Ito, T. Sakurai and T. Matsuo, *Rapid Commun. Mass Spectrom.*, 1992, **6**, 413–416.
- 7 S. Wang, Q. Chang, G. Zhang, F. Li, X. Wang, S. Yang and S. I. Troyanov, *Front. Chem.*, 2020, **8**, 607712.
- 8 R. Bakry, R. M. Vallant, M. Najam-ul-Haq, M. Rainer, Z. Szabo, C. W. Huck and G. K. Bonn, *Int. J. Nanomedicine*.
- 9 D. M. Guldi, B. M. Illescas, C. M. Atienza, M. Wielopolski and N. Martín, *Chem. Soc. Rev.*, 2009, **38**, 1587.
- 10 W. Cai, C.-H. Chen, N. Chen and L. Echegoyen, *Acc. Chem. Res.*, 2019, **52**, 1824–1833.
- 11 L. Feng, Y. Hao, A. Liu and Z. Slanina, *Acc. Chem. Res.*, 2019, **52**, 1802–1811.
- 12 S. Iijima, *Nature*, 1991, **354**, 56–58.
- 13 M. Terrones, H. Terrones, M. S. Dresselhaus, G. Dresselhaus, J. C. Charlier and E. Hernández, *Philos. Trans. R. Soc. Lond. Ser. Math. Phys. Eng. Sci.*, 2004, **362**, 2065–2098.
- 14 M. Monthieux, *Carbon meta-nanotubes: synthesis, properties, and applications*, John Wiley & Sons, Hoboken, N.J., 2012.
- 15 A. Takakura, K. Beppu, T. Nishihara, A. Fukui, T. Kozeki, T. Namazu, Y. Miyauchi and K. Itami, *Nat. Commun.*, 2019, **10**, 3040.
- 16 M. Zhang, S. Fang, A. A. Zakhidov, S. B. Lee, A. E. Aliev, C. D. Williams, K. R. Atkinson and R. H. Baughman, *Science*, 2005, **309**, 1215–1219.
- 17 Z. Wu, Z. Chen, X. Du, J. M. Logan, J. Sippel, M. Nikolou, K. Kamaras, J. R. Reynolds, D. B. Tanner, A. F. Hebard and A. G. Rinzler, *Science*, 2004, **305**, 1273–1276.
- 18 D. A. Heller, S. Baik, T. E. Eurell and M. S. Strano, *Adv. Mater.*, 2005, **17**, 2793–2799.
- 19 J. Phiri, P. Gane and T. C. Maloney, *Mater. Sci. Eng. B*, 2017, **215**, 9–28.
- 20 K. S. Novoselov, A. K. Geim, S. V. Morozov, D. Jiang, Y. Zhang, S. V. Dubonos, I. V. Grigorieva and A. A. Firsov, *Science*, 2004, **306**, 666–669.
- 21 A. C. Ferrari, F. Bonaccorso, V. Fal'ko, K. S. Novoselov, S. Roche, P. Bøggild, S. Borini, F. H. L. Koppens, V. Palermo, N. Pugno, J. A. Garrido, R. Sordan, A. Bianco, L. Ballerini, M. Prato, E. Lidorikis, J. Kivioja, C. Marinelli, T. Ryhänen, A. Morpurgo, J. N. Coleman, V. Nicolosi, L. Colombo, A. Fert, M. Garcia-Hernandez, A. Bachtold, G. F. Schneider, F. Guinea, C. Dekker, M. Barbone, Z. Sun, C. Galiotis, A. N. Grigorenko, G. Konstantatos, A. Kis, M.

- Katsnelson, L. Vandersypen, A. Loiseau, V. Morandi, D. Neumaier, E. Treossi, V. Pellegrini, M. Polini, A. Tredicucci, G. M. Williams, B. Hee Hong, J.-H. Ahn, J. Min Kim, H. Zirath, B. J. van Wees, H. van der Zant, L. Occhipinti, A. Di Matteo, I. A. Kinloch, T. Seyller, E. Quesnel, X. Feng, K. Teo, N. Rupesinghe, P. Hakonen, S. R. T. Neil, Q. Tannock, T. Löfwander and J. Kinaret, *Nanoscale*, 2015, **7**, 4598–4810.
- 22 A. A. Balandin, S. Ghosh, W. Bao, I. Calizo, D. Teweldebrhan, F. Miao and C. N. Lau, *Nano Lett.*, 2008, **8**, 902–907.
- 23 N. P. Guisinger and M. S. Arnold, *MRS Bull.*, 2010, **35**, 273–279.
- 24 R. Mas-Ballesté, C. Gómez-Navarro, J. Gómez-Herrero and F. Zamora, *Nanoscale*, 2011, **3**, 20–30.
- 25 X. J. Lee, B. Y. Z. Hiew, K. C. Lai, L. Y. Lee, S. Gan, S. Thangalazhy-Gopakumar and S. Rigby, *J. Taiwan Inst. Chem. Eng.*, 2019, **98**, 163–180.
- 26 N. O. Weiss, H. Zhou, L. Liao, Y. Liu, S. Jiang, Y. Huang and X. Duan, *Adv. Mater.*, 2012, **24**, 5782–5825.
- 27 P. Rani and V. K. Jindal, *RSC Adv*, 2013, **3**, 802–812.
- 28 M. Shahrokhi and C. Leonard, *J. Alloys Compd.*, 2017, **693**, 1185–1196.
- 29 Y. Yano, N. Mitoma, H. Ito and K. Itami, *J. Org. Chem.*, 2020, **85**, 4–33.
- 30 I. A. Stepek, M. Nagase, A. Yagi and K. Itami, *Tetrahedron*, 2022, 132907.
- 31 A. Narita, X. Feng and K. Müllen, *Chem. Rec.*, 2015, **15**, 295–309.
- 32 J. Cai, P. Ruffieux, R. Jaafar, M. Bieri, T. Braun, S. Blankenburg, M. Muoth, A. P. Seitsonen, M. Saleh, X. Feng, K. Müllen and R. Fasel, *Nature*, 2010, **466**, 470–473.
- 33 J. Liu, B.-W. Li, Y.-Z. Tan, A. Giannakopoulos, C. Sanchez-Sanchez, D. Beljonne, P. Ruffieux, R. Fasel, X. Feng and K. Müllen, *J. Am. Chem. Soc.*, 2015, **137**, 6097–6103.
- 34 P. Ruffieux, S. Wang, B. Yang, C. Sánchez-Sánchez, J. Liu, T. Dienel, L. Talirz, P. Shinde, C. A. Pignedoli, D. Passerone, T. Dumslaff, X. Feng, K. Müllen and R. Fasel, *Nature*, 2016, **531**, 489–492.
- 35 P. Han, K. Akagi, F. Federici Canova, H. Mutoh, S. Shiraki, K. Iwaya, P. S. Weiss, N. Asao and T. Hitosugi, *ACS Nano*, 2014, **8**, 9181–9187.
- 36 K. Yu. Amsharov and P. Merz, *J. Org. Chem.*, 2012, **77**, 5445–5448.
- 37 A.-K. Steiner and K. Y. Amsharov, *Angew. Chem. Int. Ed.*, 2017, **56**, 14732–14736.
- 38 M. Kolmer, A.-K. Steiner, I. Izydorczyk, W. Ko, M. Engelund, M. Szymonski, A.-P. Li and K. Amsharov, *Science*, 2020, **369**, 571–575.
- 39 R. S. Jordan, Y. Wang, R. D. McCurdy, M. T. Yeung, K. L. Marsh, S. I. Khan, R. B. Kaner and Y. Rubin, *Chem*, 2016, **1**, 78–90.
- 40 R. S. Jordan, Y. L. Li, C.-W. Lin, R. D. McCurdy, J. B. Lin, J. L. Brosmer, K. L. Marsh, S. I. Khan, K. N. Houk, R. B. Kaner and Y. Rubin, *J. Am. Chem. Soc.*, 2017, **139**, 15878–15890.
- 41 X. Yang, X. Dou, A. Rouhanipour, L. Zhi, H. J. Räder and K. Müllen, *J. Am. Chem. Soc.*, 2008, **130**, 4216–4217.
- 42 K. T. Kim, J. W. Jung and W. H. Jo, *Carbon*, 2013, **63**, 202–209.
- 43 M. G. Schwab, A. Narita, Y. Hernandez, T. Balandina, K. S. Mali, S. De Feyter, X. Feng and K. Müllen, *J. Am. Chem. Soc.*, 2012, **134**, 18169–18172.
- 44 T. H. Vo, M. Shekhirev, D. A. Kunkel, M. D. Morton, E. Berglund, L. Kong, P. M. Wilson, P. A. Dowben, A. Enders and A. Sinitskii, *Nat. Commun.*, 2014, **5**, 3189.
- 45 S. von Kugelgen, I. Piskun, J. H. Griffin, C. T. Eckdahl, N. N. Jarenwattananon and F. R. Fischer, *J. Am. Chem. Soc.*, 2019, **141**, 11050–11058.
- 46 W. Tian, W. Li, W. Yu and X. Liu, *Micromachines*, DOI:10.3390/mi8050163.
- 47 W. E. Barth and R. G. Lawton, *J. Am. Chem. Soc.*, 1966, **88**, 380–381.
- 48 L. T. Scott, E. A. Jackson, Q. Zhang, B. D. Steinberg, M. Bancu and B. Li, *J. Am. Chem. Soc.*, 2012, **134**, 107–110.
- 49 B. Liu, J. Liu, H.-B. Li, R. Bholra, E. A. Jackson, L. T. Scott, A. Page, S. Irle, K. Morokuma and C. Zhou, *Nano Lett.*, 2015, **15**, 586–595.
- 50 Z.-Z. Zhu, Z.-C. Chen, Y.-R. Yao, C.-H. Cui, S.-H. Li, X.-J. Zhao, Q. Zhang, H.-R. Tian, P.-Y. Xu, F.-F. Xie, X.-M. Xie, Y.-Z. Tan, S.-L. Deng, J. M. Quimby, L. T. Scott, S.-Y. Xie, R.-B. Huang and L.-S. Zheng, *Sci. Adv.*, 2019, **5**, eaaw0982.
- 51 J. H. Dopper, D. Oudman and H. Wynberg, *J. Org. Chem.*, 1975, **40**, 3398–3401.
- 52 K. Kawasumi, Q. Zhang, Y. Segawa, L. T. Scott and K. Itami, *Nat. Chem.*, 2013, **5**, 739–744.
- 53 J. M. Fernández-García, P. J. Evans, S. Medina Rivero, I. Fernández, D. García-Fresnadillo, J. Perles, J. Casado and N. Martín, *J. Am. Chem. Soc.*, 2018, **140**, 17188–17196.
- 54 X. Qiao, D. M. Ho and R. A. Pascal Jr., *Angew. Chem. Int. Ed. Engl.*, 1997, **36**, 1531–1532.
- 55 J. Zhang, D. M. Ho and R. A. Pascal, *Tetrahedron Lett.*, 1999, **40**, 3859–3862.
- 56 J. Lu, D. M. Ho, N. J. Vogelaar, C. M. Kraml and R. A. Pascal, *J. Am. Chem. Soc.*, 2004, **126**, 11168–11169.

- 57 J. Lu, D. M. Ho, N. J. Vogelaar, C. M. Kraml, S. Bernhard, N. Byrne, L. R. Kim and R. A. Pascal, *J. Am. Chem. Soc.*, 2006, **128**, 17043–17050.
- 58 R. G. Clevenger, B. Kumar, E. M. Menuey and K. V. Kilway, *Chem. – Eur. J.*, 2018, **24**, 3113–3116.
- 59 M. Gingras, *Chem. Soc. Rev.*, 2013, **42**, 968–1006.
- 60 R. Weitzenböck and H. Lieb, *Monatshefte Für Chem. Verwandte Teile Anderer Wiss.*, 1912, **33**, 549–565.
- 61 R. Weitzenböck and A. Klingler, *Monatshefte Für Chem. Verwandte Teile Anderer Wiss.*, 1918, **39**, 315–323.
- 62 J. Cook, *J. Chem. Soc. Resumed*, 1933, 1592–1597.
- 63 A. O. McIntosh, J. M. Robertson and V. Vand, *Nature*, 1952, **169**, 322–323.
- 64 A. O. McIntosh, J. M. Robertson and V. Vand, *J. Chem. Soc. Resumed*, 1954, 1661–1668.
- 65 M. S. Newman, W. B. Lutz and D. Lednicer, *J. Am. Chem. Soc.*, 1955, **77**, 3420–3421.
- 66 M. S. Newman and D. Lednicer, *J. Am. Chem. Soc.*, 1956, **78**, 4765–4770.
- 67 M. S. Newman and W. B. Lutz, *J. Am. Chem. Soc.*, 1956, **78**, 2469–2473.
- 68 M. S. Newman, R. S. Darlak and L. L. Tsai, *J. Am. Chem. Soc.*, 1967, **89**, 6191–6193.
- 69 M. Scholz, M. Mühlstädt and F. Dietz, *Tetrahedron Lett.*, 1967, **8**, 665–668.
- 70 M. Flammang-Barbieux, J. Nasielski and R. H. Martin, *Tetrahedron Lett.*, 1967, **8**, 743–744.
- 71 R. H. Martin, G. Morren and J. J. Schurter, *Tetrahedron Lett.*, 1969, **10**, 3683–3688.
- 72 G. J. Bodwell, J. N. Bridson, T. J. Houghton, J. W. J. Kennedy and M. R. Mannion, *Chem. – Eur. J.*, 1999, **5**, 1823–1827.
- 73 T. Otsubo, Y. Aso, F. Ogura, S. Misumi, A. Kawamoto and J. Tanaka, *Bull. Chem. Soc. Jpn.*, 1989, **62**, 164–170.
- 74 Y. Segawa, H. Ito and K. Itami, *Nat. Rev. Mater.*, 2016, **1**, 15002.
- 75 R. Jasti, J. Bhattacharjee, J. B. Neaton and C. R. Bertozzi, *J. Am. Chem. Soc.*, 2008, **130**, 17646–17647.
- 76 H. Takaba, H. Omachi, Y. Yamamoto, J. Bouffard and K. Itami, *Angew. Chem. Int. Ed.*, 2009, **48**, 6112–6116.
- 77 S. Yamago, Y. Watanabe and T. Iwamoto, *Angew. Chem. Int. Ed.*, 2010, **49**, 757–759.
- 78 E. Kayahara, T. Iwamoto, H. Takaya, T. Suzuki, M. Fujitsuka, T. Majima, N. Yasuda, N. Matsuyama, S. Seki and S. Yamago, *Nat. Commun.*, 2013, **4**, 2694.
- 79 K. Ikemoto, T. M. Fukunaga and H. Isobe, *Proc. Jpn. Acad. Ser. B*, 2022, **98**, 379–400.
- 80 T. M. Fukunaga, T. Kato, K. Ikemoto and H. Isobe, *Proc. Natl. Acad. Sci.*, 2022, **119**, e2120160119.
- 81 G. Wittig and G. Lehmann, *Chem. Ber.*, 1957, **90**, 875–892.
- 82 G. Povie, Y. Segawa, T. Nishihara, Y. Miyauchi and K. Itami, *Science*, 2017, **356**, 172–175.
- 83 G. Povie, Y. Segawa, T. Nishihara, Y. Miyauchi and K. Itami, *J. Am. Chem. Soc.*, 2018, **140**, 10054–10059.
- 84 K. Y. Cheung, S. Gui, C. Deng, H. Liang, Z. Xia, Z. Liu, L. Chi and Q. Miao, *Chem*, 2019, **5**, 838–847.
- 85 K. Y. Cheung, K. Watanabe, Y. Segawa and K. Itami, *Nat. Chem.*, 2021, **13**, 255–259.
- 86 Y. Han, S. Dong, J. Shao, W. Fan and C. Chi, *Angew. Chem. Int. Ed.*, 2021, **60**, 2658–2662.
- 87 M. A. Majewski, Y. Hong, T. Lis, J. Gregoliński, P. J. Chmielewski, J. Cybińska, D. Kim and M. Stępień, *Angew. Chem. Int. Ed.*, 2016, **55**, 14072–14076.
- 88 W. H. Perkin, *J. Chem. Soc.*, 1868, **21**, 181–186.
- 89 L. Sturm, F. Aribot, L. Soliman, H. Bock and F. Durola, *Eur. J. Org. Chem.*, 2022, **2022**, e202200196.
- 90 P. Sarkar, F. Durola and H. Bock, *Chem. Commun.*, 2013, **49**, 7552.
- 91 M. Ferreira, E. Giroto, A. Bentaleb, E. A. Hillard, H. Gallardo, F. Durola and H. Bock, *Chem. – Eur. J.*, 2015, **21**, 4391–4397.
- 92 L. Nassar-Hardy, C. Deraedt, E. Fouquet and F.-X. Felpin, *Eur. J. Org. Chem.*, 2011, **2011**, 4616–4622.
- 93 F. B. Mallory and C. W. Mallory, in *Organic Reactions*, 2005, pp. 1–456.
- 94 T. S. Moreira, M. Ferreira, A. Dall’armellina, R. Cristiano, H. Gallardo, E. A. Hillard, H. Bock and F. Durola, *Eur. J. Org. Chem.*, 2017, **2017**, 4548–4551.
- 95 G. Naulet, A. Robert, P. Dechambenoit, H. Bock and F. Durola, *Eur. J. Org. Chem.*, 2018, **2018**, 619–626.
- 96 G. Naulet, S. Huet-Exiga, H. Bock and F. Durola, *Org. Chem. Front.*, 2019, **6**, 994–997.
- 97 R. H. Martin, *Angew. Chem. Int. Ed. Engl.*, 1974, **13**, 649–660.
- 98 M. G. Belarmino Cabral, D. M. Pereira de Oliveira Santos, R. Cristiano, H. Gallardo, A. Bentaleb, E. A. Hillard, F. Durola and H. Bock, *ChemPlusChem*, 2017, **82**, 342–346.
- 99 R. Wang, K. Shi, K. Cai, Y. Guo, X. Yang, J.-Y. Wang, J. Pei and D. Zhao, *New J. Chem.*, 2016, **40**, 113–121.
- 100 M. Ferreira, G. Naulet, H. Gallardo, P. Dechambenoit, H. Bock and F. Durola, *Angew. Chem. Int. Ed.*, 2017, **56**, 3379–3382.
- 101 M. Ferreira, T. S. Moreira, R. Cristiano, H. Gallardo, A. Bentaleb, P. Dechambenoit, E. A. Hillard, F. Durola and H. Bock, *Chem. – Eur. J.*, 2018, **24**, 2214–2223.

- 102 A. Robert, P. Dechambenoit, H. Bock and F. Durola, *Can. J. Chem.*, 2017, **95**, 450–453.
- 103 A. Robert, P. Dechambenoit, E. A. Hillard, H. Bock and F. Durola, *Chem Commun*, 2017, **53**, 11540–11543.
- 104 A. Robert, G. Naulet, H. Bock, N. Vanthuyne, M. Jean, M. Giorgi, Y. Carissan, C. Aroulanda, A. Scalabre, E. Pouget, F. Durola and Y. Coquerel, *Chem. – Eur. J.*, 2019, **25**, 14364–14369.
- 105 G. Naulet, L. Sturm, A. Robert, P. Dechambenoit, F. Röhricht, R. Herges, H. Bock and F. Durola, *Chem. Sci.*, 2018, **9**, 8930–8936.
- 106 F. Aribot, A. Merle, P. Dechambenoit, H. Bock, A. Artigas, N. Vanthuyne, Y. Carissan, D. Hagebaum-Reignier, Y. Coquerel and F. Durola, *Angew. Chem. Int. Ed.*, 2023, **62**, e202304058.
- 107 C. Adams, *The knot book: an elementary introduction to the mathematical theory of knots*, American Mathematical Society, Providence, R.I, 2004.
- 108 H. L. Frisch and E. Wasserman, *J. Am. Chem. Soc.*, 1961, **83**, 3789–3795.
- 109 G. Schill and A. Lüttringhaus, *Angew. Chem. Int. Ed. Engl.*, 1964, **3**, 546–547.
- 110 C. O. Dietrich-Buchecker, J. P. Sauvage and J. P. Kintzinger, *Tetrahedron Lett.*, 1983, **24**, 5095–5098.
- 111 C. O. Dietrich-Buchecker and J.-P. Sauvage, *Angew. Chem. Int. Ed. Engl.*, 1989, **28**, 189–192.
- 112 K. S. Chichak, S. J. Cantrill, A. R. Pease, S.-H. Chiu, G. W. V. Cave, J. L. Atwood and J. F. Stoddart, *Science*, 2004, **304**, 1308–1312.
- 113 W. Zhang, A. Abdulkarim, F. E. Golling, H. J. Räder and K. Müllen, *Angew. Chem. Int. Ed.*, 2017, **56**, 2645–2648.
- 114 Y. Segawa, M. Kuwayama, Y. Hijikata, M. Fushimi, T. Nishihara, J. Pirillo, J. Shirasaki, N. Kubota and K. Itami, *Science*, 2019, **365**, 272–276.

Chapter 2: Synthesis of topologically non-trivial macrocycles

I. Introduction

Most of the daily-life objects we know are two-sided objects, they have an “inside” and an “outside”, and it is not possible to move from one side to the other without crossing its surface. Compared to knots, which are made up of threads with no thickness, ribbons have a non-zero width, and therefore a surface area. In this case, the twist of a cyclic ribbon is an additional criterion necessary for the description of its topology.¹ The best-known topologically non-trivial geometric figure in this last family is the Möbius ribbon, named after the works of Möbius and Listing.^{2,3} It consists of a ribbon closed on itself after having made a half-turn of twisting. This atypical object thus has a single face and a single edge. There is a strong correlation between topologically non-trivial knots and ribbons. Indeed, from a wire figure, it is possible to define one or more finite surfaces, called Seifert surfaces, whose edge is this wire figure. Thus, the simple Möbius strip is a topologically non-trivial Seifert surface of a twisted loop (Figure 48a). If a full twist is applied to a ribbon before closing it on itself, the object obtained (Figure 48b), called "figure of eight" has two faces and two edges, the latter being intertwined. If three half twists are applied to the strip before closing it on itself, we again obtain a Möbius strip, with a single face and a single edge, but this time the latter has the shape of a trefoil knot (Figure 48c). According to Herges,⁴ one of the oldest examples of a man-made object with a Möbius topology comes from a series of canons written by Johann Sebastian Bach in 1747, the oldest being a retrograde canon written by a medieval composer, Guillaume de Machaut. Cutting Bach’s canon and pasting it back with a half twist will give an endless Möbius-shaped score, where the two violins exchange their parts after every turn. Möbius-shaped objects have now found applications in devices, like Möbius conveyor belts and non-inductive Möbius resistors.

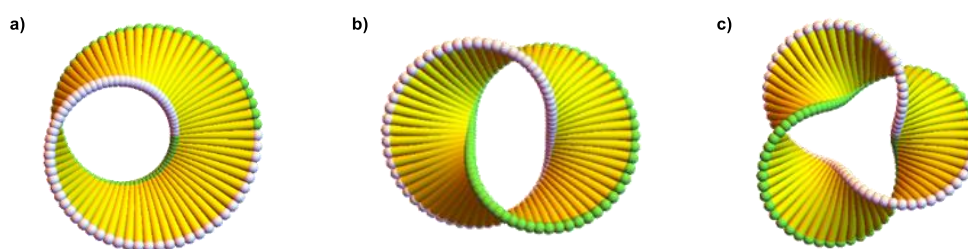


Figure 48. Representation of Möbius bands with one (a), two (b) and three (c) 180° twists.

Applying the Möbius topology to a molecular assembly would require a surface to be twisted, likely a molecular band with two edges or a π system. In 1982, Walba’s team reported the synthesis of the first band-type Möbius molecule.⁵ The rope-ladder type structure was obtained by reaction in high dilution conditions between ethylene “rungs” and two polyether “ropes” (Figure 49) .

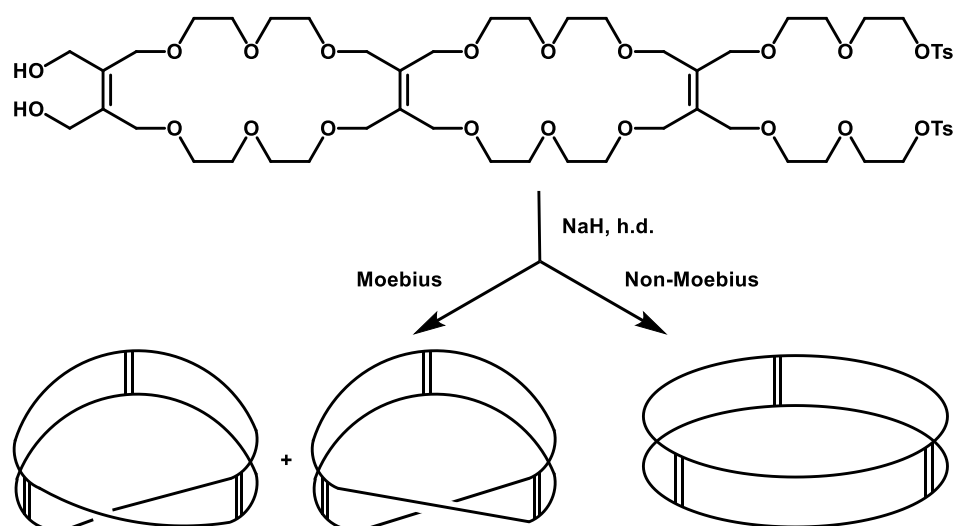


Figure 49. Rope-ladder structure obtained by Walba and co.

Several compounds with a Möbius topology have been synthesized. Möbius-shaped annulenes and porphyrinoid systems were also reported. The family of Möbius-shaped molecules quickly expanded in the last decades, but the first examples of Möbius carbon nanobelts were only reported during the last three years. The synthesis of carbon nanobelts already represented a great synthetic challenge due to the high tension induced by the macrocyclic structure. Introducing one or more twists would logically increase further the already present tension. Yet the assembly of building blocks leading to a flexible precursor, followed by a final rigidification step, proved to be the right approach for the synthesis of twisted CNBs. The strain in the cycle slowly increased over each cyclization, easing the twisting process. Thanks to this approach, Wu and Isobe,^{6,7} quickly followed by Itami,⁸ reported the synthesis of CNBs with two 180° twists (Figure 50b and 50c). The synthesis of a nanoribbon with one 180° twist was published soon after by Itami (Figure 50a),⁹ while Isobe and Wu applied their synthetic strategy to synthesize a macrocyclic nanoribbon with three 180° twists (Figure 50d).¹⁰

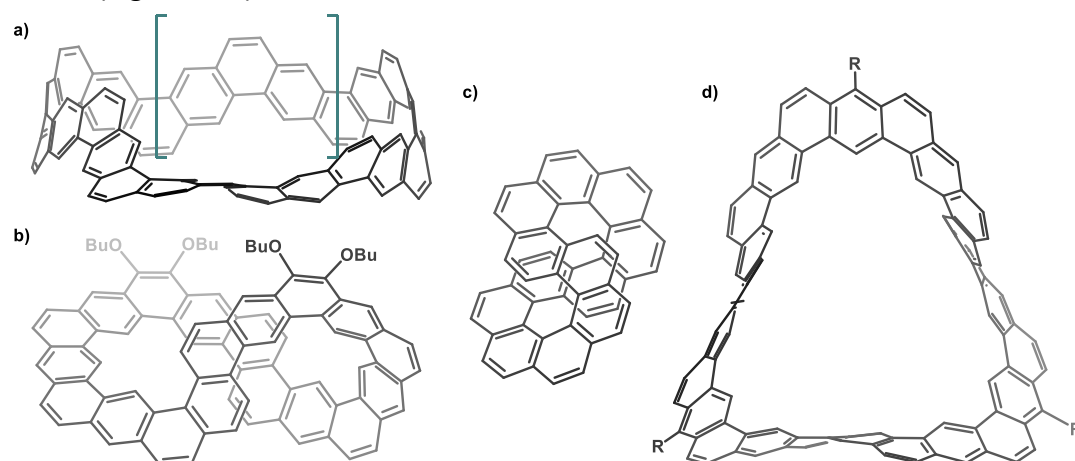


Figure 50. Topologically non-trivial aromatic nanoribbons obtained by Itami (a and c), and by Wu and Isobe (b and d).

These astonishing structures were only reported over the last three years, meaning that at the start of this Ph.D. project, the three target macrocycles were highly innovative structures

with unpredictable electronic properties. During the last three years, the focus has been put on the synthesis of *figure-of-eight* and triply twisted nanoribbons, as their retrosyntheses involve the same building blocks (Figure 51). Both macrocycles can indeed be obtained from bifunctional 3,6-phenanthrene and 1,5-naphthalene. Simulations showed that, with these building blocks, the tension that builds up during the successive formations of the C-C bonds in the triply twisted nanoribbons is barely higher than the usual distortion observed in a helicene compound. This would greatly ease the final step of photocyclisation and encouraged us to aim for a strategy using these building blocks. In this chapter, we report the synthetic approaches used for the synthesis of the *figure-of-eight* and the triply twisted nanoribbons. The first synthetic strategy relied on the formation of flexible four- and six-unit precursors by a high dilution Perkin reaction with a stoichiometric mixture of phenanthrene-3,6-diglyoxylic acid and naphthalene-1,5-diacetic acid.

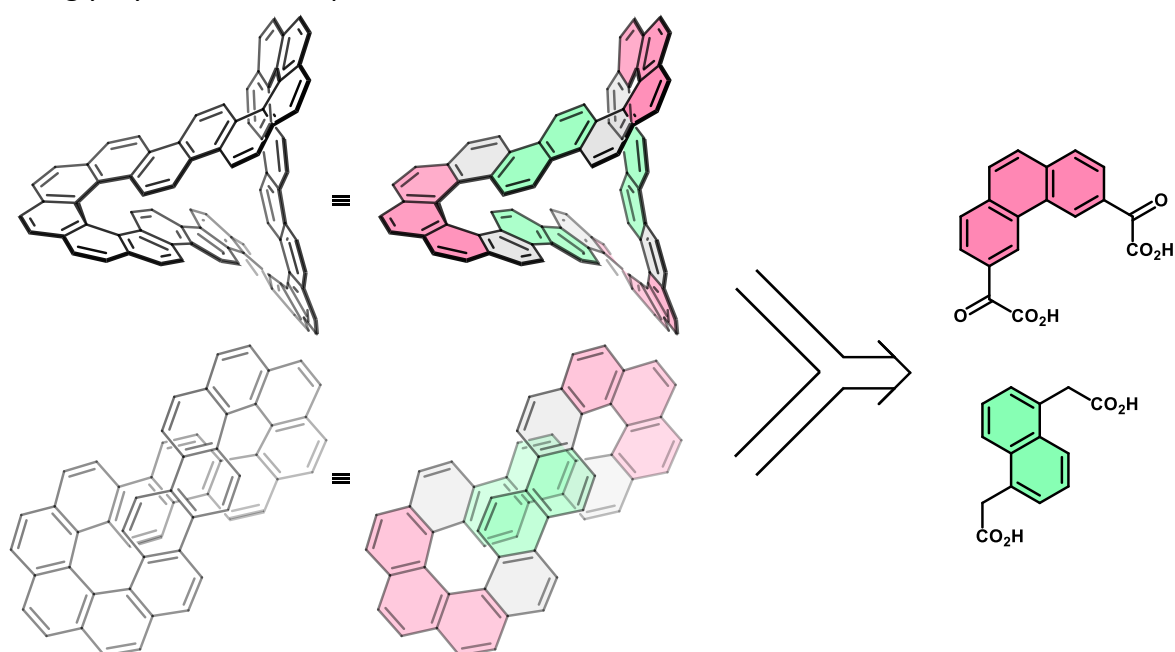


Figure 51. Retrosynthesis of the triply twisted macrocycle and the figure-of-eight.

II. Synthetic strategy involving two bifunctional building blocks

a. Synthesis of building blocks

One of the building blocks required for the macrocyclization reaction is the naphthalene-1,5-diacetic acid. Thanks to the synthetic technique developed in our group, this building block is easily obtained from commercially available 1,5-dibromonaphthalene. The reaction of *t*BuLi on the dibrominated naphthalene at -97 °C in THF leads to the formation of a dilithiated naphthalene after a double lithium-halogen exchange (4). Once a halogen-lithium exchange happens, another equivalent of *t*BuLi will react by beta-elimination with the newly formed bromobutane to yield isobutene. Two equivalents of *t*BuLi per brominated position on the aromatic core are therefore needed. After 3 hours of stirring, diethyl oxalate was added. The fast addition of a large excess of diethyl oxalate at -97 °C limits polymerisation and favours the formation of the diglyoxylic ester product. After an acidic work-up, extraction of the aqueous layer with CH₂Cl₂ and drying on MgSO₄, the solvents were removed under reduced

pressure until a yellow oil remained. The oil was let to dry in the fume hood for the night, in order to remove a maximum of remaining diethyl oxalate in soft conditions. Recrystallization in ethanol of the final yellow solid allowed to easily isolate the desired product **II-1** as thin yellow crystals with an 83% yield. Saponification of **II-1** in mild conditions yielded quantitatively the diglyoxylic acid **II-2** after filtration of the white precipitate that separated after addition of aqueous HCl to the reaction medium.

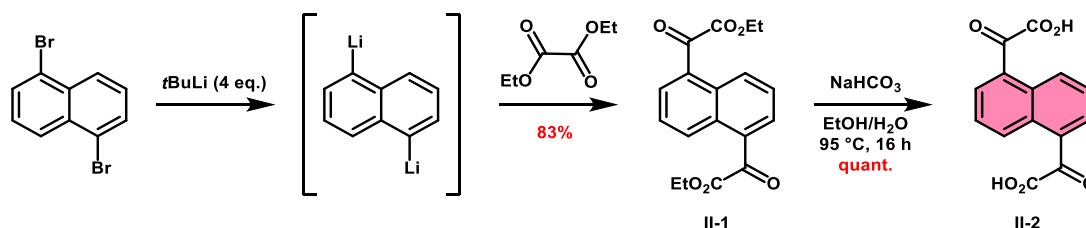


Figure 52. Synthesis of naphthalene-1,5-diglyoxylic acid **II-2** from 1,5-dibromonaphthalene.

The diglyoxylic acid obtained from this saponification can already be used as a building block for Perkin reactions but our designed approach requires acetic functions on the naphthalene building blocks. **II-2** was therefore reduced in presence of H_3PO_2 and NaI within three days in refluxing acetic acid (Figure 53). A white precipitate appeared after the addition of water to the solution. The solid was filtered and dried for a day to give pure naphthalene-diacetic acid **II-3** in 65% yield.

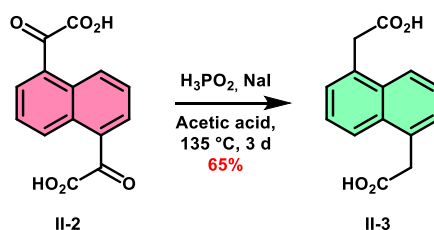


Figure 53. Synthesis of naphthalene-1,5-diacetic acid **II-3**.

The second required building block for the macrocyclization is phenanthrene-3,6-diglyoxylic acid, that should be obtained from 3,6-dibromophenanthrene according to our synthetic strategy. This brominated compound is not commercially available but its synthesis is known, in two steps from *p*-bromobenzaldehyde.^{11,12} Lithiation with *t*BuLi followed by *in situ* reaction with diethyl oxalate in the same condition as with the naphthalene gave phenanthrene-3,6-diglyoxylic diethyl ester **II-4** in 57% yield after recrystallization in ethanol. Saponification of **II-4** in mild conditions gave the phenanthrene-3,6-diglyoxylic acid **II-5** in 91% yield (Figure 54).

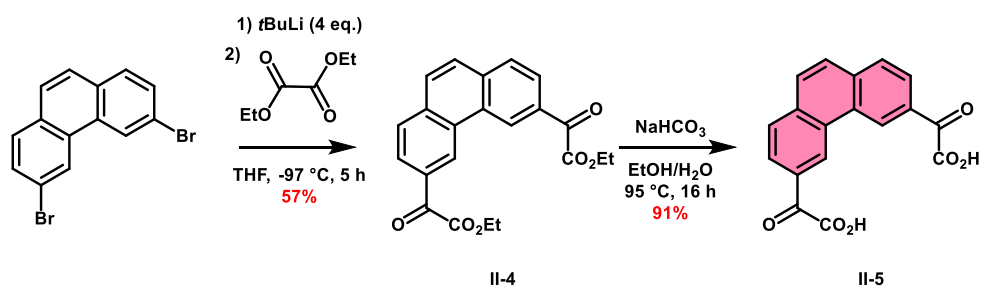


Figure 54. Synthesis of phenanthrene-3,6-diglyoxylic acid **II-5** from 3,6-dibromophenanthrene.

Diacid **II-5** was the first considered building block for our approach, but it appeared that its production is strongly limited by the photocyclization step required to form 3,6-dibromophenanthrene. Although the reaction is efficient, only a small quantity of reagent can be introduced in the photoreactor to limit $[2\pi+2\pi]$ dimerization and this restriction slows down the production of 3,6-dibromophenanthrene. A more convenient approach was therefore considered, as well as slightly different phenanthrene-based building blocks, with additional substituents. Indeed, di-alkoxy substituted 3,6-dibromophenanthrenes appeared to be good candidates for our approach, as their synthesis is efficient, fast, and versatile. Dibromination of 9,10-phenanthrenequinone yielded 3,6-dibromophenanthrenequinone **II-6** in 96% yield.¹³ This efficient step works on the tens of grams scale, producing more than enough material for the next steps of the synthesis. Reduction of 3,6-dibromophenanthrenequinone by $\text{Na}_2\text{S}_2\text{O}_4$ followed by *in situ* nucleophilic substitution on a bromoalkane gave diether-substituted dibromophenanthrenes.¹⁴ This strategy allowed to efficiently produce 3,6-dibromo-9,10-diethoxyphenanthrene **II-7** in large quantity, even though the last step's yield remains modest (Figure 55).

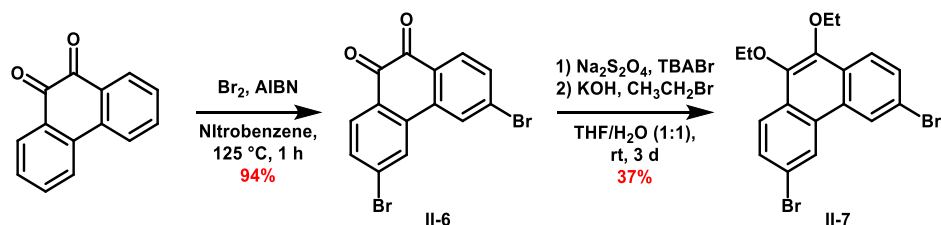


Figure 55. Synthesis of 3,6-dibromo-9,10-diethoxyphenanthrene **II-7**.

This dibrominated diethoxyphenanthrene was used for the synthesis of diethyl diethoxyphenanthrene-diglyoxylic ester **II-8** in 38% yield with the same procedure as for the synthesis of **II-4**. Saponification of the diester in basic conditions finally led quantitatively to the second diglyoxylic building block **II-9** (Figure 56).

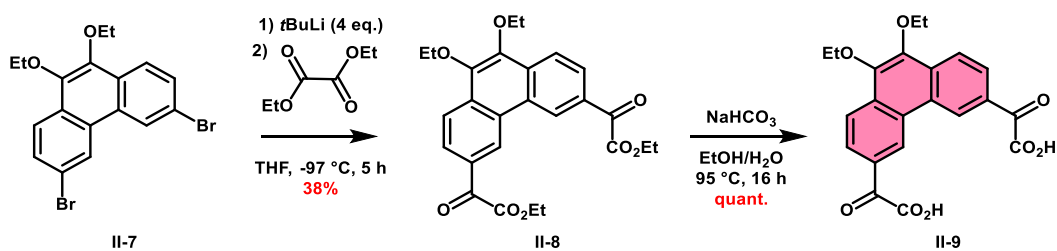


Figure 56. Synthesis of the diacidic phenanthrene building block **II-9**.

This last compound was however poorly soluble in THF, resulting in problems for respecting the strict stoichiometry in a high dilution Perkin reaction. Replacement of the ethyl chains by *n*-butyl chains was therefore considered to increase the solubility of the acidic building block. Following the same strategy, reduction of the phenanthrenequinone involving bromobutane in the second step led to the formation of 3,6-dibromo-9,10-bisbutyloxyphenanthrene **II-10** with an 85% yield after purification by column chromatography. Instead of using diethyl oxalate for the next step of the synthetic route, dimethyl oxalate was retained as a reagent. This allowed simpler purification after removing the solvent, as the resulting crude solid needed only to be washed in methanol to remove the remaining dimethyl oxalate with the other impurities. This technique led to the formation of dimethyl 9,10-bisbutyloxyphenanthrene diglyoxylic ester **II-11** with 44% yield (Figure 57).

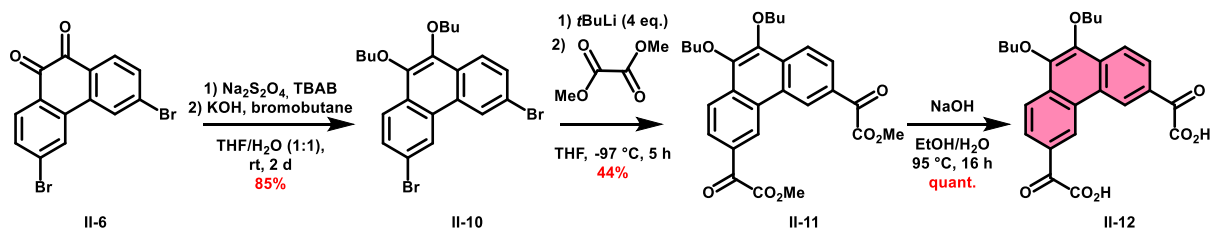


Figure 57. Synthesis of the bisbutyloxyphenanthrene-diacidic building block **II-12**.

b. Macrocyclization in stoichiometric conditions

Both building blocks were engaged in a macrocycle formation by Perkin reaction in high dilution conditions. Stoichiometric amounts of diacids **II-12** and **II-3** were dissolved in anhydrous THF. This solution was then added dropwise, over one day, to a refluxing solution of NEt_3 and Ac_2O in 1 L of anhydrous THF (Figure 58). By adding slowly both reagents to the reaction mixture, we expect that the building blocks contained in the falling drop will react together before the addition of the next drop, or at least before many drops are added. When several buildings blocks react together, forming flexible enough oligomers, the high dilution conditions favor intra- over intermolecular condensation, leading preferentially to macrocyclic compounds and limiting the formation of long linear oligomers.

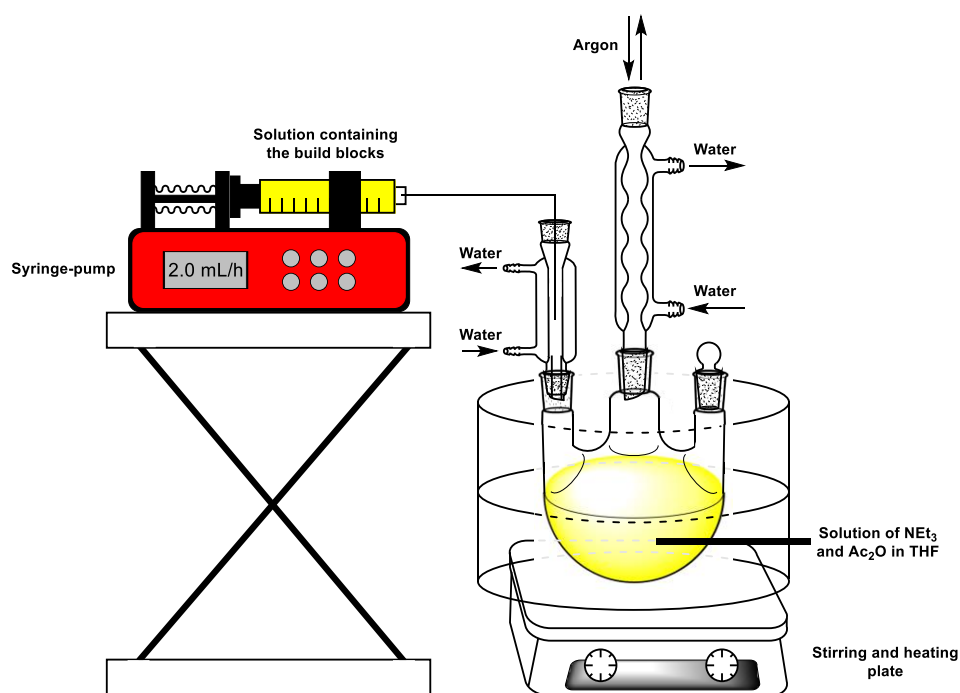


Figure 58. Set-up used for high-dilution Perkin reactions.

After the addition of the reagents, the mixture was stirred at reflux for three more days before addition of ethanol, bromoethane and DBU. After one day of reflux, the mixture was quenched with 100 mL of aqueous HCl (10%w). The aqueous layer was extracted with dichloromethane and the organic layers were then united and dried over MgSO_4 . After the solvent was removed under reduced pressure, the crude mixture was separated by silica gel column chromatography. ^1H NMR spectra of the isolated fractions showed that only one set of fractions contained a product with expected multiplicity and integration for either the four- or six-block flexible macrocycles. The ^1H NMR spectra of both macrocycles are similar, but mass spectrometry analysis of the sample revealed, to our surprise, that the product was neither the four- nor the six-block macrocycle. This analysis showed that the isolated product **II-13** was a cyclophane-like structure containing only two units, obtained in 8% yield. Despite changing the reaction conditions, only this small macrocycle, which we dubbed *microcycle*, is formed when using the bifunctional building blocks **II-3** and **II-12**.

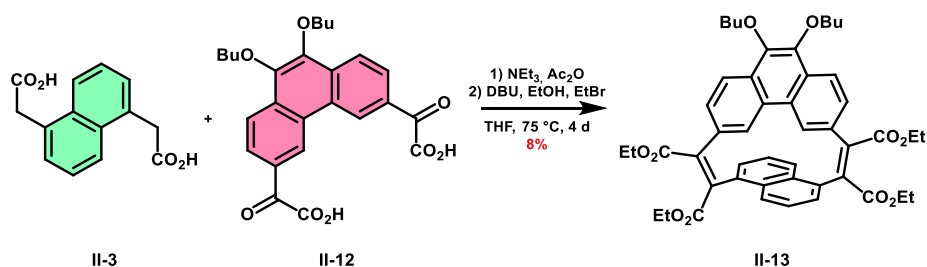


Figure 59. High dilution Perkin reaction, leading to the formation of phenanthrocyclophanediene **II-13**.

This revealed that 3,6-disubstituted phenanthrene, with its pincer-like structure, can be used to produce macrocycles containing only two units. We took advantage of this serendipitous discovery and explored further the synthesis of cyclophane-like macrocycles from

bifunctional phenanthrenes. These results will be addressed in the next chapter. As the high dilution Perkin reaction does not lead to the expected flexible larger macrocycles, a new strategy has been adopted to form them.

III. Synthesis of the macrocycles through controlled assembly

Using the protection and deprotection techniques known in our group, it is possible to synthesize two complementary flexible bifunctional precursors composed of three building blocks.¹⁵ This approach could be used to form two such precursors. One would be composed of a central naphthalene unit and two terminal phenanthrenes. The second one would be composed of a central phenanthrene unit and two terminal naphthalenes. Once isolated and after saponification, the latter could react with another phenanthrene unit to give a cyclic *figure-of-eight* precursor, or react with the complementary trimer to give the precursor of a triply twisted nanoribbon (Figure 60).

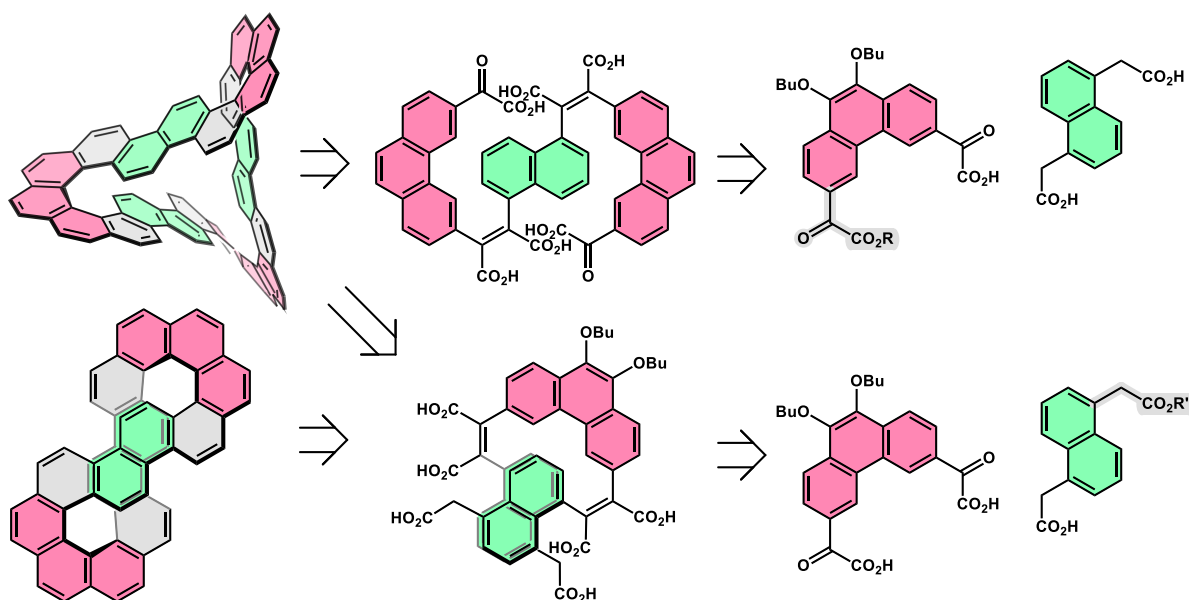


Figure 60. Synthetic strategy leading to the selective synthesis of both nanoribbons.

a. Synthesis of the monoprotected building blocks

i. Monoprotected naphthalene

In addition to the previously synthesized diacid building blocks **II-3** and **II-12**, two monoprotected building blocks are required for this strategy. The first is a known monoprotected naphthalene. Esterification of naphthalene-1,5-diacetic acid **II-3** in the presence of SOCl_2 in methanol led to the formation of diester **II-14** in 77% yield, isolated after recrystallization in MeOH (Figure 61).

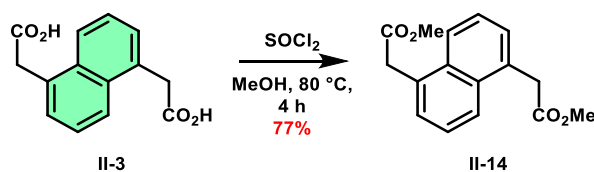


Figure 61. Esterification of naphthalene-1,5-diacetic acid **II-3**.

This diester was then saponified with only one equivalent of KOH in THF. After 70 minutes at reflux, a statistical mixture of products composed of the starting material **II-14** and the carboxylate forms of diacid **II-3** and mono-acid mono-ester **II-15** is obtained (Figure 62).

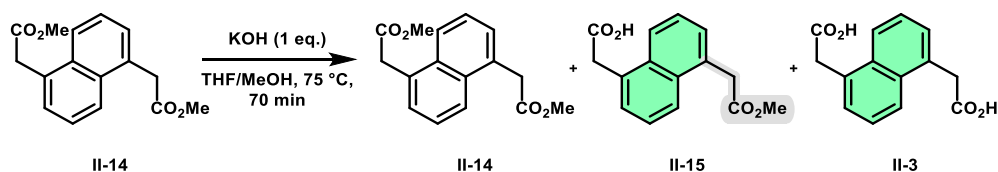


Figure 62. Monosaponification of diester **II-14**.

Once the solvent was removed under reduced pressure and the mixture dried, a succession of filtrations and pH-dependent precipitations allowed to easily isolate each compound. First the solid crude basic mixture was triturated in dichloromethane and filtered. This separated the diester **II-14** from the two insoluble ionic products (Figure 63a). The remaining solid was then dissolved in water and aqueous HCl (10%w) was added. This addition caused the formation of a white precipitate. The mixture was filtered and the solid triturated once again in dichloromethane. As the monoester was now in its protonated form, its solubility in dichloromethane drastically increased, while the diacid remained poorly soluble. The second filtration isolated the monoester **II-15** from the diacid **II-3** (Figure 63b). The dichloromethane was dried and removed under reduced pressure to yield **II-15** in 23% yield.

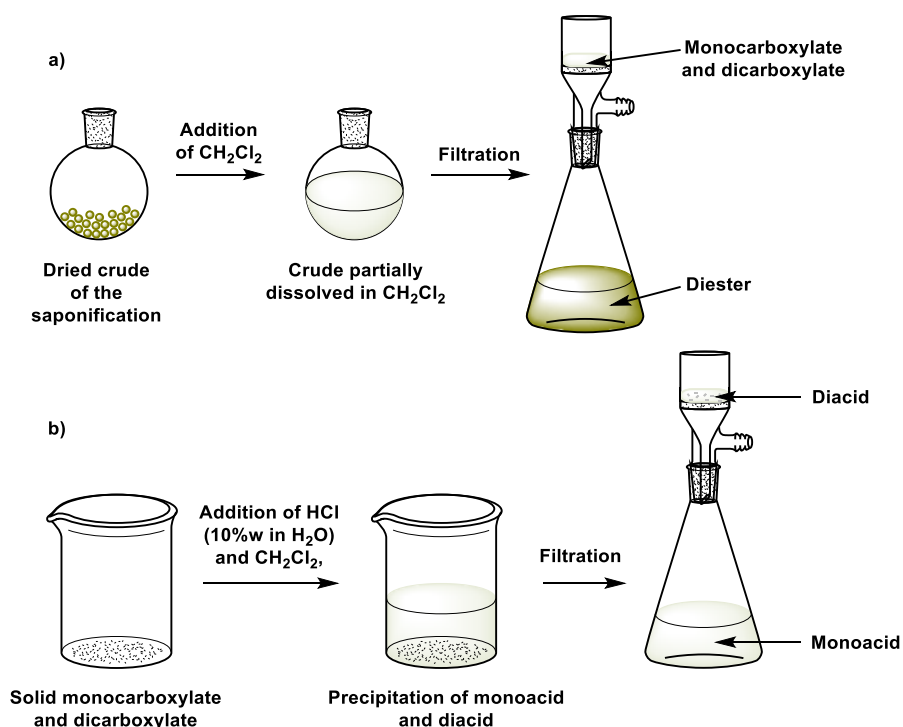


Figure 63. pH-controlled filtrations leading to the isolation of diester **II-14**, diacid **II-3** and monoprotected naphthalene **II-15**.

ii. Monoprotected phenanthrene

The second monoprotected building block is a phenanthrene-diglyoxylic monoester-monoacid. Dimethyl 9,10-bisbutyloxyphenanthrene-diglyoxylic ester **II-11** was saponified partially in a similar way as the naphthalene building block (Figure 64).

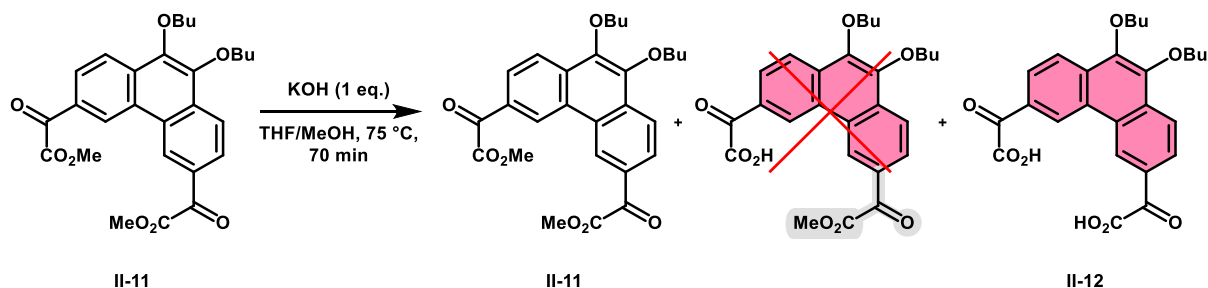


Figure 64. Monosaponification of diester **II-11.8**

After 70 minutes at reflux, the solvent was removed under reduced pressure. The products were separated by several pH-controlled filtrations. The soluble diester was successfully isolated from the mixture. The second filtration of the mixture of monoacid and diacid revealed that the diacid was partially soluble in dichloromethane and that, annoyingly, no monoester was produced in this reaction. As changing the concentration did not solve this problem, alternatives were considered.

The second approach consisted in using diethyl 9,10-bisbutyloxyphenanthrene-diglyoxylic ester **II-16**, obtained with the same conditions as for the synthesis of **II-11**, replacing dimethyl oxalate by diethyl oxalate. Unfortunately, the equimolar saponification again did not lead to the monoester (Figure 65).

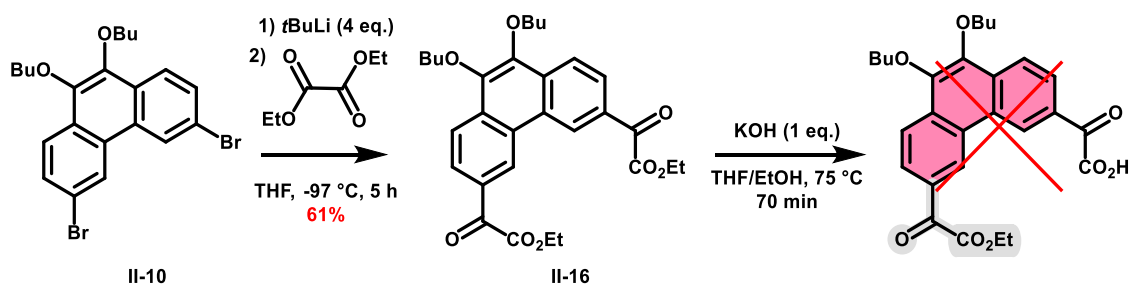


Figure 65. Synthesis of diethyl 9,10-bisbutyloxyphenanthrene-diglyoxylic ester **II-16** and monosaponification attempt.

The third attempt was done on the phenanthrene diethyl ether unit, as the solubility of the corresponding diacid was lower than the diacid with butyl ether functions. This strategy also proved to be unsuccessful, but we decided to insist on the idea of focusing on solubility. Our goal was to find conditions where the diester was soluble in the reaction medium, but once it reacted with an equivalent of KOH , the resulting mono-carboxylate would precipitate, limiting its reaction with a second equivalent of base. Using toluene instead of THF , the dimethyl 9,10-bisbutyloxyphenanthrene-diglyoxylic ester **II-11** was reacted with only one equivalent of KOH dissolved in methanol. After 70 minutes at reflux, a white precipitate was

formed, but analyses of the crude by ^1H NMR and TLC revealed that the reaction led once again only to the formation of the diester and the diacid. We finally decided to decrease the amount of methanol used during the reaction, generally representing 10% of the solvent used. Doing so would also impact the solubility of KOH in the reaction mixture. LiOH was then considered as a substitute to KOH and its solubility was not impacted by the low polarity of the solvent mixture. Using LiOH as a base allowed to decrease the amount of methanol to a concentration of only 1% (Figure 66).

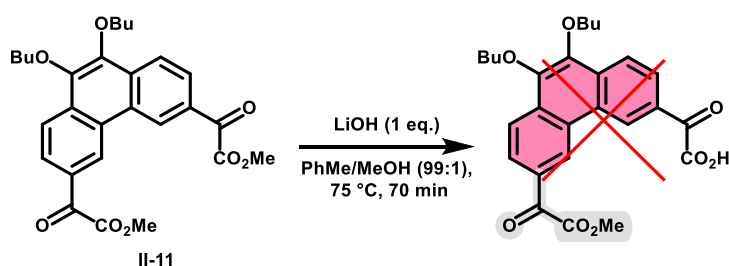


Figure 66. Final attempt on the monosaponification of II-11.

Once again, the formation of a white precipitate was observed. TLC showed that a third product was this time formed. pH-Controlled filtrations did not lead to the isolation of each compound, so purification on silica gel column chromatography was necessary. This purification allowed to isolate only a few milligrams of the expected monoprotected compound and the diacid could not be extracted from the silica gel. Unfortunately, this method proved to be not optimizable and not even reproducible, therefore we decided to try one last strategy. This time, the monoester would not be formed by saponification of the diester II-11, but by monoesterification of diacid II-12. This reaction would be performed by action of one equivalent of diazomethane, produced from commercially available N-methyl-N-nitroso-*p*-toluenesulfonamide, named Diazald (Figure 67a). Once formed, diazomethane can react with carboxylic acids to give methyl esters (Figure 67b).

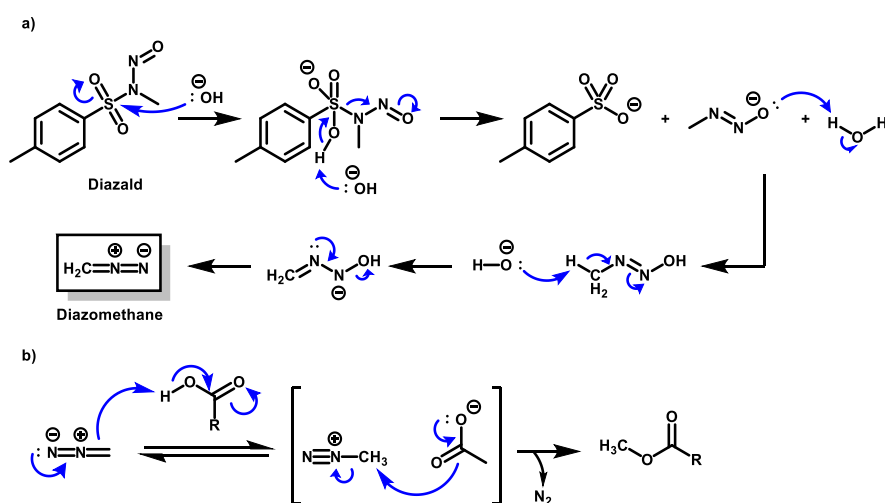


Figure 67. Formation of diazomethane from Diazald (a) and esterification of carboxylic acid to methyl esters (b).

As diazomethane is a very sensitive and toxic gas, it must be produced from a commercially available precursor and trapped in a solvent. The reaction of one equivalent of Diazald, in diethyl ether and kept in a 0 °C cooling bath, with an aqueous solution of KOH, produces dissolved diazomethane. The biphasic solution is composed of an aqueous lower layer, and an organic upper layer containing the diazomethane. Upon addition of the base, the organic layer went from orange to a bright yellow, pointing the formation of diazomethane. The organic layer was carefully taken with a glass dropper and added dropwise to a solution of the diacid **II-12** in THF. After stirring for one hour at room temperature, a TLC of the reaction was performed, where three spots appeared. Purification of the crude mixture by column chromatography allowed isolating the diester and the second spot, but the latter appeared to be unreacted Diazald. This means that the conversion of Diazald into diazomethane is not quantitative, and so it is difficult to have a precise control on the stoichiometry of the reaction. This approach was therefore abandoned.

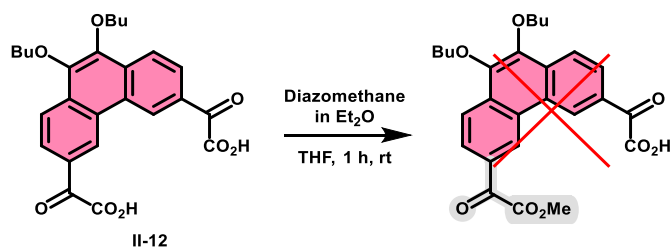


Figure 68. Monoesterification attempt of 9,10-bisbutyloxyphenanthrene-diglyoxylic acid **II-12**.

With the synthesis of the second monoprotected building block proving more challenging than anticipated, we decided to concentrate on the synthesis of the trimer that not require this block.

b. Synthesis of the trimer with acetic acid functions

The phenanthrene-diglyoxylic acid **II-12** and the monoprotected naphthalene **II-15** were combined in a double Perkin reaction to form the flexible bifunctional precursor with a central phenanthrene and two external naphthalenes. After two days of reaction, the mixture was quenched with HCl (10%w in H₂O) and the aqueous layer was extracted with dichloromethane. The organic layers were united and dried over MgSO₄, and the solvent was removed under reduced pressure. The crude was then purified by silica gel column chromatography. The desired product **II-17** could be isolated and was characterized by NMR spectroscopy, but the purification also allowed to isolate an interesting secondary product. Analysis of the NMR spectra showed that this product was the result of a single condensation and therefore composed of a phenanthrene linked to only one naphthalene. This resulted in a new type of flexible intermediate **II-18** containing two building blocks and functionalized with both an acetic methyl ester and a glyoxylic ethyl ester (Figure 21).

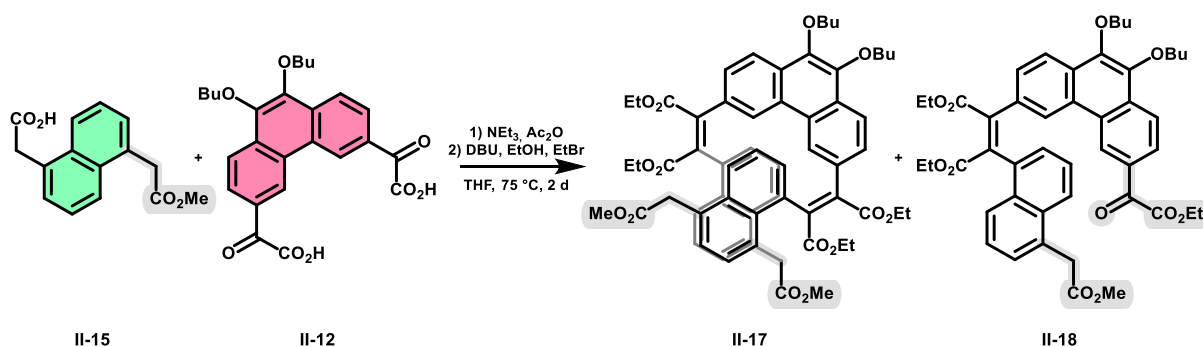


Figure 69. Synthesis of doubly linked phenanthrene **II-17** and asymmetric compound **II-18**

Using stoichiometric amounts of both building blocks at low concentration, the formation of this intermediate was optimized with a yield reaching 45%. It would be later used as an alternative precursor for another synthetic approach (see paragraph II d).

Conditions for the synthesis of the trimer **II-17** were optimized by increasing the concentration and the time of reaction. This increased the efficiency, reaching a 50% yield of **II-17** (Figure 70). This flexible intermediate was then saponified in the presence of KOH. After stirring one night in a refluxing mixture of ethanol and water, the reaction was cooled down to room temperature and HCl was added to the orange solution. Upon addition of the acidic solution, a bright orange precipitate appeared. The latter was filtered, dried, and analyzed by ^1H NMR spectroscopy. The NMR spectra showed that the flexible hexaacid intermediate **II-19** was obtained with a 89% yield (Figure 70).

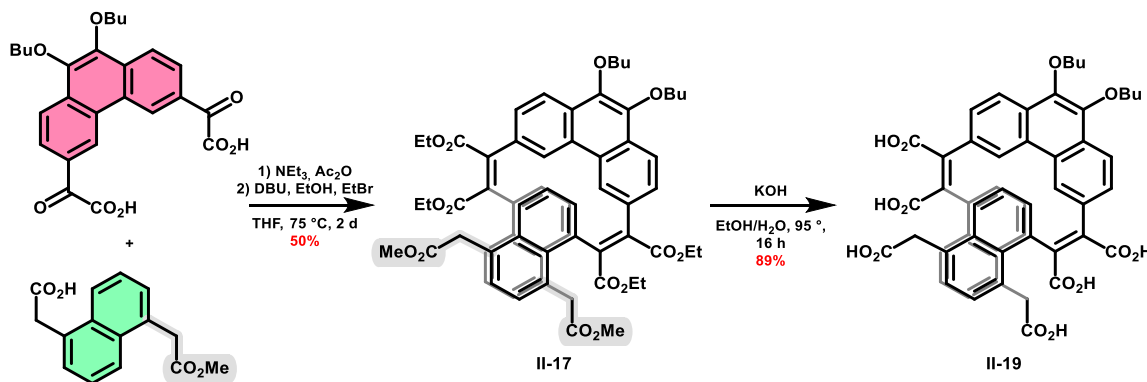


Figure 70. Optimized synthesis of trimer **II-17** and saponification leading to acidic trimer **II-19**.

c. Synthesis of the flexible intermediate functionalized with glyoxylic acids

The approach to the second flexible intermediate, which is functionalized with glyoxylic acids, is similar to the one used for the synthesis of **II-19**. Complementary to this first flexible intermediate, the new one requires two peripheral phenanthrenes with glyoxylic functions and one central naphthalene. This synthesis was first planned as a Perkin reaction involving two equivalents of monoprotected diglyoxylic phenanthrene and one equivalent of naphthalene-diacetic acid. Unfortunately, we were not able to synthesize the required monoprotected phenanthrene (see II a). This inconvenience greatly affected our approach, as the second trimer could not be efficiently produced in an usual and controlled way.

Another approach for the synthesis of a structurally similar precursor was considered but not attempted, based on successive Perkin reactions between complementary naphthalene and benzene-based building blocks (Figure 71). However, using the resulting trimer may not be as efficient as using the one constituted of two phenanthrenes and a naphthalene. With this approach, the number of bonds to be formed during the last photocyclization step is greatly increased. Furthermore, comparison to the flexible macrocycle only composed of naphthalenes and phenanthrenes suggested that its spatial conformation may not be as favorable for the formation of a triply twisted nanoribbon.

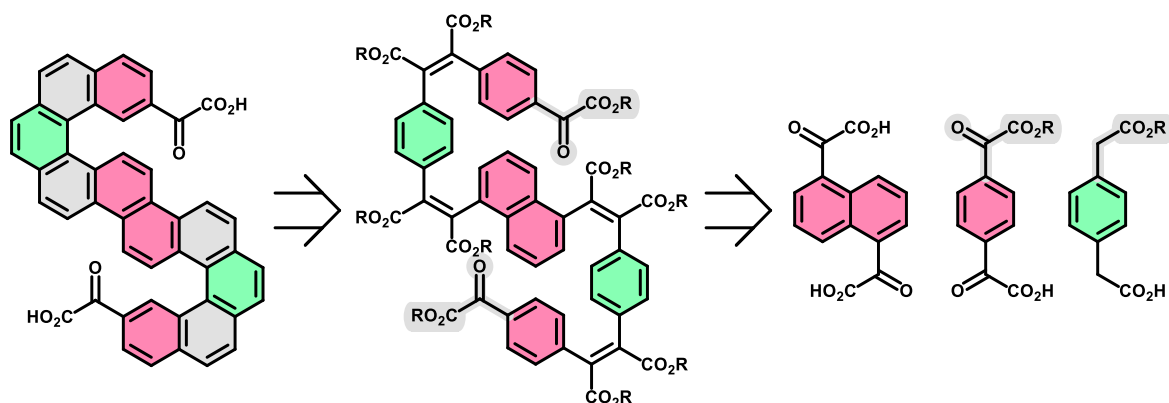


Figure 71. Synthesis of a structurally similar complementary precursor for the synthesis of the macrocyclic nanoribbons.

We decided to focus on the previously obtained precursors **II-18** and **II-19** to synthesize the target macrocycles.

d. Toward the synthesis of the macrocycles

The flexible intermediates **II-18** and **II-19** were used in two different synthetic routes to obtain the desired nanoribbons. The first one involves the unexpectedly obtained monoacetic monoglyoxylic precursor **II-18**. The reaction of one equivalent of this intermediate with another equivalent of itself would ideally lead to a mixture of macrocycles containing two units, four units, six units etc. We know from the first attempts at the macrocyclization reaction that only the two-block macrocycles were formed when using diacidic building blocks. In the case of **II-18**, the naphthalene and the phenanthrene are already linked, and a high dilution Perkin reaction with saponified **II-18** might favor the formation of a two-unit “microcycle” (Figure 72). Worst, the saponification of the precursor might fail, as the basic conditions required might cause the formation of oligomers during the reaction.

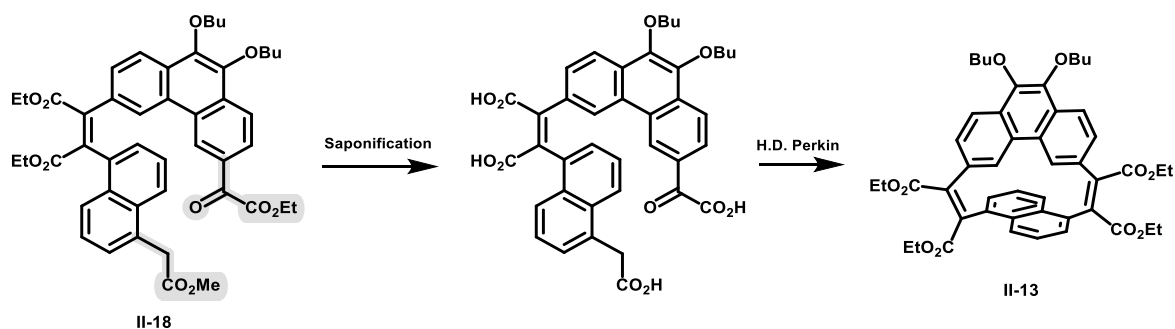


Figure 72. Most probable result of the high dilution Perkin reaction using a monosubstituted phenanthrene.

One way to avoid these problems would be to pre-rigidify the precursor **II-18** before the saponification. The formation of a helicene from **II-18** would lock the position of the complementary functions in space, and, after saponification, macrocyclization of this rigidified precursor should lead to a mixture of partially rigidified [2+2] and [3+3] macrocycles (Figure 73).

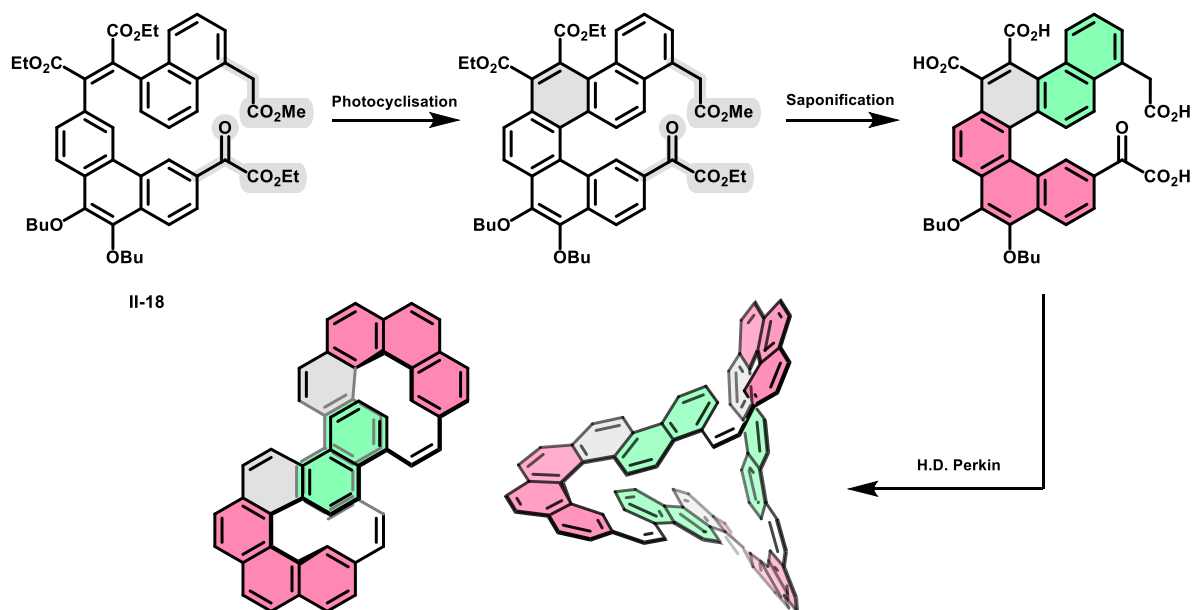


Figure 73. Alternative approach for the synthesis of the macrocyclic nanoribbons

The flexible precursor **II-18** and iodine were dissolved in ethyl acetate and stirred for two days at room temperature under irradiation from a 150 W mercury immersion lamp inside a borosilicate immersion tube. The ethyl acetate plays two roles in this Mallory photocyclization: it is used as both a solvent and as a scavenger to neutralize the HI produced during the oxidation step of the reaction. Thus, there is no need to add propylene oxide or ethylene oxide as scavenger to the reaction. Because the reagents and products of this reaction are highly colored, the solution was diluted enough so that light could well penetrate the mixture. After two days, TLC showed that the starting material had reacted entirely. The solution was concentrated under reduced pressure, washed with aqueous sodium sulfite Na_2SO_3 and dried on MgSO_4 , and the remaining solvent was removed under vacuum. Purification of the crude on column chromatography yielded the desired benzo-[5]helicene

II-20, but also an overcyclized product in equal quantity. When stirring over only one night, the same reaction gave the helicenic compound **II-20** after purification on silica gel as a racemic mixture with a 67% yield (Figure 74).

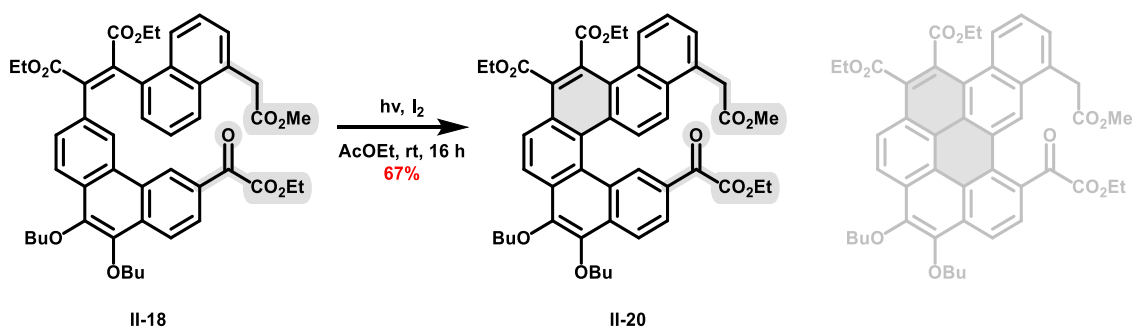


Figure 74. Synthesis by Mallory photocyclization of benzo-[5]helicene **II-20** functionalized with one acetic and one glyoxylic ester function.

Once **II-20** isolated and characterized, it was saponified by KOH in a mixture of ethanol and water (Figure 75). After one day of stirring at reflux, aqueous HCl was added to the solution. A precipitate appeared and was filtered, but the NMR spectra recorded showed that the saponification was either not finished or other impurities were present. Pursuing the saponification for a longer time did not solve this issue, nor did a decrease of concentration. The saponification was then attempted in milder conditions, with KOH replaced by NaHCO₃. Unfortunately, none of the conditions tested allowed to form the desired saponified benzo-[5]helicene. We could not provide any explanation, but the proximity between the acetate formed after addition of the base and the glyoxylic function might cause some undesired intramolecular reaction such as formation of an anhydride. Without the saponified helicene, this synthetic approach could not be pursued further.

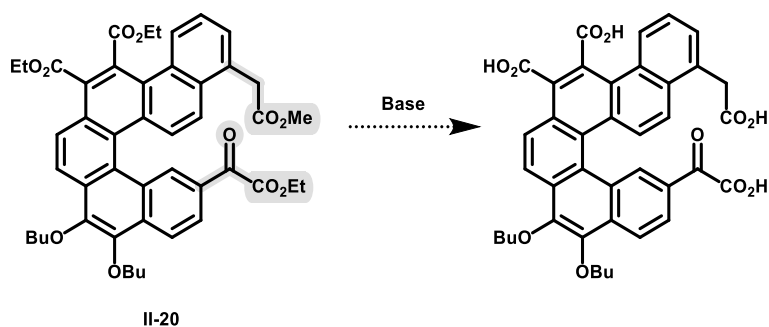


Figure 75. Inconclusive saponification of benzo-[5]helicene **II-20**.

The second synthetic route can only lead to the formation of the macrocyclic precursors of the figure-of-eight nanoribbon and implies the hexaacidic flexible intermediate **II-19** which can be co-macrocyclized with another equivalent of phenanthrene diglyoxylic acid **II-12** (Figure 76). The two reagents were dissolved in THF and added dropwise over one day to a refluxing solution of NEt₃ and Ac₂O in 1 L of THF. After the addition, the solution was stirred at reflux for three more days. To subsequently esterify in situ, the reaction was stirred for two days at reflux after addition of ethanol, DBU and bromoethane. After work-up and

evaporation of the solvent, the crude residue was purified by column chromatography. Analysis of the collected fractions revealed that only one seemed to contain the expected macrocycle.

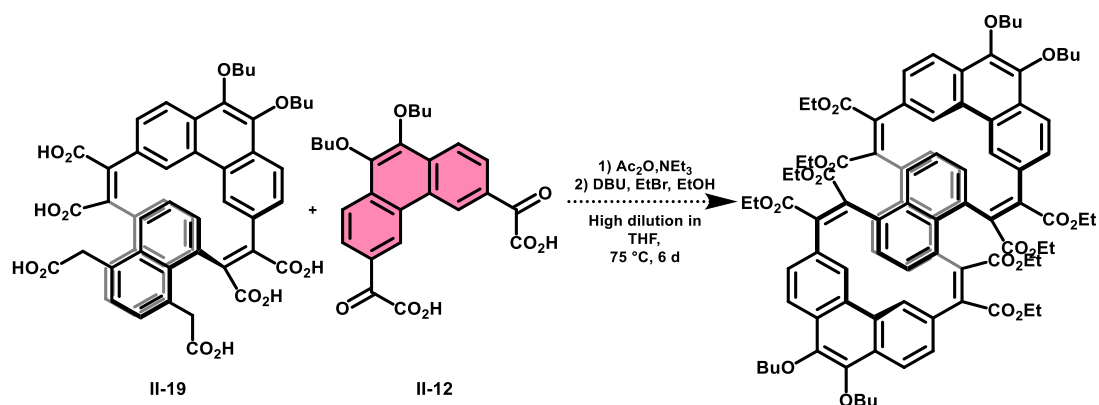


Figure 76. Macrocyclization of trimer II-19 with bifunctional phenanthrene II-12.

The ^1H NMR spectra showed that the compound was asymmetric, with the correct number of aromatic protons, but with four ethyl chains missing. The ^{13}C NMR spectrum revealed remaining non-ester carbonyls. These results suggest that the isolated product II-21 could be a flexible precursor to the figure-of-eight nanoribbons, with half its expected number of ester functions (Figure 77).

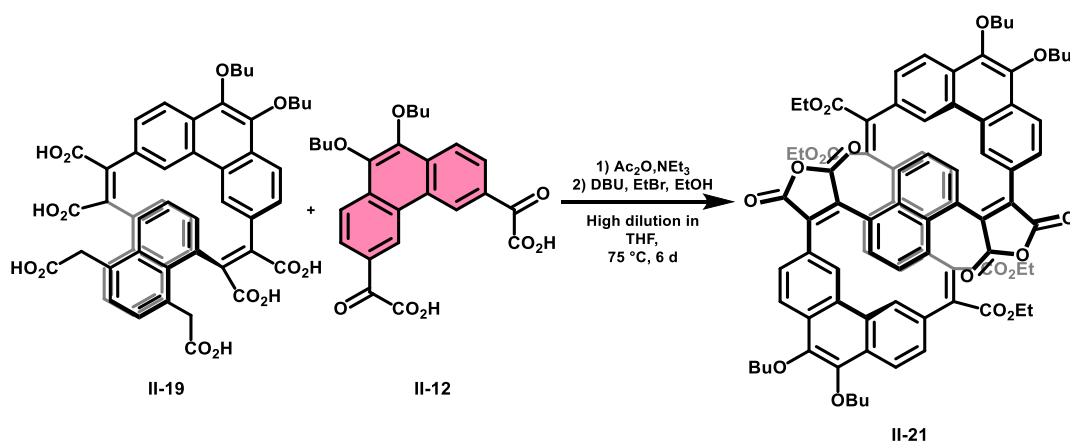


Figure 77. Supposed macrocycle isolated after the macrocyclization reaction.

In spite of numerous attempts at this reaction, the fully esterified macrocycle was never obtained. We decided to replace the esterification step with an *in situ* imidification step after the Perkin condensation. Before this, we wanted to see how replacing esters by imides would influence the final rigidification reaction. A test molecule has been made for this purpose. Phenanthrene diglyoxylic acid II-12 and two equivalents of commercially available 1-naphthalene-acetic acid were condensed by Perkin reaction (Figure 78). After two days of reflux for the condensation step, 3-aminopentane was added to the reaction and the solution was stirred for another two days at reflux. Purification of the crude gave the flexible diimide compound II-22 in 32% yield.

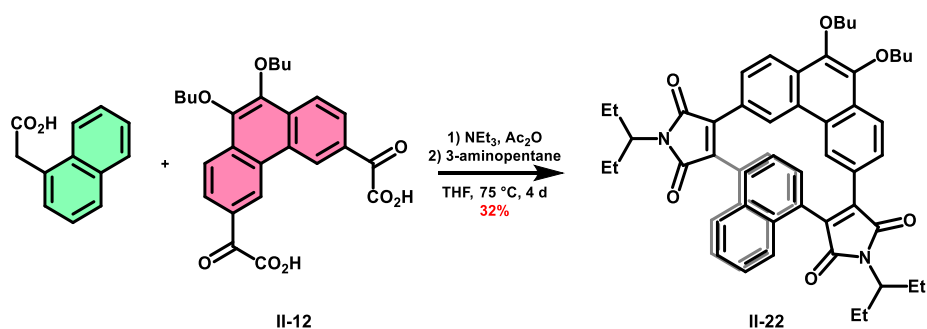


Figure 78. Synthesis of trimer II-22.

The latter was finally photocyclized (Figure 79). After one night of stirring at room temperature in a mixture of ethyl acetate and toluene (1:3), the solvent was removed and the residue was purified by column chromatography to give dibenzo-[7]helicene diimide II-23.

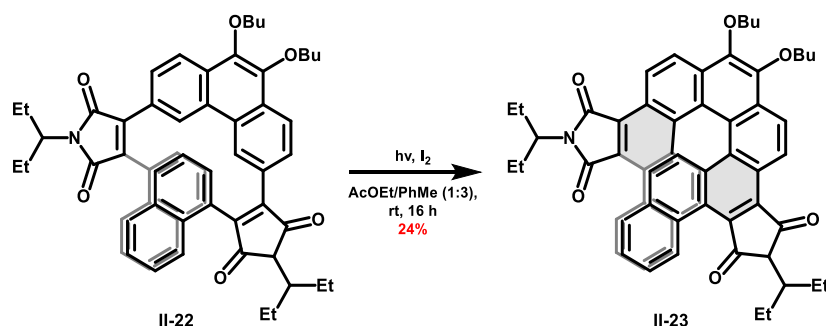


Figure 79. Synthesis of dibenzo-[7]helicene diimide II-23.

Thus, the substitution of the esterification step by an imidification step seemed to be a good alternative for the synthesis of the final rigid macrocycle. The bifunctional flexible intermediate II-19 and phenanthrene-diglyoxylic acid II-12 were once again engaged in a macrocyclization reaction under the same conditions as previously. After four days of stirring at reflux, 3-aminopentane was added and the mixture stirred for another two days (Figure 80). The crude was purified on column chromatography and GPC, but the expected macrocycle could not be detected.

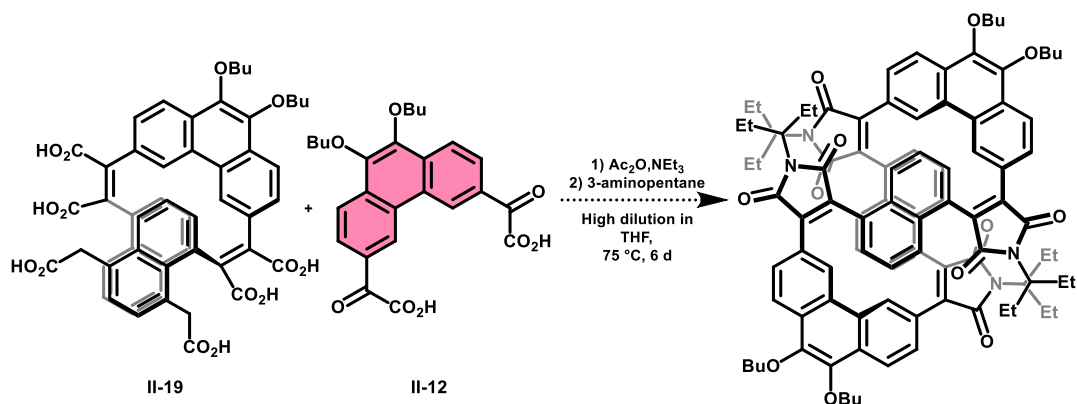


Figure 80. Synthesis of a flexible precursor for the figure-of-eight functionalized with cyclic imides.

The flexible precursor of the figure-of-eight could not be obtained whatever the functionalization of the maleic bridges. This could stem from too much flexibility or from a non-favorable conformation of the trimer **II-19**. Despite the rigidity imposed by the C=C double bonds, the naphthalenes still retain a high degree of conformational freedom due to the two single bonds on the maleic bridges. The naphthalenes can freely move between several conformations, two of which are very close in energy. The first one is like the one drawn in the previous reaction schemes. The second one is a helical structure, with the phenanthrene intertwined between the two naphthalene (Figure 81). This structure is slightly more stable, with a calculated energy of 163.68 kJ/mol. As the reaction is heated at reflux, the energy provided should allow to switch from one conformation to another, but remaining in this conformation could limit the formation of the macrocycle.

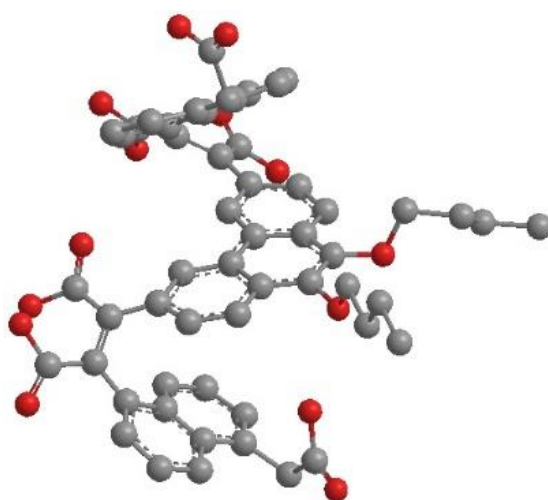


Figure 81. Representation of one of several conformations adopted by the trimer **II-19**.

Another approach to favor the formation of the macrocycle was therefore considered. Given the known regioselectivity of the Mallory photocyclization, the anticipated rigidification of the hexaester intermediate **II-17**, prior to the saponification and macrocyclization, should lead mostly to the formation of a dibenzo-[7]helicene. This rigidified precursor will pre-arrange the acetic functions in space to favor the formation of a macrocycle during the high dilution Perkin reaction. The flexible hexaester **II-17** and iodine were dissolved in ethyl acetate and stirred for one night under illumination in a photoreactor. The solution was concentrated, washed with an aqueous solution of $\text{Na}_2\text{S}_2\text{O}_3$ and dried over MgSO_4 . The solvent was removed under reduced pressure and the residue was purified over silica gel. After purification, the dibenzo-[7]helicene **II-24** was obtained in 88% yield (Figure 82).

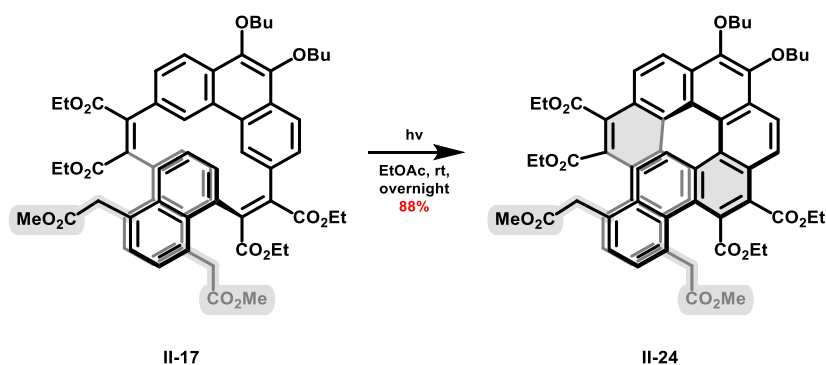


Figure 82. Synthesis of dibenzo-[7]helicene II-24.

This product was then reacted with KOH (Figure 83). As for benzo-[5]helicene **II-20**, the expected saponified product could not be isolated after days of stirring in a refluxing mixture of water and ethanol. Because the product was poorly soluble in the chosen mixture of solvents, we added a little THF, enough to dissolve the starting material. Even then, the dibenzo-[7]helicene-hexaacid could not be obtained. Using NaHCO₃ instead of KOH did not lead to the desired product either.

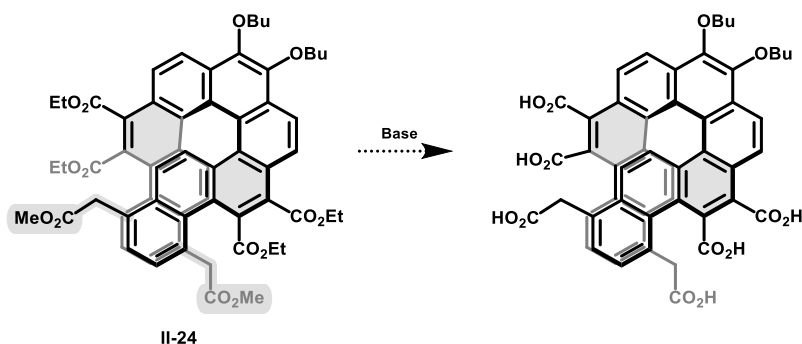


Figure 83. Saponification attempts on II-24.

Facing again unpredictable problems with such an apparently trivial saponification, we had no other choice than to try an unusual method for the synthesis of the targeted rigid hexaacid. This time, the trimer was saponified first, and the flexible hexaacid intermediate was then illuminated (Figure 84). Photocyclization of saponified compounds are usually avoided because of bad yields. Surprisingly, hexaacid **II-19** was reasonably soluble in ethyl acetate. Because of the acidic conditions due to the formation of hydrogen iodide, transesterification reactions may happen between ethyl acetate and hexaacid **II-19**. To limit this unwanted reaction, the solvent was mixed with toluene so the amount of ethyl acetate would only represent one quarter of the mixture. After one night of stirring under irradiation, a TLC was performed. Because of their high polarity, it is difficult to distinguish the starting material from the products. Nonetheless, this TLC revealed that not only a highly polar compound or mixture of compound was still present, but also several slightly less polar side products. We attempted to purify the crude on column chromatography, but even the use of high polarity mixtures of eluents could not separate the different products of this reaction. After this attempt, we noted that the residue was peculiarly soluble in chloroform. It was dissolved in

chloroform and injected to be purified over Gel Permeation Chromatography (GPC), a type of size exclusion chromatography (see Chapter 3). The chromatograph showed that the crude contained a high number of different products with similar sizes. Because these compounds have one or more acid functions, they tend to drag on the GPC's column in a similar manner to that on a silica gel column. The separation was thus difficult, and analysis of each fraction showed that it consisted of compounds that underwent one or more photocyclisations or transesterifications. Still, one of the fraction was found to be the dibenzo-[7]helicene hexaacid **II-25**, isolated in 10% yield.

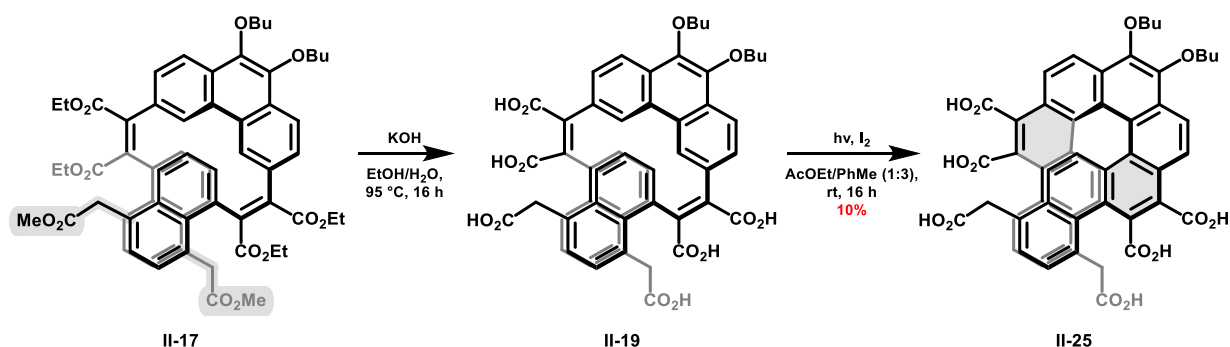


Figure 84. Synthesis of the dibenzo-[7]helicene-hexaacid **II-23**.

This encouraging result showed that the synthesis of a rigidified, acidic precursor usable in a Perkin reaction was achievable. Most of the side products isolated after the purification on GPC proved to be results of transesterification reactions. Only a minimal quantity of ethyl acetate was used to limit these undesired reactions, but it proved to be unsuccessful. This reaction still needs to be optimized and substitution of ethyl acetate by THF, propylene oxide or using pure toluene could resolve the issues of transesterification.

Conclusion

The synthesis of two topologically non-trivial macrocyclic nanoribbons was attempted by several approaches. In the first one, two bifunctional building blocks react together in a high dilution Perkin reaction. A mixture of four- and six-block macrocycles was expected, but we only obtained a single two-block macrocycle displaying planar chirality. Though unexpected, this interesting result was further explored. We designed new ether-functionalized phenanthrene-diglyoxylic acids and confirmed the need for a controlled assembly of the building blocks to obtain the desired macrocycles.

This was the base of our second approach, in which Perkin reactions between bifunctional and monoprotected building blocks could lead to the synthesis of complementary flexible precursors, which would then be assembled for the synthesis of both macrocycles. Many unexpected difficulties were encountered. The monoprotected phenanthrene could not be synthesized, thus limiting this approach to the synthesis of the trimer with two peripheral naphthalenes and a central phenanthrene. The Perkin reaction involving one equivalent of phenanthrene and two monoprotected naphthalenes gave the desired trimer and a flexible precursor functionalized by both an acetic and a glyoxylic ester. The latter was rigidified to

give a benzo-[5]helicene but this compound could not be saponified and thus could not be used in a high dilution Perkin reaction.

The trimer consisting of a central phenanthrene and two naphthalenes was saponified and macrocyclized with one equivalent of phenanthrene-diglyoxylic acid, but this reaction did not lead to the flexible precursor of the figure-of-eight. The flexible intermediate hexaester was therefore photocyclized to a dibenzo-[7]helicene to preorganize the acetic acid functions in space. Inexplicably, this helicene could not be fully saponified. The photocyclisation was performed on the flexible hexaacid precursor, and surprisingly led to a small quantity of dibenzo-[7]helicene-hexaacid. Because of many side products, this method still needs to be optimized, but could be a successful approach to a figure-of-eight nanoribbon via Perkin reactions.

References

- 1 C. Adams, *The knot book: an elementary introduction to the mathematical theory of knots*, American Mathematical Society, Providence, R.I, 2004.
- 2 J. B. Listing, *Der Census räumlicher Complexe: oder Verallgemeinerung des euler'schen Satzes von den Polyedern*, Dieterich, 1862, vol. 10.
- 3 A. Mobius, *Abhandlungen* *Sachsische Gesellschaft der Wissenschaften*, 1865, **17**, 473–512.
- 4 R. Herges, *Chem. Rev.*, 2006, **106**, 4820–4842.
- 5 D. M. Walba, R. M. Richards and R. C. Haltiwanger, *J. Am. Chem. Soc.*, 1982, **104**, 3219–3221.
- 6 W. Fan, T. Matsuno, Y. Han, X. Wang, Q. Zhou, H. Isobe and J. Wu, *J. Am. Chem. Soc.*, 2021, **143**, 15924–15929.
- 7 Q. Zhou, X. Hou, J. Wang, Y. Ni, W. Fan, Z. Li, X. Wei, K. Li, W. Yuan, Z. Xu, M. Zhu, Y. Zhao, Z. Sun and J. Wu, *Angewandte Chemie International Edition*, 2023, **62**, e202302266.
- 8 M. Krzeszewski, H. Ito and K. Itami, *J. Am. Chem. Soc.*, 2022, **10**.
- 9 Y. Segawa, T. Watanabe, K. Yamanoue, M. Kuwayama, K. Watanabe, J. Pirillo, Y. Hijikata and K. Itami, *Nature Synthesis*, 2022, **1**, 535–541.
- 10 W. Fan, T. M. Fukunaga, S. Wu, Y. Han, Q. Zhou, J. Wang, Z. Li, X. Hou, H. Wei, Y. Ni, H. Isobe and J. Wu, *Nature Synthesis*, DOI:10.1038/s44160-023-00317-3.
- 11 K. S. Jeong, Y. S. Kim, Y. J. Kim, E. Lee, J. H. Yoon, W. H. Park, Y. W. Park, S.-J. Jeon, Z. H. Kim, J. Kim and N. Jeong, *Angewandte Chemie International Edition*, 2006, **45**, 8134–8138.
- 12 H. R. Talele, M. J. Gohil and A. V. Bedekar, *Bulletin of the Chemical Society of Japan*, 2009, **82**, 1182–1186.
- 13 B. Kobin, L. Grubert, S. Blumstengel, F. Henneberger and S. Hecht, *J. Mater. Chem.*, 2012, **22**, 4383.
- 14 B. V. Phulwale, S. K. Mishra, M. Nečas and C. Mazal, *J. Org. Chem.*, 2016, **81**, 6244–6252.
- 15 G. Naulet, L. Sturm, A. Robert, P. Dechambenoit, F. Röhrich, R. Herges, H. Bock and F. Durola, *Chem. Sci.*, 2018, **9**, 8930–8936.

Chapter 3: Phenanthrocyclophanes

I. Introduction

Various attempts of macrocyclization reactions of a bifunctional phenanthrene with a bifunctional naphthalene always led to the formation of products of [1+1] macrocyclization. These results showed that the pincer-like arrangement of the glyoxylic acid functions on the phenanthrene favored the formation of cyclophane-like macrocycles. In these cases, naphthalene building blocks lead to quite congested chiral macrocycles but shorter benzene-based diacetic compounds would also be able to form small [1+1] macrocycles, which could then act as flexible precursors of substituted coronenes.

The synthesis of coronene was first reported in 1932 by Scholl and Meier (Figure 85a),¹ and various substituted and π -expanded coronenes has since been made.² Coronenes inherently have a circularly condensed π electron system,^{3,4} often have a high symmetry and tend to form charge-transfer complexes⁵ or adducts with electron-poor molecules.⁶ Many new coronene-based structures have been designed for various applications such as charge-transfer based supramolecular rotors,⁷ supramolecular hydrogels⁸ and coronene-based host-guest nanostructures.⁹ Despite the large range of applications, the synthetic strategies leading to coronenes are not very diverse. Coronenes are usually obtained by expansion of perylene^{10,11} or rigidification of cyclophanes.^{12–15} Our group already proved that the Perkin strategy could be used for the synthesis of dibenzocoronenes (Figure 85b).¹⁶

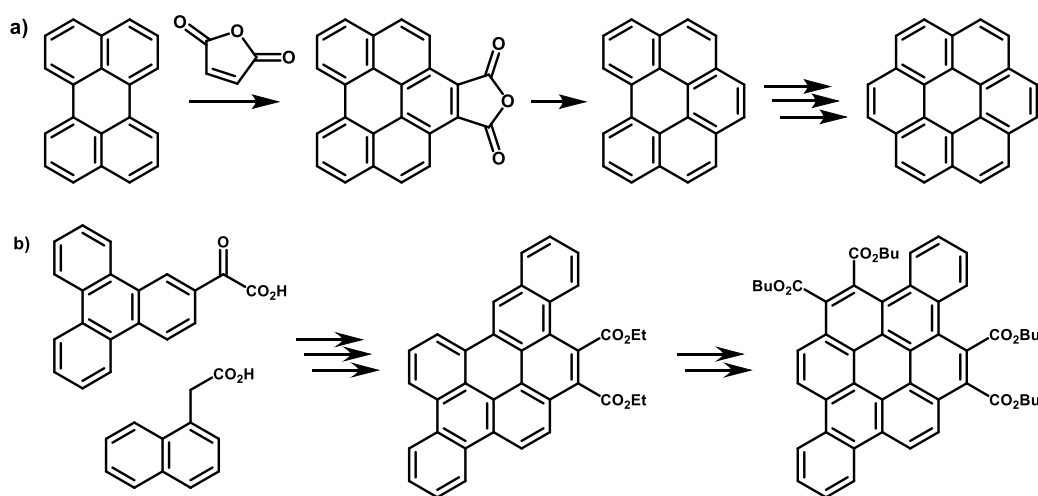


Figure 85. Synthesis of coronene by perylene expansion by Scholl and Meier (a) and our group (b).

The approach used for their synthesis mimicked the synthesis by expansion of perylene and led to the formation of dibenzocoronenes from a triphenylene- and a naphthalene-based building block. In the second part of this chapter, we report the synthesis of three phenanthroparacyclophanes with push-pull geometries, which could be photocyclised into tetra- and hexa-ester coronenes. All three coronenes are of D_{2h} symmetry, and the attempts for the synthesis of an asymmetric hexasubstituted coronene and a coronene of higher symmetry will be discussed.

II. Microcycles: naphthalenophenanthrocyclophanes

The first strategy that we used for the synthesis of our macrocyclic nanoribbons used a stoichiometric mixture of bifunctional building blocks to obtain four- or six-units macrocycles. The reaction conditions used unexpectedly led to two-block macrocycles (Figure 86). Because the signals appearing in the ^1H NMR spectra of the two-, four- and six-block macrocycles share the same integrals and multiplicities, this result had to be confirmed by MS. A characteristic shift is however observed in ^1H NMR. The “inner” protons (positions 4 and 5) of the phenanthrene were shielded compared to what is normally observed for these doublets in other cases. This shielding is due to the position of the protons above the naphthalene core in its shielding cone. The short distance between the naphthalene and the phenanthrene forces these two arene units to be orthogonal. The protons in position 4 and 5 of the phenanthrene are thus pointing toward the center of the naphthalene. Although this shielding effect is noticeable, it is less pronounced than in other aromatic systems such as porphyrins.

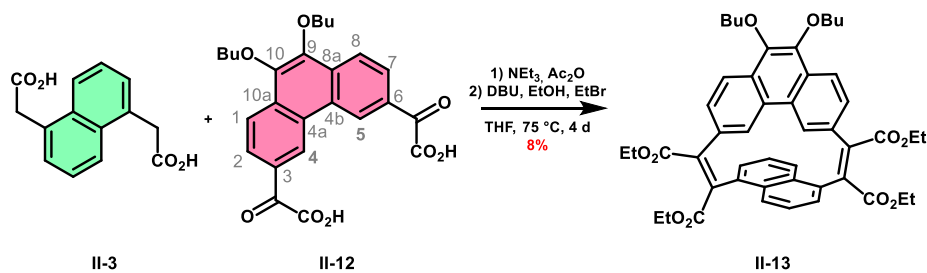


Figure 86. Synthesis of phenanthrocyclophane II-13.

This synthesis proved to be reproducible, although in modest yields, always leading to a mixture of the [1+1] macrocycle and linear oligomers. A mixture of products is sometimes obtained after attempted separation. Neither changing the eluent nor recrystallization could separate the products. Another purification method, based on size exclusion, was therefore used. The mixture was dissolved in chloroform and injected into a recycling GPC. Being a type of size-exclusion chromatography (SEC), this process separates the different analytes based on their size or hydrodynamic volume. The stationary phase is composed of porous gel beads packed inside the column, while the mobile phase is an organic solvent, in our case chloroform. Upon entering the column, small molecules will enter the pores and stay longer inside the column, while large molecules will be excluded from entering the pores and thus elute first. Because it does not rely on the chemical or physical interaction between the stationary and mobile phase, this process allows to efficiently separate compounds of similar polarity but different size. This purification method proved to be highly valuable as it allowed us to isolate products that we could not separate by classical silica gel chromatography. UV-visible (254 and 366 nm) and refractive index detectors allow monitoring the separation process. Gaussian signals corresponding to different molecule sizes are displayed on the chromatogram and separate more and more with each cycle.

With this purification method, the separation of the mixture was feasible and showed that it was composed of two products. The first one was the "micro" cyclic two-block tetraester, while the second was an asymmetric macrocycle with half the expected number of ester functions. Since the size of the first product was not the same as the previous macrocycle, half esterified four-block macrocycle was first considered. Nevertheless, the doublets corresponding to the "inner" protons of the phenanthrene were once again more shielded compared to what is normally observed for these signals and suggested that this product was an asymmetric version of a [1+1] *microcycle*. This hypothesis was confirmed by 2D NMR and high temperature ^1H NMR. The ^1H NMR spectra of the compound in deuterated tetrachloroethane at room and high temperature ($>100^\circ\text{C}$) were the same, showing that the asymmetry was due to the missing ester rather than due to a stable asymmetric conformation of a larger, slightly flexible product. Unfortunately, it was not possible to determine precisely the structure of the molecule without the crystallographic structure. ROESY and NOESY NMR performed on **II-13** showed no spatial coupling between the different alkyl chains. Besides knowing that only two of the four supposed ester functions are present and that it has a cyclophane structure, the exact structure of this byproduct is still uncertain.

Slow evaporation of a solution of symmetrical *microcycle* **II-13** in ethanol gave single crystals suitable for X-Ray diffraction (XRD). The resolved structure (Figure 87a) is a racemic mixture of macrocycles with a planar chirality (Figure 87b). In the unit cell, same enantiomers stack together in chiral columns (Figure 87c). Each column is linked to its neighbors by π - π interactions between naphthalenes. The distance between the two aromatic cores is only 2.3 Å, and the naphthalene is unusually distorted, with an end-to-end twist of 14° . The short distance between the two aromatic cores makes it impossible to convert an enantiomer into its mirror image and conveys long-term enantio-stability. This was confirmed by a simulation by Dr. Yoann Coquerel, our collaborator at the University of Aix-Marseille, that showed that a 5 Å long C=C bond would be required for the racemization process.

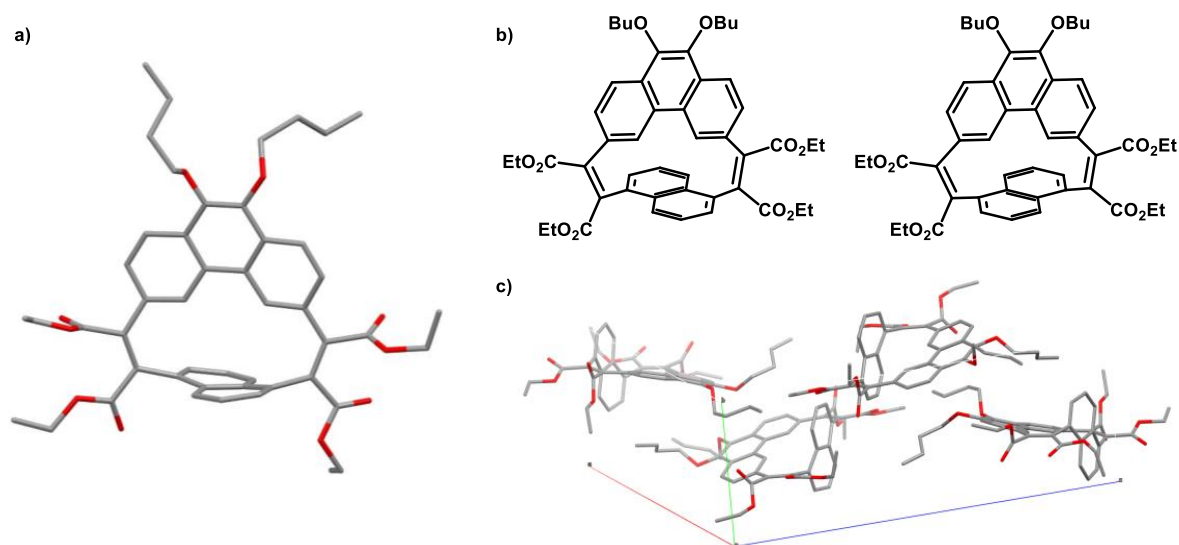


Figure 87. XRD structure of **II-13** (a) along representation of the two possible enantiomers (b) and of the unit cell (c).

Considering the high versatility of our synthetic approach, the interesting unusual and stable chirality of the compound, as well as the possible push-pull functionalization and geometry, we felt encouraged to synthesize a small family of *microcycles* with the prospect of studying their photophysical and chiroptical properties.

Naphthalene-1,5-diacetic acid **II-3** and phenanthrene-3,6-diglyoxylic acid **II-5** were Perkin-condensed in high dilution. After purification by column chromatography, *microcycle III-1* was obtained in 8% yield. The same reaction was then performed with 9,10-diethoxyphenanthrene-3,6-diglyoxylic acid **II-9** instead of **II-5**. After purification by silica gel chromatography and GPC, *microcycle III-2* was obtained (Figure 88). Slow diffusion of a solution of **III-1** in chloroform into a solution of ethanol gave single crystals suitable for XRD, but we failed to crystallize **III-2**.

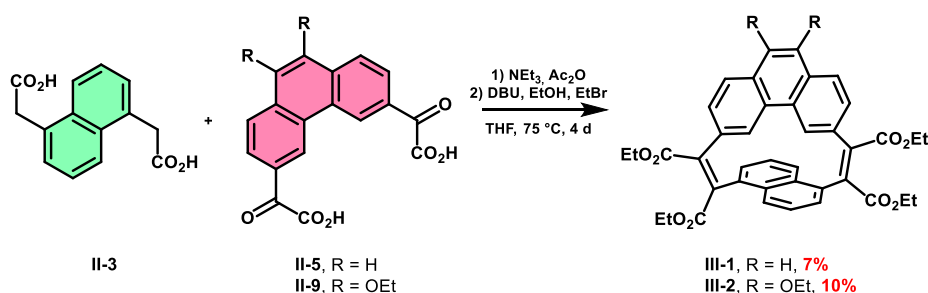


Figure 88. Synthesis of *microcycles III-1 and III-2*

The synthesis of these two *microcycles* would allow us to compare the physical properties of **II-13** with those of a similar compound with slightly shorter (**III-2**) or no (**III-1**) donating groups. To complete the study, we also desired a *microcycle* with more electron accepting groups, an obvious and straightforward choice being cyclic maleimides in place of the dialkyl maleate bridges. Phenanthrene-diacetic acid **II-12** and naphthalene-diglyoxylic acid **II-3** were once again condensed in high dilution. After stirring at reflux for four days, 3-aminopentane was added to the solution. The mixture was then stirred for another two days before work-up and purification. Dibutoxy-*microcycle*-diimide **III-3** was finally isolated with a 54% yield, significantly higher than the yields obtained for the *microcycles* with ester functions. This improvement in yield is hardly explainable, since it is logically independent from the cyclisation step. The presence of the five-membered cyclic maleimide bridges may nevertheless be favored by reducing the ring tension.

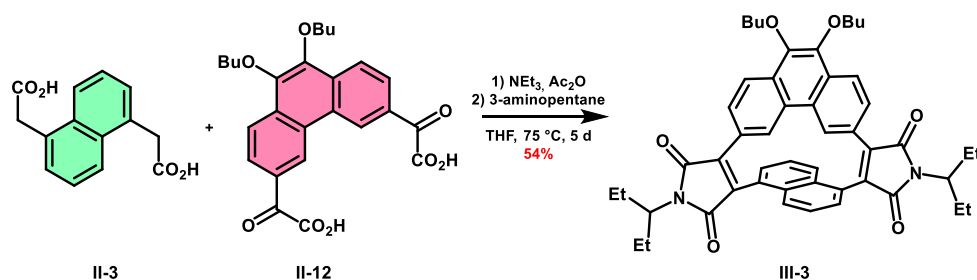


Figure 89. Synthesis of *dibutoxy-microcycle-diimide III-3*.

Single crystals suitable for XRD were obtained by slow evaporation of a solution of **III-3** in chloroform and *iso*-propanol. The structure (Figure 90a) revealed that even if the distance between the two aromatic core was the similar (2.4 Å) to the one in **II-13**, the naphthalene was surprisingly much less distorted, with an end-to-end twist of 8°. This could mean that the conversion from the maleic anhydride to the ester functions is not easy, as it induces more strain in the naphthalene.

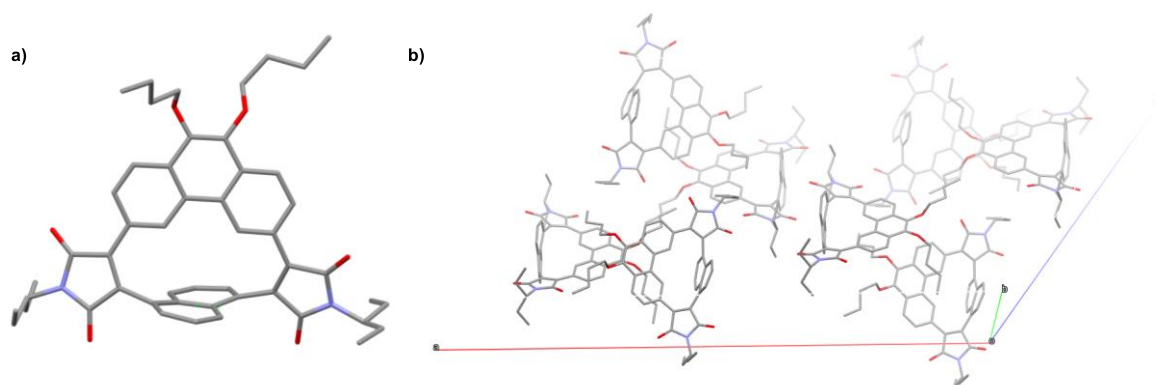


Figure 90. XRD structure of **III-3** (a) and of its unit cell (b).

With this family of four microcycles synthesized and characterized, their photophysical and chiroptical properties had to be studied. The racemic mixtures of all four compounds were sent to Dr. Michal Šámal, our collaborator at the IOCB in Prague, who separated all enantiomers by chiral HPLC, with a mixture of heptane and dichloromethane (1:1) as the mobile phase. The enantiopure samples were then sent back to us for additional analyses. We could grow single crystals of the two enantiomers of **II-13** and of one enantiomer of **III-2**. Unfortunately, the latter were too weakly diffracting, and the structure could not be resolved. The structure of the two enantiomers of **II-13** was determined, including their absolute configuration (Figure 91). The first one, **II-13-E1**, is of (*pS*, *pS*) chirality, making the second, **II-13-E2**, (*pR*, *pR*). Thus we could assign the electronic circular dichroism (ECD) and circularly polarized luminescence (CPL) spectra to the corresponding configurations.

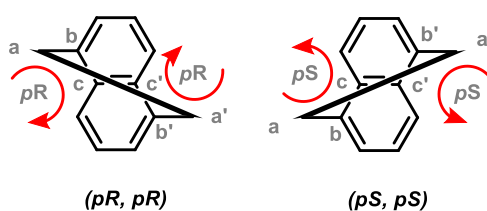


Figure 91. Assignment of the chiral centers using the Cahn-Ingold-Prelog priority convention.

Although many of the compounds obtained by our team are chiral, this property is not our main purpose, and we are not well equipped at the CRPP to investigate them. To study the chiral properties of the naphthalene-based microcycles, I had the opportunity to spend several days at the ISCR in Rennes where our collaborator Dr. Ludovic Favereau trained me in the measurement and interpretation of chiroptical properties.

The luminescence of the racemic compounds was investigated first. Upon excitation by light, electrons of the ground state S_0 will reach one of the excited singlet states S_n .¹⁷ Generally, the promotion of an electron from the highest occupied molecular orbital (HOMO) to the lowest unoccupied molecular orbital (LUMO) is the most energetically favored absorption transition. In some cases, for example when using heavy transition metals, the system can undergo intersystem crossing to a triplet state. The excited electron will in this case have the same spin as the electron it was associated with in the ground state, in contrast to the singlet state where they are of opposite spin. Radiative decay from these higher-energy excited states back to the ground state is called fluorescence in the case of $S_n \rightarrow S_0$ transitions, and phosphorescence in the case of $T_n \rightarrow S_0$ transitions. The transitions can be characterized by their characteristic time $\tau = 1/k_{\text{process}} \text{ s}^{-1}$, by the quantum yield of luminescence $\Phi = k_r/(k_r+k_{nr})$, where k_r is the radiative rate constant and k_{nr} the non-radiative rate constant. The different electronic states and transitions can be represented on a Jablonski-Perrin diagram (Figure 92).

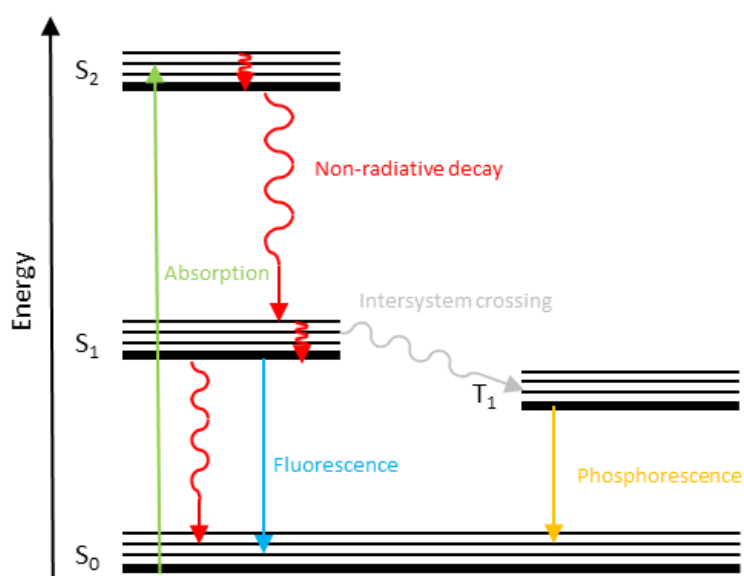


Figure 92. Simplified Jablonski-Perrin diagram. Thick lines represent electronic states, thinner lines their vibrational states. Straight arrows represent radiative processes, wiggly arrows non-radiative processes.

The absorption spectra of the cyclophanes were measured (Figure 93) at six different known concentrations. By the Beer-Lambert law, the molar attenuation coefficient ϵ of each microcycle could be determined. The absorption spectra of **II-13**, **III-1** and **III-2** are similar, with λ_{max} around 290 nm and lowest energy transitions between 340 and 400 nm. On the other hand, λ_{max} of **III-3** is at higher energy, at 250 nm, and its lower-energy transitions are red-shifted compared to the other three macrocycles. This comes from the strong push-pull system in the imide-containing microcycle.

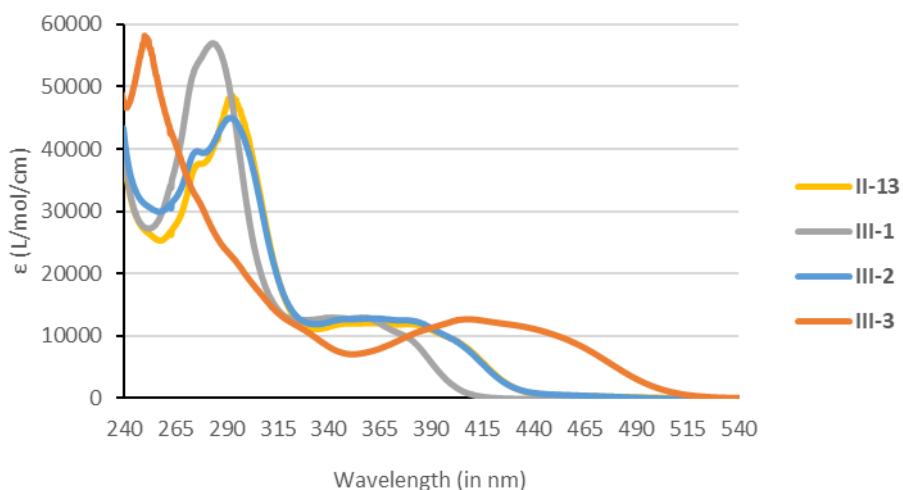


Figure 93. Absorption spectra of the four microcycles, measured in dichloromethane at room temperature.

Absorption at a certain wavelength means that an electron is promoted to an excited state of higher energy, or one of its vibrational states. Once excited, the molecule will try to return to its ground state S_0 via radiative or non-radiative desexcitation. Kasha's rule states that radiative decay will generally be produced when originating from the lowest excited state of a given multiplicity (singlet or triplet). Collision with other molecules will lead to nonradiative internal conversion from an excited state of higher energy to the lowest excited state. If no internal conversion occurs, S_1 might depopulate radiatively to S_0 . Vibrational relaxation or solvent reorganization generally causes the emitted photon to have a lower energy than the absorbed photon. The resulting shift is called Stokes shift. Because of the numerous energetically different possible transitions back to a vibrational ground state, the emission band is often broad. The emission spectra of each microcycle were measured in dichloromethane at room temperature (Figure 94). All four are luminescent, with Stokes shifts of 200 nm for **II-13**, 186 nm for **III-1**, 225 nm for **III-2** and 228 nm for **III-3**.

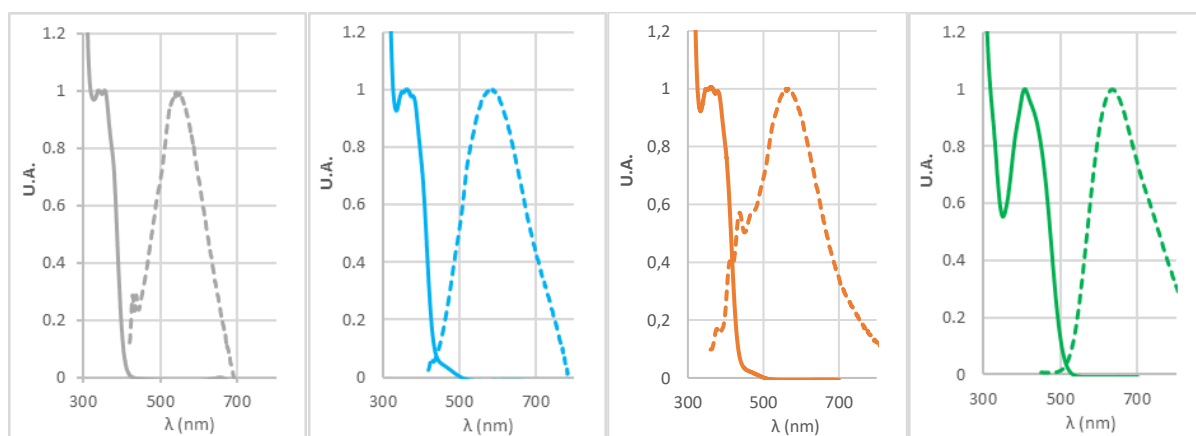


Figure 94. Normalized absorption (continuous) and fluorescence (dashed) spectra of **III-1** (grey), **III-2** (blue), **II-13** (orange) and **III-3** (green) in dichloromethane at room temperature. Emission was measured upon excitation at 380 nm for **III-1** and **III-2**, 350 nm for **II-13** and 400 nm for **III-3**.

Quantum yields of fluorescence for each compound were measured in dichloromethane at room temperature with Coumarin 153 as a standard.¹⁸ This method relies on the comparison

of the emission of the analyzed fluorophore with the emission of a standard fluorophore of known quantum yield and with absorption and emission at similar energies as the samples. The emission spectra of the standard and the products were measured with an absorbance $A < 0.1$ to avoid internal filter effects, and the spectra were integrated. The quantum yields can then be calculated from eq. 1:

Equation 1

$$\Phi_f^i = \frac{F^i f_s n_i^2}{F^s f_i n_s^2} \Phi_f^s$$

In this equation, Φ_f^i and Φ_f^s are the quantum yields of fluorescence of the sample and of the standard. F^i and F^s are the integrated emission intensities of sample and standard. f_i and f_s are the absorption factors, calculated with $f_x = 1 - 10^{-A_x}$, where A is the absorbance. n_i and n_s are the refractive indices of the sample and reference solutions. Dibutoxy-microcycle diimide **III-3** had the highest quantum yield (8%), while diethoxy- and dibutoxy-microcycle tetraester (**III-2** and **II-13**) had lower quantum yields (1%). Microcycle tetraester **III-1** was the least luminescent of the four molecules, with a quantum yield below 1%. These results can be used to calculate the brightness B for the compounds, a widely used measure of emission performance. The brightness is defined simply by $B = \epsilon_\lambda \times \Phi$, with ϵ_λ the molar extinction coefficient at the excitation wavelength and Φ the emission quantum yield. The four emitters having comparable ϵ_λ , their brightness will be mostly defined by their quantum yield of fluorescence. As expected, dibutoxy-microcycle diimide **III-3** proved to be the brightest of the family ($B_{\text{III-3}} = 974.4$), shining more than four times brighter than the other microcycles ($B_{\text{III-1}} = 9.4$, $B_{\text{III-2}} = 125.2$ and $B_{\text{II-13}} = 119.4$).

Rigid luminescent compounds usually have higher quantum yields due to limited non-radiative decay via vibrational relaxation. Yet our compounds are functionalized by “floppy” alkyl chains that might decrease the fluorescence. Other sources of competing processes could include reabsorption by neighboring molecules or population of the triplet state. At room temperature, intersystem crossing often competes with non-radiative decay, as the process is spin-forbidden. Lowering the temperature allows however to limit the occurrence of non-radiative decay by limiting collisions with the solvent or trapping the compound in a matrix. The emission spectrum of microcycle tetraester **III-1** was measured in 2-methyl tetrahydrofuran at 77 K. At this temperature, new emissions appear weakly at 570, 625 and 690 nm, in addition to the major emission at 440 nm. Gated fluorescence spectroscopy allows to “hide” the fluorescence of the compounds by only measuring processes with a long lifetime such as phosphorescence. The delayed emission spectrum of **III-1** at 77 K displays three emission bands at the same wavelengths as in the prompt emission spectrum, without the emission corresponding to the fluorescence. The same phenomenon is observed for **II-13** and **III-2**. In the case of dibutoxy-microcycle diimide **III-3**, both spectra show emission at the same wavelengths. This means that in the case of **III-3**, the system might emit *via* Thermally Activated Delayed Fluorescence (TADF). In this process, the excited system undergoes a first ISC to a triplet state. If the triplet state has an energy level close to a singlet state, it can

undergo reverse intersystem crossing (RISC) and convert back to a singlet state that will finally emit fluorescence. Thus the triplet state might be populated, which decreases the quantum yield of fluorescence.

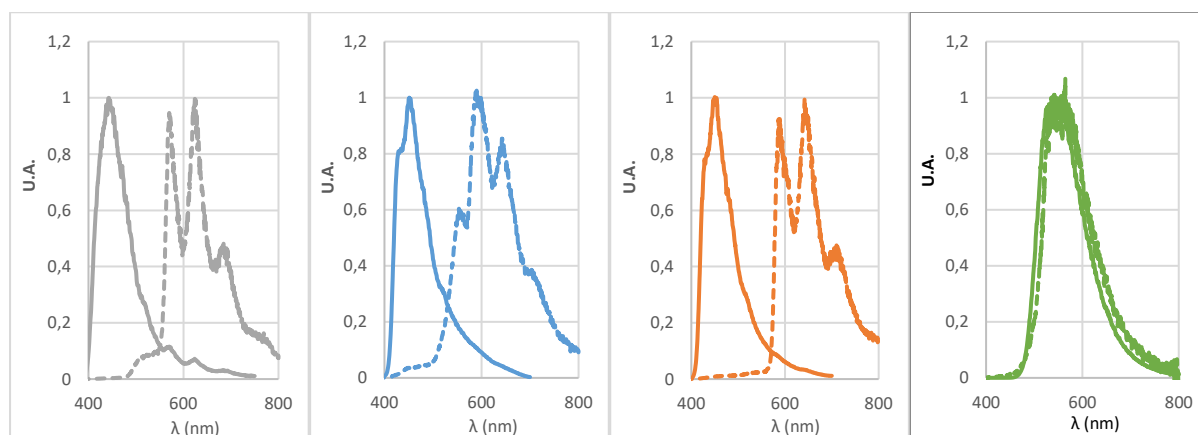


Figure 95. Normalized emission (continuous) and delayed emission (dashed) spectra of **III-1** (grey), **III-2** (blue), **II-13** (orange) and **III-3** (green) in 2-methyl-tetrahydrofuran at 77 K. Emission and time gated emission were respectively measured upon excitation at 350 and 340 nm for all the compounds. The delay time for delayed emission was 32 ms.

Because of their chirality, the enantiomers of the microcycles can discriminate between left and right circularly polarized light, meaning that they show circular dichroism (CD).¹⁹ Circular dichroism analysis relies on the interactions of a chiral, non-racemic, sample with circularly polarized light. CD, measured as ellipticity θ (in mdeg), is defined by $CD = A^l - A^r$, with A^l and A^r the absorptions of left and right circularly polarized light. By the Beer-Lambert law, this equation yields a molar quantity $\Delta\varepsilon = \varepsilon^l - \varepsilon^r = \frac{CD}{c \times b}$, with c the concentration (in mol/L) and b the path length (in cm). The CD of two enantiomers is theoretically exactly opposite. The dissymmetry factor g_{abs} can be obtained from the equation $g_{abs} = \frac{\Delta\varepsilon}{\varepsilon}$. The CD spectra of the four microcycles were measured with a spectropolarimeter. Each enantiomer was irradiated by left and right circularly polarized light beams, and the two circularly polarized lights were being absorbed to a different extent. The Cotton effects, the dichroic peaks measured, for each pair of enantiomers were indeed exactly opposite for each compound, and the spectra, describing the ellipticity as a function of the wavelength, were converted to display the molar quantity as a function of the wavelength (Figure 96). With both $\Delta\varepsilon$ and ε measured, the dissymmetry factors g_{abs} of each microcycle was calculated. The maximum g_{abs} obtained for **III-1**, **III-2**, **II-13** and **III-3** were 2.6×10^{-3} , 2.9×10^{-3} , 2.9×10^{-3} and 2.4×10^{-3} , respectively, which correspond to the range of values usually expected for organic fluorophores.

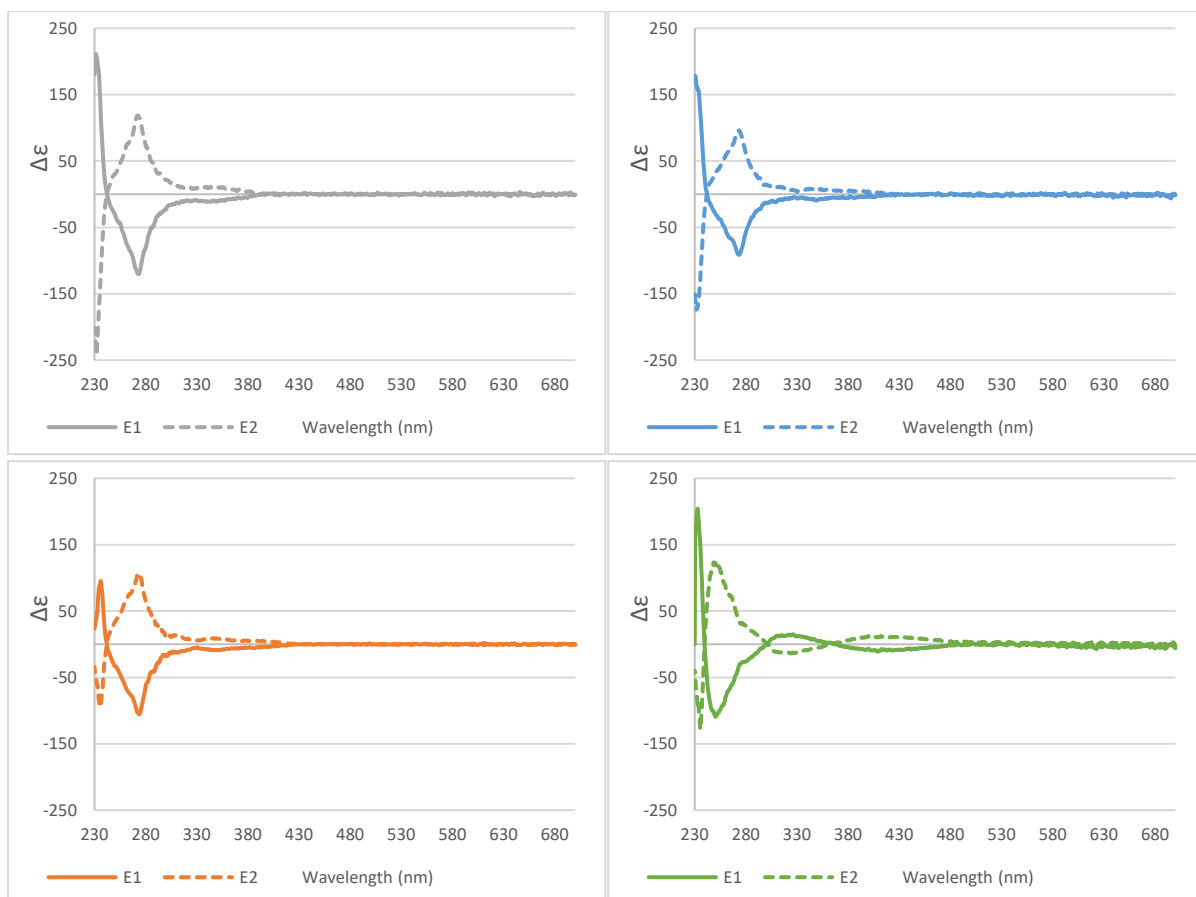


Figure 96. Electronic Circular Dichroism (ECD) spectra measured for **III-1** (grey), **III-2** (blue), **II-13** (orange) and **III-3** (green) in dichloromethane at room temperature.

Non-racemic chiral emissive compounds can emit left or right circularly polarized luminescence (CPL).²⁰ Contrary to CD, non-polarized light is used to excite the sample. The difference between left and right polarized emitted light is then measured. Even with efficient CPL emitters, the difference is small, and this technique requires many acquisitions. The dissymmetry factor g_{lum} is then used to quantify the polarization of emission. This factor can be calculated with $g_{lum} = 2 \frac{(I_L - I_R)}{(I_L + I_R)}$, with I_L and I_R the intensity of left- and right polarized emitted light, at the wavelength of maximum emission. The dissymmetry factor is indeed given for a single transition. For most emissive organic compounds, this value is constant throughout the emission band. The CPL of the four *microcycles*, dissolved in dichloromethane, was measured at room temperature (Figure 97). The spectra obtained are accumulated over twenty measurements. The measured difference of intensity gave access to the dissymmetry factors of **III-1** (1.1×10^{-3}), **III-2** (1.7×10^{-4}), **II-13** (1.9×10^{-4}) and **III-3** (1.2×10^{-4}). Organic CPL emitters often have a g_{lum} factor of the order of 10^{-3} , with a few examples having slightly lower (10^{-4}) values. In analogy with the brightness B calculated for the racemic mixtures, it is possible to calculate the brightness for CPL of each compound, defined by $B_{CPL} = B \times \frac{|g_{lum}|}{2}$. The values of B_{CPL} followed the same trend as the brightness B , **III-3** giving the highest value (0.056), followed by **III-2** and **II-13** (0.010 and 0.012) and **III-1** showing the lowest brightness (0.005).

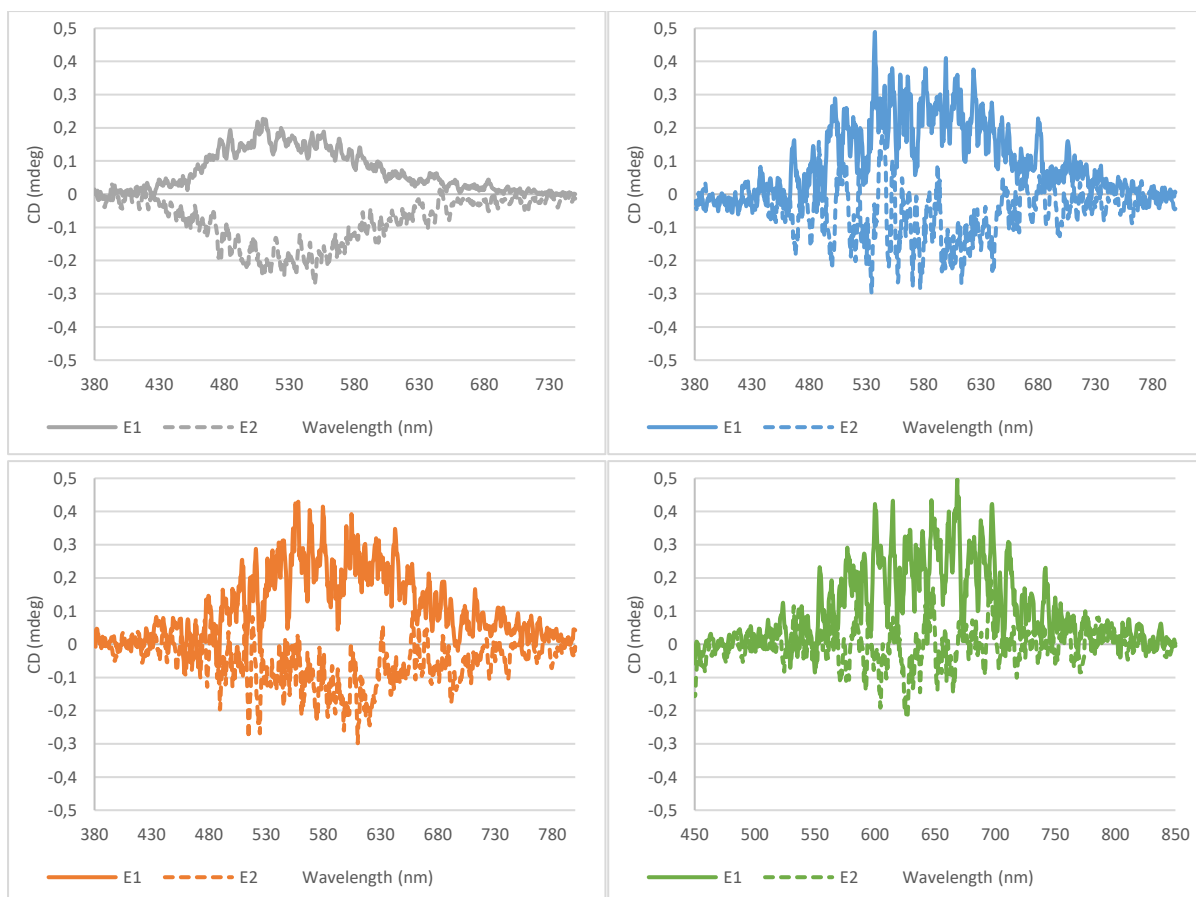


Figure 97. Circularly polarized luminescence spectra of **III-1** (grey), **III-2** (blue), **II-13** (orange) and **III-3** (green). The measurements were done with solutions of **III-1**, **III-2**, **II-13** and **III-3** in dichloromethane at room temperature, excited at 310 nm (**III-1**, **III-2**, **II-13**) and 380 nm (**III-3**). Each spectrum was accumulated twenty times.

Finally, the influence of the solvent on the emission was investigated. Solvent polarity can indeed influence the emission spectra of fluorophores, especially polar compounds, by its effect on the dipole moment of the excited state.²¹ This effect, called solvatochromism, is less visible in absorption spectra. This is due to the short time at which the absorption process occurs ($f_s = 10^{-15}$ s), too short for allowing motion of the fluorophore or the solvent (around 10-100 ps = 10^{-11} - 10^{-10} s). Fluorescence processes have however longer lifetimes (1-10 ns) and thus are more affected by this phenomenon. The absorption spectra of **III-3** showed that the solvent polarity had no effect on this fluorophore. The fluorescence spectrum displayed however a more energetic emission in toluene than in dichloromethane, a more polar solvent. This fluorescence solvatochromism indicates that the excited state of the compound has a larger dipole moment than the ground state. In a polar solvent, the solvent dipoles can reorient and relax around the dipole of the excited state, resulting in a lower energy for the latter. As the absorption is not influenced by the polarity, no ECD spectra were measured for this compound. Its CPL was however measured and yielded a g_{lum} of 4.6×10^{-4} .

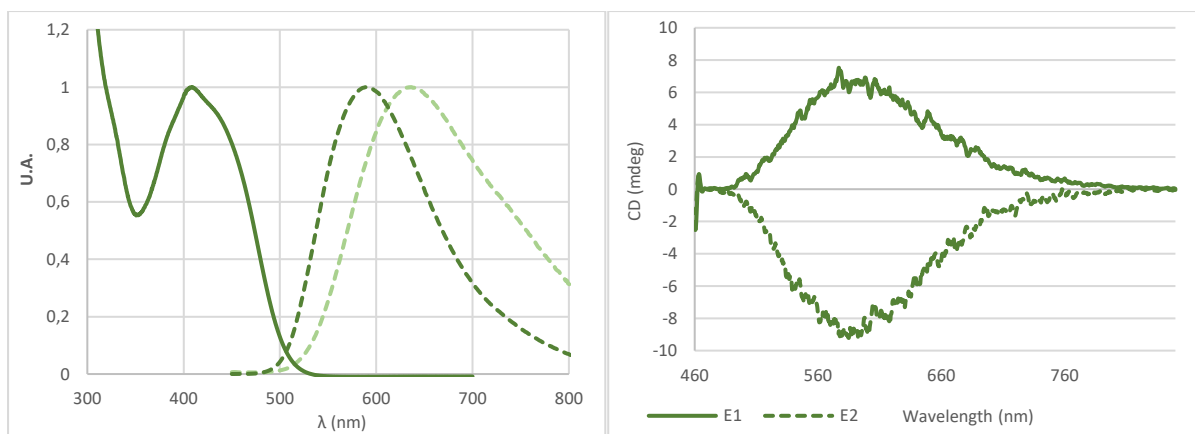


Figure 98. Left: normalized absorption (continuous) and emission (spectra) spectra of **III-3** in toluene at room temperature. Normalized emission of **III-3** in dichloromethane at room temperature (light green, dashed) is displayed for comparison. Right: CPL spectra of **III-3** in toluene at room temperature.

The chiroptical properties of the microcycles proved to be modest for rigid organic fluorophores. However, the ease and repeatability of the synthesis of the cyclophane-like structures make pincer-like 3,6-disubstituted phenanthrenes good building blocks for the synthesis of strained macrocycles containing only two units. This, as well as the push-pull geometry induced by the Perkin reaction and the functionalization of the phenanthrene, motivated us to further investigate the synthesis of two-unit phenanthrocyclophanes.

III. Phenanthroparacyclophanes and substituted coronenes

a. Synthesis of macrocycles with a D_{2h} symmetry

The diverse phenanthrene building blocks and the variable functionalization of the maleic bridges gave us the possibility to synthesize a family of chiral naphthalene-containing microcycles. Similarly, by replacing the naphthalene fragment with a simple benzene, a family of achiral microcycles with D_{2h} symmetry can be designed.²² Practically, a high dilution Perkin reaction involving stoichiometric amounts of commercially available phenylene-1,4-diacetic acid and phenanthrene-diglyoxylic acid **II-12** led to phenanthroparacyclophane **III-4** in 28% yield after purification on column chromatography and recrystallization in ethanol (Figure 99). The ^1H NMR spectrum of **III-4** shows a less important shielding effect of the signals corresponding to protons in positions 4 and 5 than in the case of the chiral microcycles. As the benzene is less restrained than the naphthalene, its partial rotation is still possible and its orientation, not perpendicular to phenanthrene, leads to a weaker anisotropic effect. The spectrum however does not allow concluding whether rotation of the benzene is complete around the axis of its two *para* positions: the high symmetry of the compound leads to the phenylene protons giving a singlet whatever the extent of the rotation.

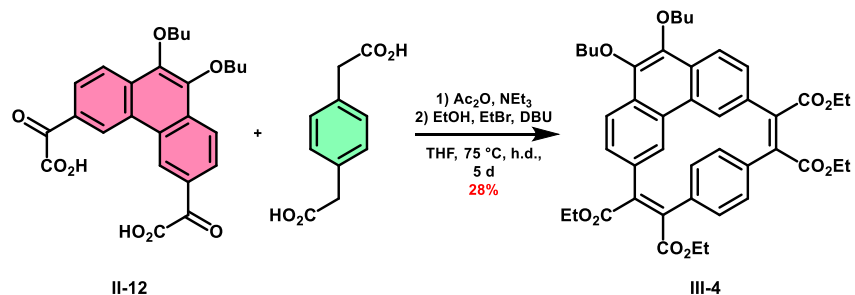


Figure 99. Synthesis of dibutoxy-phenanthroparacyclophane tetraester **III-4**.

The structure of this macrocycle makes it an excellent precursor for a hexasubstituted coronene by double intramolecular photo-dehydrocyclisation. **III-4** and I_2 were dissolved in a mixture of ethyl acetate and toluene and irradiated for one night by a UV lamp. The solvent was then removed *in vacuo*, and the residue was dissolved in dichloromethane, washed by an aqueous solution of sodium thiosulfate and dried over $MgSO_4$. Purification on silica gel gave dibutoxy-coronene tetraester **III-5** with a 65% yield (Figure 100).

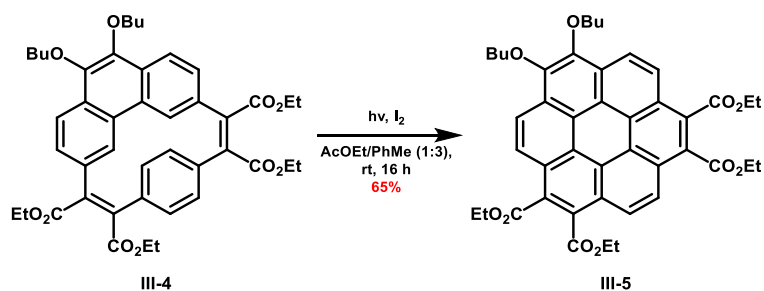


Figure 100. Photocyclization leading to the formation of dibutoxy-coronene tetraester **III-5**.

Recrystallizing product **III-5** in ethanol gave single crystals suitable for XRD. The structure was resolved and showed that, in the crystalline state, the compound packs in an offsetted columnar arrangement with close π - π interactions (Figure 101). The columnar packing of aromatic compounds functionalized by long ester chains is an exciting result that we may apply in our group for obtaining liquid crystals. **III-5** itself was not liquid-crystalline at any temperature.

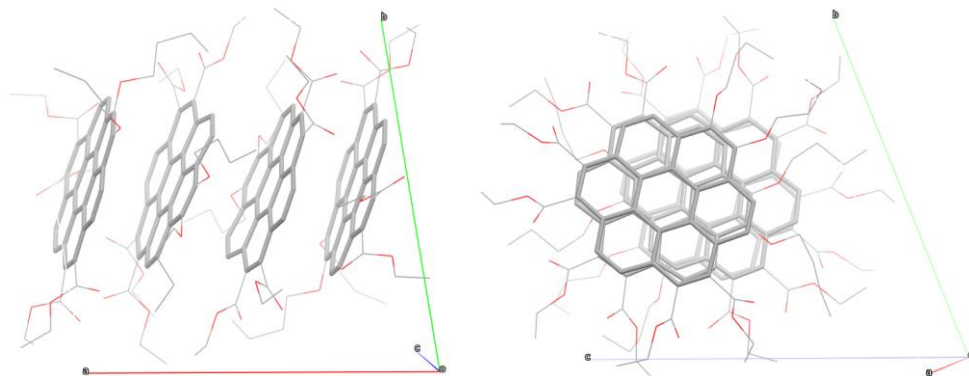


Figure 101. Coronene **III-5** seen along crystallographic *c* (left) and *a* (right). Hydrogens were omitted for clarity. Ester and ether groups = thin, aromatic cores = thick.

In order to understand the influence of substituents on the optical properties, we decided to expand the family of microcycles and substituted coronenes with two more members each, with either a weaker or a stronger push-pull effect.

Phenanthrene **II-12** and phenylene-1,4-diacetic acid were once again macrocyclized. This time, after the condensation step, 3-aminopentane was added instead of ethanol and bromoethane in order to form imide instead of diester groups. Purification of the residue by column chromatography gave microcycle **III-6** in 35% yield. After a photocyclisation in the same conditions as for compound **III-4**, the residue was purified over silica gel to isolate dibutoxy-coronene diimide **III-7** in 30% yield (Figure 102). The yield is significantly lower than the one of coronene tetraester **III-5** and could be due to the poor solubility of both **III-6** and **III-7** in organic solvents. No single crystals of these two compounds could be obtained, probably for the same reason.

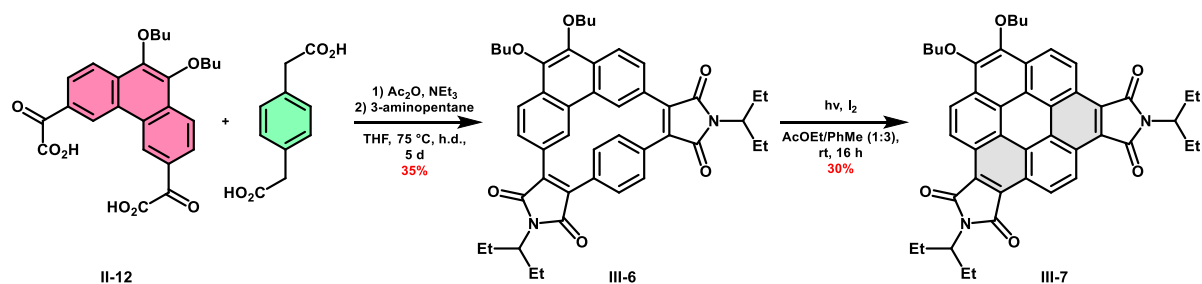


Figure 102. Synthesis of phenanthroparacyclophane diimide **III-6** and coronene diimide **III-7**.

In parallel, a macrocyclisation reaction involving phenanthrene diglyoxylic acid **II-5** and 1,4-phenylene diacetic acid led to phenanthroparacyclophane **III-8** after purification on column chromatography. The microcycle **III-8** was finally photocyclised for two days. The coronene tetraester **III-9** was obtained quantitatively after a work-up of the residue with an aqueous solution of sodium thiosulfate.

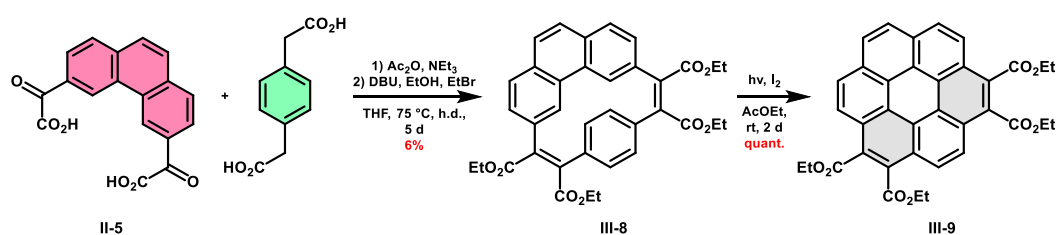


Figure 103. Synthesis of phenanthroparacyclophane **III-8** and coronene tetraester **III-9**.

Slow diffusion of a dichloromethane solution of **III-9** into butanol gave single crystals suitable for XRD. It crystallizes in a manner similar to **III-5**, although its structure is more planar than the latter (Figure 104).

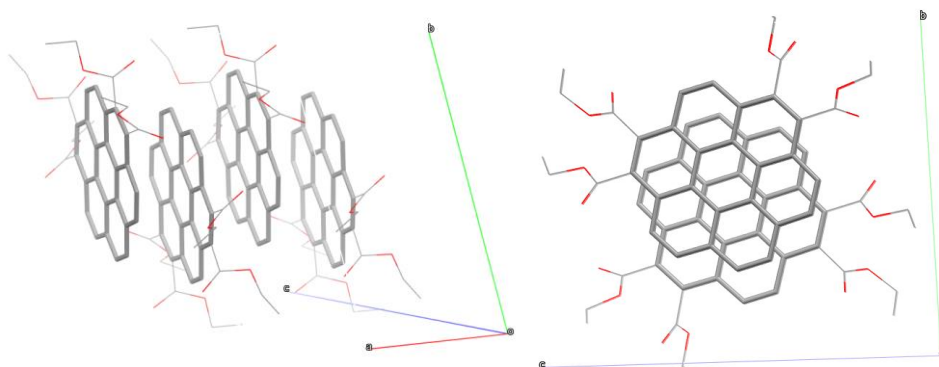


Figure 104. Coronene **III-9** seen along crystallographic *c* (left) and *a* (right). Hydrogens were omitted for clarity. Ester and ether groups = thin, aromatic cores = thick.

Planarised compounds **III-9** (tetraester), **III-5** (dialkoxy tetraester) and **III-9** (dialkoxy diimide) are a small family of substituted coronenes, with an increasing push-pull effect. Their photophysical properties were investigated.

The absorption spectra of all coronenes and their cyclophane precursors were measured in dichloromethane at room temperature. The planar structure and the aromatic character of coronene mean that it may aggregate in solution. This would be observable with UV-visible spectroscopy. But no hypsochromic or bathochromic shifts were observed when increasing the concentration, which suggests that no H- or J- aggregates were formed.

Emission spectra were measured in dichloromethane at room temperature (Figure 105). The quantum yields of luminescence were determined using Coumarin 153 in ethanol as standard. The three coronenes **III-5**, **III-7** and **III-9** proved to be fluorescent, with the two dibutoxy-coronenes showing the highest quantum yields (18% each), while **III-9** was slightly less emissive (11%). The macrocyclic precursors had no apparent emission, except for **III-6**, although with a very weak quantum yield of luminescence (*ca.* 1%)

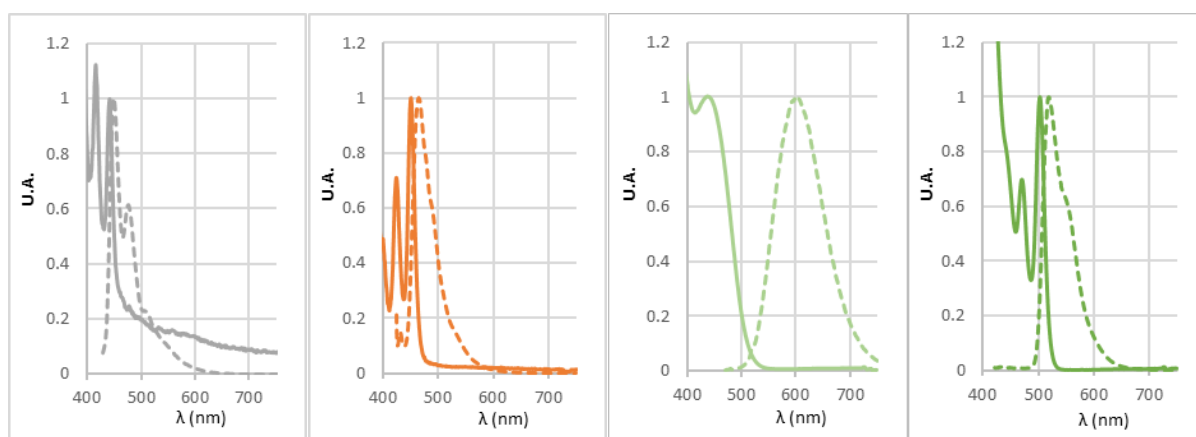


Figure 105. Normalized absorption (continuous) and fluorescence (dashed) spectra of **III-5** (first spectrum), **III-6** (second spectrum), **III-7** (third spectrum) and **III-9** (fourth spectrum) in CH_2Cl_2 at room temperature. Emission was measured upon excitation at 420 nm for **III-5**, 450 nm for **III-6**, 390 nm for **III-7** and 425 nm for **III-9**.

These results showed once again that the Perkin strategy allows an easy and fast access to carboxy-substituted polycyclic arenes, whose luminescence depends on the substitution pattern.

b. Synthesis of an asymmetric coronene

The protecting techniques for the Perkin reaction allow in principle the design of a coronene functionalized by three different substituents. Its formation would require a first Perkin reaction forming a maleic bridge with a cyclic imide before a Perkin macrocyclization creating a maleic bridge with two ester functions (Figure 106). This builds on the results of Frédéric Aribot, who proved during his doctorate that it was possible to selectively saponify ester functions in the presence of cyclic maleimides in mild conditions. It would thus be conceivable to attach a bifunctional phenanthrene to a bifunctional benzene by a single maleimide link, and, after saponification of the protecting groups, create the macrocycle with a maleic ester link. Unfortunately, since mono-protected phenanthrene could not be obtained, the first condensation would have to be carried on between a mono-protected phenylene building block and an unprotected bifunctional phenanthrene, hoping that an chosen stoichiometry would lead to the desired mono-condensation.

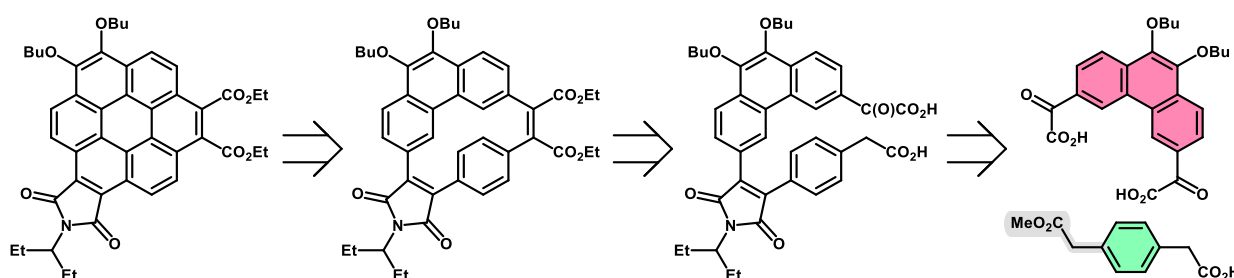


Figure 106. Retrosynthesis of the target asymmetric coronene.

Phenylene-1,4-diacetic acid was first esterified by thionyl chloride in methanol. After stirring for four hours at reflux, the solution was cooled to room temperature and the solvent was removed under reduced pressure. Recrystallization of the residue in methanol gave dimethyl phenylene-1,4-diacetate **III-10** quantitatively as white crystals. This diester was then partially saponified in presence of only one equivalent of KOH in THF. Similarly to the purification of the mono-protected diacetic naphthalene block, pH-controlled filtrations led to the isolation of the desired monoester-monoacid **III-11** (Figure 107).

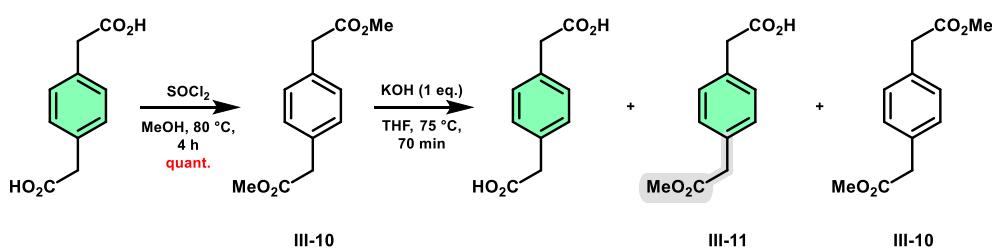


Figure 107. Synthesis of dimethyl phenylene-1,4-diacetate **III-10** and subsequent partial saponification leading to monoester **III-11**.

The best way to favor the formation of an acyclic diblock intermediate would have been to use a monoprotected phenanthrene, but since its synthesis was not successful (See Chapter 2), another approach, less controlled, had to be used. As the Perkin reaction between monoprotected naphthalenes and diacidic phenanthrene surprisingly gave mainly monocondensation (see Chapter 2), we were confident that we could obtain the same results with a monoprotected phenylene instead of a naphthalene, and therefore efficiently attach only one phenylene-based building block to a bifunctional phenanthrene. Stoichiometric amounts of monoprotected phenylene **III-11** and dibutoxy-phenanthrene-diglyoxylic acid **II-12** were then coupled in a diluted Perkin reaction followed by imidification, instead of the usual diester. After the work-up and purification on column chromatography, two products were isolated. The first one was a phenanthrene substituted by two monoprotected phenylenes **III-13**. The second product was as expected a phenanthrene substituted by a single monoprotected phenylene block. The ^1H NMR spectrum of the sample revealed nevertheless that it was not the desired product. Contrary to the previous monocoupling reaction between phenanthrene and naphthalene, the condensation was this time followed by an imidification reaction, instead of a diester formation. Upon addition of a primary amine to the reaction mixture, an undesired decarboxylation occurred, to give **III-14**, which bears an aldehyde moiety instead of a glyoxylic acid (Figure 108).

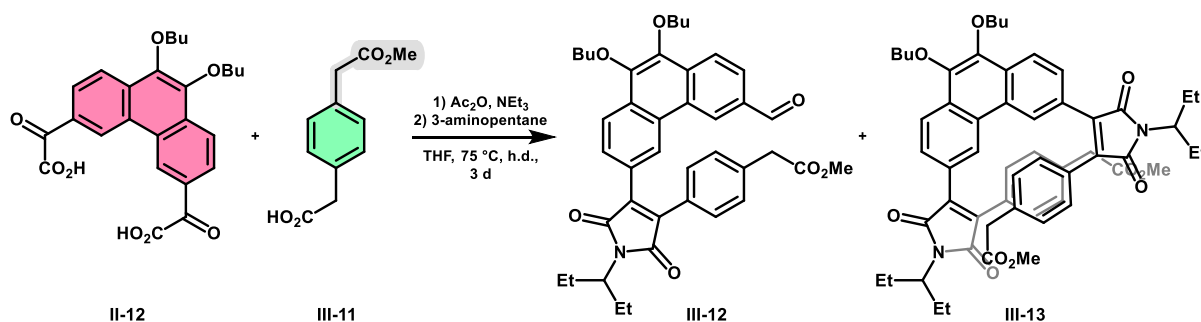


Figure 108. Perkin reaction leading to disubstituted phenanthrene **III-12** and monosubstituted phenanthrene **III-13**.

The intermediate **III-13** cannot lead to the hexasubstituted asymmetric coronene, but a final ring closing traditional (aldehydic) Perkin reaction would still be possible after saponification of this product. The resulting phenanthroparacyclophane and subsequent coronene would then be functionalized by a cyclic imide, two ethers and a single ester function (Figure 109). The time was missing to investigate further this approach.

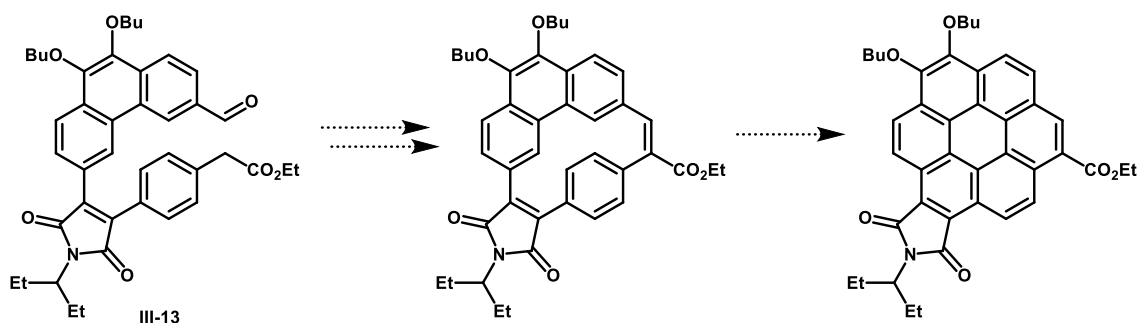


Figure 109. Potential macrocyclisation of intermediate aldehyde **III-13** and resulting coronene by photocyclization.

With no access to the monoprotected phenanthrene and no ways of protecting the glyoxylic acid during the Perkin reaction, the synthesis of the asymmetric coronene was not pushed forward. Another less elegant approach to obtain the target diether-imide-diester could be based on the monoimidification of dibutoxy-coronene tetraester. In the same manner as the monosaponification, this reaction would lead to a mixture of coronene tetraester, coronene imide diester and coronene diimide, that should be separable by column chromatography or even better on GPC.

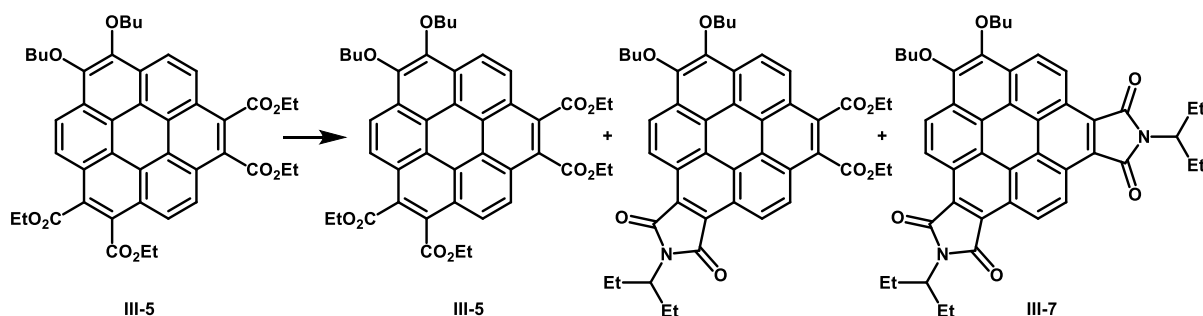


Figure 110. Potential statistical monoimidification of dibutoxycoronene tetraester **III-5**.

c. Synthesis of macrocycles with a D_{3h} symmetry

After the synthesis of the coronenes with a D_{2h} symmetry and in parallel to the synthesis of the asymmetric coronene, the final target of this project was the synthesis of a coronene with a D_{3h} symmetry. For this objective, we have adopted a strategy based on the homocoupling of brominated precursors. Two possible retrosyntheses were designed. In the first (Figure 111a) the homocoupling of two monobrominated precursors would lead to the formation of a stilbene functionalized with two acetic esters. After saponification, this stilbene could react with one equivalent of phenylene-diglyoxylic acid in a high dilution Perkin reaction to form the macrocyclic precursor of coronene hexaester. In the second (Figure 111b), one equivalent of phenylene-diglyoxylic acid could react with two equivalents of monoprotected phenylene-diacetic acid to form a flexible trimer with two terminal acetic ester functions. Each acetic function could then be brominated, and the resulting product could be engaged in an intramolecular homocoupling reaction to give the required macrocyclic precursor. As this approach was new for our group, and the production of phenylene-diglyoxylic acid being relatively cumbersome, only the first approach was investigated.

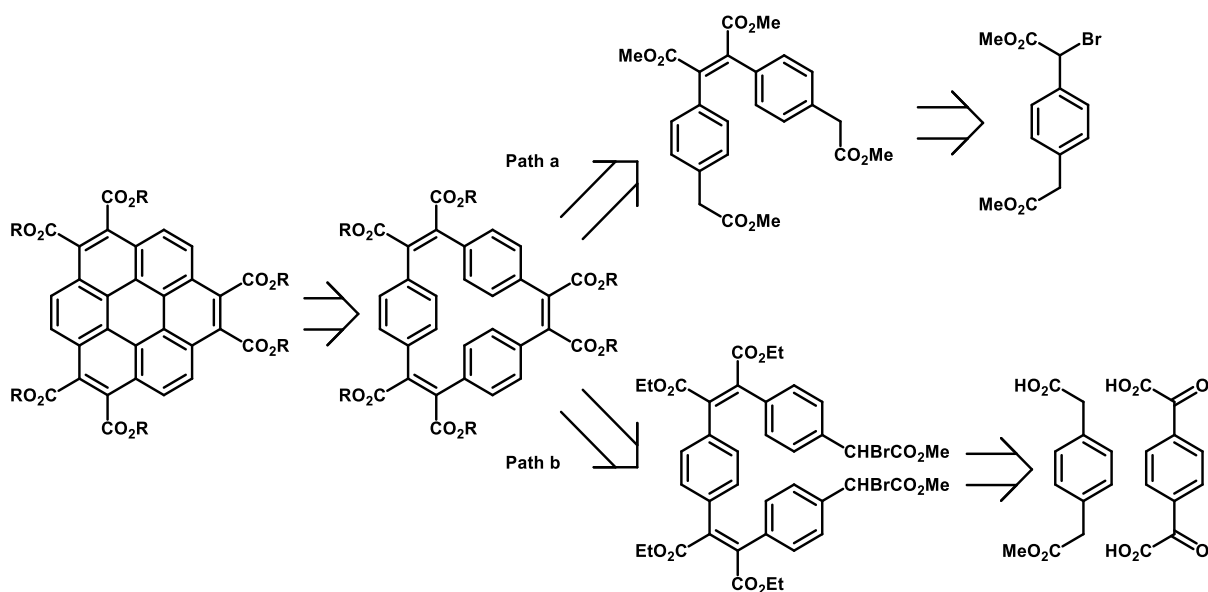


Figure 111. Synthetic approaches possible for the synthesis of a coronene hexaester.

Phenylene diacetic ester **III-10**, N-bromosuccinimide (NBS) and azobisisobutyronitrile (AIBN) were dissolved in chloroform and the mixture was stirred at reflux for 5 h (Figure 112). The residue was easily purified on silica gel and three compounds were obtained: the monobrominated product **III-14** (57% yield), the dibrominated compound **III-15** and the starting material (both 20% yield).

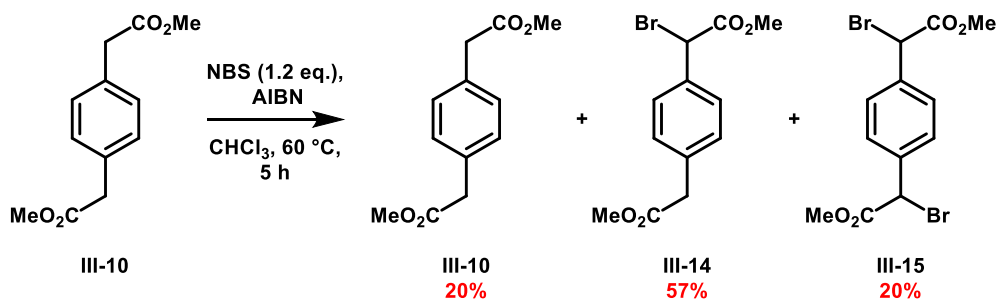


Figure 112. Monobromination reaction of phenylene diacetic ester **III-10**.

In the literature, the coupling was optimal when using NaOH as a base and dimethylformamide (DMF) as a solvent.²³ A test reaction was thus done with the dimbrominated compound **III-15** in diluted conditions (Figure 113), with the hope of directly forming the flexible trimer in one step, but only polymers were formed during this reaction.

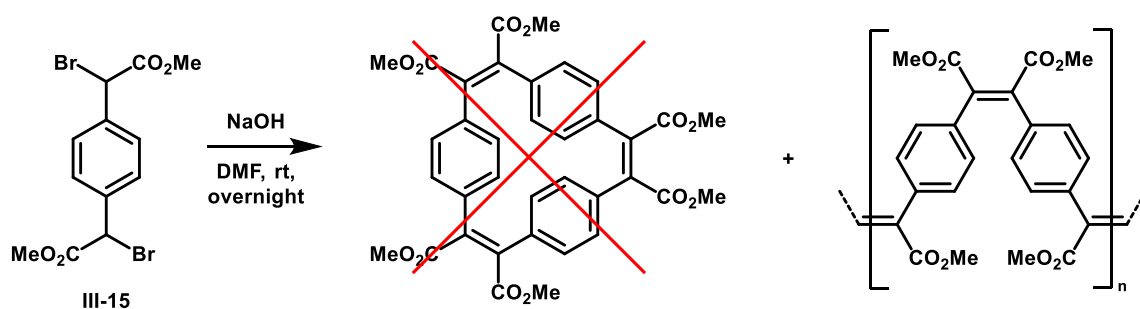


Figure 113. Macrocyclization attempt with III-15.

As planned initially, we tried to homocouple the monobrominated compound III-14 in DMF in the presence of NaOH (Figure 114). Once again, and a lot more surprisingly, only polymers were obtained. Due to lack of time, this reaction was however only tested once. The optimization of this approach (choice of base and dilution) could not only lead to symmetrically hexasubstituted coronenes, but could also yield a second strategy for the controlled assembly of diacetic building blocks.

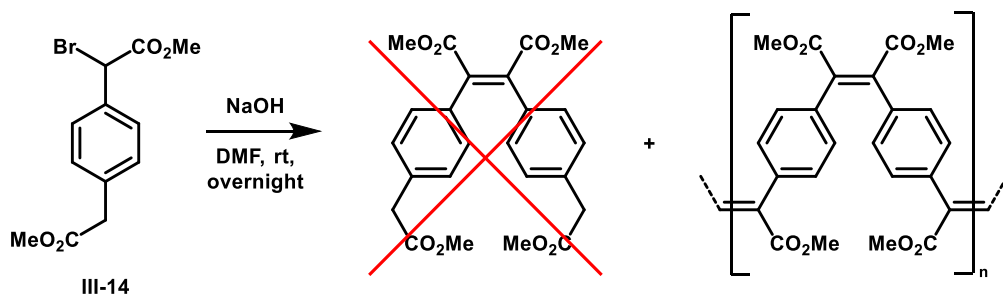


Figure 114. Homocoupling attempt with III-14.

Conclusion

The macrocyclization reactions involving a disubstituted 3,6-phenanthrene and short complementary bifunctional building blocks (from naphthalene or benzene) always led to phenanthrocyclophanes. The formation of such two-unit macrocycles was surely induced by the pincer-like arrangement of the 3,6-substituted phenanthrene, contrary to the other usual bifunctional building blocks with functionalization in opposite directions. This specificity was exploited and applied to the synthesis of phenanthroparacyclophanes.

A family of short chiral macrocycles composed of only two building blocks was first obtained with the Perkin strategy and their chiroptical properties were studied. These *microcycles* proved to be unique structures with two close orthogonal units and robust enantiostability. Their ECD and CPL revealed usual dissymmetry factors for such organic chiral chromophores. All these *microcycles* proved to be fluorescent, although with low quantum yields.

The use of phenanthrene with and without alkoxy substituents and the use of either maleimide or maleic ester bridges allowed the synthesis of three achiral phenanthroparacyclophanes. These proved to be good precursors for tetra- and hexafunctionalized coronenes with push-pull geometries. The coronenes were obtained in a

small number of steps, although with moderate yields, and proved to be fluorescent. The single crystals obtained for two of these structures showed columnar stacks with close interactions. This propensity to stack in columns suggests that with longer alkyl moieties, liquid crystalline homologs might be obtainable.

Attempts to obtain a microcycle and the corresponding coronene with three differently substituted peripheral segments led to a difunctional diblock intermediate with a terminal aldehyde function instead of the expected glyoxylic acid function. This aldehyde was not macrocyclized due to lack of time.

Two approaches were tested for the synthesis of a D_{3h} symmetric coronene hexaester. The first one was based on a combination of the Perkin reaction with a coupling between two dibrominated building blocks. The second one was based on a macrocyclic benzoin condensation. Both failed on our first attempts, but our minor efforts were not exhaustive.

References

- 1 R. Scholl and K. Meyer, *Berichte Dtsch. Chem. Ges. B Ser.*, 1932, **65**, 902–915.
- 2 S. Kumar and Y. Tao, *Chem. – Asian J.*, 2021, **16**, 621–647.
- 3 M. A. Dobrowolski, A. Ciesielski and M. K. Cyrański, *Phys. Chem. Chem. Phys.*, 2011, **13**, 20557.
- 4 N. Fedik and A. I. Boldyrev, *J. Phys. Chem. A*, 2018, **122**, 8585–8590.
- 5 A. K. Kandalam, B. Kiran, P. Jena, X. Li, A. Grubisic and K. H. Bowen, *J. Chem. Phys.*, 2007, **126**, 084306.
- 6 H. Takemura and K. Sako, *Tetrahedron Lett.*, 2005, **46**, 8169–8172.
- 7 Y. Yoshida, Y. Kumagai, M. Mizuno, K. Isomura, Y. Nakamura, H. Kishida and G. Saito, *Cryst. Growth Des.*, 2015, **15**, 5513–5518.
- 8 K. V. Rao, K. Jayaramulu, T. K. Maji and S. J. George, *Angew. Chem.*, 2010, **122**, 4314–4318.
- 9 J. Liu, X. Zhang, H.-J. Yan, D. Wang, J.-Y. Wang, J. Pei and L.-J. Wan, *Langmuir*, 2010, **26**, 8195–8200.
- 10 E. Clar and M. Zander, *J. Chem. Soc. Resumed*, 1957, 4616–4619.
- 11 E. Clar, Ü. Sanigök and M. Zander, *Tetrahedron*, 1968, **24**, 2817–2823.
- 12 J. Craig, B. Halton and S. Lo, *Aust. J. Chem.*, 1975, **28**, 913–916.
- 13 J. Davy and J. Reiss, *Aust. J. Chem.*, 1976, **29**, 163–171.
- 14 P. Jessup and J. Reiss, *Aust. J. Chem.*, 1977, **30**, 843–850.
- 15 T. Liu, J. Yang, F. Geyer, F. S. Conrad-Burton, R. Hernández Sánchez, H. Li, X. Zhu, C. P. Nuckolls, M. L. Steigerwald and S. Xiao, *Angew. Chem. Int. Ed.*, 2020, **59**, 14303–14307.
- 16 M. Ferreira, T. S. Moreira, R. Cristiano, H. Gallardo, A. Bentaleb, P. Dechambenoit, E. A. Hillard, F. Durola and H. Bock, *Chem. – Eur. J.*, 2018, **24**, 2214–2223.
- 17 M. Sauer, J. Hofkens and J. Enderlein, *Handbook of fluorescence spectroscopy and imaging: from single molecules to ensembles*, WILEY-VCH-Verlag, Weinheim, 2011.
- 18 A. M. Brouwer, *Pure Appl. Chem.*, 2011, **83**, 2213–2228.
- 19 N. Berova, L. D. Bari and G. Pescitelli, *Chem. Soc. Rev.*, 2007, **36**, 914–931.
- 20 L. Arrico, L. Di Bari and F. Zinna, *Chem. – Eur. J.*, 2021, **27**, 2920–2934.
- 21 J. R. Lakowicz, Ed., in *Principles of Fluorescence Spectroscopy*, Springer US, Boston, MA, 2006, pp. 205–235.
- 22 L. Soliman, E. Ramassamy, K. Dujarric, G. Naulet, P. Dechambenoit, H. Bock and F. Durola, *Chem. Commun.*, 2024, **60**, 4439–4442.
- 23 J. Lyu and C. W. Bielawski, *Polym. Chem.*, 2022, **13**, 613–621.

Chapter 4: Macrocyclic hexamer of phenanthrenes

I. Introduction

In previous projects of our team, it has been shown that some rigid conjugated macrocycles may have topologically persistent non-trivial geometries even though they were not strictly non-trivial topologically due to incomplete condensation of the ribbon geometry. The figure-of-eight shape for example can be induced by two rigidly linked helical moieties, as reported in the literature by our group or later by Matsuda and Hirose (Figure 115).^{1,2} These macrocycles are not topologically non-trivial, due to the single bonds linking the [5]helicene parts (See Chapter 1), yet the nodal surface of the π -type molecular orbitals has the shape of a figure-of-eight.

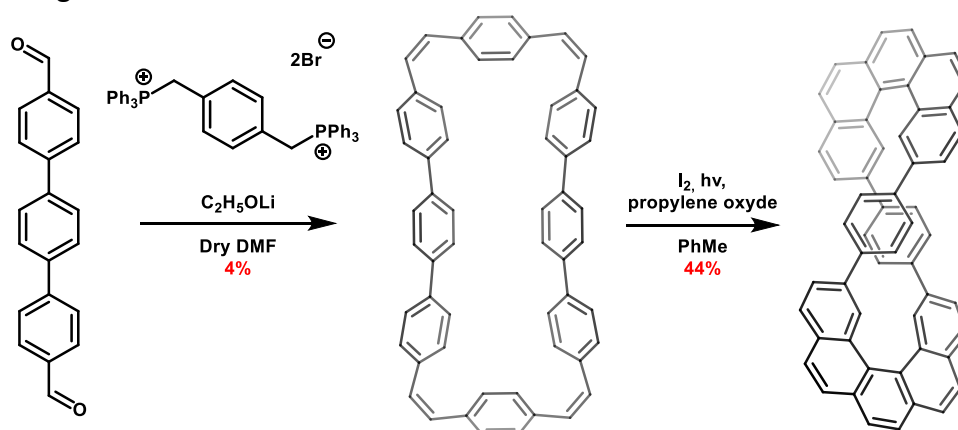


Figure 115. Figure-of-eight-shaped dimer synthesized by Matsuda's and Hirose's groups.

This particular shape can also be induced by the insertion of a “node” in the macrocycle. By coupling a spirobifluorenyl to two trimers of carbazole, Shi and coworkers synthesized a figure-of-eight type macrocycle (Figure 116)³ despite the single bonds linking the different aromatic units.

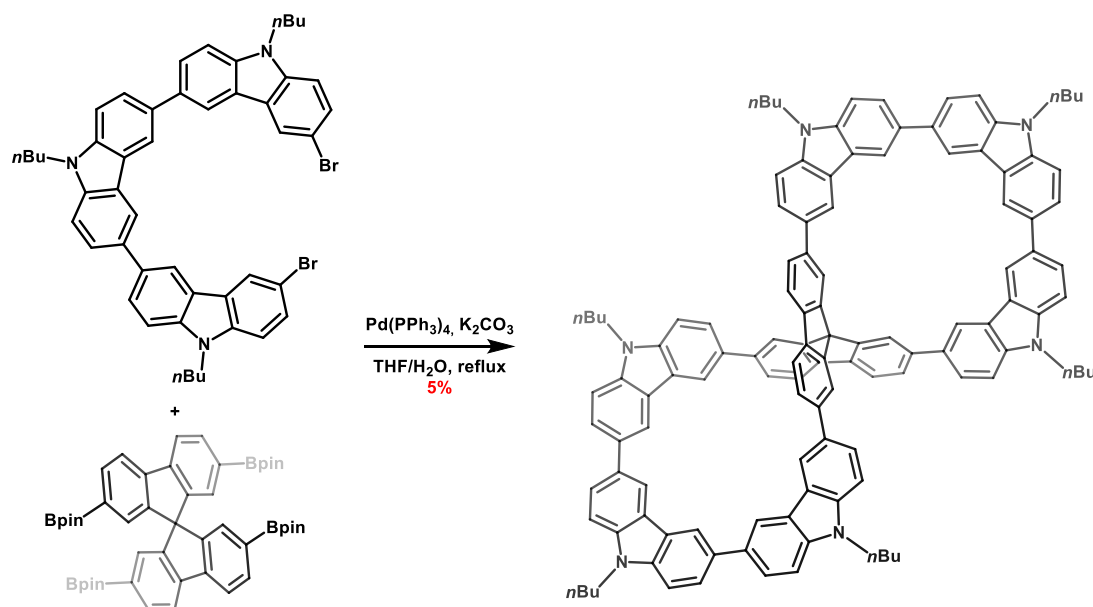


Figure 116. Spirobifluorenyl-based figure-of-eight macrocycle obtained by Shi.

Weaker intramolecular interactions can also be used to stabilise such a geometry. By homocoupling phenanthrenediynes, Luo's team obtained arylbutadiyne macrocycles of different sizes.⁴ While the macrocycle with three phenanthrene units is a planar triangle, rigid saddle-shaped macrocycles are obtained with four or five units. A hexaarylbutadiyne was also obtained using a palladium-catalyzed Glaser coupling in pseudo-high dilution conditions (Figure 117). In the crystal, this flexible compound adopts a figure-of-eight topology, where two diyne links adopt a *trans* conformation and force a *cis* conformation of the four other links. This shape is stabilized by the π - π interactions between the superposed phenanthrenes.

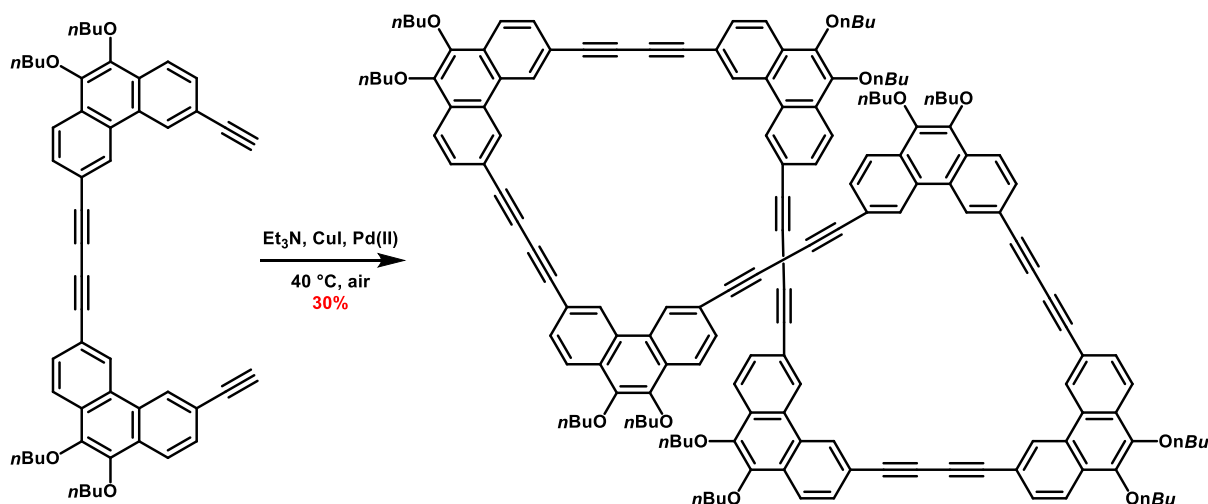


Figure 117. Synthesis of a figure-of-eight-shaped macrocyclic arylbutadiyne by Luo et al.

During his doctoral thesis in our group, from 2014 to 2017, Antoine Robert synthesized a macrocyclic Perkin tetramer of biphenyl units linked by maleic bridges, starting from a stoichiometric mixture of two complementary biphenyl building blocks.⁵ After a first column on silica gel, the purification of this reaction was optimized by GPC. Two products with similar ¹H NMR spectra were isolated, yet they were of different sizes as indicated by the chromatogram. Mass spectrometry revealed that the smaller macrocycle was the targeted product of the reaction, which was then used to synthesize a saddle-shaped macrocycle containing four phenanthrenes. The second product was a macrocyclic hexamer of biphenyls, obtained in just sufficient quantity to be characterized (Figure 118).

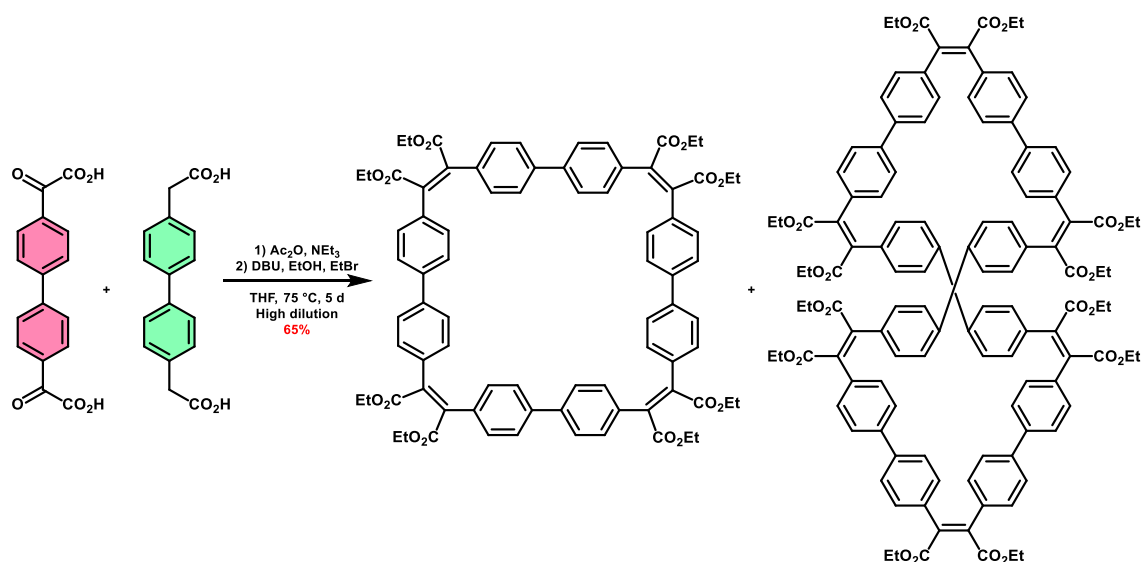


Figure 118. Products isolated by Antoine Robert after a macrocyclization of two complementary bifunctionalized biphenyls.

Contrary to the tetramer, whose photocyclization led to a rigid macrocycle, photocyclization of this larger macrocycle would lead, according to geometrical simulations, to a flexible macrocyclic hexamer of phenanthrenes. With six possible rotations around single bonds, it can adopt several conformations (Figure 119). When all single bonds are in *trans* conformation, the macrocycle will adopt a *crown* geometry, with a cavity in its center. If the single bonds alternate between *cis* and two consecutive *trans* conformations, the macrocycle adopts a flatter *chair* geometry. Finally, the macrocycle can adopt a folded *figure-of-eight* geometry when the single bond conformations are successively *cis-cis-trans-cis-cis-trans*. In semi-empirical simulations, the latter appears to be the energetically most favored conformation. This structure is stabilized by π - π stacking between the central phenanthrenes, leading to a more packed structure, and the small angles between two adjacent phenanthrenes allow an efficient electronic delocalization around the whole macrocycle.

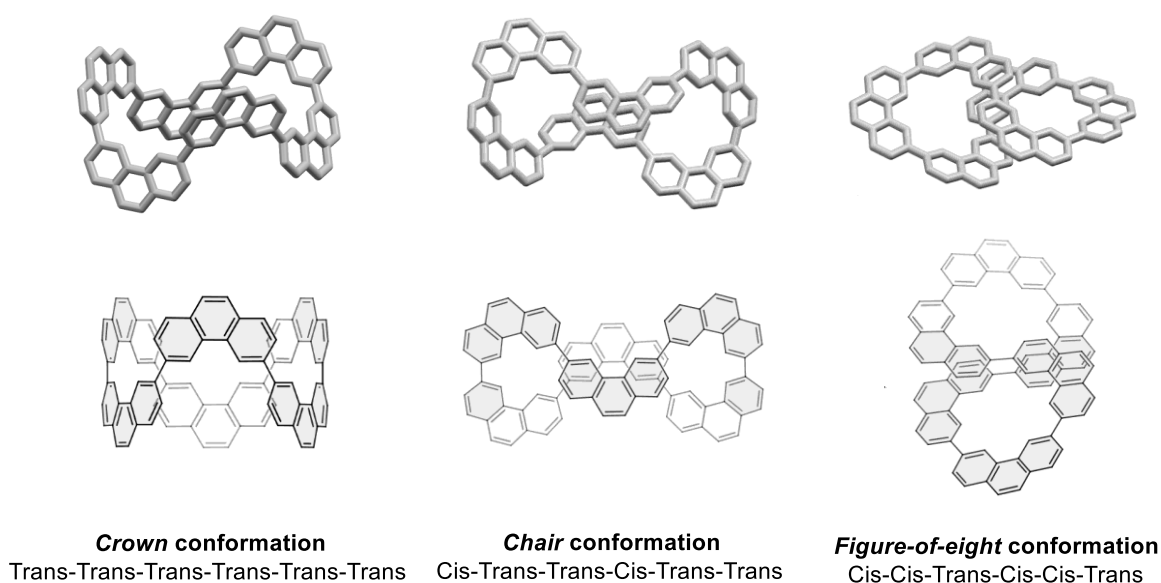


Figure 119. Possible conformations of a macrocyclic hexamer of phenanthrenes.

During the synthesis of the macrocyclic tetramer of biphenyl blocks, the hexameric counterpart was isolated as an impurity. As the macrocycle could be obtained using a stoichiometric mixture of elementary building blocks, a macrocyclization reaction in higher concentration conditions was performed, but did not yield the expected hexameric macrocycle. A stepwise controlled synthesis for this macrocyclic hexamer was therefore set up. Two trimers of biphenyl building blocks, one functionalized by glyoxylic acids and the other by acetic acids, were first to be synthesized. A macrocyclization reaction between these two trimers should then lead to the macrocyclic hexamer of maleate-bridged biphenyls, which could finally be photocyclised into a macrocyclic hexamer of phenanthrenes.

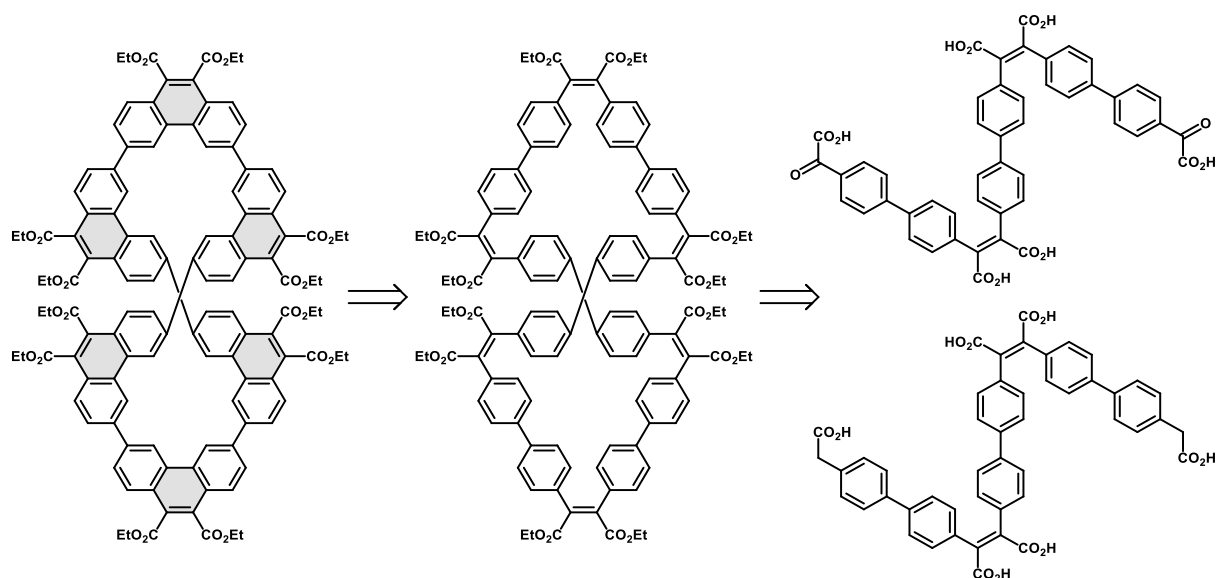


Figure 120. Retrosynthesis for the approach to a macrocyclic hexamer of phenanthrene.

II. Capping a brominated trimer with Suzuki-Miyaura coupling

a. Presentation of the strategy

The two complementary bifunctional flexible precursors required for the synthesis of the macrocycle are composed of the same type and succession of aryl parts, and only differ by their external functions. Thus a different synthetic strategy combining Perkin reactions and Pd-catalyzed coupling reactions can be considered in order to first develop the formation of a common precursor, which can be differentiated at the last step (Figure 121). A dibrominated common precursor resulting from a double Perkin condensation is “capped” by a benzene functionalized either by a glyoxylic ester or an acetic ester. The dibrominated intermediate required for this strategy is readily obtainable from commercially available *p*-bromophenylacetic acid and from easily made 4,4'-biphenyl-diglyoxylic acid. The two boronic esters required for the Suzuki-Miyaura coupling are also easily obtainable by borylation of suitably functionalized bromobenzenes.

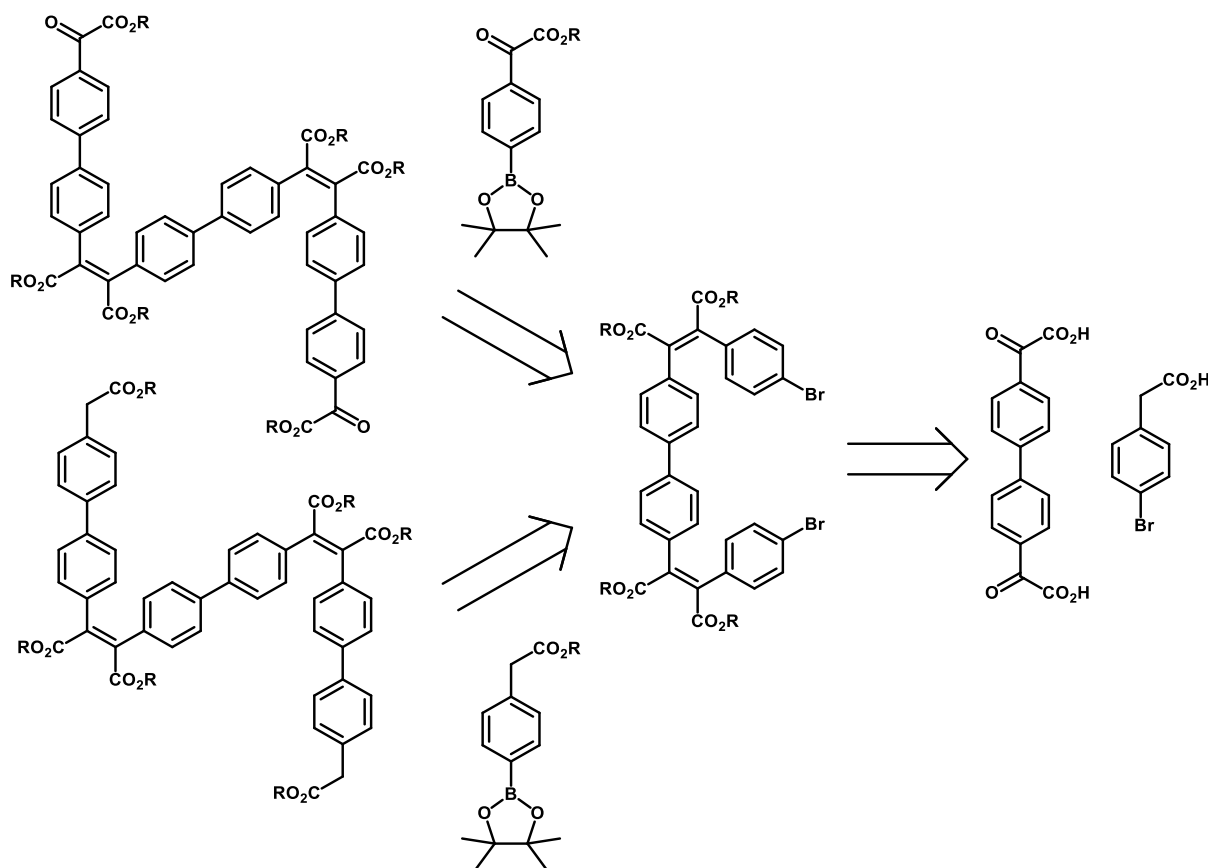


Figure 121. Retrosynthesis for both trimers by Suzuki-Miyaura and Perkin reactions.

b. Synthesis of the building blocks

The first required building block is biphenyl-4,4'-diglyoxylic acid. Commercially available 4,4'-dibromobiphenyl was lithiated to obtain biphenyl-4,4'-diglyoxylic ester **IV-1**. Contrary to the lithiation reaction reported in the previous chapters, the second lithium-halogen exchange is fast with biphenyls and does not require an important temperature increase. *n*BuLi can thus be used instead of *t*BuLi, as the *n*-bromobutane formed after the halogen-lithium exchange will not react as an electrophile with the formed organolithium intermediates.

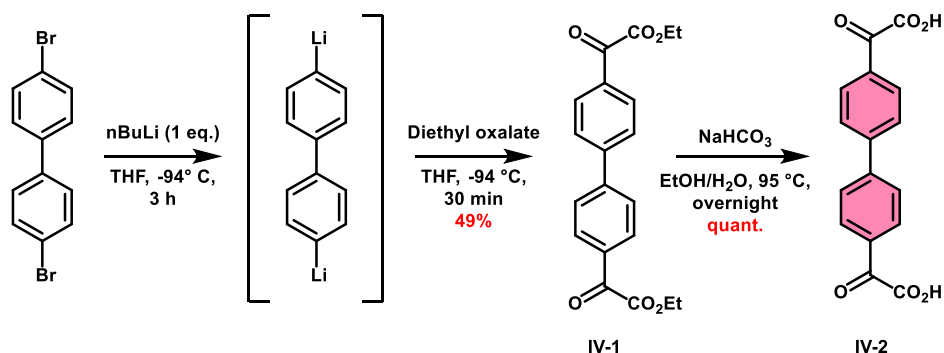


Figure 122. Synthesis of biphenyl-4,4'-diglyoxylic acid **IV-2**.

This diglyoxylic acid was Perkin-condensed with two equivalents of commercially available *p*-bromophenylacetic acid (Figure 123). After addition of acetic anhydride and trimethylamine, the solution was stirred at reflux. The condensation usually happens over the course of one

was synthesized by previous doctoral students by a Friedel-Crafts acylation of bromobenzene with ethyl oxalyl chloride ClCOCO_2Et (Figure 125).

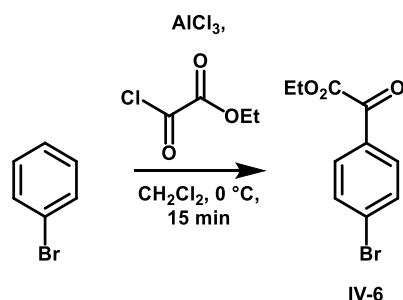


Figure 125. Synthesis of *p*-bromophenyl-glyoxylic ethyl ester **IV-6**.

Suzuki-Miyaura coupling creates C-C bonds between arylboronic esters and haloarenes in mildly basic conditions. The saponification of the glyoxylic ester is also performed in mildly basic conditions. Undesired saponification could therefore happen during the Suzuki coupling of substrates containing glyoxylic ester functions. To test the efficiency of this approach for the synthesis of the complementary bifunctional flexible precursors, the first Suzuki coupling was thus realized with the phenyl boronic ester **IV-5** functionalized with an acetic methyl ester, more resilient in the reaction conditions than its glyoxylic homolog. This reaction was first performed by refluxing the reagents overnight in toluene with a $[\text{Pd}(\text{PPh}_3)_4]$ complex. After the work-up, the residue was purified by column chromatography and the trimeric intermediate **IV-7** was isolated in 4% yield. The reaction time was increased up to 5 days, resulting in an improvement of the yield, which still remained modest (14%). Other conditions were tried, using $[\text{PdCl}_2(\text{PPh}_3)_2]$ as the catalyst in a mixture of toluene, ethanol and water (Figure 126). TLCs revealed that the reaction was not progressing anymore after five days of stirring at reflux. Purification of the residue led to the isolation of two major products, present in equal quantity. The first one was the desired trimer **IV-7**, while the second was a partially saponified version of the latter, whose ^1H NMR spectrum showed that albeit the acetic methyl ester moieties were indeed resistant to saponification during the coupling, this was not the case of the ethyl ester functions on the maleic bridges.

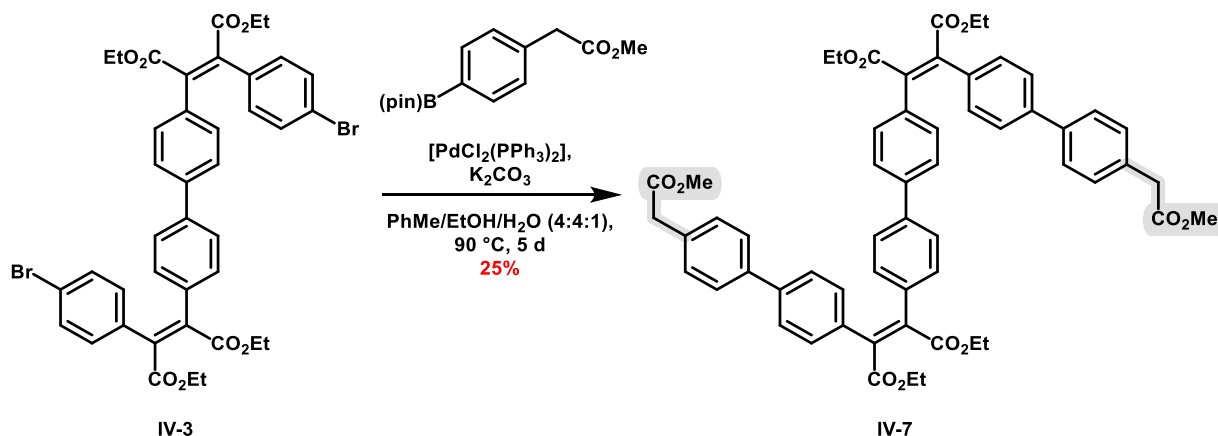


Figure 126. Synthesis of diacetic trimer **IV-7** by Suzuki-Miyaura coupling.

The difference of polarity between these two products was noticeable, yet the partially saponified trimer, missing two ester functions, was still purifiable by column chromatography on silica gel. Trimers who would have been subjected to further saponification however would not be purifiable by such a process, because of the high affinity of the silica with the acidic functions. As the product **IV-7** was significantly sensible to undesired saponification, to which its diglyoxylic homolog would have been even more sensible, we decided to change the approach for a longer, yet more usual and efficient, strategy.

III. Controlled assembly of monoprotected building blocks

The second approach was based on the controlled assembly of mono-protected building blocks to synthesize the two complementary flexible trimers (Figure 127). Following the usual Perkin procedures, two parallel syntheses are necessary, which imply the formation of three new building blocks: a biphenyl diacetic acid, a monoprotected biphenyl diacetic acid and a monoprotected biphenyl diglyoxylic acid.

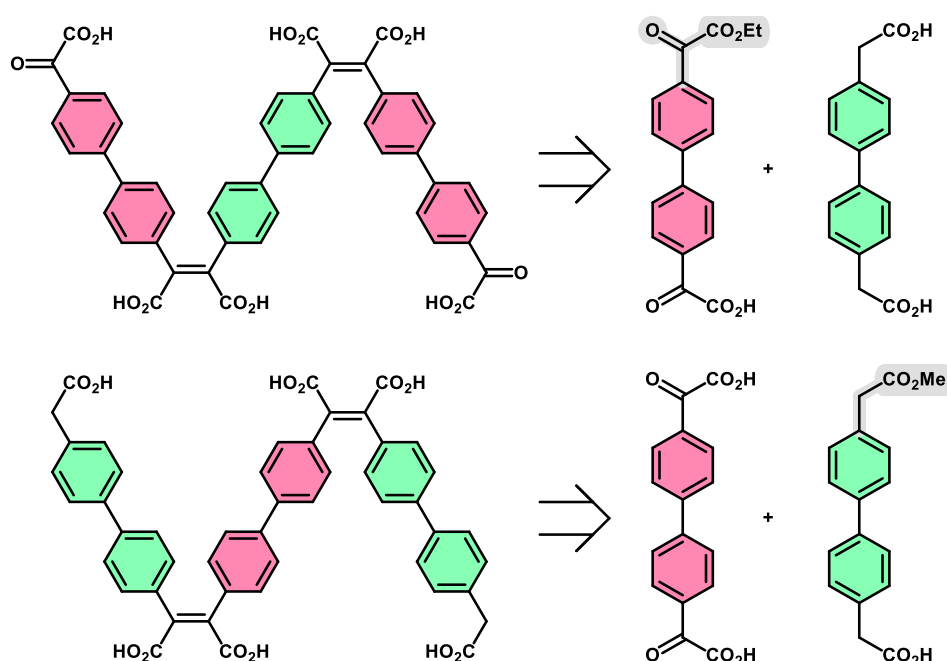


Figure 127. Retrosynthesis of the trimers using protection and deprotection techniques.

a. Synthesis of the building blocks

The biphenyl-4,4'-diglyoxylic acid **IV-2** was first reduced slowly and mildly by hypophosphorous acid (50%w in water) and sodium iodide. After stirring for three days at reflux, addition of water caused a precipitate to appear. Filtrating and washing the white powder with water gave the diacetic acid **IV-8** in 86% yield.

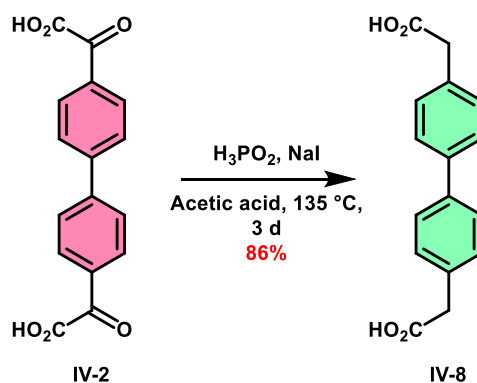


Figure 128. Synthesis of biphenyl-4,4'-diacetic acid **IV-9** by reduction of the diglyoxylic acid **IV-2**.

This product can be used with two complementary monoprotected diglyoxylic building blocks, or used to synthesize a monoprotected diacetic acid building block. First the diacetic acid **IV-8** was esterified with MeOH and SOCl_2 (Figure 129). Purification of the residue on silica gel gave the corresponding dimethyl ester **IV-9**. The latter can then react with one equivalent of potassium hydroxide to give a statistical mixture of more or less saponified products. As in previous monosaponifications, each compound could easily be separated by successive pH-controlled precipitations and filtrations and the expected biphenyl-diacetic monoester-monoacid **IV-10** could be isolated in 43% yield.

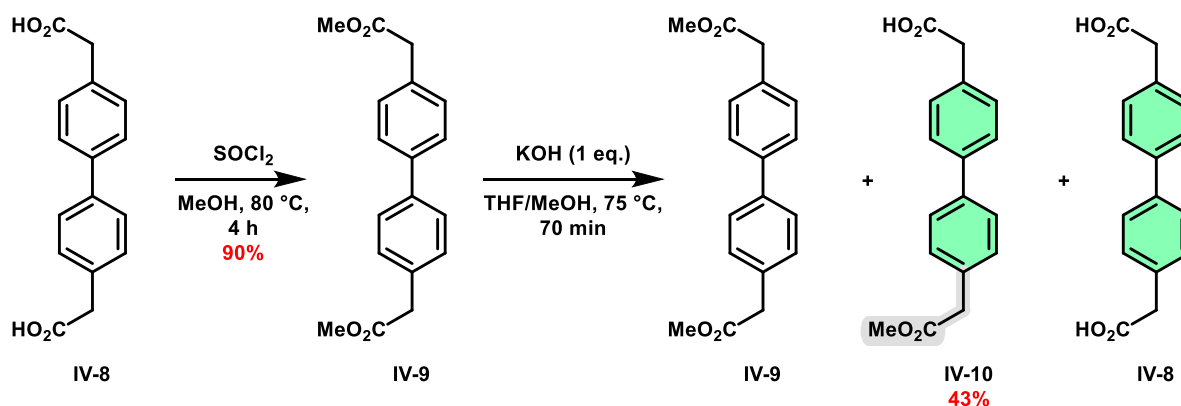


Figure 129. Synthesis of monoprotected 4,4'-biphenyl diacetic acid **IV-10**.

The same approach was used with biphenyl-4,4'-diglyoxylic ethyl ester **IV-1** (Figure 130) which is rapidly obtained from 4,4'-dibromobiphenyl in one step and can directly be used in a monosaponification reaction. Here, each filtration took a lot more time, due to the higher hydrophilicity of the glyoxylic functions. The monoprotected diglyoxylic biphenyl **IV-11** could nonetheless be isolated, with a yield of 39%. As usual, the two other products can be easily recycled.

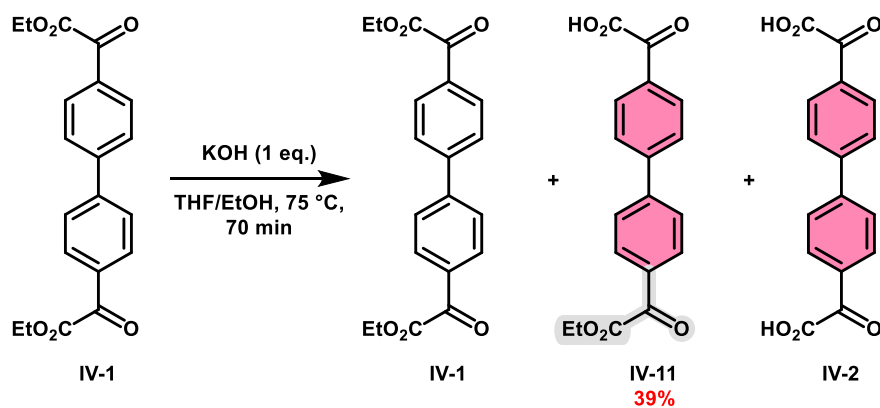


Figure 130. Synthesis of monoprotected 4,4'-biphenyl diglyoxylic acid IV-10.

b. Synthesis of the complementary trimers

One equivalent of biphenyl diacetic acid **IV-10** and two equivalents of monoprotected biphenyl diglyoxylic acid **IV-11** were engaged in a Perkin reaction (Figure 131). Except for macrocyclisation reactions, the Perkin reaction is usually more efficient in high concentration conditions. This statement proved to be true for the synthesis of this trimeric flexible precursor, which gave the best yields when using very high concentrations of reagents. Yet, asymmetric byproducts, missing two ester functions, were at first often isolated. This result pointed toward a too short esterification time, which was increased from 16 hours to 48 h. After optimization, the targeted compound could be isolated in 52% yield after purification by column chromatography.

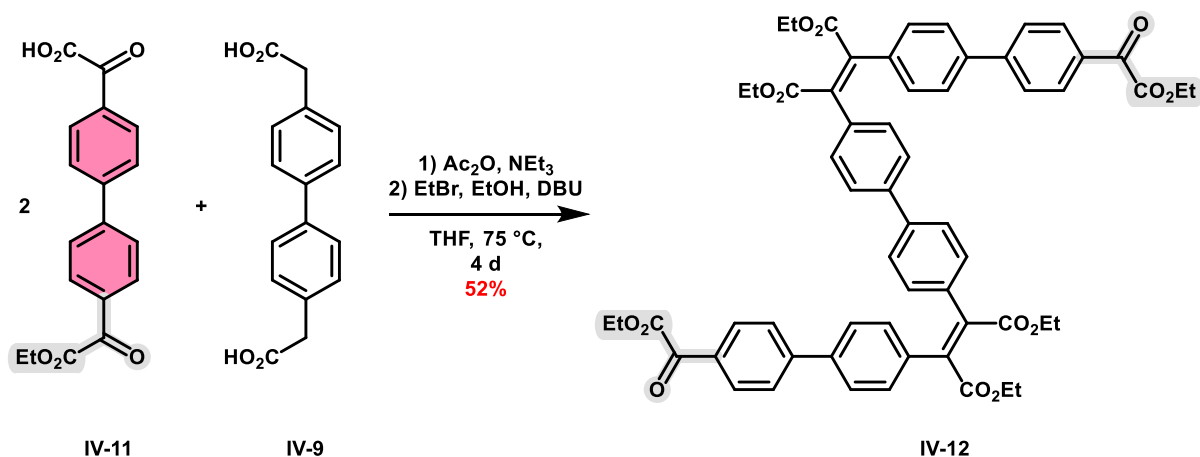


Figure 131. Synthesis of trimer diglyoxylic ethyl ester IV-12 by Perkin reaction.

This protected intermediate was then saponified in mild conditions. Compared to previous products of Perkin reactions, this hexaester, and the partially or fully saponified compounds, are poorly soluble in a basic mixture of ethanol and water. This resulted in incomplete saponification, giving a mixture of partially saponified products. Addition of THF to the mixture led to a homogeneous reaction medium and allowed the saponification to proceed to completion, yielding quantitatively the hexaacid **IV-13**.

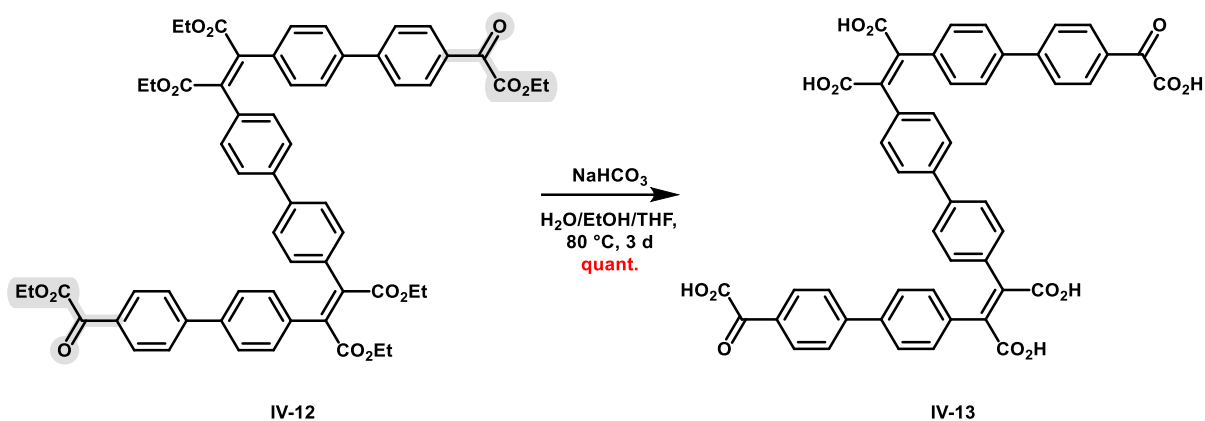


Figure 132. Synthesis of trimeric diglyoxylic acid **IV-13** by saponification.

The opposite Perkin reaction of biphenyl-diglyoxylic acid and mono-protected biphenyl-diacetic acid gave the complementary trimeric precursor **IV-7**. After four days of stirring at reflux, the residue was purified and the trimer **IV-7** was isolated in 49% yield (Figure 133).

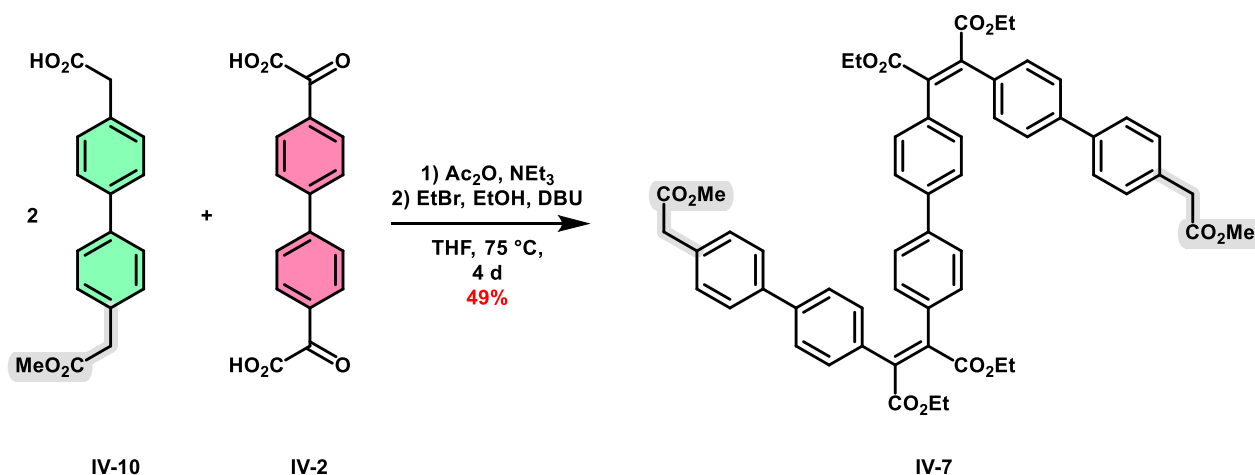


Figure 133. Synthesis of trimeric diacetic methyl ester **IV-7** by Perkin reaction.

This protected intermediate, either obtained from Suzuki coupling or from Perkin reaction, was saponified, again with added THF to improve solubility. After stirring for three days at reflux, the acidic trimer **IV-14** was obtained quantitatively after addition of aqueous HCl (10%w) and liquid-liquid extraction with a mixture of $\text{CH}_2\text{Cl}_2/\text{THF}$ (Figure 134).

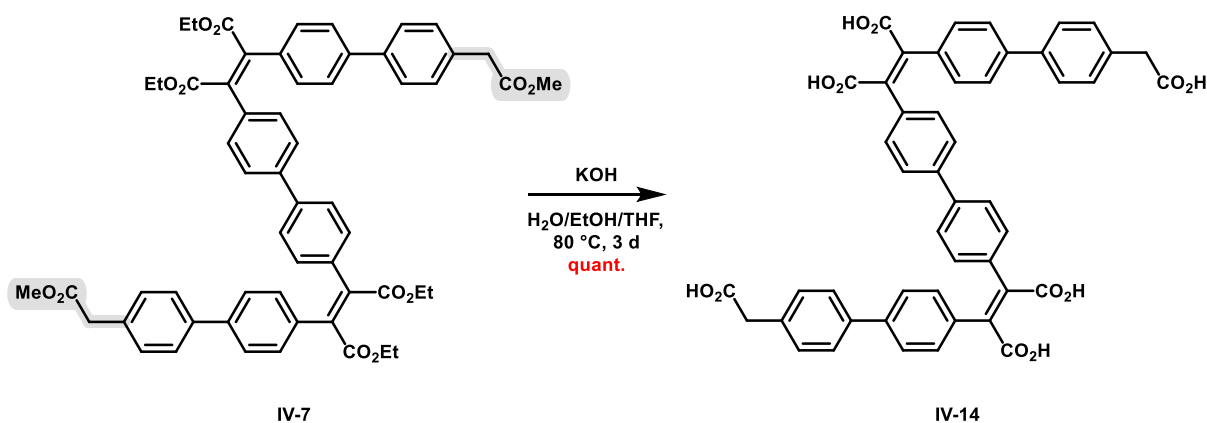


Figure 134. Synthesis of trimeric diacetic acid **IV-14** by saponification.

We also tried an alternative synthesis of this trimeric diacetic acid precursor **IV-14**. The Perkin reaction leading to this product being significantly less efficient than the one leading to its diglyoxylic homolog **IV-13**, more easily accessible and in larger quantities, we tested the reduction of glyoxylic acid moieties on a functionalized flexible Perkin product into acetic moieties. Trimer **IV-13** was reduced in the usual conditions for the reduction of simple glyoxylic acid building blocks (Figure 135). After stirring at reflux for three days, the reaction was cooled down and water was added. A precipitate appeared and was filtered, dried and analyzed by ^1H NMR spectroscopy. This revealed a mixture of products, among them the diacetic product **IV-14**, identifiable by a singlet at 3.6 ppm of the methylene protons. The reduction was therefore possible, although it was not complete after three days and had to be optimized. The residue was put to react for another three days at reflux, but the reaction still gave a mixture of products. Increasing the concentration had however a beneficial effect, as after three more days of stirring, the trimer **IV-14** was obtained with a 49% yield. This reaction proved to be reproducible and efficient, which added a new tool to the Perkin strategy by allowing to form flexible diacetic intermediates from their diglyoxylic analogs that are sometimes more easily obtained.

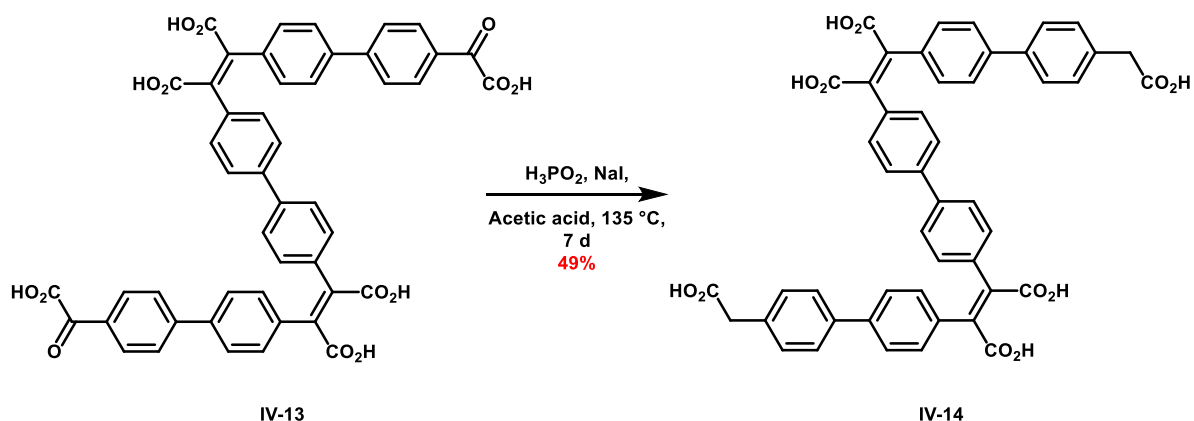


Figure 135. Synthesis of trimeric diacetic acid **IV-14** by reduction of trimer **IV-13**.

Thus, several approaches for the synthesis of the trimers were explored. The synthesis by Perkin reaction proved to be the most efficient approach. Sufficient amounts of

complementary trimeric macrocyclization precursors were obtained to attempt the synthesis of the target macrocycles.

c. Synthesis of the macrocycles

The two complementary precursors **IV-13** and **IV-14** were Perkin-condensed in high dilution. The reaction was at first tried in 1 L of solvent, with a concentration of 10^{-5} mol/L, but no macrocycle could be obtained. The concentration was finally increased 3×10^{-5} mol/L and after purification of the residue on silica gel, the macrocycle **IV-15** was isolated in 10% yield.

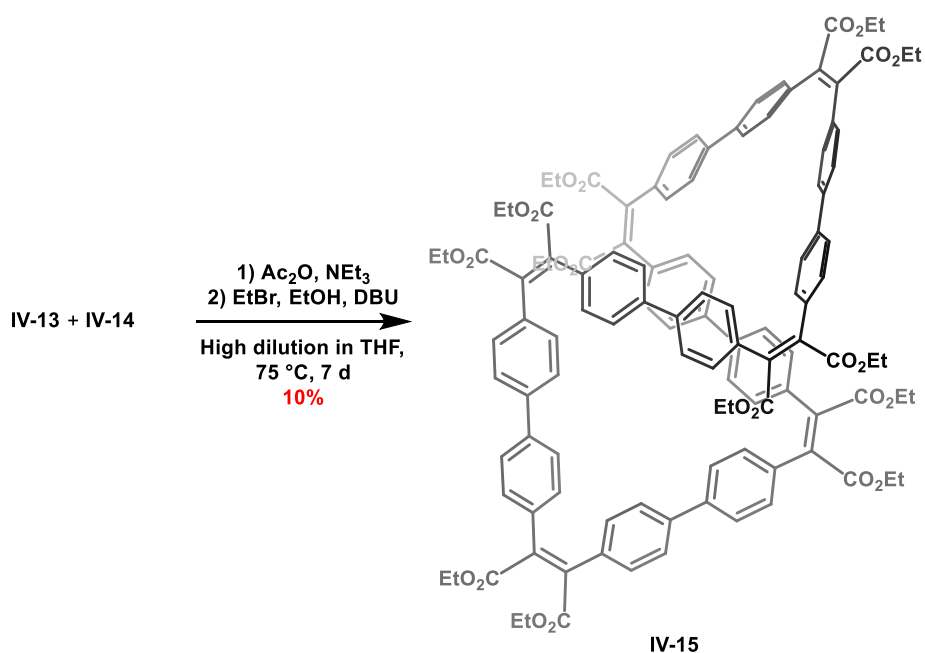


Figure 136. Synthesis of macrocycle **IV-15** by Perkin reaction.

This many-proton macrocycle is highly symmetrical, in opposition to its linear precursors. This greatly helped with its identification and characterization. Whereas the linear trimers **IV-7** and **IV-12** were identifiable in ^1H NMR by six doublets and three ester chains, the ^1H NMR spectrum of the hexameric macrocycle **IV-15** has only two doublets of the second order and one ester chain. Analogously, the ^{13}C NMR spectrum has only eight signals.

As soon as the flexible macrocycle was isolated and characterized, the final step of the synthesis could be attempted. The macrocycle **IV-15** was dissolved in ethyl acetate and irradiated in the photoreactor for one night (Figure 137). The next day, only a single spot could be observed by TLC. The residue was analyzed by ^1H NMR and disappointingly appeared to be a mixture of partially photocyclised macrocycles. Because of their very similar polarities, it was not possible to separate the compounds by column chromatography. Purification on GPC also turned out to be inefficient due to their similar hydrodynamic volumes. Thus better conditions for a direct and complete photocyclisation had to be found.

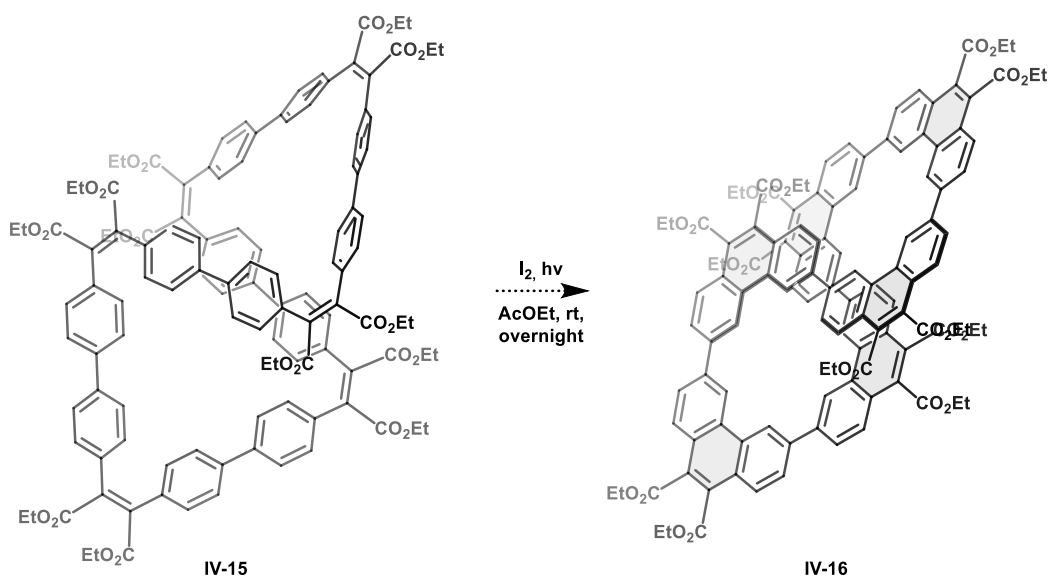


Figure 137. Photocyclisation attempt to form macrocyclic phenanthrene hexamer **IV-16**.

Among the several possible choices to improve this reaction and promote the full photocyclisation of the macrocycle, we decided to use cyclic imides on the maleic bridges to favor the formation of the C-C bonds. If the synthetic strategy used for the asymmetric coronene (See Chapter 3) required formation of the cyclic imide during the assembly of the first, non-cyclized, precursor, this is not the case here. Because all the maleic bridges had to be functionalized with imides, all these functions could be introduced later and at the same time during the macrocycle-forming Perkin reaction. Both trimers **IV-13** and **IV-14** were then condensed in the same dilution conditions as for the synthesis of **IV-15** but with subsequent addition of an amine for the functionalization of the carboxylic groups (Figure 138). After purification on column chromatography, macrocycle **IV-17** was obtained as a bright yellow solid with a 19% yield. In the same manner as with macrocycle **IV-15**, this macrocycle has a high symmetry, leading to simple NMR spectra.

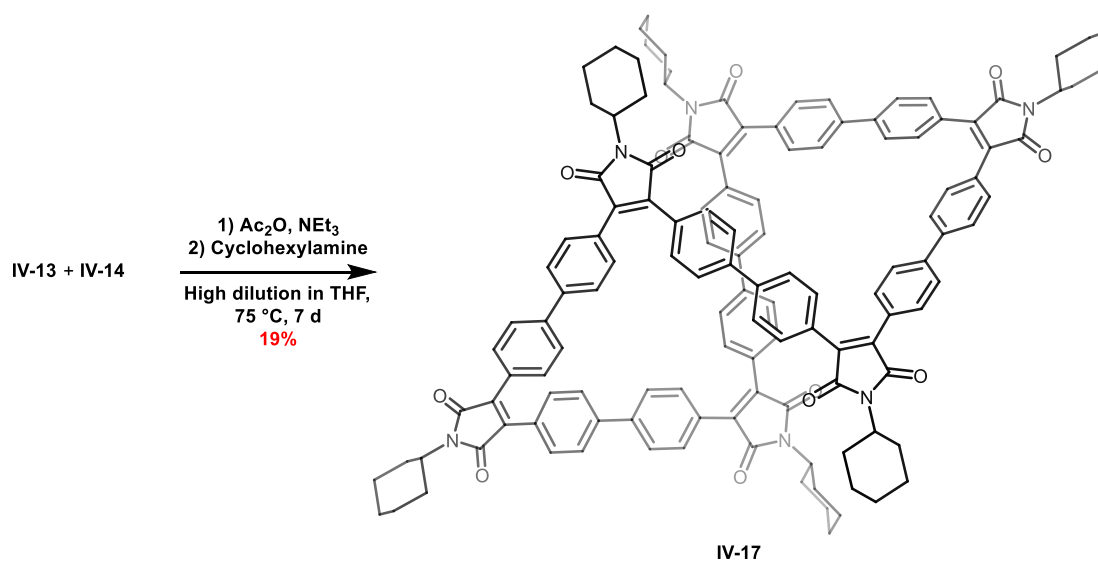


Figure 138. Synthesis of macrocycle **IV-17** by high dilution Perkin reaction.

Once isolated and characterized, the Mallory photocyclisation of the macrocyclic hexaimide **IV-17** was attempted (Figure 139). The reaction was first performed in chlorobenzene, to avoid any solubility issues, over one night at room temperature in a photoreactor. The next day, TLC revealed a single spot, at the same position as the starting material. NMR of the residue showed that it was indeed only composed of the starting macrocycle. We thus let the reaction run for a longer time. Following the reaction by ^1H NMR showed however that even after being irradiated for one week, only the starting material was present in the medium and no C-C bonds were formed. We decided to fix the reaction time at one week and change the solvent, but ethyl acetate, 1,4-dioxane or THF did not change anything. Then we modified the irradiation system itself. For the previous reactions, a 150 W mercury lamp was used inside a borosilicate immersion tube. The glass wall separating the lamp from the solution filters the high energy wavelengths, thus allowing mild photocyclisation conditions. For our last try, we changed the borosilicate immersion tube for a more UV-transparent quartz immersion tube. This time, the product would be irradiated with wavelengths of higher energy. After one day of stirring at room temperature, the ^1H NMR spectrum of the crude showed the presence of different compounds than the starting material, although the TLCs showed only one spot. Nevertheless, the ^1H NMR spectrum of the isolated compound appeared to be the starting material, the other major peaks observed in the crude mixture being degradation products of the solvent.

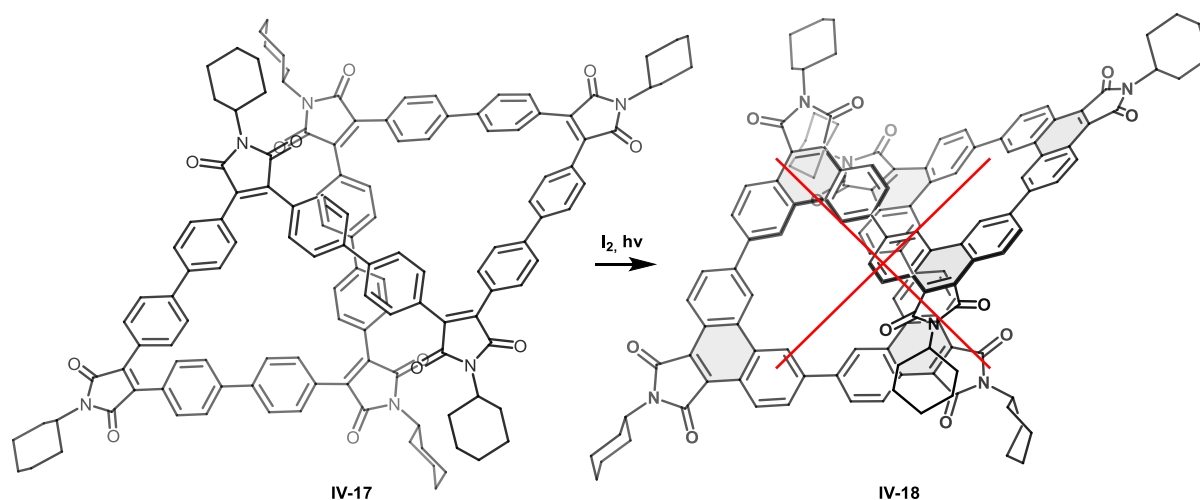


Figure 139. Photocyclisation attempt on macrocycle **IV-18**.

Conclusion

Previously our group showed that a macrocyclic hexamer of biphenyls can be obtained by our Perkin strategy. Upon photocyclisation of this macrocycle, a flexible macrocycle containing six phenanthrene units should be obtained. While still maintaining some flexibility due to the single bonds linking the phenanthrenes, the macrocycle should adopt a figure-of-eight-shaped conformation. To form this macrocycle in improved quantity, a synthetic approach based on two complementary trimeric precursors was tested. Two strategies were explored for the synthesis of these trimers.

The first strategy combined Perkin and Suzuki-Miyaura coupling reactions. It was based on the assumption that a single trimer, functionalized by bromine functions, could be synthesized by Perkin reaction and would serve as a common precursor to reduce the number of synthetic steps. This trimer could then be coupled to a phenylboronic ester, functionalized by glyoxylic or acetic ester substituents, to yield the desired trimers. The building blocks required for the synthesis of the dibrominated trimer were easily and efficiently obtained. They were then used in a Perkin reaction that yielded the dibrominated trimer in high yields. The *p*-pinacolboranophenyl-acetic methyl ester was obtained in two steps from commercially available *p*-bromophenyl-acetic acid. The latter and the previously obtained dibrominated trimer were then used in Suzuki-Miyaura coupling reactions. Even after optimizing the conditions, the yields for the coupling were critically low, as the basic conditions used for this coupling also produced partially saponified compounds that could only be partly isolated. This sensibility to the basic conditions of the coupling reaction appeared to be an important problem, as glyoxylic ester groups can be even more easily hydrolyzed. Yet, a similar approach using Stille coupling might be considered, which does not require basic conditions, thus protecting the ester functions during the coupling. This approach has yet to be tested, and the organostannanes required for the coupling have to be synthesized.

As this approach proved to be less effective than expected, we adapted the usual protection and deprotection approach for the synthesis of the trimers. The biphenyl diacetic acid building block was obtained from the reduction of the biphenyl-diglyoxylic acid. This product could be used as a building block for the Perkin reaction or transformed into a diacetic ester before monosaponification to synthesize the monoprotected diacetic building block. The monoprotected diglyoxylic building block was on the other hand obtained in two steps from commercially available 4,4'-dibromobiphenyl. These building blocks were finally used to synthesize the desired trimers, which were then coupled by a high-dilution Perkin reaction to yield the macrocyclic hexamer. After one day in the photoreactor, a mixture of partially photocyclised products was obtained and no product could be isolated detected. This forced us to find conditions that favor a complete photocyclisation of the macrocycle. We thought this could be induced by the presence of cyclic imides on the maleic bridges. A macrocyclic hexamer with cyclic maleimides was thus synthesized. The photocyclisation of this product was however not successful, as the starting material proved to be non-reactive whatever the conditions. The synthesis of this final rigidified macrocycle should still be possible, as several conditions for the photocyclisation of the ester-functionalized macrocycle have to be tested yet. The biphenyl based trimer could also be used together with smaller intermediates or building blocks to obtain other phenanthrenes containing macrocycles, such as a macrocycle containing a [5]helicene linked to two phenanthrenes, and which should adopt a Möbius geometry.

References

- 1 H. Kubo, D. Shimizu, T. Hirose and K. Matsuda, *Org. Lett.*, 2020, **22**, 9276–9281.

- 2 A. Robert, G. Naulet, H. Bock, N. Vanthuyne, M. Jean, M. Giorgi, Y. Carissan, C. Aroulanda, A. Scalabre, E. Pouget, F. Durolo and Y. Coquerel, *Chem. – Eur. J.*, 2019, **25**, 14364–14369.
- 3 Y. Shi, C. Li, J. Di, Y. Xue, Y. Jia, J. Duan, X. Hu, Y. Tian, Y. Li, C. Sun, N. Zhang, Y. Xiong, T. Jin and P. Chen, *Angew. Chem. Int. Ed.*, 2024, **n/a**, e202402800.
- 4 Z. Luo, X. Yang, K. Cai, X. Fu, D. Zhang, Y. Ma and D. Zhao, *Angew. Chem. Int. Ed.*, 2020, **59**, 14854–14860.
- 5 A. Robert, P. Dechambenoit, E. A. Hillard, H. Bock and F. Durolo, *Chem Commun*, 2017, **53**, 11540–11543.

General conclusion

Over the last decade, the synthetic strategy developed in our group proved to be a powerful and versatile tool for the formation of large polycyclic aromatic compounds. Flexible conjugated intermediates are first formed by Perkin condensation of arylglyoxylic acids with arylacetic acids. The intermediates can then be rigidified by different means. This strategy led to the formation of a large variety of conjugated molecules, linear or branched, flat or twisted, and has even been proven to be highly efficient for the formation of macrocyclic compounds. In addition, protection and deprotection techniques allowed the controlled assembly of the building blocks. This led to the synthesis of macrocycles with atypical structures such as macrocyclic poly-helicenes with figure-of-eight or Möbius nanoribbon shapes and even a cyclophane bridged by three [5]helicenes. Among those latest examples of macrocycles obtained in our team, some of them display molecular orbitals whose nodal surface is a cyclic ribbon with non-trivial topologies. These peculiarities do not, however, extend to the topology of the macrocycles themselves, as the single bonds linking the [5]helicene parts allow the macrocycles to be drawn with a planar graph. Homologous fully condensed macrocycles with a non-trivial topology were designed and new synthetic strategies were adapted.

A first approach, relying on two complementary naphthalene- and phenanthrene-based bifunctional building blocks, was attempted. This method did not lead to the desired four-unit flexible precursors of topologically non-trivial macrocycles but instead, due to the geometry of the bifunctional phenanthrene, to a cyclophane-like macrocycle containing only two orthogonal aromatic units. A second approach, based on the controlled assembly of the right number of building blocks, was therefore designed. Two complementary flexible bifunctional precursors would be synthesized and used to reach the formation of two of the desired macrocycles. As the monoprotected phenanthrene could not be synthesized, this approach was limited to the synthesis of the precursor containing a central phenanthrene and two peripheral naphthalenes but the latter could not yield the precursor of the figure-of-eight shaped macrocycle after a reaction with another equivalent of the phenanthrene building block. A helicenic equivalent of this precursor was designed to favor the formation of the target macrocycle, but its synthesis has yet to be optimized.

During the first approach for the synthesis of the topologically non-trivial macrocycles, several 3,6-bifunctionalized phenanthrene-based building blocks were synthesized. Due to the pincer-like arrangement of their glyoxylic acid functions, high dilution Perkin reaction involving such compounds and another equivalent of bifunctional building block always led to [1+1] macrocycles only. The unique chiral macrocycles obtained using these building blocks displayed an infinite enantioselectivity, due to their highly constrained structures. Their photophysical and chiroptical properties were studied and showed usual dissymmetry factors in ECD and CPL, although with low quantum yields. Replacement of the naphthalene-based building block by a shorter phenylene-based building block led to phenanthroparacyclophanes. These compounds proved to be good precursors for fluorescent tetra- and hexasubstituted

coronene. Several approaches for the synthesis of D_{3h} symmetrical and asymmetrical coronenes were tested without success.

Finally, the targeted synthesis of a macrocyclic hexamer of phenanthrenes, serendipitously observed in our group years ago, was attempted. A first synthetic strategy, combining Perkin and Suzuki-Miyaura coupling reactions, was initially investigated but the frailty of the ester even in weakly basic conditions limited this approach. A second, longer but more usual approach was finally used, with bifunctional and monoprotected building blocks reacting together to form complementary flexible trimers. Those trimers were synthesized and engaged together in a macrocycle-forming Perkin reaction to yield a cyclic hexamer of biphenyl units. The rigidification of this macrocycle was however only partial. A second macrocycle was therefore synthesized, with cyclic imides on the maleic bridges. This second macrocycle was ultimately non-reactive during the Mallory photocyclisation. New conditions for the total photocyclisation of the ester-functionalized should be found and would hopefully lead to a macrocyclic hexamer of phenanthrenes with a figure-of-eight shaped conformation.

Very disappointingly, the macrocycles with a non-trivial topology could not be obtained. Despite the many unexpected difficulties, a dibenzo-[7]helicene intermediate functionalized by acetic acids could be synthesized, although not in sufficient quantity to follow the synthesis. The synthetic path leading to this precursor of a macrocycle with a figure-of-eight shape has however been traced (through sweat, tears, and organic solvents). Unique, luminescent, cyclophane-like structures were unexpectedly obtained and characterized. Finally, two cyclic precursors of flexible macrocycles with a figure-of-eight shaped conformation were obtained.

Although the limits of the synthetic strategy developed by our group started to appear, new synthetic tools and opportunities also emerged. 3,6-Disubstituted phenanthrenes could be used as building blocks favoring the formation of two-units macrocycles. Later, the naphthalene may then be substituted by functionalized naphthalenes or longer acenes, or the phenanthrene may also be replaced by another aromatic core with a similar pincer-like arrangement of its acid functions. Preliminary result also showed that it was possible to perform the glyoxylic to acetic reduction on products of Perkin reaction still functionalized with glyoxylic acids, in order to form their acetic acid counterparts. This encouraging result may greatly ease some synthetic approaches by having more convergent syntheses. Finally, previous results obtained in the lab showed that the Perkin reaction was resilient to heteroatom-containing aromatic core, such as thiophenes and pyrazine. Including N-heterocyclic compounds such as bipyridines in flexible Perkin products could lead to allosteric compounds, as well as providing a possibility of reversible rigidification, controlled by metalation and demetalation.

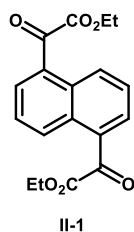
Experimental Part

General

All purchasable chemicals were of the best commercially available grade and used without further purification. Thin layer chromatography was carried out using aluminium sheets of silica gel (Merck, 60 F254). Column chromatography was carried out using silica gel (Merck, silica gel 60, 35-75 μm). Mass spectrometry analyses (GCMS (EI and FI), field ionisation (FD) and electrospray (ESI)) were performed by the CESAMO (ISM, Bordeaux, France) HRMS ESI spectra were obtained on a QExactive™ benchtop Orbitrap mass spectrometer coupled to a Vanquish UHPLC system (Thermo Scientific, San Jose, USA) using electrospray ionization mode. HRMS EI, FI and FD mass spectra spectra were obtained on an Accutof GCv mass spectrometer (JEOL). Nuclear Magnetic Resonance spectra were acquired on a JEOL ECS-40 spectrometer. ^1H and ^{13}C spectra were referenced to residual solvent peaks (chloroform: 7.26 and 77.16 ppm; dichloromethane: 5.32 and 53.84 ppm; DMSO: 2.50 and 39.52 ppm; acetone: 2.05 and 205.26/29.84 ppm). UV-visible spectra were recorded on a JASCO-730 spectrometer at 21 °C with 1 cm wide quartz cells. Emission and excitation spectra were recorded on a JASCO-FP8300 spectrometer at 21 °C using 1 cm wide quartz cells. Quantum yields were measured as described in the literature,¹ using Coumarin 153 in EtOH as a standard.

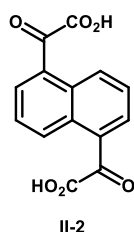
Synthetic procedures

Chapter 2:



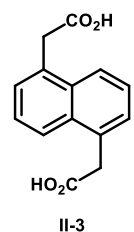
Diethyl 1,5-naphthalenediglyoxylate II-1 1,5-dibromonaphthalene (11.440 g, 40 mmol, 1 eq.) was dissolved in dry THF (400 mL). The solution was cooled down to $-97\text{ }^{\circ}\text{C}$ and *t*BuLi (1.6 M in pentane, 100 mL, 160 mmol, 4 eq.) was slowly added. The mixture was stirred under argon at $-97\text{ }^{\circ}\text{C}$ for 1 h followed by 2 more hours of stirring while slowly returning to rt. The solution was cooled down to $-97\text{ }^{\circ}\text{C}$ and diethyl oxalate (20 mL, 294 mmol, 7.3 eq.) was added quickly. The reaction medium was stirred at $-97\text{ }^{\circ}\text{C}$ for 30 min, then the cooling bath was removed, and the solution stirred for another 30 min at rt. The reaction was stopped by addition of HCl (1M, 100 mL) and the aqueous layer extracted with DCM. The organic layers were assembled before being dried over MgSO_4 . The solvent was then removed under vacuum and the resulting yellow solid left to dry overnight. Its recrystallization in ethanol yielded the product as yellow crystals ($m = 11.071\text{ g}$, 83 %).

^1H NMR (400 MHz, CDCl_3 , δ in ppm): 9.29 (d, $^3J = 8\text{ Hz}$, 2H), 8.05 (d, $^3J = 7\text{ Hz}$, 2H), 7.76 (t, $^3J = 8\text{ Hz}$, 2H), 4.49 (q, $^3J = 7\text{ Hz}$, 4H), 1.44 (t, $^3J = 7\text{ Hz}$, 6H).



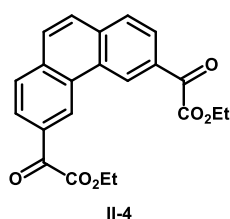
1,5-naphthalenediglyoxylic acid II-2 Diester **II-1** (5 g, 15.2 mmol, 1 eq.) was dissolved in EtOH (150 mL). A solution of NaHCO_3 (5 g in 300 mL H_2O) was then poured into the solution. The mixture was heated to reflux overnight. HCl (10 %w in H_2O , 100 mL) was added to the limpid green solution and the mixture was filtered. The white solid was dried and used in the next step without further purification (quantitative).

^1H NMR (400 MHz, $\text{DMSO}-d_6$, δ in ppm): 9.05 (d, $^3J = 9\text{ Hz}$, 2H), 8.06 (d, $^3J = 7\text{ Hz}$, 2H), 7.79 (t, $^3J = 9\text{ Hz}$, 2H).



1,5-naphthalenediacetic acid II-3 Diglyoxylic acid **II-2** (6.560 g, 24.1 mmol, 1 eq.) was dissolved in acetic acid (80 mL). H_3PO_2 (50 %w in water, 6.5 mL, 60.2 mmol, 2.5 eq.) and NaI (4.33 g, 28.9 mmol, 1.2 eq.) were added and the mixture was degassed. The solution was heated to reflux and stirred under argon for 3 days. After being cooled down, water was added and the white precipitate was filtered and dried under vacuum to remove traces of acetic acid and water. The white solid is then used without further purification ($m = 3.830$ g, 65 %).

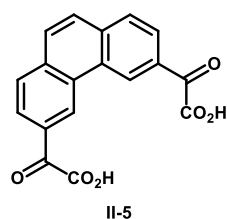
^1H NMR (400 MHz, DMSO-d_6 , δ in ppm): 7.87 (d, $^3\text{J} = 8$ Hz, 2H), 7.46 (t, $^3\text{J} = 8$ Hz, 2H), 7.41 (d, $^3\text{J} = 6$ Hz, 2H), 4.01 (s, 4H).



Diethyl phenanthrene-3,6-diglyoxylate II-4 3,6-Dibromophenanthrene (2.50 g, 7.4 mmol, 1 eq.) was dissolved in dry THF (200 mL). The solution was cooled down to -94 °C and $t\text{BuLi}$ (1.7 M in pentane, 13.2 mL, 22.4 mmol, 4 eq.) was slowly added. The mixture was stirred under argon at -94 °C for 1 h followed by 2 more hours of stirring while the reaction was allowed to warm up to room temperature. The solution was cooled down again to -94 °C and a solution of diethyl oxalate (10.2 mL, 75.1 mmol, 10.1 eq.) was quickly added. The reaction was stirred at -94 °C for 30 min, then the cooling bath was removed, and the solution stirred for another 30 min at room temperature. The reaction was stopped by addition of HCl (10 %w in water, 100 mL), the phases were separated, the aqueous phase was extracted with DCM, and the combined organic phases were dried with MgSO_4 . The solvent was removed under vacuum and the yellow solid obtained was recrystallized in ethanol to yield the product as a crystalline powder ($m = 1.52$ g, 57%).

^1H NMR (400 MHz, CD_2Cl_2 , δ in ppm): 9.45 (d, $^4\text{J} = 2$ Hz, 2H), 8.24 (dd, $^3\text{J} = 8$ Hz, $^4\text{J} = 2$ Hz, 2H), 8.09 (d, $^3\text{J} = 8$ Hz, 2H), 8.00 (s, 2H), 4.56 (q, $^3\text{J} = 7$ Hz, 4H), 1.51 (t, $^3\text{J} = 7$ Hz, 6H).

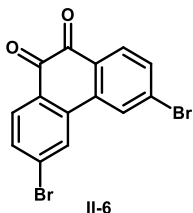
^{13}C NMR (100 MHz, CDCl_3 , δ in ppm): 186.1, 163.8, 136.2, 131.1, 130.2, 130.1, 129.7, 127.2, 126.4, 62.8, 14.34.



Phenanthrene-3,6-diglyoxylic acid II-5 Diethyl phenanthrene-3,6-diglyoxylate 2 (1.52 g, 4.2 mmol, 1 eq.) was dissolved in ethanol (100 mL). A solution of NaHCO_3 in water (10 g in 200 mL) and was added, and the mixture was stirred at reflux overnight. After cooling down to

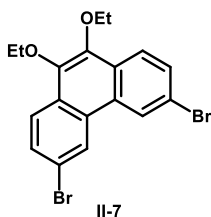
room temperature, HCl (10 %w in water) was added and a precipitate appears. The solid is filtered off and dried (m = 1.17 g, 91%).

^1H NMR (400 MHz, DMSO- d_6 , δ in ppm): 9.35 (d, $^4J = 2$ Hz, 2H), 8.29 (d, $^3J = 8$ Hz, 2H), 8.23 – 8.18 (m, 4H).



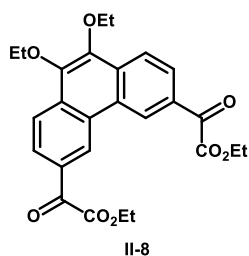
3,6-dibromophenanthrene-9,10-quinone II-6 9,10-phenanthrenequinone (5.2 g, 25 mmol, 1 eq.) and AIBN (136 mg, 0.83 mmol, 0.3 eq.) were dissolved in nitrobenzene (25 mL). Bromine (1.5 mL, 29 mmol, 1.2 eq.) was added and the mixture heated to 120 °C. When vapors of HBr appeared, bromine (1.3, 25 mmol, 1 eq.) was added drop wisely and the solution was stirred for 1 h at 120 °C. After being cooled down, EtOH was added to the mixture and the precipitate was filtered. The solid was washed with EtOH until the washing solution turned colorless to yield an orange solid (m = 8.560 g, 94%).

^1H NMR (400 MHz, CDCl_3 , δ in ppm): 8.11 (d, $^4J = 2$ Hz, 2H), 8.06 (d, $^3J = 8$ Hz, 2H), 8.65 (dd, $^3J = 8$ Hz, $^4J = 2$ Hz, 2H).



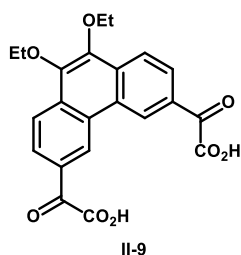
3,6-dibromo-9,10-diethoxyphenanthrene II-7 3,6-dibromophenanthrene-9,10-quinone II-6 (6 g, 16.4 mmol, 1 eq.) was dissolved in anhydrous DMF (200 mL). $\text{Na}_2\text{S}_2\text{O}_4$ (15.7 g, 90.2 mmol, 5.5 eq.) is then added and the mixture is stirred under argon at rt for 20 min. The solution turns black. KOH (13.8 g, 245.9 mmol, 15 eq.), TBAB (3.170 g, 9.8 mmol, 0.6 eq.) and bromoethane (9.7 mL, 130 mmol, 7.9 eq.) are successively added and the mixture is stirred under argon at 60 °C for 3d. The deep yellow solution is then cooled to rt and poured in brine (400 mL). The aqueous layer is extracted with diethyl ether (3x150 mL), the assembled organic layers were dried over MgSO_4 and the solvent was finally removed under vacuum. After purification by column chromatography (SiO_2 , cyclohexane/ethyl acetate (9:1)), the product is obtained as a white solid (m = 2.57 g, 37%).

^1H NMR (400 MHz, CDCl_3 , δ in ppm): 8.64 (d, $^4J = 2$ Hz, 2H), 8.11 (d, $^3J = 8$ Hz, 2H), 7.70 (dd, $^3J = 8$ Hz, $^4J = 2$ Hz, 2H), 4.27 (q, $^3J = 7$ Hz, 4H), 1.48 (t, $^3J = 7$ Hz, 6H).



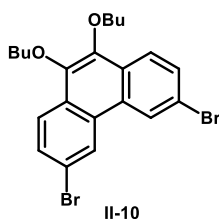
Diethyl 9,10-diethoxyphenanthrene-3,6-diglyoxylate II-8 3,6-dibromo-9,10-diethoxyphenanthrene **II-7** (2.57 g, 6.1 mmol, 1 eq.) was dissolved in dry THF (60 mL). The solution was cooled down to $-97\text{ }^{\circ}\text{C}$ before slow addition of *t*BuLi (1.7 M in pentane, 14.3 mL, 24.2 mmol, 4 eq.). The mixture was stirred under argon at $-97\text{ }^{\circ}\text{C}$ for 1 h, and then for another 2 h while being progressively heated up to rt. The solution was then cooled down to $-97\text{ }^{\circ}\text{C}$ and diethyl oxalate (6.1 mL, 44.8 mmol, 7.3 eq.) was added. After being stirred for 30 min at $-97\text{ }^{\circ}\text{C}$, the cooling bath was removed, and the solution was stirred 1 h at rt. Water (50 mL) and HCl (2 M in H_2O , 50 mL) were added to the mixture and the aqueous phases were extracted with DCM. The organic layers were assembled, dried over MgSO_4 and the solvent slowly removed. After recrystallization of the resulting oil in EtOH, thin yellow crystals were obtained ($m = 1.080\text{ g}$, 38 %).

$^1\text{H NMR}$ (400 MHz, CDCl_3 , δ in ppm): 9.37 (d, $^4J = 1\text{ Hz}$, 2H), 8.38 (d, $^3J = 9\text{ Hz}$, 2H), 8.24 (dd, $^3J = 9\text{ Hz}$, $^4J = 1\text{ Hz}$, 2H), 4.55 (q, $^3J = 7\text{ Hz}$, 4H), 4.35 (q, $^3J = 7\text{ Hz}$, 4H), 1.51 (t, $^3J = 7\text{ Hz}$, 12H).



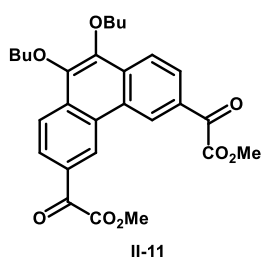
9,10-diethoxyphenanthrene-3,6-diglyoxylic acid II-9 Diethyl 9,10-diethoxyphenanthrene-3,6-diglyoxylate **II-8** (1.070 g, 2.3 mmol, 1 eq.) was dissolved in EtOH and a solution of NaHCO_3 (2 g in mL) was added. The mixture was then stirred at reflux overnight. After being cooled down to rt, HCl (37 %w, 10 mL) was added and the mixture was filtered to yield the diglyoxylic acid as a yellow solid ($m = 940\text{ mg}$, quantitative).

$^1\text{H NMR}$ (400 MHz, DMSO-d_6 , δ in ppm): 9.29 (d, $^4J = 2\text{ Hz}$, 2H), 8.40 (d, $^3J = 9\text{ Hz}$, 2H), 8.19 (dd, $^3J = 9\text{ Hz}$, $^4J = 2\text{ Hz}$, 2H), 4.29 (q, $^3J = 7\text{ Hz}$, 4H), 1.43 (t, $^3J = 7\text{ Hz}$, 6H).



3,6-dibromo-9,10-bisbutyloxyphenanthrene II-10 3,6-dibromophenanthrenequinone **II-6** (6 g, 16.4 mmol, 1 eq.), TBAB (6 g, 18.6 mmol, 1.1 eq.) and Na₂S₂O₄ (28.8 g, 165.4 mmol, 10.1 eq.) were dissolved in H₂O/THF (240 mL, 1:1). The solution was stirred at rt under argon until it became homogeneous. KOH (12 g, 213.9 mmol, 13 eq.) and 1-bromobutane (9.7 mL, 90 mmol, 5.5 eq.) were then added and the mixture was stirred at rt under argon for 3 days. The crude was diluted in water (200 mL) and the aqueous layer was extracted with DCM. The organic layers were then assembled and dried over MgSO₄ and the solvent removed under reduced pressure. After purification by silica gel column chromatography (cyclohexane), the product was obtained as a white solid (m = 6.5 g, 85%).

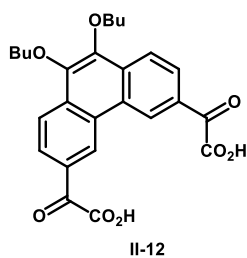
¹H NMR (400 MHz, CDCl₃, δ in ppm): 8.64 (d, ⁴J = 2 Hz, 2H), 8.09 (d, ³J = 9 Hz, 2H), 7.70 (dd, ³J = 9 Hz, ⁴J = 1.6 Hz, 2H), 4.18 (t, ³J = 7 Hz, 4H), 1.86 (m, 4H), 1.57 (m, 4H), 1.01 (t, ³J = 7 Hz, 6H).



Dimethyl 9,10-bis(butyloxy)phenanthrene-3,6-diglyoxylate II-11 3,6-dibromo-9,10-bis(butyloxy)phenanthrene **II-10** (2.740 g, 5.7 mmol, 1 eq.) was dissolved in dry THF (60 mL). The solution was cooled down to -97 °C and *t*BuLi (1.6 M in pentane, 14.3 mL, 22.8 mmol, 4 eq.) was slowly added. The mixture was stirred under argon at -97 °C for 1 h followed by 2 more hours of stirring while the reaction was allowed to warm up to room temperature. The solution was cooled down again to -97 °C and a solution of dimethyl oxalate (4.910 g, 41.6 mmol, 7.3 eq.) in dry THF (15 mL) was added quickly. The reaction medium was stirred at -97 °C for 30 min, then the cooling bath was removed, and the solution stirred for another 90 min at room temperature. The reaction was stopped by addition of HCl (10 %w in water, 100 mL) and the phases were separated, the aqueous phase was extracted with DCM, and the combined organic phases were dried with MgSO₄. The solvent was removed under vacuum and the yellow solid obtained was washed with MeOH (m = 1.236 g, 44 %).

¹H NMR (400 MHz, CDCl₃, δ in ppm): 9.39 (s, 2H), 8.37 (d, ³J = 9 Hz, 2H), 8.24 (dd, ³J = 9 Hz, ⁴J = 1 Hz, 2H), 4.26 (t, ³J = 7 Hz, 4H), 4.08 (s, 6H), 1.89 (m, 4H), 1.61 (m, 4H), 1.02 (t, ³J = 7 Hz, 6H).

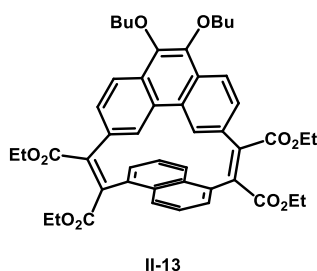
¹³C NMR (100 MHz, CDCl₃, δ in ppm): 185.5, 164.0, 145.8, 134.4, 130.2, 128.4, 127.3, 126.5, 123.5, 73.8, 53.1, 32.5, 19.5, 14.1.



9,10-bis(butyloxy)phenanthrene-3,6-diglyoxylic acid II-12 Dimethyl 9,10-bis(butyloxy)phenanthrene-3,6-diglyoxylate **II-11** (1.81 g, 3.5 mmol, 1 eq.) was dissolved in THF (15 mL). A solution of NaOH (2 g) in a mixture of water (200 mL) and MeOH (20 mL) was added, and the mixture was stirred at reflux overnight. After being cooled down to room temperature, HCl (10 %w in water) was then added to the medium until a yellow precipitate appears. The solid was filtered and dried to yield the diglyoxylic acid as a yellow solid (1.58 g, quantitative).

^1H NMR (400 MHz, DMSO- d_6 , δ in ppm): 9.30 (d, $^4J = 2$ Hz, 2H), 8.37 (d, $^3J = 9$ Hz, 2H), 8.22 (dd, $^3J = 9$ Hz, $^4J = 2$ Hz, 2H), 4.20 (t, $^3J = 6$ Hz, 4H), 1.83 (m, 4H), 1.53 (m, 4H), 0.96 (t, $^3J = 7$ Hz, 6H).

^{13}C NMR (100 MHz, DMSO- d_6 , δ in ppm): 188.0, 165.8, 145.1, 133.5, 129.9, 127.6, 127.4, 125.5, 123.5, 73.4, 31.9, 18.9, 13.9.



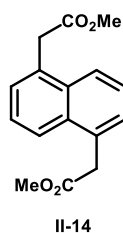
Tetraester bisbutyloxymicrocycle II-13 3,6-diglyoxylic-9,10-bisbutyloxyphenanthrene acid **II-12** (746 mg, 1.6 mmol, 1 eq.) and 1,5-naphthalenediacetic acid **II-3** (391 mg, 1.6 mmol, 1 eq.) were dissolved in dry THF (500 mL). Acetic anhydrid (1.2 mL, 12.8 mmol, 8 eq.), NEt_3 (0.9 mL, 6.4 mmol, 4 eq.) were added and the solution was heated for 24 h at reflux under argon. EtOH (2.6 mL, 44.8 mmol, 28 eq), EtBr (2.4 mL, 32 mmol, 20 eq.) and DBU (2.4 mL, 16 mmol, 10 eq.) were then added and the mixture was heated to reflux overnight. After being cooled down to rt, HCl (10%w, 300 mL) was added, and the aqueous layer was extracted with DCM. The organic layers were assembled before being dried over MgSO_4 . The solvent was then removed under reduced pressure. Purification of the crude by column chromatography (cyclohexane/acetone (6:4)) and Gel Permeability Chromatography yielded the product as an orange solid (m = 103 mg, 8%).

^1H NMR (400 MHz, CD_2Cl_2 , δ in ppm): 7.95 (d, $^3J = 9$ Hz, 2H), 7.89 (d, $^3J = 9$ Hz, 2H), 7.52 (t, $^3J = 8$ Hz, 2H), 7.45 (dd, $^3J = 9$ Hz, $^4J = 2$ Hz, 2H), 7.30 (d, $^3J = 7$ Hz, 2H), 6.62 (d, $^4J = 2$ Hz, 2H), 4.49

(q, $^3J = 7$ Hz, 4H), 4.31 (q, $^3J = 7$ Hz, 4H), 4.06 (t, $^3J = 7$ Hz, 4H), 1.76 (m, 4H), 1.54 (4H), 1.43 (t, $^3J = 7$ Hz, 6H), 1.26 (t, $^3J = 7$ Hz, 6H), 0.93 (t, $^3J = 7$ Hz, 6H).

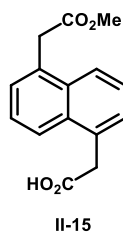
^{13}C NMR (100 MHz, CD_2Cl_2 , δ in ppm): 168.8, 166.5, 144.4, 135.3, 134.9, 130.2, 130.0, 129.4, 129.1, 128.6, 127.6, 127.2, 126.3, 126.0, 125.1, 122.3, 73.5, 62.0, 62.0, 32.4, 19.4, 14.0, 13.9, 13.7.

FD-HRMS: m/z calcd for $\text{C}_{48}\text{H}_{50}\text{O}_{10}\text{Na}^+$ [M+Na] $^+$: 809.32962, found 809.32719.



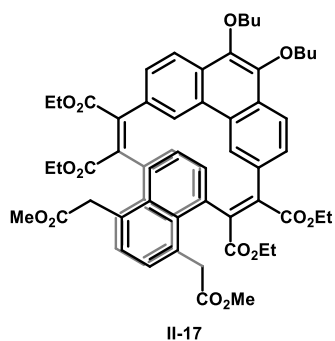
Dimethyl 1,5-naphthalenediacetate II-14 Diacetic acid **II-3** (4.35 g, 17.8 mmol, 1 eq.) was dissolved in MeOH (175 mL). SOCl_2 (17.4 mL, 240.4, 13.5 eq.) was then slowly added, and the solution was heated to reflux for 4 h. Once cooled down to rt, the crude was put in a fridge and a white precipitate appeared. The crude was then filtered and dried to yield the diester as a white solid (3.730 g, 77%).

^1H NMR (400 MHz, CD_2Cl_2 , δ in ppm): 7.92 (d, $^3J = 8$ Hz, 2H), 7.48 (t, $^3J = 8$ Hz, 2H), 7.41 (m, 2H), 4.06 (s, 4H), 3.65 (s, 6H).



1,5-naphthalenediacetic acid, 1-methylester II-15 Diester **II-14** (4.480 g, 16.5 mmol, 1 eq.) was dissolved in THF (300 mL). A solution of KOH (923 mg, 16.5 mmol, 1 eq.) dissolved in MeOH (50 mL) is then added to the solution and the mixture is heated to reflux for 70 min. The mixture is then cooled down to rt and the solvent evaporated under reduced pressure. A minimum of CH_2Cl_2 is added and the crude is filtered. The filtrate is evaporated under reduced pressure to yield a white solid corresponding to the unreacted diester **II-14**. The residue is collected and triturated in a mixture of HCl (1M) and CH_2Cl_2 . The mixture is filtered and the remaining solid, corresponding to the diacid, is collected. The aqueous layer is extracted with CH_2Cl_2 . The organic layers are then reassembled, dried with MgSO_4 and the solvent is removed under vacuum to yield a white solid corresponding to the monoester (m = 970 mg, 23%).

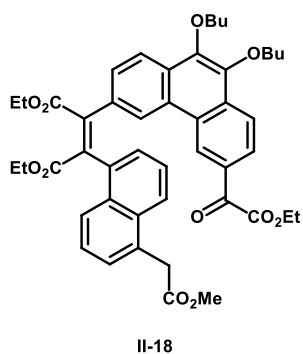
^1H NMR (400 MHz, CD_2Cl_2 , δ in ppm): 7.92 (t, $^3J = 8$ Hz, 2H), 7.47 (td, $^3J = 8$ Hz, $^4J = 2$ Hz, 2H), 7.41 (m, 2H), 4.09 (s, 2H), 4.06 (s, 2H), 3.64 (s, 3H).



Bisnaphthalene diacetic ester, monophenanthrene trimer II-17 Acid 9,10-bisbutyloxyphenanthrene-3,6-diglyoxylic **II-12** (446 mg, 0.95 mmol, 1 eq.) and 1,5 naphthalenediacetic acid, 1-methylester **II-15** (749 mg, 2.9 mmol, 3 eq.) were dissolved in 10 mL of anhydrous THF. Ac₂O (0.7 mL, 7.6 mmol, 8 eq.) and NEt₃ (0.5 mL, 3.8 mmol, 4 eq.) were added and the mixture was stirred at 75 °C for 24 h under argon. DBU (1.4 mL, 9.5 mmol, 10 eq.), EtOH (1.6 mL, 26.6 mmol, 28 eq.) and EtBr (1.4 mL, 19 mmol, 20 eq.) were then added to the mixture which was stirred for another 16 h at 75 °C. The reaction media was then cooled down to rt and a large excess of HCl (10%w) was put in the mixture. The organic layers were extracted with CH₂Cl₂, put together and dried over MgSO₄. The solvent was removed under reduced pressure and the resulting red oil was purified by column chromatography over silica gel (cyclohexane/acetone (6:4)) and recrystallization in EtOH to yield the product as a yellow solid (m = 510 mg, 50%).

¹H NMR (400 MHz, CD₂Cl₂, δ in ppm): 8.03 (d, ³J = 9 Hz, 1H), 7.92 (m, 3H), 7.84 (d, ³J = 9 Hz, 2H), 7.69 (d, ³J = 9 Hz, 2H), 7.54 (m, 1H), 7.40 (m, 4H), 7.28 (t, ³J = 7 Hz, 2H), 7.13 (d, ³J = 7 Hz, 1H), 7.05 (m, 2H), 4.40 (p, ³J = 7 Hz, 4H), 4.24 (q, ³J = 7 Hz, 4H), 4.05 (d, ²J = 15 Hz, 3H), 3.92 (m, 6H), 3.58 (s, 3H), 3.57 (s, 3H), 1.65 (m, 4H), 1.40 (m, 10H), 1.23 (t, ³J = 7 Hz, 3H), 0.86 (t, ³J = 7 Hz, 6H).

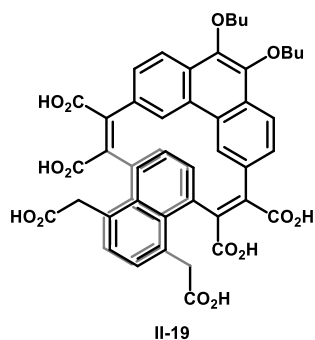
¹³C NMR (100 MHz, CD₂Cl₂, δ in ppm): 172.1, 168.4, 168.3, 167.7, 143.8, 143.3, 143.2, 136.3, 134.0, 133.9, 132.8, 132.6, 132.5, 132.4, 131.8, 129.7, 129.0, 128.8, 127.8, 127.8, 127.4, 126.9, 126.7, 126.0, 125.5, 125.4, 125.0, 123.3, 123.1, 122.4, 73.5, 62.3, 62.3, 52.4, 39.3, 32.7, 19.7, 14.4, 14.2, 14.1.



Naphthalene acetic ester, phenanthrene glyoxylic ester dimer II-18 Acid 9,10-bisbutyloxyphenanthrene-3,6-diglyoxylic (933 mg, 2 mmol, 1 eq.) and 1,5

naphthalenediacetic acid, 1 methylester (512 mg, 2 mmol, 1 eq.) were dissolved in 40 mL of anhydrous THF. Ac₂O (0.7 mL, 7.6 mmol, 3.8 eq.) and NEt₃ (0.5 mL, 3.8 mmol, 1.9 eq.) were added and the mixture was stirred overnight at 75 °C under argon. DBU (1.4 mL, 9.5 mmol, 4.8 eq.), EtOH (1.6 mL, 26.6 mmol, 14 eq.) and EtBr (1.4 mL, 19 mmol, 10 eq.) were then added to the mixture which was stirred for another 16 h at 75 °C. The reaction media was then cooled down to rt and a large excess of HCl (10%w) was put in the mixture. The organic layers were extracted with CH₂Cl₂, put together and dried over MgSO₄. The solvent was removed under reduced pressure and the resulting red oil was purified by column chromatography over silica gel (cyclohexane/acetone (6:4)) as a yellow solid (m = 715 mg, 45%).

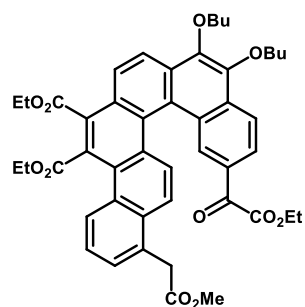
¹H NMR (400 MHz, CD₂Cl₂, δ in ppm): 8.82 (d, ⁴J = 1 Hz, 1H), 8.37 (d, ⁴J = 1 Hz, 1H), 8.21 (d, ³J = 9 Hz, 1H), 8.04 (dd, ³J = 9 Hz, ⁴J = 1 Hz, 1H), 8.00 (d, ³J = 8 Hz, 1H), 7.88 (d, ³J = 8 Hz, 1H), 7.81 (dd, ³J = 6 Hz, ⁴J = 3 Hz, 1H), 7.49 (dd, ³J = 8 Hz, ³J = 7 Hz, 1H), 7.35 (m, 3H), 7.23 (dd, ³J = 9 Hz, ⁴J = 2 Hz, 1H), 4.52 (q, ³J = 7 Hz, 2H), 4.38 (m, 2H), 4.21 (qd, ³J = 7 Hz, ⁴J = 2 Hz, 2H), 4.12 (qd, ³J = 6 Hz, ⁴J = 3 Hz, 2H), 4.05 (qd, ³J = 6 Hz, ⁴J = 3 Hz, 2H), 3.86-4.02 (2H), 3.53 (s, 3H), 1.82-1.71 (m, 4H), 1.47 (t, ³J = 7 Hz, 3H), 1.37 (t, ³J = 7 Hz, 3H), 1.20 (t, ³J = 7 Hz, 3H), 0.95 (t, ³J = 7 Hz, 3H), 0.92 (t, ³J = 7 Hz, 3H).



Bisnaphthalene monophenanthrene trimer hexaacid II-19 The trimer hexaester **II-17** (910 mg, 0.86 mmol, 1 eq.) was dissolved a mixture of THF/EtOH/water (5:30:65, 100 mL). KOH (1 g, 56 mmol, in excess) was dissolved in 10 mL EtOH and was added to the reaction media. The mixture was then stirred overnight at 75 °C. The crude was then cooled back to rt and the aqueous layer was extracted with CH₂Cl₂. The aqueous layers were collected and aqueous HCl (10%w) was added until formation of a red precipitate. The solid was filtered and dried to yield the fully saponified trimer as a bright red solid (m = 706 mg, 89%).

¹H NMR (400 MHz, acetone-*d*₆, δ in ppm): 8.81 (d, ³J = 6 Hz, 2H), 8.28 (d, ³J = 6 Hz, 2H), 7.97 (d, ³J = 9 Hz, 2H), 7.91 (d, ³J = 9 Hz, 2H), 7.71 (d, ³J = 9 Hz, 4H), 7.49 (d, ³J = 6 Hz, 2H), 7.45 (d, ³J = 9 Hz, 2H), 7.35 (dd, ³J = 9 Hz, ³J = 7 Hz, 2H), 4.14 (m, 4H) 4.08 (t, ³J = 7 Hz, 4H), 1.74 (m, 5H), 1.45 (m, 4H), 0.88 (t, ³J = 7 Hz, 6H).

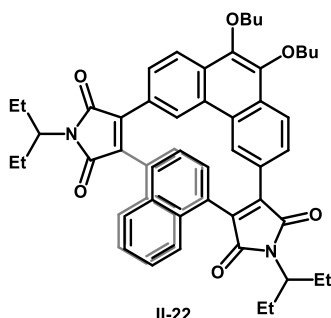
¹³C NMR (100 MHz, acetone-*d*₆, δ in ppm): 172.7, 170.9, 166.1, 145.4, 142.0, 139.8, 133.5, 133.4, 131.9, 131.7, 129.8, 129.1, 128.7, 128.4, 127.8, 127.7, 127.6, 126.8, 126.6, 125.8, 125.8, 123.5, 74.1, 60.5, 39.2, 33.0, 30.7, 20.8, 19.9, 14.5, 14.1, 9.0.



II-20

Benzo-[5]helicene tetraester II-20 The flexible precursor **II-18** (715 mg, 0.9 mmol, 1 eq.) and I₂ (550 mg) were dissolved in AcOEt (1.8 L). The solution was stirred overnight at room temperature under air in a Peschl photoreactor with irradiation from a medium pressure 150 W mercury immersion lamp inside a borosilicate immersion tube in which cooling water circulated. The solvent was evaporated and the crude product was washed with an aqueous solution of Na₂SO₃. The phases were separated, the aqueous phase was extracted with DCM, and the combined organic phases were dried with MgSO₄ and concentrated under vacuum. Purification of the crude on column chromatography gave the product as a dark powder (464 mg, 67%).

¹H NMR (400 MHz, CDCl₃, δ in ppm): 8.58 (d, ⁴J = 2 Hz, 1H), 8.43 (d, ³J = 9 Hz, 1H), 8.42 (d, ³J = 9 Hz, 1H), 8.35 (d, ³J = 8 Hz, 1H), 8.15 (d, ³J = 9 Hz, 1H), 8.14 (dd, ³J = 9 Hz, ⁴J = 2 Hz, 1H), 8.01 (d, ³J = 9 Hz, 1H), 7.76 (d, ³J = 9 Hz, 1H), 7.58 (m, 2H), 4.45 (m, 12H), 4.06 (d, ²J = 16 Hz, 1H), 3.65 (s, 3H), 3.33 (m, 2H), 1.95 (m, 4H), 1.66 (m, 4H), 1.51 (t, ³J = 7 Hz, 3H), 1.35 (t, ³J = 7 Hz, 3H), 1.08 (t, ³J = 7 Hz, 3H), 1.06 (t, ³J = 7 Hz, 3H), 0.75 (t, ³J = 7 Hz, 3H).

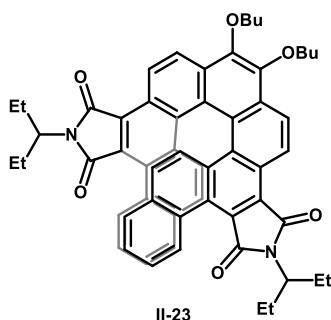


II-22

Bisnaphthalene, monophenanthrene trimer diimide II-22 Acid 9,10-bisbutyloxyphenanthrene-3,6-diglyoxylic **II-12** (466 mg, 1 mmol, 1 eq.) and 1-naphthaleneacetic acid (475 mg, 2.5 mmol, 2.5 eq.) were dissolved in 50 mL of anhydrous THF. Ac₂O (0.8 mL, 8 mmol, 8 eq.) and NEt₃ (0.8 mL, 4 mmol, 4 eq.) were added and the mixture was stirred at 75 °C for 3 d under argon. 3-aminopentane (2 mL, 17 mmol, 17 eq.) were then added to the mixture which was stirred for another 3 d at 75 °C. The reaction media was then cooled down to rt and a large excess of HCl (10%w) was put in the mixture. The organic layers were extracted with DCM, put together and dried over MgSO₄. The solvent was

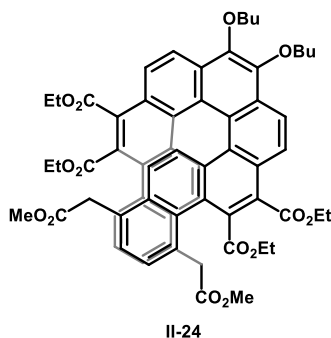
removed under reduced pressure and the resulting red oil was purified by column chromatography over silica gel (eluent: CH₂Cl₂) to yield the product as a red oil (m = 340 mg, 37%).

¹H NMR (400 MHz, CD₂Cl₂, δ in ppm): 8.81 (s, 1H), 8.76 (s, 1H), 7.98 (d, ³J = 7 Hz, 2H), 7.91 (d, ³J = 8 Hz, 3H), 7.86 (d, ³J = 9 Hz, 3H), 7.57 (m, 6H), 7.44 (m, 2H), 7.33 (m, 4H), 4.13 (m, 2H), 4.04 (t, ³J = 7 Hz, 4H), 2.16 (m 4H), 1.91 (m, 4H), 1.73 (m, 4H), 1.48 (m, 4H), 1.07 (t, ³J = 7 Hz, 12H), 0.91 (t, ³J = 7 Hz, 6H).



Dibenzo-[7]helicene diimide II-23 The flexible precursor **II-22** (340 mg, 0.4 mmol, 1 eq) was dissolved in AcOEt and toluene (1:3, 1.8 L). The solution was stirred overnight at room temperature under air in a Peschl photoreactor with irradiation from a medium pressure 150 W mercury immersion lamp inside a borosilicate immersion tube in which cooling water circulated. The solvent was evaporated and the crude product was washed with an aqueous solution of Na₂SO₃. The phases were separated, the aqueous phase was extracted with DCM, and the combined organic phases were dried with MgSO₄ and concentrated under vacuum. Purification of the crude by column chromatography gave the product as a bright orange (84 mg, 24%).

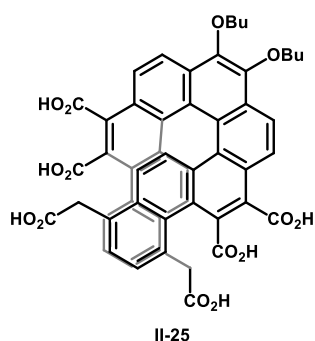
¹H NMR (400 MHz, CD₂Cl₂, δ in ppm): 9.41 (d, ³J = 9 Hz, 2H), 8.61 (d, ³J = 9 Hz, 2H), 8.41 (d, ³J = 8 Hz, 2H), 7.49 (t, ³J = 7 Hz, 2H), 7.39 (d, ³J = 7 Hz, 2H), 7.35 – 7.23 (m, 4H), 6.88 (d, ³J = 9 Hz, 2H), 6.74 (d, ³J = 9 Hz, 2H), 4.61 (dt, ²J = 10 Hz, ³J = 7 Hz, 2H), 4.38 (dt, J = 10 Hz, ³J = 7 Hz, 2H), 4.21 (m, 2H), 2.07 (m, 4H), 1.90 (tt, ²J = 13.9, ³J = 7.2 Hz, 4H), 1.75 (dq, ²J = 14.8 Hz, ³J = 7.4 Hz, 4H), 1.14 (t, ³J = 7 Hz, 6H), 1.02 (t, ³J = 7 Hz, 6H), 1.02 (t, ³J = 7 Hz, 6H).



Dibenzo-[7]helicene hexaester II-24 The flexible precursor **II-17** (340 mg, 0.3 mmol, 1 eq) was dissolved in AcOEt (800 mL). The solution was stirred overnight at room temperature under air in a Peshl photoreactor with irradiation from a medium pressure 150 W mercury immersion lamp inside a borosilicate immersion tube in which cooling water circulated. The solvent was evaporated and the crude product was washed with an aqueous solution of Na₂SO₃. The phases were separated, the aqueous phase was extracted with DCM, and the combined organic phases were dried with MgSO₄ and concentrated under vacuum. Purification of the crude on column chromatography gave the product as a dark powder (298 mg, 88%).

¹H NMR (400 MHz, CD₂Cl₂, δ in ppm): 8.51 (d, ³J = 9 Hz, 2H), 8.10 (d, ³J = 9 Hz, 2H), 7.27 (d, ³J = 7 Hz, 2H), 6.96 (dd, ³J = 9, ³J = 7 Hz, 2H), 6.91 (d, ³J = 9 Hz, 2H), 6.82 (d, ³J = 9 Hz, 2H), 6.77 (d, ³J = 9 Hz, 2H), 4.64 (dq, ²J = 11 Hz, ³J = 7 Hz, 2H), 4.59 (dt, ²J = 10 Hz, ³J = 7 Hz, 2H), 4.50 (dq, ²J = 11 Hz, ³J = 7 Hz, 2H), 4.37 (dq, ²J = 11 Hz, ³J = 7 Hz, 2H), 4.33 (dt, ²J = 10 Hz, ³J = 7 Hz, 2H), 4.21 (d, ²J = 16 Hz, 2H), 4.14 (dq, ²J = 11 Hz, ³J = 7 Hz, 2H), 3.84 (d, ²J = 16 Hz, 2H), 3.59 (s, 6H), 2.03 (m, 4H), 1.71 (m, 6H), 1.51 (t, ³J = 7 Hz, 6H), 1.20 (t, ³J = 7 Hz, 6H), 1.10 (t, ³J = 7 Hz, 6H).

¹³C NMR (100 MHz, CD₂Cl₂, δ in ppm): 172.3, 170.2, 168.5, 145.4, 131.0, 130.4, 130.3, 129.9, 129.1, 128.9, 128.5, 128.4, 128.3, 126.2, 125.4, 124.8, 124.7, 124.6, 123.4, 122.6, 121.1, 74.4, 62.6, 62.4, 52.3, 39.4, 33.0, 20.0, 14.4, 14.2, 13.9.



Dibenzo-[7]helicene hexaacid II-25 The flexible precursor **II-19** (100 mg, 0.1 mmol, 1 eq) was dissolved in AcOEt and toluene (1:9, 800 mL). The solution was stirred overnight at room temperature under air in a Peshl photoreactor with irradiation from a medium pressure 150 W mercury immersion lamp inside a borosilicate immersion tube in which cooling water circulated. The solvent was evaporated and the crude product was washed with an aqueous solution of Na₂SO₃. The phases were separated, the aqueous phase was extracted with DCM and THF, and the combined organic phases were dried with MgSO₄ and concentrated under vacuum. Purification of the crude on column chromatography (MeCN/THF) and on GPC gave the product as a red powder (10 mg, 10%).

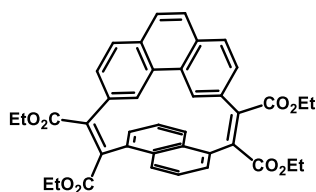
¹H NMR (400 MHz, acetone-*d*₆, δ in ppm): 9.09 (d, ³J = 9 Hz, 2H), 8.70 (d, ³J = 9 Hz, 2H), 7.82 (d, ³J = 8 Hz, 2H), 7.42 (d, ³J = 7 Hz, 2H), 7.13 (dd, ³J = 8 Hz, ³J = 7 Hz, 2H), 6.85 (d, ³J = 9 Hz, 2H),

6.62 (d, $^3J = 9$ Hz, 2H), 4.63 (dt, $^2J = 10$ Hz, $^3J = 7$ Hz, 2H), 4.37 (dt, $^2J = 10$ Hz, $^3J = 7$ Hz, 2H), 3.92 (d, $^2J = 17$ Hz, 2H), 3.83 (d, $^2J = 17$ Hz, 2H), 1.78 (m, 4H), 1.14 (t, $^3J = 7$ Hz, 6H).

^{13}C NMR (100 MHz, acetone- d_6 , δ in ppm): 172.9, 165.0, 163.3, 146.7, 133.8, 132.0, 131.5, 131.0, 130.9, 130.7, 129.8, 129.3, 128.1, 127.2, 126.6, 126.4, 125.4, 124.7, 124.6, 123.9, 123.5, 74.9, 38.4, 33.4, 30.7, 20.3, 14.5.

Chapter 3:

The compounds **III-10** and **III-11** were synthesized using published procedures.² The procedures for phenanthroparacyclophanes **III-4**, **III-6**, **III-8** and functionalized coronenes **III-5**, **III-7** and **III-9** were also reported by our group in the literature.³ The procedure for the monobromination of phenyl diacetic methyl ester was adapted from the literature.⁴

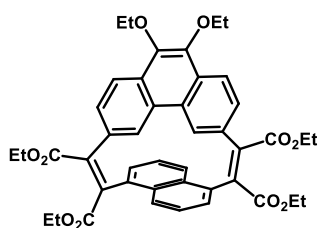


III-1

Microcycle tetraester III-1 3,6-diglyoxylic acid phenanthrene **II-5** (322 mg, 1 mmol, 1 eq.) and 1,5-naphthalenediacetic acid **II-3** (244 mg, 1 mmol, 1 eq.) were dissolved in a THF/DMF (9:1). The solution was added dropwise with a push-syringe over 24 h in a solution of Ac₂O (14 mL, 148 mmol, 148 eq.) and NEt₃ (15 mL, 111 mmol, 111 eq.) in THF (1 L) heated to reflux and under argon. After the end of the addition, the solution was stirred for 4 more days at reflux under argon. The mixture was then concentrated under reduced pressure and EtOH (10 mL, 176 mmol, 176 eq.), EtBr (12.5 mL, 168 mmol, 176 eq.) and DBU (23.6, 158 mmol, 158 eq.) were added. The solution was heated at reflux overnight. After being cooled down to rt, HCl (10 %w, 200 mL) was added and the aqueous layer was extracted with DCM. The organic layers were assembled and dried over MgSO₄. The solvent was then removed under reduced pressure and the crude was purified by column chromatography (cyclohexane/acetone (6:4)) and recrystallization in EtOH to yield a yellow solid (m = 45 mg, 7%).

^1H NMR (400 MHz, CD₂Cl₂, δ in ppm): 7.94 (d, $^3J = 8$ Hz, 2H), 7.71 (d, $^3J = 9$ Hz, 2H), 7.60 (s, 2H), 7.55 (dd, $^3J = 9$ Hz, $^3J = 7$ Hz, 2H), 7.49 (dd, $^3J = 9$ Hz, $^4J = 2$ Hz, 2H), 7.34 (d, $^3J = 7$ Hz, 2H), 6.73 (d, $^4J = 2$ Hz, 2H), 4.52 (q, $^3J = 7$ Hz, 4H), 4.35 (q, $^3J = 7$ Hz, 4H), 1.46 (t, $^3J = 7$ Hz, 6H), 1.29 (t, $^3J = 7$ Hz, 6H).

^{13}C NMR (100 MHz, CD₂Cl₂, δ in ppm): 169.2, 166.9, 144.6, 135.6, 135.2, 132.3, 131.2, 130.0, 129.7, 129.5, 128.4, 127.8, 127.5, 126.7, 126.4, 125.7, 62.4, 62.4, 14.4, 14.3.



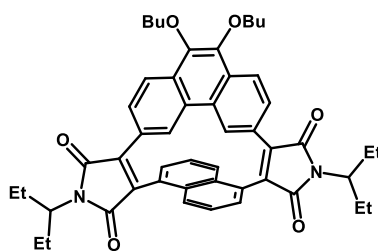
III-2

Bisethoxymicrocycle tetraester III-2 3,6-diglyoxylic-9,10-bisethoxy-phenanthrene acid **II-9** (410 mg, 1 mmol, 1 eq.) and 1,5-naphthalenediacetic acid **II-3** (244 mg, 1 mmol, 1 eq.) were dissolved in dry THF (200 mL). Ac₂O (1.5 mL, 16 mmol, 8 eq.), NEt₃ (1.2 mL, 8 mmol, 4 eq.) were added and the solution was heated for 24 h at reflux under argon. EtOH (3 mL, 51 mmol, 51 eq), EtBr (3 mL, 40 mmol, 40 eq.) and DBU (3.5 mL, 23 mmol, 23 eq.) were then added and the mixture was heated to reflux overnight. After being cooled down to rt, HCl (10 %w, 300 mL) was added and the aqueous layer was extracted with DCM. The assembled organic layers were dried over MgSO₄. The solvent was then removed under reduced pressure and the crude was purified by column chromatography (cyclohexane/acetone (6:4)) and GPC to yield a yellow solid (m = 60 mg, 10%).

¹H NMR (400 MHz, CDCl₃, δ in ppm): 7.96 (d, ³J = 9 Hz, 2H), 7.93 (d, ³J = 8 Hz, 2H), 7.52 (t, ³J = 8 Hz, 2H), 7.48 (dd, ³J = 9, ⁴J = 2 Hz, 2H), 7.33 (d, ³J = 7 Hz, 2H), 6.67 (d, ⁴J = 2 Hz, 2H), 4.55 (q, ³J = 7 Hz, 4H), 4.35 (q, ³J = 7 Hz, 4H), 4.16 (q, ³J = 7 Hz, 4H), 1.47 (t, ³J = 7 Hz, 6H), 1.39 (t, ³J = 7 Hz, 6H), 1.29 (t, ³J = 7 Hz, 6H).

¹³C NMR (100 MHz, CD₂Cl₂, δ in ppm): 169.2, 166.9, 144.7, 144.6, 135.7, 135.2, 130.7, 130.4, 129.4, 129.1, 127.9, 127.6, 126.7, 126.4, 125.5, 122.7, 69.6, 62.4, 62.4, 15.9, 14.4, 14.3.

FD-HRMS: m/z calcd for C₄₄H₄₂O₁₀Na⁺ [M+Na]⁺: 753.26812, found 753.26485.



III-3

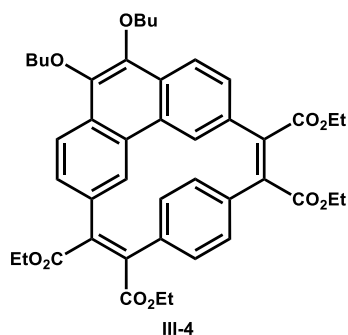
Bisbutyloxymicrocycle functionalized with imides III-3 3,6-dibromo-9,10-bisbutyloxyphenanthrene (466 mg, 1 mmol, 1 eq.) **II-12** and 1,5-naphthalenediacetic acid **II-3** (244 mg, 1 mmol, 1 eq.) dropwise with a push-syringe over 24 h in a solution of Ac₂O (14 mL, 12.8 mmol, 8 eq.) and NEt₃ (15 mL, 6.4 mmol, 4 eq.) in dry THF (1 L) heated to reflux under argon. After the addition was completed, the mixture was stirred a 75 °C under argon for another 3 d. The solution was then concentrated, 3-aminopentane (16.5 mL, mmol, eq) was then added and the mixture was heated to reflux for 3 d. After being cooled down to rt, HCl (10%w, 300 mL) was added and the aqueous layer was extracted with DCM. The assembled organic layers were dried over MgSO₄. The solvent was then removed under reduced pressure

and the crude was purified by column chromatography (eluent: CH₂Cl₂) and recrystallization in EtOH to yield an orange solid (m = 421 mg, 54%).

¹H NMR (400 MHz, CD₂Cl₂, δ in ppm): 8.66 (dd, ³J = 9 Hz, ⁴J = 2 Hz, 2H), 8.11 (d, ³J = 9 Hz, 2H), 7.84 (d, ³J = 8 Hz, 2H), 7.56 (dd, ³J = 9 Hz, ³J = 7 Hz, 2H), 7.36 (d, ³J = 7 Hz, 2H), 6.69 (d, ⁴J = 2 Hz, 2H), 4.20 – 4.09 (m, 6H), 2.26 – 2.10 (m, 4H), 1.97 – 1.86 (m, 4H), 1.86 – 1.77 (m, 4H), 1.55 (h, ³J = 7 Hz, 4H), 1.06 (t, ³J = 7 Hz, 12H), 0.98 (t, ³J = 7 Hz, 6H).

¹³C NMR (100 MHz, CD₂Cl₂, δ in ppm): 171.6, 171.4, 145.1, 138, 136.7, 133.9, 130.8, 130.6, 129.0, 127.9, 127.8, 127.5, 126.3, 126.2, 125.6, 122.7, 73.9, 56.5, 54.4, 54.1, 53.8, 53.6, 53.3, 32.8, 25.9, 25.8, 19.8, 14.1, 11.6.

FD-HRMS: m/z calcd for C₅₀H₅₂O₆N₂ [M]: 776.38254, found 776.38296.



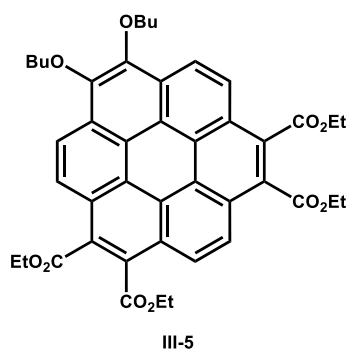
Flexible bis(butyloxy)coronene tetraester precursor III-4 9,10-Bis(butyloxy)phenanthrene-diglyoxylic acid **II-12** (700 mg, 1.5 mmol, 1 eq.) and 1,4-phenylenediacetic acid (291 mg, 1.5 mmol, 1 eq.) were dissolved in dry THF (50 mL). This solution was added dropwise over 24 h to a refluxing solution of Ac₂O (11.3 mL, 120 mmol) and NEt₃ (8.3 mL, 60 mmol) in THF (1 L) under argon. After the addition ended, the reaction was stirred at reflux under argon for 2 more days. The solvent was then removed until ca. 150 mL remained and DBU (22.3 mL, 150 mmol), EtOH (24.5 mL, 420 mmol) and EtBr (22.4 mL, 300 mmol) were added. The solution was stirred at reflux overnight. After being cooled down to room temperature, HCl (10%w in water, 100 mL) was added and the phases were separated, the aqueous phase was extracted with DCM, and the combined organic phases were dried with MgSO₄ and concentrated. The resulting oil was purified by column chromatography in DCM on silica gel and recrystallization in EtOH to yield the product as a yellow solid (313 mg, 28%).

¹H NMR (400 MHz, CD₂Cl₂, δ in ppm): 8.01 (d, ³J = 9 Hz, 2H), 7.39 (dd, ³J = 9 Hz, ⁴J = 2 Hz, 2H), 7.32 (d, ⁴J = 2 Hz, 2H), 7.21 (s, 4H), 4.46 (q, ³J = 7 Hz, 4H), 4.30 (q, ³J = 7 Hz, 4H), 4.16 (t, ³J = 7 Hz, 4H), 1.83 (quint., ³J = 7 Hz, 4H), 1.51 (m, 4H), 1.41 (t, ³J = 7 Hz, 6H), 1.29 (t, ³J = 7 Hz, 6H), 0.97 (t, ³J = 7 Hz, 6H).

¹³C NMR (100 MHz, CD₂Cl₂, δ in ppm): 169.0, 166.9, 144.8, 142.9, 138.1, 132.8, 130.5, 130.1, 129.1, 128.2, 127.0, 126.8, 122.6, 74.0, 62.39, 62.35, 32.9, 31.0, 19.8, 14.3, 14.3, 14.1.

ESI-HRMS: m/z calcd for C₄₄H₄₈O₁₀²³Na [M+Na]: 759.31397, found 759.31581.

UV-vis (CH₂Cl₂) λ_{\max} (ϵ L.mol⁻¹.cm⁻¹): 240 (4.98^{E4}), 270 (2.5^{E4}), 300 (3.1^{E4}), 335 (1.4^{E4}), 380 (1.16^{E4}).



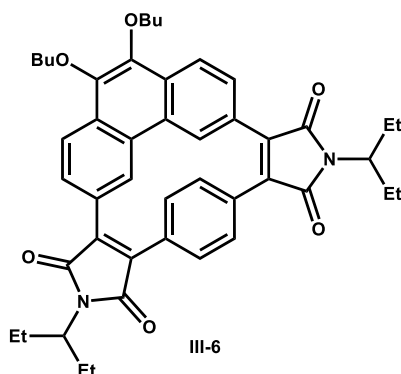
Bis(butyloxy)coronene tetraester III-5 The flexible coronene precursor **III-3** (80 mg, 0.11 mmol, 1 eq.) and iodine (300 mg) were dissolved in PhMe/AcOEt (3:1, 800 mL). The solution was stirred overnight at room temperature under air in a Pechl photoreactor with irradiation from a medium pressure 150 W mercury immersion lamp inside a borosilicate immersion tube in which cooling water circulated. The solvent was then removed and the crude product was purified by column chromatography in chloroform on silica gel and recrystallisation in EtOH to yield the final product as yellow crystals (52 mg, 65%).

¹H NMR (400 MHz, CD₂Cl₂, δ in ppm): 9.37 (d, ³J = 9 Hz, 2H), 9.29 (s, 2H), 9.22 (d, ³J = 9 Hz, 2H), 4.74 (q, ³J = 7 Hz, 4H), 4.73 (q, ³J = 7 Hz, 4H), 4.62 (t, ³J = 7 Hz, 4H), 2.17 – 2.07 (m, 4H), 1.84 – 1.72 (m, 4H), 1.60 (t, ³J = 7 Hz, 6H), 1.599 (t, ³J = 7 Hz, H), 1.12 (t, ³J = 7 Hz, 6H).

¹³C NMR (100 MHz, CD₂Cl₂, δ in ppm): 68.8, 168.7, 146.6, 130.6, 128.8, 127.1, 125.7, 125.6, 124.7, 124.6, 123.7, 123.1, 122.7, 119.9, 75.0, 63.0, 33.2, 20.0, 14.5, 14.3.

ESI-HRMS: m/z calcd for C₄₄H₄₈O₁₀²³Na [M+Na]: 755.28377, found 755.28484.

UV-vis (CH₂Cl₂) λ_{\max} (ϵ L.mol⁻¹.cm⁻¹): 280 (2.36^{E4}), 320 (6.76^{E4}), 335 (8.15^{E4}), 365 (2.44^{E4}), 430 (1.96^{E3}), 450 (3.65^{E3}).



Flexible bis(butyloxy)coronene diimide precursor III-6 9,10-Bis(butyloxy)phenanthrene diglyoxylic acid **II-12** (477 mg, 1.0 mmol, 1 eq.) and 1,4-phenylenediacetic acid (194 mg, 1.0 mmol, 1 eq.) were dissolved in dry THF (50 mL). This solution was added dropwise over 24 h to a refluxing mixture of Ac₂O (14 mL, 148 mmol) and NEt₃ (16 mL, 118 mmol) in THF (1 L)

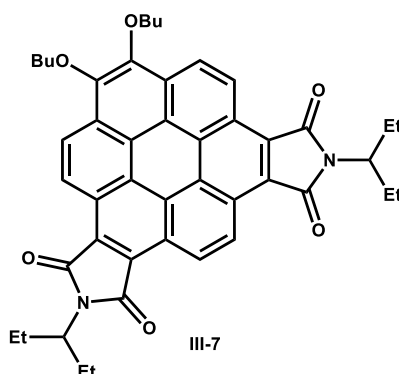
under argon. After the addition ended, the reaction media was heated under argon for 2 more days. The solvent was then removed until ca. 150 mL remained and 3-aminopentane (20 mL, 171 mmol) was added. The solution was stirred at reflux for another 2 days. After being cooled down to room temperature, excess HCl (10%w in water) was added and the phases were separated, the aqueous phase was extracted with DCM, and the combined organic phases were dried with MgSO₄ and the solvent removed under reduced pressure. The resulting oil was purified by column chromatography in DCM on silica gel and recrystallization in EtOH to yield the product as a yellow solid (254 mg, 35%).

¹H NMR (400 MHz, CD₂Cl₂, δ in ppm): 8.41 (dd, ³J = 9 Hz, ⁴J = 2 Hz, 2H), 8.20 (d, ³J = 9 Hz, 2H), 7.26 (s, 4H), 7.05 (d, ⁴J = 2 Hz, 2H), 4.25 (t, ³J = 7 Hz, 4H), 4.07 (m, 2H), 2.11 (m, 4H), 1.95 – 1.78 (m, 8H), 1.61 (m, 6H), 1.03 (t, ³J = 7 Hz, 6H), 0.99 (t, ³J = 7 Hz, 12H).

¹³C NMR (100 MHz, CD₂Cl₂, δ in ppm): 171.3, 170.8, 145.3, 137.4, 137.3, 133.7, 130.8, 130.2, 127.5, 127.5, 126.6, 125.7, 122.7, 74.2, 56.5, 32.9, 25.9, 19.8, 14.2, 11.5.

ESI-HRMS: m/z calcd for C₄₆H₅₀O₆²³Na [M+Na]: 749.35721, found 749.35782.

UV-vis (CH₂Cl₂) λ_{max} (ε L.mol⁻¹.cm⁻¹): 250 (7.3^{E4}), 310 (1.9^{E4}), 385 (1.5^{E4}), 450 (1.2^{E4}).

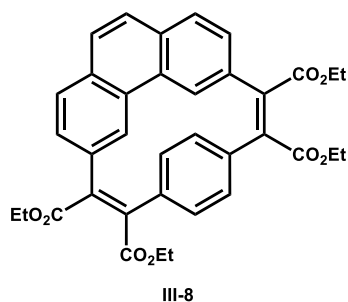


Bis(butyloxy)coronene diimide III-7 The flexible coronene precursor **III-6** (253 mg, 0.35 mmol, 1 eq.) and iodine (300 mg) were dissolved in PhMe/AcOEt (3:1, 800 mL). The solution was stirred overnight at room temperature under air in a Pechl photoreactor with irradiation from a medium pressure 150 W mercury immersion lamp inside a borosilicate immersion tube in which cooling water circulated. The solvent was then removed and the crude product was purified by column chromatography in CHCl₃ on silica gel and recrystallized in EtOH to yield the final product as yellow crystals (76 mg, 30%).

¹H NMR (400 MHz, CDCl₃, δ in ppm): 9.99 (d, ³J = 9 Hz, 2H), 9.88 (s, 2H), 9.36 (d, ³J = 9 Hz, 2H), 4.69 (t, ³J = 7 Hz, 4H), 4.40 (m, ³J = 7 Hz, 2H), 2.48 – 2.32 (m, 4H), 2.14 – 2.01 (m, 4H), 1.90 – 1.76 (m, 4H), 1.20 (t, J = 7 Hz, 6H), 1.19 (t, J = 7 Hz, 12H).

¹³C NMR (100 MHz, CD₂Cl₂, δ in ppm): 170.4, 170.3, 146.8, 126.7, 125.4, 124.1, 123.9, 123.3, 122.9, 122.8, 122.0, 118.3, 74.9, 56.0, 33.2, 25.7, 19.8, 14.3, 11.8.

UV-vis (CH₂Cl₂) λ_{max} (ε L.mol⁻¹.cm⁻¹): 265 (4.5^{E4}), 295 (5.0^{E4}), 315 (5.6^{E4}), 390 (7.2^{E4}), 475 (7.3^{E3}), 505 (1.1^{E4}).



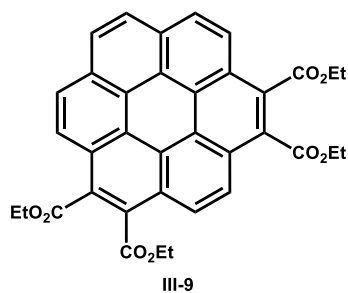
Flexible coronene tetraester precursor III-8 Phenanthrene-3,6-diglyoxylic acid **II-5** (620 mg, 1.9 mmol, 1 eq.) and 1,4-phenylenediacetic acid (373 mg, 1.9 mmol, 1 eq.) were dissolved in dry THF (50 mL). This solution was added dropwise over 24 h to a refluxing mixture of Ac₂O (11.3 mL, 102 mmol) and NEt₃ (8.3 mL, 60 mmol) in THF (1 L) under argon. After the addition, the reaction was stirred at reflux under argon for 2 more days. The solvent was then partially removed and DBU (10 mL, 67 mmol), EtOH (12 mL, 205 mmol) and EtBr (10 mL, 135 mmol) were added. The solution was stirred at reflux overnight. After being cooled down to room temperature, HCl (10%w in water, 100 mL) was added the phases were separated, the aqueous phase was extracted with DCM, and the combined organic phases were dried with MgSO₄ and concentrated. The resulting oil was purified by column chromatography in DCM on silica gel and recrystallization in EtOH to yield the product as a pale-yellow solid (73 mg, 6%).

¹H NMR (400 MHz, CDCl₃, δ in ppm): 7.74 (d, ³J = 8 Hz, 2H), 7.69 (s, 2H), 7.46 – 7.39 (m, 4H), 7.23 (s, 4H), 4.54 (q, ³J = 7 Hz, 4H), 4.34 (q, ³J = 7 Hz, 4H), 1.47 (t, ³J = 7 Hz, 6H), 1.33 (t, ³J = 7 Hz, 6H).

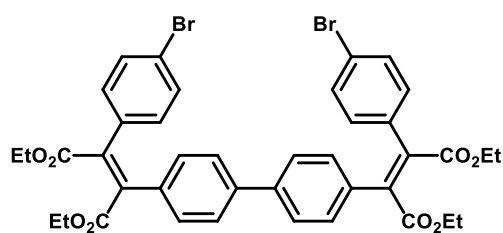
¹³C NMR (100 MHz, CDCl₃, δ in ppm): 169.0, 166.8, 142.5, 137.6, 133.1, 132.1, 129.7, 128.6, 128.18, 127.9, 127.6, 126.3, 62.2, 62.1, 14.31, 14.27.

ESI-HRMS: m/z calcd for C₃₆H₃₂O₈²³Na [M+Na]: 615.20004, found 615.19928.

UV-vis (CH₂Cl₂) λ_{max} (ε L.mol⁻¹.cm⁻¹): 290 (3.71^{E4}), 325 (1.78^{E4}), 365 (1.15^{E4}).



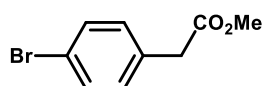
Coronene tetraester III-9 The flexible precursor **III-8** (37 mg, 0.06 mmol, 1 eq) was dissolved in AcOEt (400 mL). The solution was stirred for 2 days at room temperature under air in a



IV-3

Dibrominated trimer IV-3 4,4'-biphenyldiglyoxylic acid **IV-2** (3.1 g, 10.4 mmol, 1 eq.) and 4-bromophenylacetic acid (5.6 g, 22.9 mmol, 2.2 eq.) were dissolved in THF (250 mL). Ac₂O (8.9 mL, 83.2 mmol, 8 eq.) and NEt₃ (8.9 mL, 41.6 mmol, 4 eq.) were added and the solution was heated to reflux under argon for 1 h. After return to rt, DBU (15.5 mL, 104 mmol, 10 eq.), EtOH (17 mL, 291.2 mmol, 28 eq.) and EtBr (15.5 mL, 208 mmol, 20 eq.) were added and the mixture was heated to reflux overnight. After being cooled down to rt, HCl (10 %w, 250 mL) was added and the aqueous layers were extracted with DCM. The organic layers were assembled and dried over MgSO₄. The solvent was then removed under reduced pressure and after addition of EtOH to the red oil, a yellow precipitate appears. The precipitate was filtrated and washed with EtOH to yield the product as a yellow solid (m = 7.4 g, 89%).

¹H NMR (400 MHz, CDCl₃, δ in ppm): 7.40 (d, ³J = 9 Hz, 4H), 7.33 (d, ³J = 8. Hz, 4H), 7.13 (d, ³J = 9 Hz, 4H), 7.00 (d, ³J = 9 Hz, 4H), 4.30 (q, ³J = 7 Hz, 4H), 4.28 (q, ³J = 7 Hz, 4H), 1.30 (t, ³J = 7 Hz, 6H), 1.29 (t, ³J = 7 Hz, 6H).

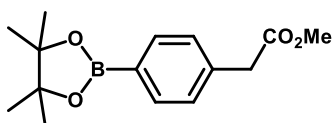


IV-4

Methyl 4-bromophenylacetate IV-4 4-bromophenylacetic acid (20 g, 93 mmol, 1 eq.) was dissolved in MeOH (500 mL). SOCl₂ (50 mL, 689 mmol, 13.5 eq.) was carefully added through the water condenser and the solution was then heated to reflux for 4 h. After cooling down to rt, the solution was concentrated under reduced pressure and the resulting oil was purified over silica gel column chromatography (eluent: CHCl₃) to yield the product as a yellow oil (m = 21 g, quantitative).

¹H NMR (400 MHz, CDCl₃, δ in ppm): 7.45 (dd, ³J = 9 Hz, 2H), 7.15 (dd, ³J = 9 Hz, 2H), 3.69 (s, 3H), 3.58 (s, 2H).

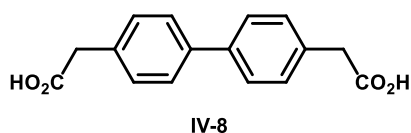
¹³C NMR (100 MHz, CDCl₃, δ in ppm): 171.7, 133.0, 131.8, 131.2, 121.3, 52.3, 40.7.



IV-5

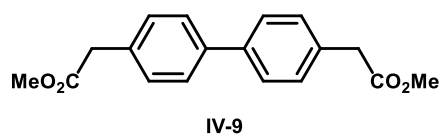
Methyl [4-(4,4,5,5-tetramethyl-1,3,2-dioxaborolan-2-yl)phenyl]acetate IV-5 Methyl 4-bromo-phenylacetate (4.7 g, 20.5 mmol, 1 eq.) was dissolved in anhydrous 1,4-dioxane (90 mL). $B_2(\text{pin})_2$ (6.1 g, 24 mmol, 1.2 eq.), AcOK (5.9 g, 60 mmol, 2.9 eq.) and [1,1'-Bis(diphenylphosphino)ferrocene] palladium chloride (0.9 g, 1.2 mmol, cat.) were added and the red mixture was heated at 90 °C for 2.5 h under argon. After being cooled down to rt, the mixture was diluted in DCM and water was added to dissolve the remaining salts. The aqueous layer was then extracted with DCM, and the organic layers assembled, dried over $MgSO_4$ and the solvent removed under vacuum. The resulting black solid was purified with column chromatography over silica gel (eluent: petroleum ether/acetone (9:1)) to yield the product of borylation as a yellow oil (m = 5.1 g, 90%).

1H NMR (400 MHz, $CDCl_3$, δ in ppm): 7.77 (d, $^3J = 8$ Hz, 2H), 7.29 (d, $^3J = 8$ Hz, 3H), 3.68 (s, 3H), 3.64 (s, 2H), 1.34 (s, 12H).



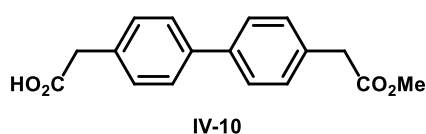
4,4'-biphenyle diacetic acid IV-8 Diglyoxylic acid IV-2 (2.54 g, 8.5 mmol, 1 eq.) was dissolved in acetic acid (50 mL). H_3PO_2 (50 %w in water, 2.3 mL, 21.3 mmol, 2.5 eq.) and NaI (1.53 g, 10.2 mmol, 1.2 eq.) were added to the mixture. The solution was heated to reflux and stirred under argon for 3 days. After being cooled down, water was added and the white precipitate was filtered and dried under vacuum to remove traces of acetic acid and water. The white solid is then used without further purification (m = 1.99 g, 86%).

1H NMR (400 MHz, acetone- d_6 , δ in ppm): 7.62 (d, $^3J = 8$ Hz, 4H), 7.41 (d, $^3J = 8$ Hz, 4H), 3.68 (s, 4H).



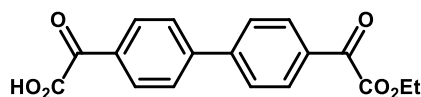
Dimethyl 4,4'-biphenyle diacetic ester IV-9 Diacetic acid IV-8 (1 g, 3.74 mmol, 1 eq.) was dissolved in MeOH (500 mL). $SOCl_2$ (12 mL, 164.8, 13.5 eq.) was then slowly added and the solution was heated to reflux for 4 h. Once cooled down to rt, the solvent was removed under reduced pressure and the crude was purified over silica gel ($CHCl_3$) to yield the product as a white solid (m = 1 g, 90%).

1H NMR (400 MHz, $CDCl_3$, δ in ppm): 7.53 (d, $^3J = 8$ Hz, 4H), 7.34 (d, $^3J = 8$ Hz, 2H), 3.71 (s, 6H), 3.67 (s, 4H).



4,4'-biphenyle diacetic acid, 4-methylester IV-10 Diester **IV-9** (1.175 g, 3.9 mmol, 1 eq.) was dissolved in THF (200 mL). A solution of KOH (220 mg, 3.9 mmol, 1 eq.) dissolved in MeOH (10 mL) was then added to the solution and the mixture was heated to reflux for 70 min. The mixture was then cooled down to rt and the solvent evaporated under reduced pressure. A minimum of CH₂Cl₂ is added and the crude is filtered. The filtrate is evaporated under reduced pressure to yield a white solid corresponding to the unreacted diester **IV-9**. The residue is collected and triturated in a mixture of HCl (1M) and CH₂Cl₂. The mixture is filtered and the remaining solid, corresponding to the diacid, is collected. The aqueous layer is extracted with CH₂Cl₂. The organic layers are then reassembled, dried with MgSO₄ and the solvent is removed under vacuum to yield a white solid corresponding to the monoester (m = 477 mg, 43%).

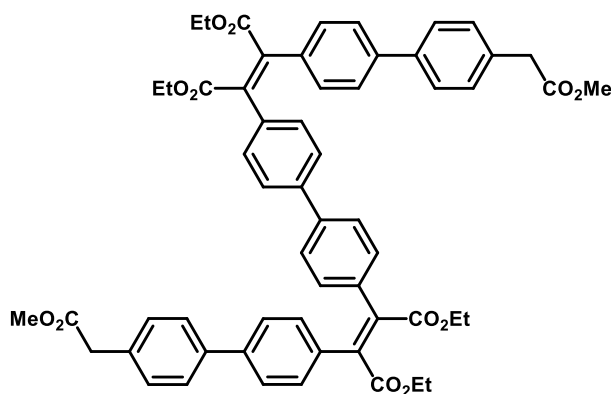
¹H NMR (400 MHz, acetone-d₆, δ in ppm): 7.58 (m, 4H), 7.37 (m, 4H), 3.67 (m, 2H), 3.65 (s, 2H), 3.63 (s, 3H).



IV-11

4,4'-biphenyle diglyoxylic acid, 4-ethylester IV-11 Diester **IV-1** (3.400 g, 9.6 mmol, 1 eq.) was dissolved in THF (200 mL). A solution of KOH (555 mg, 9.6 mmol, 1 eq.) dissolved in MeOH (50 mL) is then added to the solution and the mixture is heated to reflux for 70 min. The mixture is then cooled down to rt and the solvent evaporated under reduced pressure. A minimum of CH₂Cl₂ is added and the crude is filtered. The filtrate is evaporated under reduced pressure to yield a white solid corresponding to the unreacted diester **IV-1**. The residue is collected and triturated in a mixture of HCl (1M) and CH₂Cl₂. The mixture is filtered and the remaining solid, corresponding to the diacid, is collected. The aqueous layer is extracted with CH₂Cl₂. The organic layers are then reassembled, dried with MgSO₄ and the solvent is removed under vacuum to yield a white solid corresponding to the monoester (m = 1.221 g, 39%).

¹H NMR (400 MHz, acetone-d₆, δ in ppm): 8.19 (m, 2H), 8.15 (m, 2H), 8.01 (m, 4H), 4.49 (q, ³J = 7 Hz, 2H), 1.41 (t, ³J = 7 Hz, 3H).



IV-7

Biphenyl trimer with two acetic ester functions IV-7

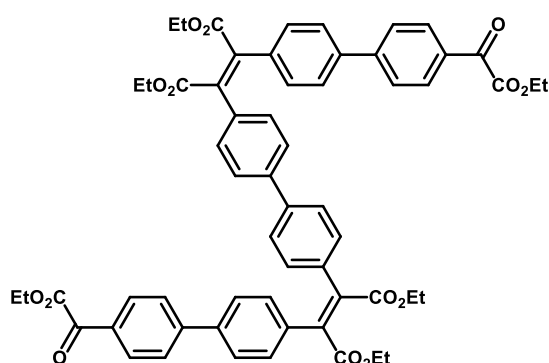
- With Suzuki-Miyaura coupling:

Dibrominated trimer **IV-3** (2.6 g, 3.2 mmol, 1 eq.) and the boronate ester **IV-5** were dissolved in a solution of $[\text{PdCl}_2(\text{PPh}_3)_2]$ (240 mg, 0.3 mmol, 10 mol%) and K_2CO_3 (460 mg, 3.3 mmol, 1 eq.) in a mixture of toluene, ethanol and water (180 mL, 4:4:1). The mixture was stirred at 90 °C for 5 days under argon. After being cooled down to room temperature, HCl (10%w in water) was added, and the aqueous layer was extracted with DCM. The organic layers were assembled, dried over MgSO_4 and the solvent was removed under reduced pressure. The resulting oil was purified on silica gel (petroleum ether/acetone (6:4)) to yield the trimer **IV-7** as a yellow solid (760 mg, 25%).

- With the Perkin Strategy:

4,4'-biphenyl diglyoxylic acid **IV-2** (358 mg, 1.2 mmol, 1 eq.) and monoprotected 4,4'-biphenyl diacetic acid **IV-10** (891 mg, 3.1 mmol, 2.5 eq.) were dissolved in 20 mL of anhydrous THF. Ac_2O (0.9 mL, 9.5 mmol, 8 eq.) and NEt_3 (0.8 mL, 5.5 mmol, 4.6 eq.) were added and the mixture was stirred overnight at 75 °C under argon. DBU (1.5 mL, 10 mmol, 8.3 eq.), EtOH (1.7 mL, 29.1 mmol, 24 eq.) and EtBr (1.5 mL, 20.2 mmol, 17 eq.) were then added to the mixture which was stirred for another 48 h at 75 °C. The reaction media was then cooled down to rt and a large excess of HCl (10%w) was put in the mixture. The aqueous layers were extracted with CH_2Cl_2 . The organic layers were finally put together and dried over MgSO_4 . The solvent was removed under reduced pressure and the resulting orange oil was purified by column chromatography over silica gel (petroleum ether/acetone (7:3)) as a yellow solid (m = 258 mg, 49%).

$^1\text{H NMR}$ (400 MHz, CD_2Cl_2 , δ in ppm): 7.51 (d, $^3J = 8$ Hz, 4H), 7.44 (m, 8H), 7.31 (d, $^3J = 8$ Hz, 4H), 7.18 (d, $^3J = 9$ Hz, 8H), 4.29 (q, $^3J = 7$ Hz, 4H), 4.28 (q, $^3J = 7$ Hz, 4H), 3.68 (s, 6H), 3.65 (s, 4H), 1.31 (t, $^3J = 7$ Hz, 6H), 1.30 (t, $^3J = 7$ Hz, 6H).



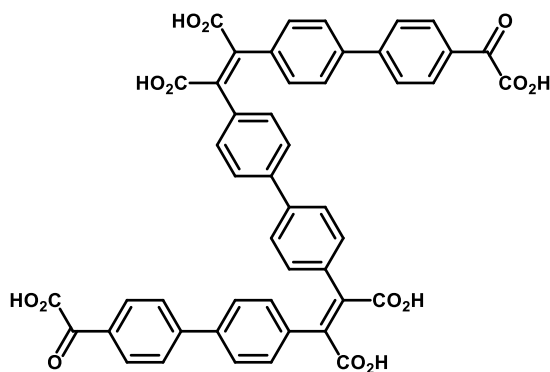
IV-12

Biphenyl trimer with two glyoxylic ester functions IV-12 4,4'-biphenyl diacetic acid **IV-9** (459 mg, 1.7 mmol, 1 eq.) and monoprotected 4,4'-biphenyl diglyoxylic acid **IV-11** (1.221 g, 3.7 mmol, 2.2 eq.) were dissolved in 75 mL of anhydrous THF. Ac_2O (1.3 mL, 13.6 mmol, 8 eq.) and NEt_3 (1 mL, 6.8 mmol, 4 eq.) were added and the mixture was stirred overnight at 75 °C

under argon. DBU (2.5 mL, 17 mmol, 10 eq.), EtOH (2.7 mL, 47.6 mmol, 28 eq.) and EtBr (2.5 mL, 34 mmol, 20 eq.) were then added to the mixture which was stirred for another 48 h at 75 °C. The reaction media was then cooled down to rt and a large excess of HCl (10%w) was put in the mixture. The aqueous layers were extracted with CH₂Cl₂, the organic layers put together and dried over MgSO₄. The solvent was then removed under reduced pressure and the resulting orange oil was purified by column chromatography over silica gel (petroleum ether/acetone (6:4)) as a yellow oil (m = 1 g, 52%).

¹H NMR (400 MHz, CDCl₃, δ in ppm): 8.05 (d, ³J = 9 Hz, 4H), 7.66 (d, ³J = 9 Hz, 4H), 7.47 (d, ³J = 9 Hz, 4H), 7.39 (d, ³J = 9 Hz, 4H), 7.23 (d, ³J = 8 Hz, 4H), 7.17 (d, ³J = 8 Hz, 4H), 4.45 (q, ³J = 7 Hz, 4H), 4.32 (q, ³J = 7 Hz, 8H), 1.42 (t, ³J = 7 Hz, 6H), 1.32 (t, ³J = 7 Hz, 6H), 1.31 (t, ³J = 7 Hz, 6H).

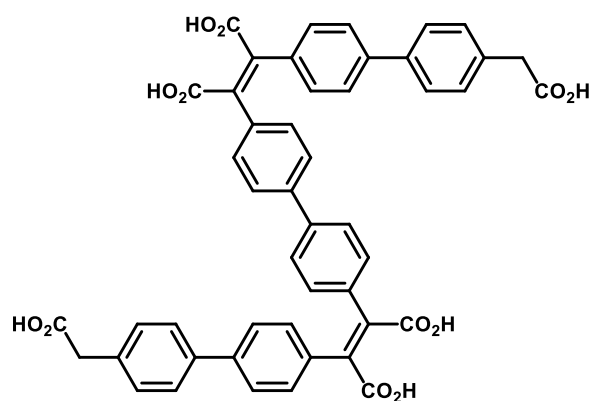
¹³C NMR (100 MHz, CDCl₃, δ in ppm): 185.9, 168.0, 167.8, 163.8, 146.6, 140.1, 139.2, 139.0, 137.6, 135.2, 133.9, 131.5, 130.8, 130.7, 130.4, 127.5, 127.2, 126.8, 62.5, 62.0, 31.1, 14.3, 14.2.



IV-13

Biphenyl trimer with two glyoxylic acid functions IV-13 The trimer hexaester **IV-12** (1.290 mg, 1.2 mmol, 1 eq.) was dissolved a mixture of THF/EtOH/H₂O (1:1:8, 200 mL). NaHCO₃ (2 g, in excess) was dissolved in water (100 mL) and was added to the reaction media. The mixture was then stirred overnight at 75 °C. The crude was then cooled back to rt and aqueous HCl (10%) was added. A bright yellow precipitate appears. THF and CH₂Cl₂ were added and the aqueous layer was extracted with CH₂Cl₂. The organic layers were assembled, dried over MgSO₄ and the solvent removed under reduced pressure. The product is obtained as an orange powder (m = 990 mg, quantitative).

¹H NMR (400 MHz, DMSO-d₆, δ in ppm): 8.04 (d, ³J = 9 Hz, 4H), 7.98 (d, ³J = 9 Hz, 4H), 7.92 (d, ³J = 9 Hz, 4H), 7.89 (d, ³J = 9 Hz, 4H), 7.62 (m, 8H).



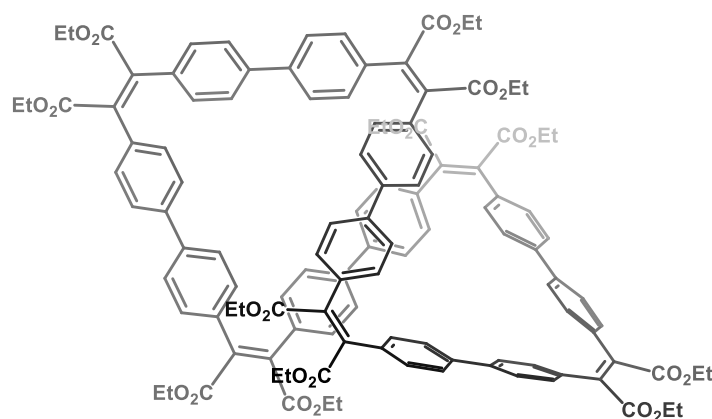
IV-14

Biphenyl trimer with two acetic acid functions IV-14

The trimer hexaester **IV-7** (515 mg, 0.6 mmol, 1 eq.) was dissolved a mixture of THF/EtOH (1:1, 75 mL). KOH (600 g, in excess) was dissolved in water (100 mL) and was added to the reaction media. The mixture was then stirred overnight at 75 °C. The crude was then cooled back to rt and aqueous HCl (10%) was added. A bright yellow precipitate appears. THF and CH₂Cl₂ were added, and the aqueous layer was extracted with CH₂Cl₂. The organic layers were assembled, dried over MgSO₄ and the solvent removed under reduced pressure. The product is obtained as an orange powder (m = 480 mg, quantitative).

¹H NMR (400 MHz, DMSO-*d*₆, δ in ppm): 7.89 (d, ³J = 9 Hz, 4H), 7.80 (d, ³J = 9 Hz, 4H), 7.68 (d, ³J = 8 Hz, 4H), 7.61 (d, ³J = 8 Hz, 4H), 7.58 (d, ³J = 8 Hz, 4H), 7.37 (d, ³J = 8 Hz, 4H), 3.62 (s, 4H).

¹³C NMR (100 MHz, DMSO-*d*₆, δ in ppm): 206.6, 172.6, 165.1, 141.9, 140.7, 137.9, 137.4, 137.2, 135.2, 130.2, 130.2, 127.5, 127.1, 126.8, 126.7, 126.5, 79.2, 40.3, 30.7.

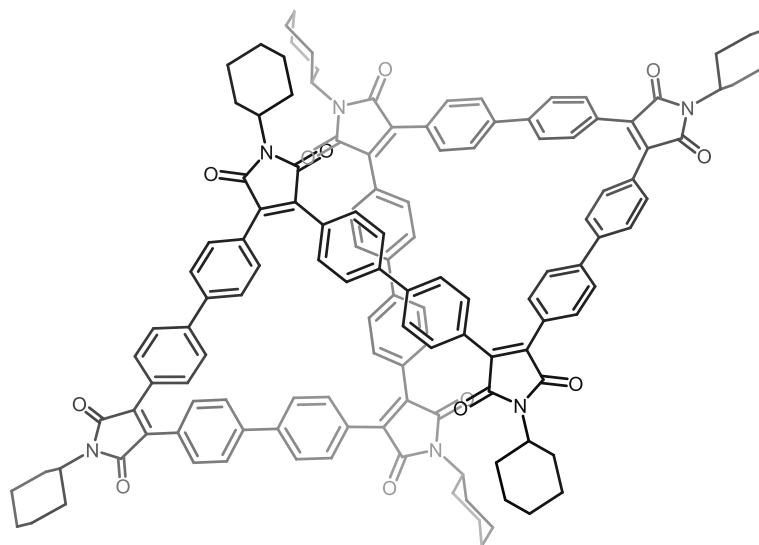


IV-15

Macrocyclic hexamer dodecaester IV-15 The two trimers of biphenyl **IV-13** (636 mg, 0.8 mmol, 1 eq.) and **IV-14** (615 mg, 0.8 mmol, 1 eq.) were dissolved in a THF/DMF (9:1, 50 mL) mixture. The solution was added dropwise with a push-syringe over 24 h in a solution of Ac₂O (mL, 10.6 mmol, 14 eq.) and NEt₃ (1 mL, 7.2 mmol, 9 eq.) in THF (250 mL) heated to reflux and under argon. After the end of the addition, the solution was stirred for 4 more days at reflux

under argon. EtOH (3.7 mL, 63.3 mmol, 83 eq.), EtBr (12.52.5 mL, 33.7 mmol, 44 eq.) and DBU (2.5, 16.7 mmol, 22 eq.) were then added. The solution was heated at reflux overnight. After being cooled down to rt, HCl (10 %w, 200 mL) was added and the aqueous layer was extracted with DCM. The organic layers were assembled and dried over MgSO₄. The solvent was then removed under reduced pressure and the crude was purified by column chromatography (CHCl₃) and recrystallization in EtOH to yield a yellow solid (m = 150 mg, 10%).

¹H NMR (400 MHz, CDCl₃, δ in ppm): 7.37 (d, ³J = 9 Hz, 24H), 7.17 (d, ³J = 9 Hz, 24H), 4.31 (q, ³J = 7 Hz, 24H), 1.30 (t, ³J = 7 Hz, 36H).



IV-17

Macrocyclic hexamer hexaimide IV-15 The two trimers of biphenyl IV-13 (577 mg, 0.7 mmol, 1 eq.) and IV-14 (558 mg, 0.7 mmol, 1 eq.) were dissolved in a THF/DMF (9:1, 50 mL) mixture. The solution was added dropwise with a push-syringe over 24 h in a solution of Ac₂O (1 mL, 10.6 mmol, 14 eq.) and NEt₃ (1 mL, 7.2 mmol, 9.4 eq.) in THF (250 mL) heated to reflux and under argon. After the end of the addition, the solution was stirred for 4 more days at reflux under argon. Cyclohexylamine (5 mL, 43.6 mmol, 62 eq.) was then added and the solution was heated at reflux for two days. After being cooled down to rt, HCl (10 %w, 200 mL) was added and the aqueous layer was extracted with DCM. The organic layers were assembled and dried over MgSO₄. The solvent was then removed under reduced pressure and the crude was purified by column chromatography (CH₂Cl₂/ petroleum ether (9:1)) to yield the product as a yellow solid (m = 263 mg, 19%).

¹H NMR (400 MHz, CD₂Cl₂, δ in ppm): 7.60 (d, 3J = 9 Hz, 24H), 7.55 (d, 3J = 9 Hz, 24H), 4.06 (tt, J = 12 Hz, J = 4 Hz, 6H), 2.15 (m, 12H), 1.87 (d, J = 13 Hz, 12H), 1.77 (d, J = 10 Hz, 12H), 1.70 (d, J = 12 Hz, 6H), 1.39 (q, J = 13 Hz, 12H), 1.27 (m, 6H).

¹³C NMR (100 MHz, CD₂Cl₂, δ in ppm): 170.8, 141.8, 135.9, 130.9, 128.9, 127.5, 51.6, 31.0, 30.4, 29.5, 26.5, 25.6.

Crystallographic Data

Single crystal X-ray diffraction

The crystallographic data were collected with a Bruker APEX II Quasar diffractometer, equipped with a graphite monochromator centred on the path of MoK α radiation. Single crystals of **III-9** were obtained by slow diffusion of a dichloromethane solution of **III-9** into butanol, whereas single crystals of **III-5** were obtained by recrystallisation in ethanol. The selected single crystals were coated with CargilleTM NHV immersion oil and mounted on a fiber loop, followed by data collection at 120 K for 10, and 298 K for **III-9**. At 120 K, the single crystals of **III-9** break into a microcrystalline powder so that the structure was not determined at low temperature. The program SAINT was used to integrate the data, which was thereafter corrected using SADABS. The structure was solved using SHELXT and refined by a full-matrix least-squares method on F² using SHELXL-2019. All non-hydrogen atoms were refined with anisotropic displacement parameters, whereas hydrogen atoms were assigned to ideal positions and refined isotropically using suitable riding models.

The crystals of coronene tetraester **III-9** are weakly diffracting. Therefore, the data were cut at 0.90 Å, as there is no diffraction above and R_{int} becomes larger. The result is a quite low Θ_{\max} value and data/parameters ratio. DFIX constraint was used between C26 and C27.

The CIF files have been deposited at the Cambridge Crystallographic Data Centre as supplementary publication no. CCDC 2335164-2335165.

Table: crystallographic data

Compound	coronene tetraester III-9	bisbutyloxycoronene tetraester III-5
Formula	C ₃₆ H ₂₈ O ₈	C ₄₄ H ₄₄ O ₁₀
FW (g·mol ⁻¹)	588.58	732.79
Crystal color	yellow	yellow
Crystal size (mm)	0.40 x 0.10 x 0.03	0.30 x 0.22 x 0.11
Crystal system	triclinic	triclinic
Space group	P-1	P-1
Temperature	298 K	120 K
<i>a</i> (Å)	6.9314(5)	15.186(2)
<i>b</i> (Å)	13.7810(9)	15.823(2)
<i>c</i> (Å)	16.0680(12)	16.474(2)
α (°)	86.662(4)	69.815(5)
β (°)	82.997(4)	88.884(6)
γ (°)	76.021(3)	81.886(6)
<i>V</i> (Å ³)	1477.62(18)	3676.6(9)
<i>Z</i>	2	4
<i>d</i> _{calc}	1.323	1.324
μ (mm ⁻¹)	0.094	0.093
θ_{\min} - θ_{\max}	1.959° - 23.412°	1.318° - 24.499°
Refl. coll. / unique	109471 / 4305	43227 / 12032
Completeness to 2 θ	0.994	0.982
<i>R</i> _{int}	0.1040	0.0806
Refined	401 / 1	985 / 0
^a <i>R</i> ₁ (<i>I</i> > 2 σ (<i>I</i>))	0.0620	0.0844
^b <i>wR</i> ₂ (all data)	0.2076	0.2602
Goodness of fit	1.097	1.059
CCDC number	2335165	2335164

$$^a R_1 = \sum ||F_o| - |F_c|| / \sum |F_o| \text{ and } ^b wR_2 = [\sum w(F_o^2 - F_c^2)^2 / \sum w(F_o^2)^2]^{1/2}$$

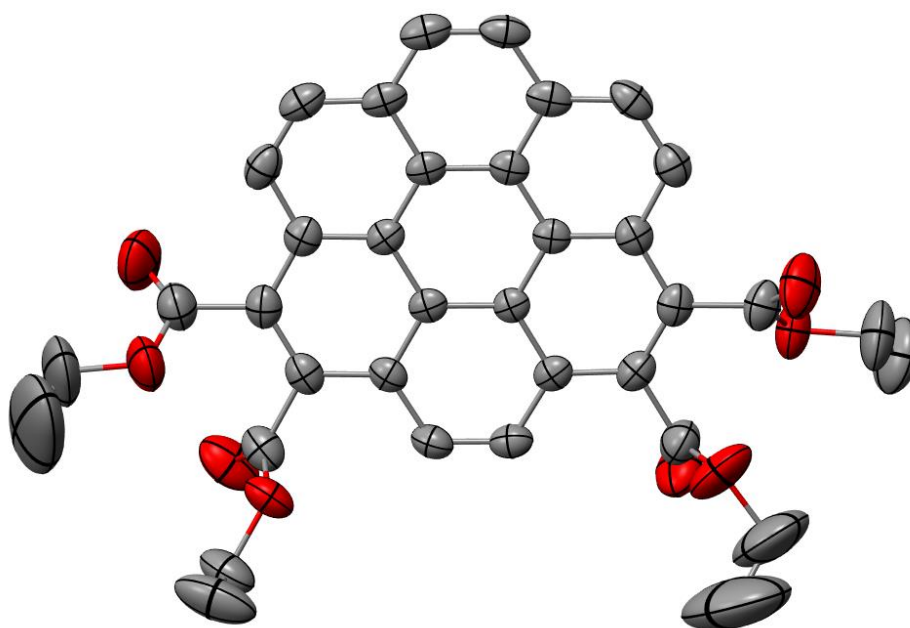


Figure 140. ORTEP-type view of the coronene tetraester 5 in the crystal at 298 K. Thermal ellipsoids are depicted at a 50 % probability level. Hydrogen atoms are omitted, for clarity. C: grey, O: red.

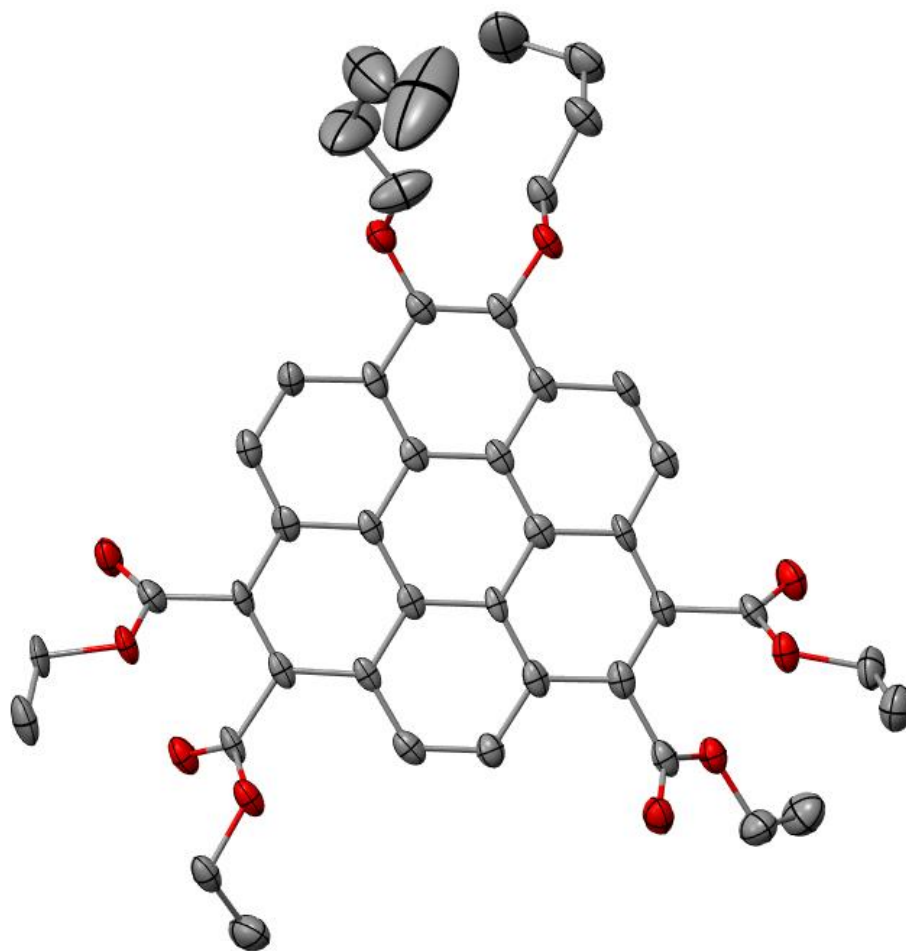


Figure 141. ORTEP-type view of bisbutyloxycoronene tetraester 10 in the crystal at 120 K. Thermal ellipsoids are depicted at a 50 % probability level. Only one of the two molecule of the asymmetric unit is depicted, and hydrogen atoms are omitted, for clarity. C: grey, O: red.

References

- 1 A. M. Brouwer, *Pure Appl. Chem.*, 2011, **83**, 2213–2228.
- 2 F. Aribot, A. Merle, P. Dechambenoit, H. Bock, A. Artigas, N. Vanthuyne, Y. Carissan, D. Hagebaum-Reignier, Y. Coquerel and F. Durola, *Angew. Chem. Int. Ed.*, 2023, **62**, e202304058.
- 3 L. Soliman, E. Ramassamy, K. Dujarric, G. Naulet, P. Dechambenoit, H. Bock and F. Durola, *Chem. Commun.*, DOI:10.1039/D4CC00935E.
- 4 J. Lyu and C. W. Bielawski, *Polym. Chem.*, 2022, **13**, 613–621.
- 5 A. Robert, P. Dechambenoit, E. A. Hillard, H. Bock and F. Durola, *Chem Commun*, 2017, **53**, 11540–11543.

Titre : Nanorubans cycliques aromatiques

Résumé :

La synthèse de macrocycles conjugués à partir de fragments aromatiques polycycliques a fait l'objet de recherches approfondies au cours des dernières décennies en raison de leurs structures et propriétés physiques inhabituelles. Notre équipe a développé une voie de synthèse pour la formation de nouveaux composés aromatiques polycycliques carboxy-substitués basée sur une version modifiée de la réaction historique de Perkin. Cette stratégie permet la formation d'une grande variété de molécules conjuguées, linéaires ou ramifiées, plates ou torsadées, et s'est même révélée très efficace pour la formation de composés macrocycliques. De plus, les techniques de protection et de déprotection permettent d'assembler de manière contrôlée un grand nombre d'éléments et de concevoir des molécules aux formes de plus en plus atypiques. Au cours des dernières années, notre groupe a rapporté la synthèse de cyclo-poly-[5]helicènes avec des formes persistantes en forme de huit ou de bandes de Möbius. Malgré leurs géométries similaires à celles des rubans cycliques torsadés, ces composés ne peuvent pas être strictement considérés comme des nanorubans cycliques torsadés en raison des liaisons simples restantes reliant les parties [5]helicène. À partir des stratégies de synthèse existantes, nous en avons conçu des adaptées pour la formation d'équivalents entièrement condensés de ces poly-[5]helicènes macrocycliques, qui présenteraient alors des topologies non triviales de nanorubans torsadés. Nous rapportons ici les différentes approches tentées pour la synthèse de ces nouvelles structures moléculaires.

Mots clés : CAPs, Macrocycles, Nanorubans

Title: Cyclic aromatic nanoribbons

Abstract:

The synthesis of conjugated macrocycles from polycyclic aromatic fragments has been a subject of extensive research the last decades because of their unusual structures and physical properties. Our team has developed a synthetic pathway for the formation of new carboxy-substituted polycyclic aromatic compounds based on a modified version of the historical Perkin reaction. This strategy allows the formation of large variety of conjugated molecules, linear or branched, flat or twisted, and has even been proved highly efficient for the formation of macrocyclic compounds. In addition, protection and deprotection techniques allow the controlled assembly of a large number of elements and molecules with increasingly atypical shapes can be designed. Over the last few years, our group reported the synthesis of cyclo-poly-[5]helicenes with persistent figure-of-eight or Möbius band shapes. Despite their geometries similar to twisted cyclic ribbons, these compounds cannot be strictly considered as twisted cyclic nanoribbons due to the remaining single bonds linking the [5]helicene parts. From the existing synthetic strategies, we have designed adapted ones for the formation of fully condensed equivalents of these macrocyclic poly-[5]helicenes, which would then display non trivial topologies of twisted nanoribbons. Herein, we report the different approaches attempted for the synthesis of these novel molecular structures.

Keywords : PACs, Macrocycles, Nanoribbons

Unité de recherche

Centre de Recherche Paul Pascal, CNRS-UMR 5031,

115 Avenue du Dr Albert Schweitzer 33600 Pessac